
**HOST DEFENCE PEPTIDES
(HDPs) AS NOVEL
BIOPRESERVATIVES FOR FOOD
INDUSTRY APPLICATIONS**

Eliana Dell'Olmo

Dottorato in Biotecnologie – 32° ciclo

Università di Napoli Federico II



Dottorato in Biotecnologie – 32° ciclo

Università di Napoli Federico II



HOST DEFENCE PEPTIDES (HDPs) AS NOVEL BIOPRESERVATIVES IN FOOD INDUSTRY APPLICATIONS

Dottorando: Eliana Dell'Olmo

Relatore: Prof. Angela Arciello

Coordinatore: Prof. Marco Moracci

Settore Scientifico Disciplinare BIO-10

*A tutti coloro che hanno
deciso di combattere
per i propri sogni*

ABSTRACT	1
RIASSUNTO	3
CHAPTER 1. GENERAL INTRODUCTION	9
CHAPTER 2. ApoB derived peptides as novel antimicrobial and anti-biofilm agents towards <i>Salmonella</i> strains	33
CHAPTER 3. ApoB derived peptides as novel antifungal agents	55
CHAPTER 4. Biocompatibility assessment of ApoB derived peptides	79
CHAPTER 5. Novel ApoB peptides based active coatings for food industry applications	99
CHAPTER 6. General discussion and concluding remarks	119
APPENDICES	132
• Abbreviations	
• List of publications	
• List of communications	
• Experience in foreign laboratories	
• Acknowledgments	
• Italian acknowledgments	
• Papers	

ABSTRACT

Today, food loss and waste are a major concern worldwide, since approximately one-third of all the food produced for human consumption is either lost or wasted. Several reasons have been identified for this phenomenon. Among these, food spoilage associated to microbial contamination represents the main factor affecting organoleptic product quality (aspect, texture, taste, and aroma). The emergence of antibiotic resistance (ABR) along the food chain is a major global public health issue, with several studies reporting the colonization and/or the infection of food animals and products by antibiotic-resistant strains. This phenomenon along with the increasing concerns about the safety of chemical preservatives, make the development of novel and natural food preservatives urgent. In this scenario, naturally occurring Host Defence Peptides (HDPs) have attracted increasing importance. HDPs are small molecules, widespread in all the living organisms endowed with several activities, such as antimicrobial, anti-biofilm, antifungal and immunomodulatory. The main aim of this PhD project has been the evaluation of the applicability of novel HDPs, identified in the human Apolipoprotein B, as novel biopreservatives for food industry applications. We demonstrated that ApoB derived peptides are endowed with significant antimicrobial and anti-biofilm activity towards two *Salmonella* strains, bacteria mainly responsible for food contamination. Moreover, peptides ability to act as antifungal agents has been investigated towards *Candida* and *Aspergillus* strains and very promising results have been obtained. In addition, biocompatibility and side effects of ApoB derived peptides have been investigated to assess their safety upon human consumption. Finally, novel coating solutions, based on chitosan functionalized with ApoB derived peptides, have been designed and it has been evaluated their ability to prevent bacterial attachment on different surfaces; indeed, obtained coating solutions have been found to be capable to prevent biofilm attachment and to decrease microbial load in chicken meat samples during storage at 4 °C.

The overall obtained results highlight the applicability of ApoB derived peptides as novel agents to be employed in food industry to prevent and control food spoilage.

RIASSUNTO

Negli ultimi anni, lo spreco di cibo rappresenta una delle principali preoccupazioni a livello mondiale. È stato stimato che circa un terzo del cibo destinato al consumo umano viene perso o sprecato; tra le cause responsabili di questo fenomeno, la contaminazione microbica è sicuramente quella che ha un maggiore impatto. Essa, infatti, oltre ad accelerare il processo di deterioramento del cibo, ne altera le proprietà organolettiche (aspetto, consistenza, gusto e aroma). Tra i principali contaminanti microbici, si annoverano i batteri e i funghi resistenti agli antibiotici convenzionali; diversi studi riportano che batteri resistenti, quali *Staphylococcus aureus* resistente alla meticillina (MRSA), *Campylobacter spp.* multi-resistenti e la famiglia delle *Enterobacteriaceae* dello spettro-beta-lattamico (ESBL), sono in grado di colonizzare o infettare gli animali e/o i prodotti alimentari lungo tutta la catena di produzione.

I batteri resistenti agli antibiotici possono raggiungere l'uomo in due modi principali: (i) indirettamente lungo la catena alimentare attraverso il consumo di alimenti o prodotti derivati contaminati, o (ii) per contatto diretto con animali colonizzati/infetti. Inoltre, ceppi batteri patogeni sono in grado di aderire alle superfici degli impianti di produzione e formare il cosiddetto *biofilm* batterico. Il *biofilm* è un agglomerato di cellule batteriche immerse in una matrice polimerica che funge da protezione per diversi fattori, incluse le terapie antibiotiche. È stato, infatti, stimato che batteri immersi nella matrice del *biofilm* sono mille volte più resistenti agli antibiotici rispetto alle singole cellule batteriche in forma planctonica.

Oltre ai batteri resistenti, i funghi rappresentano un'altra importante fonte di contaminazione in ogni fase della catena alimentare, data la loro capacità di crescere in diversi ambienti, anche particolarmente stringenti. Oltre al loro impatto negativo sulla qualità degli alimenti, alcuni generi di funghi come *Aspergillus*, *Penicillium*, *Alternaria* e *Fusarium* hanno la capacità di produrre metaboliti secondari che prendono il nome di micotossine e che possono avere effetti tossici su esseri umani e animali. I funghi, principalmente sotto forma di spore aeree (sia sessuali che asessuali), possono stabilirsi e crescere in diverse fasi della vita del prodotto, cioè durante la crescita sul campo, post-raccolta, durante le fasi di lavorazione, stoccaggio e manipolazione da parte del produttore, grossista, dettagliante e consumatore. Per questo motivo, è difficile mantenere un'adeguata sicurezza e qualità alimentare fino a quando i prodotti

non raggiungono il consumatore e poi per tutta la durata di conservazione proposta.

Oggi giorno sono state sviluppate diverse metodologie di conservazione degli alimenti, con l'obiettivo di soddisfare le esigenze dei consumatori in materia di sicurezza microbiologica, valori nutrizionali e proprietà organolettiche. Tra i principali metodi di sterilizzazione, il trattamento termico degli alimenti è ancora molto frequente. Si tratta di una procedura che richiede l'esposizione del cibo a temperature comprese tra 60 e 100 °C per alcuni secondi o minuti. Anche se molto efficiente, questo metodo prevede il trasferimento di un'elevata quantità di energia termica agli alimenti, alterandone le proprietà nutritive e sensoriali. Inoltre, i conservanti alimentari sintetici comunemente utilizzati, come nitrati, benzoati, solfiti, sorbati e formaldeide, sono noti sia per le reazioni allergiche che potrebbero scatenare sia per i loro effetti collaterali.

A causa della sempre più grande preoccupazione dei consumatori riguardo i rischi per la salute e, data la crescente domanda di cibi meno processati e che non contengano sostanze chimiche, si stanno facendo strada i cosiddetti conservati naturali. I più comuni tra i conservanti naturali sono gli agenti chimici ricavati da piante, animali e microrganismi, di solito coinvolti nel sistema di difesa dell'ospite. In particolare, la bio-conservazione alimentare si sta spingendo verso lo sviluppo di nuovi composti antimicrobici naturali di varia origine, tra cui sistemi di derivazione animale (lisozima, lattoferrina e magainine), prodotti di origine vegetale (fitoalessine, erbe aromatiche e spezie) e metaboliti microbici (batteriocine, perossido di idrogeno e acidi organici).

In questo scenario, i peptidi di difesa dell'ospite (Host Defence Peptides, HDPs), chiamati dapprima peptidi antimicrobici (Anti-Microbial Peptides, AMPs), hanno attirato notevole attenzione, dal momento che non sono dannosi per la salute umana e hanno la capacità di preservare il cibo senza alterarne la qualità. Diversi studi hanno dimostrato che essi sono dotati di attività antimicrobica ad ampio spettro, essendo efficaci su batteri, virus, funghi e protozoi. Gli HDPs naturali hanno dimensioni che vanno da 12 a 50 amminoacidi, sono per lo più cationici a causa di un alto contenuto di residui di lisina e arginina e contengono oltre il 50% di amminoacidi idrofobici. Queste proprietà sono alla base della loro capacità di interagire selettivamente con le membrane batteriche e, in alcuni casi, di penetrare le membrane cellulari.

Negli ultimi anni, il gruppo di ricerca presso cui è stato svolto il presente progetto di Dottorato, ha identificato una sequenza dalla putativa azione antimicrobica nell'apolipoproteina B umana. Di tale sequenza sono state prodotte tre diverse varianti, due più lunghe, qui denominate r(P)ApoB^L^{Pro} e r(P)ApoB^L^{Ala}, che differiscono per la sostituzione di un residuo di prolina con un'alanina in posizione sette, e una versione più breve di tale sequenza, qui denominata r(P)ApoB^S^{Pro}. Tali peptidi sono stati prodotti efficientemente per via ricombinante in cellule di *Escherichia coli*, sotto forma di proteina chimerica. I peptidi derivanti dall'apolipoproteina B umana sono stati poi oggetto di caratterizzazione strutturale e funzionale. Essi sono risultati dotati di attività antimicrobica ad ampio spettro, in quanto in grado di inibire la crescita di batteri Gram-positivi e Gram-negativi; si sono, inoltre, rivelati degli efficienti agenti anti-biofilm e in grado di modulare la risposta immunitaria. Inoltre, i peptidi non hanno mostrato né effetti tossici su linee cellulari eucariotiche né effetti emolitici quando analizzati su globuli rossi, ciò che apre interessanti prospettive alla loro applicabilità.

Alla luce dei promettenti risultati pregressi, l'obiettivo principale del presente progetto di Dottorato è stato la valutazione dell'applicabilità e dell'efficacia di r(P)ApoB^L^{Pro}, r(P)ApoB^S^{Pro} e r(P)ApoB^L^{Ala} quali nuovi conservanti alimentari, dal momento che alcuni peptidi sono stati già approvati e commercializzati dalla *Food and Drug Administration (FDA)* come nuovi conservanti alimentari. Il più comune ed anche il primo ad essere stato commercializzato è la nisina, un peptide antimicrobico isolato da *Lactococcus lactis* e dotato di una significativa attività antibatterica verso batteri Gram-positivi. Inoltre, esso è risultato molto stabile ad alte temperature e innocuo per cellule eucariotiche in coltura. Un altro esempio molto noto è rappresentato dalla lattoferrina, aggiunta alla formula del latte per neonati.

Gli obiettivi principali del presente lavoro di tesi possono essere schematizzati in quattro punti fondamentali:

1) Caratterizzazione delle proprietà antimicrobiche e anti-*biofilm* dei peptidi derivanti da ApoB utilizzando ceppi di *Salmonella*; in particolare, sono stati selezionati i ceppi *Salmonella typhimurium* ATCC® 14028 e *Salmonella enteritidis* RIVM 706.

2) Caratterizzazione dell'attività antifungina di r(P)ApoB^L^{Pro}, r(P)ApoB^S^{Pro} e r(P)ApoB^L^{Ala}; a tal proposito, è stato selezionato il

ceppo *Candida albicans* ATCC 10231 come modello di lievito e il ceppo *Aspergillus niger* N402 come modello di fungo filamentoso;

3) Valutazione dei possibili effetti collaterali dei peptidi in esame; a tal proposito, è stata analizzata la loro tossicità, la digeribilità e il potenziale effetto pro-infiammatorio;

4) Funzionalizzazione di superfici selezionate con il peptide r(P)ApoB_L^{Pro}; a tal proposito, è stato selezionato il chitosano con l'obiettivo di ottenere sistemi efficienti per il rivestimento di superfici di interesse industriale o per la conservazione di carne di pollo.

Gli esperimenti condotti per valutare l'attività antimicrobica dei peptidi hanno portato a dimostrare che i peptidi r(P)ApoB_L^{Pro}, r(P)ApoB_S^{Pro} e r(P)ApoB_L^{Ala} sono in grado di inibire la crescita di entrambi i ceppi di *Salmonella* in esame. Inoltre, esperimenti di microscopia elettronica a scansione hanno evidenziato la capacità dei peptidi derivanti dall'apolipoproteina B di interagire con la membrana batterica alterando così la morfologia delle cellule. Inoltre, saggi volti alla valutazione degli effetti di tali peptidi sul *biofilm* formato da *Salmonella typhimurium* ATCC® 14028 e *Salmonella enteritidis* RIVM 706 hanno rivelato la capacità dei peptidi r(P)ApoB_L^{Pro}, r(P)ApoB_S^{Pro} e r(P)ApoB_L^{Ala} di destrutturare la matrice del *biofilm* batterico senza però alterare la vitalità cellulare. La valutazione dell'attività antifungina dei peptidi derivanti dall'apolipoproteina B umana è stata svolta durante il periodo di ricerca all'estero (*visiting period* di 6 mesi) presso il gruppo di ricerca diretto dal Professore Henk P. Haagsman dell'Università di Utrecht (*Faculty of Veterinary Medicine, Utrecht University, The Netherlands*). I risultati ottenuti hanno indicato che i peptidi in esame sono capaci di inibire completamente la crescita di *Candida albicans* ATCC 10231 in tempi di incubazioni molto brevi. Inoltre, saggi di permeabilità di membrana hanno mostrato che i peptidi r(P)ApoB_L^{Pro}, r(P)ApoB_S^{Pro} e r(P)ApoB_L^{Ala} interagiscono con le membrane fungine dopo un breve periodo di incubazione, causandone la destrutturazione. Questi risultati sono stati confermati da esperimenti in *real time*, effettuati utilizzando un microscopio confocale a scansione laser. Tali esperimenti hanno evidenziato la capacità del peptide fluorescente r(C)ApoB_L^{Pro} di interagire quasi istantaneamente con la superficie delle cellule di *Candida albicans* ATCC 10231, ciò che determina l'immediato

influsso della sonda ioduro di propidio. Risultati interessanti sono stati ottenuti anche nel caso del fungo *Aspergillus niger* N402, dal momento che i peptidi in esame si sono rivelati in grado di inibire l'attività metabolica delle spore di tale fungo.

In letteratura è noto che i funghi filamentosi sono caratterizzati da diverse fasi di crescita; in genere, essi appaiono sotto forma di spore dormienti. Quando, però, le condizioni ambientali sono favorevoli, le spore possono incamerare acqua e nutrienti rigonfiandosi. Ciò porta alla formazione delle cosiddette *swollen spores*. In questa fase si registrano importanti cambiamenti anche a livello della parete e della membrana cellulare. Da questo momento in poi inizia il processo di germinazione delle ife fino alla formazione dei miceli ramificati. Nel corso del presente progetto di tesi, si è deciso di valutare l'effetto dei peptidi in esame sull'attività metabolica dei funghi nelle diverse fasi di crescita. Sulla base dei risultati ottenuti, i peptidi derivanti dall'apolipoproteina B sono risultati in grado di inibire in maniera significativa l'attività metabolica delle spore rigonfiate e delle ife, mentre gli effetti dei peptidi sui miceli sono risultati meno pronunciati. Anche in questo caso sono stati condotti esperimenti in *real time*, che hanno mostrato l'accumulo del peptide fluorescente r(C)ApoB_L^{Pro} nelle spore rigonfiate e nelle ife in germinazione.

In seguito, si è proceduto alla valutazione di eventuali effetti tossici dei peptidi in esame. In particolare, sono stati effettuati saggi di vitalità cellulare che non hanno evidenziato alcun effetto tossico dei peptidi nei confronti di cellule eucariotiche di stomaco SNU-1 (ATCC® CRL-5971™) e di intestino HT-29 (ATCC® HTB-38™). Sono stati, inoltre, condotti esperimenti di digestione in fluidi che simulassero l'ambiente gastrico ed intestinale; è stato dimostrato che i peptidi sono altamente suscettibili alla degradazione da parte degli enzimi selezionati, ciò che suggerisce una loro elevata digeribilità. Inoltre, i peptidi r(P)ApoB_L^{Pro}, r(P)ApoB_S^{Pro} e r(P)ApoB_L^{Ala} sono risultati non indurre alcuna risposta infiammatoria in monociti umani THP-1, ciò che porterebbe ad escludere effetti collaterali legati ad un'eventuale risposta immunitaria.

I promettenti risultati ottenuti hanno consentito, inoltre, di progettare esperimenti mirati a valutare l'applicabilità dei peptidi in campo alimentare. A tale scopo, si è proceduto con la funzionalizzazione di una matrice edibile di chitosano, noto agente antimicrobico, con il peptide r(P)ApoB_L^{Pro}. Le matrici ottenute sono state poi utilizzate per rivestire superfici di interesse industriale, quali polistirene e acciaio

inossidabile, e sono risultate possedere una significativa azione antimicrobica, con effetti sinergici tra chitosano e r(P)ApoBL^{Pro}. La matrice di chitosano funzionalizzata con il peptide è stata anche utilizzata per rivestire campioni di pollo, al fine di prevenire contaminazioni batteriche durante la conservazione. Nel caso del chitosano funzionalizzato con il peptide, la carica batterica dei campioni di pollo è risultata significativamente inferiore di quella determinata nel caso dei campioni di controllo durante tutto il periodo di conservazione (5 giorni).

Nel complesso, i dati ottenuti supportano in maniera robusta la possibilità di impiego dei peptidi in esame quali nuovi agenti antibatterici o bio-conservanti per l'industria alimentare.

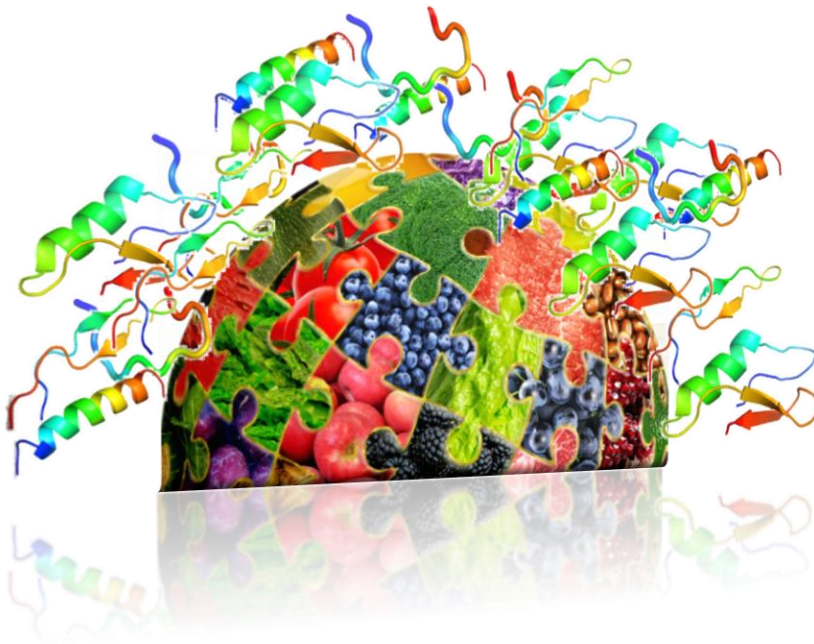
CHAPTER 1

General Introduction

Eliana Dell'Olmo

Department of Chemical Sciences, PhD in Biotechnology

University of Naples "Federico II"



General Introduction

1.1 Antimicrobial resistance

The modern era of antibiotics started with penicillin discovery by Sir Alexander Fleming in 1928 (**Sengupta, Chattopadhyay, and Grossart 2013; Piddock 2012**). Since then, antibiotics have completely modified medical approach in the treatment of infectious diseases (**Adedeji 2016**). For more than one decade, antibiotics have been described as “miraculous” pharmaceuticals. Immediately after, in first 1950’s, penicillin-resistant bacteria have been isolated. This was a consequence of Antimicrobial Resistance (AR) phenomenon that threatened the advantages obtained with antibiotic discovery (**Spellberg and Gilbert 2014**). To overcome this situation, novel β -lactams have been developed and introduced in the market (**Sengupta, Chattopadhyay and Grossart 2013; Spellberg and Gilbert 2014**). However, during the 1960’s, methicillin-resistant *Staphylococcus aureus* strains have been isolated in the United states and the United kingdom (**ANTIBIOTIC RESISTANCE THREATS in the United States 2013**). Unfortunately, resistance phenomenon has been described for almost all the antibiotics developed so far.

Nowadays, emergence of resistance to multiple antimicrobial agents in pathogenic bacteria has become a serious public health threat with great social and economic impacts. The main consequence of this phenomenon is the absence of effective strategies to counteract the growth of these superbug resistant bacteria. The term “MultiDrug-Resistant Organisms (MDROs)” has been introduced to describe bacteria resistant to more than one antimicrobial agent (**Alastruey-Izquierdo et al. 2013; Roberts et al. 2009; Cosgrove et al. 2003; Ibrahim et al. 2000**). Epidemic antibiotic resistance has been identified in numerous pathogens in several contexts, including a global pandemic infection of methicillin-resistant *Staphylococcus aureus* (MRSA) (**Moran et al. 2006**), vancomycin-resistant *enterococci* (VRE), and a growing number of additional pathogens that are developing resistance to many common antibiotics (**Golkar and Gene 2014**). Resistance development is generally the result of genetic mutations or is due to the transfer of resistance determinants from one microorganism to another (**Martínez, Coque, and Baquero 2015; Perry, Westman, and Wright 2014; D’Costa et al. 2006; Sommer, Dantas, and Church 2009**). Recent advances in

genomics and metagenomics have revealed that many natural ecosystems contain many genes whose functions can be co-opted to confer resistance to antimicrobials (**Martinez et al. 2015; Perry 2014; D'Costa et al. 2006; Sommer et al. 2009**). Bacterial communities can exhibit tolerance to environmental factors even if single cells do not possess this ability. It has been hypothesized that this tolerance might be crucial for the development of resistance phenotype. Cell-cell interactions usually lead to the formation of spatially complex matrices composed by polysaccharides and extracellular DNA, embedding bacterial cells that consequently form a biofilm community (**Flemming and Wingender 2010**). It has been reported that microbes in a biofilm community gain additional antibiotic resistance, that can be up to 1,000 times higher than that gained by the corresponding planktonic cells (**Ceri et al. 1999**). Biofilm-specific resistance mechanisms, which are distinct from the well-characterized resistance mechanisms developed at the level of single cells, may act in an orchestrated manner to confer high levels of antibiotic resistance in biofilm communities (**Penesyan, Gillings, and Paulsen 2015**). Components of the biofilm matrix form a mechanical shield that acts to inhibit the effects of antibiotics (Figure 1).

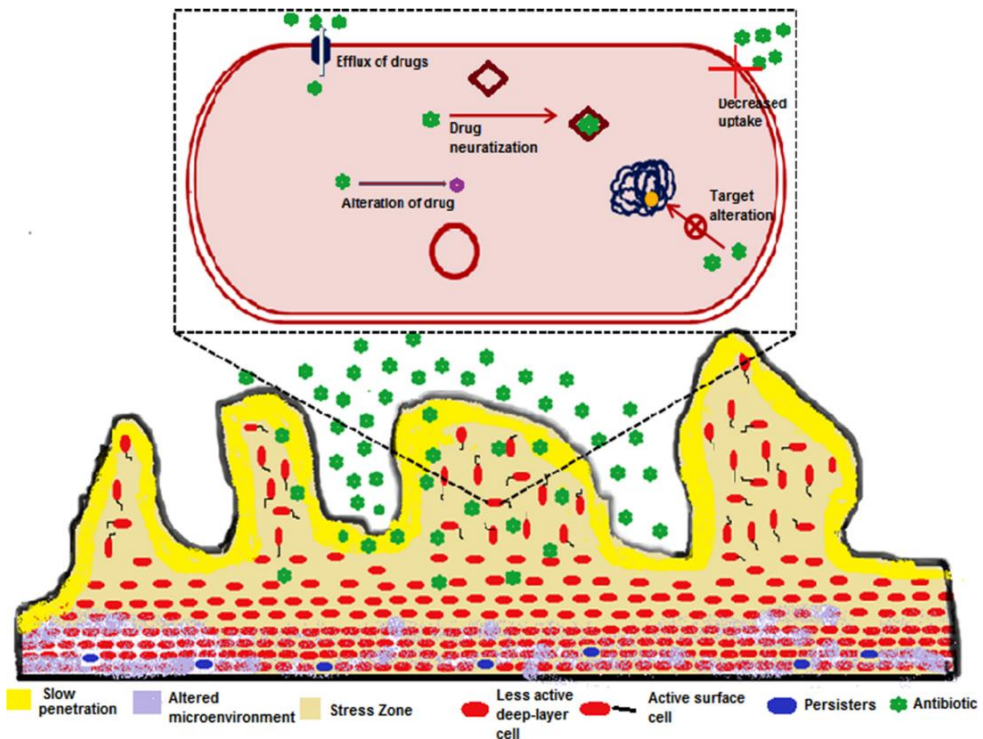


Figure 1. Schematic representation of differences between planktonic cell resistance and biofilm matrix resistance (**Sharma, Misba, and Khan 2019**).

1.2 Antifungal resistance

The antibiotic resistance is a well-established problem worldwide, and the increasing emergence of antifungal resistance also poses a serious threat to human health. The effects of fungal infections in humans are dramatic. Indeed, it has been reported that mortality rate associated to these infections is higher than those due to malaria or breast cancer (**Brown et al. 2012**). There are four main classes of antifungal agents employed in the treatment of infections in humans: (i) polyenes molecules that act by targeting ergosterol, which is one of the main constituents of fungal cell wall; (ii) pyrimidine molecules that are able to affect DNA synthesis; (iii) echinocandins, the newest antifungal compounds, that are able to inhibit (1-3)- β -D-glucan synthase and disrupts cell wall biosynthesis; and, finally, (iv) azoles that are the most widely used antifungal agents and exploit their activity by inhibiting lanosterol 14- α -demethylase (**Fisher et al. 2018a**). It has been reported that the

restricted panel of antifungals and the long prophylactic time are the main causes of resistance development (**Atashgahi et al. 2018**). On the other hand, fungi are endowed with a very high genome plasticity that allows them to adapt their metabolism to overcome antifungal treatments (**Healey et al. 2016**). Four main resistance strategies have been identified in fungi in different fields. Mutations resulting in conformational changes of drug target site are the most common form of resistance in pathogenic fungi (**Lucas, Hawkins, and Fraaije 2015**). Changes of promoter region are one of the main strategies adopted by fungi; indeed, they result in upregulation of fungicide target expression, a mechanism widely described for clinical and plant-pathogenic fungi (**Hamamoto et al. 2000**). A third resistance mechanism involves reduction of intracellular drug accumulation by upregulation of efflux pumps, whereas a fourth resistance mechanism implies the activation of stress response pathways by heat shock protein Hsp90. This last mechanism can unleash cryptic diversity, thus potentiating the evolution of resistance to azoles, echinocandins, and polyenes in *Candida* and *Aspergillus* species (**Robbins, Caplan, and Cowen 2017; Hawkins et al. 2014**).

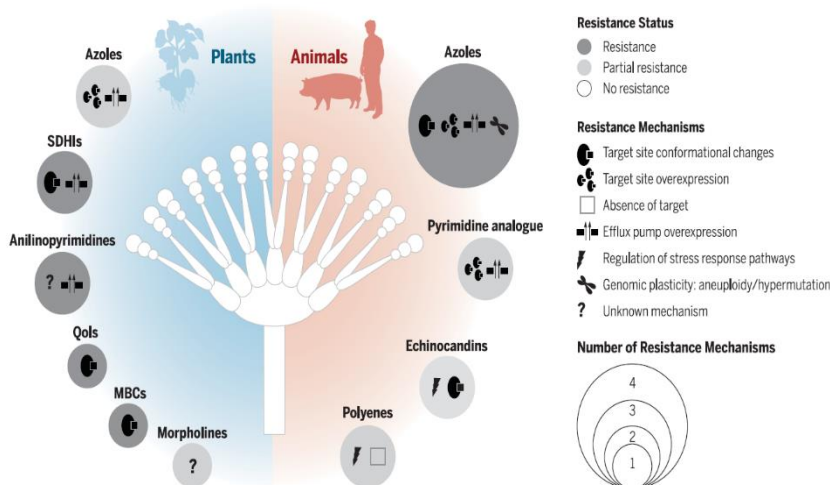


Figure 2. Schematic representation of different antifungal agents and main mechanisms of resistance development (**Fisher et al. 2018b**).

1.3 Resistance in food chain

Bacterial resistance to conventional antibiotics has increased drastically during the last decades, making difficult the effective treatment of infections caused by antibiotic-resistant bacteria (ABR) **(Tanwar et al. 2014; Li. and Webster 2018)**. While resistance phenotypes observed in human medicine are generally attributed to an inappropriate use of antibiotics in humans, there is increasing evidence that the use of antibiotics in farm animals is responsible for the development of resistant food-borne pathogens that may be transmitted to humans as food contaminants **(Marshall and Levy 2011)**. The emergence of ABR along the food chain is thus a major global public health issue, with several studies reporting the colonization and/or the infection of food animals and products by antibiotic-resistant strains, such as methicillin-resistant *Staphylococcus aureus* (MRSA) **(Price et al. 2012)**, antibiotic-resistant *Campylobacter* spp. **(Ewnetu and Mi het 2010)**, and extended spectrum beta-lactamase (ESBL) producing *Enterobacteriaceae* (viz. *Salmonella* spp., *Shigella* spp., *Escherichia coli*, *Klebsiella* spp., etc.) **(Fischer et al. 2012; Al Bayssari et al. 2015)**.

Antibiotic-resistant bacteria may reach humans (i) indirectly along the food chain through consumption of contaminated food or food derived products, and (ii) by a direct contact with colonized/infected animals or biological substances, such as blood, urine, feces, saliva, and semen among others **(Chang et al. 2015)** (Figure 3). Bacteria growth on food surfaces is the main cause of food spoilage. Because of this, it is difficult to maintain proper food safety and quality until the products reach the consumer and then throughout proposed shelf-life period **(The Open University 2018)**.

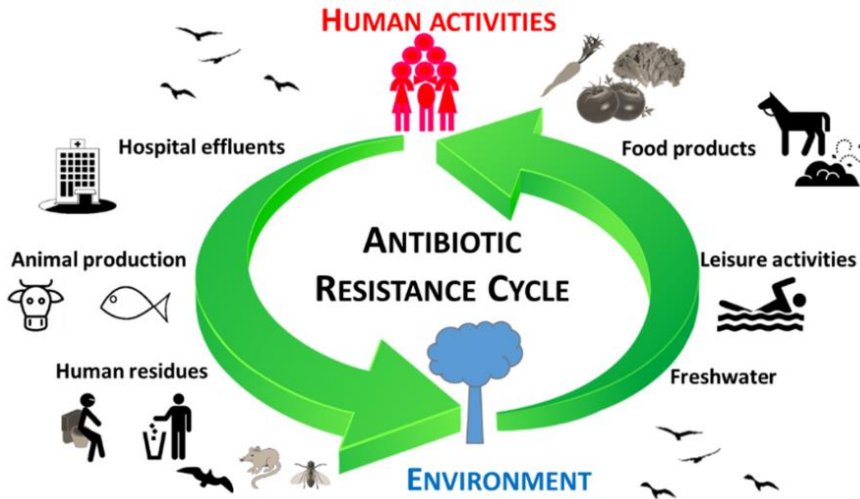


Figure 3. Schematic representation of antibiotic resistance spread along the food chain production (**Dolan et al. 2016**).

Moreover, most of food-borne pathogens are able to attach to surfaces, grow and form biofilm. It is well known that bacteria growing in biofilm matrix are ten thousand times more resistant to conventional antibiotics than their planktonic counterpart (**Gebreyohannes et al. 2019**). Furthermore, bacteria attachment can occur on very different surfaces, such as food, plastic, and stainless steel, that are components of production infrastructure (**Galié et al. 2018**) (Figure 4). Due to their features, biofilms have a negative impact on human health and economy worldwide (**Vallet-Regí et al. 2019**).

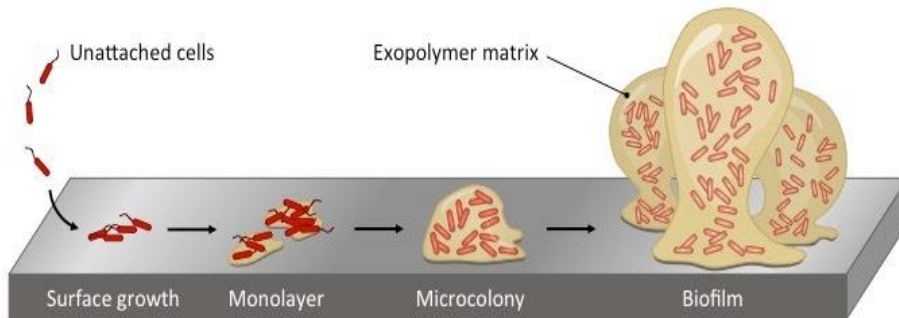


Figure 4. Schematic representation of the main stages of biofilm development: biofilm attachment, monolayer duplication, microcolony formation and mature biofilm (**Unosson 2015**).

Several studies report that *Salmonella* spp. strains are able to form biofilm on surfaces that are commonly found in food processing environments, such as metal, plastic and rubber, due to fimbriae and lipopolysaccharides (**Iñiguez-Moreno et al. 2018**). Moreover, *Salmonella* strains are also able to produce cellulose, with the consequent immersion of bacterial cells in a hydrophobic network (**Solomon et al. 2005**).

The fast increase and development of antibiotic resistant strains and the concerns of consumers about pre-treatment and chemical agents' addition to natural food make the development of novel molecules endowed with antibacterial and anti-biofilm properties urgent.

Among spoilage microorganisms, fungi represent one of the major issues at any stage of the food chain because of their ability to grow in different and even harsh environments (**Pitt and Hocking 2009a**). Beyond their negative impact on food quality, some fungal genera, such as *Aspergillus*, *Penicillium*, *Alternaria*, and *Fusarium*, have the ability to produce secondary metabolites that can have toxic effects on humans and animals, and are, therefore, named mycotoxins (**Gruber-Dorninger et al. 2016**). In this context, it is crucial to reduce food losses by controlling fungal contamination at all stages of food process chains. Three main stages are characterized by fungal contaminations: (i) the field, where water, soil, and air are natural fungal niches; (ii) raw materials, such as post-harvest crops, meats, and milk where fungal occurrence is related to food management during harvest or collecting, transportation, storage, and packaging (**Pitt and Hocking 2009a**), and (iii) food processing

process while manufacturing dairy, bakery, dry-ripened, and drink products. Generally, chemical preservatives including benzoate, propionate, sorbate, nitrate, nitrite, and sulphites, are used to avoid fungal spoilage (**Silva and Lidon 2016**). Putative adverse effects of certain fungicides and preservatives on environment and human health have led to the discovery of more natural methods, including bio-preservation processes.

1.4 Bio-preservation and novel biopreservatives

Nowadays, the increasing demand of consumers for natural food samples along with the increasing concerns about human health open the way to the development of novel strategies for food preservation. In this scenario, bio-preservation represents a novel food preservation technique in which antimicrobial activity of naturally occurring organisms and their metabolites are exploited (**Singh 2018**). Natural preservatives are defined as chemical agents derived from plants, animals, and microorganisms. As the demand for bio-preservation in food industry has increased, new natural antimicrobial compounds of various origin are being developed, including animal-derived systems (lysozyme, lactoferrin, and magainins), plant-derived products (phytoalexins, herbs, and spices), and microbial metabolites (bacteriocins, hydrogen peroxide, and organic acids) (**Lavermicocca et al. 2003**). An example of bio-preservation strategy is represented by Lactic Acid Bacteria (LAB), that generally are Gram-negative bacteria, such as *Lactococcus*, *Streptococcus*, *Lactobacillus*, *Pediococcus*, *Leuconostoc*, *Enterococcus*, *Carnobacterium*, *Aerococcus*, *Oenococcus*, *Tetragenococcus*, *Vagococcus*, and *Weisella* (**Singh 2018**). LAB usually present common features, such as low content of G+C in their DNA (<55%), which provides more thermostability to the organism, resistance to bacteriophages, resistance to proteases activity, ability to produce polysaccharides, high resistance to freezing and lyophilization, ability to adhere and colonize digestive mucosa, and ability to produce antimicrobial substances. They are classified as GRAS (Generally Recognize As Safe) organisms (**Singh 2018**). *Lactic acid bacteria* are mostly used in fermented, food such as dairy products, raw meat and vegetables, and they play an important role in the protection of food from contamination and spoilage. Among natural preservatives, also bacteriocins play a key role. Bacteriocins are ribosomally synthesized small polypeptide

molecules, that exert antagonistic activity against closely related and unrelated groups of bacteria (García-Bayona et al. 2017).

Characteristics	Archaea	Gram negative bacteria	Gram positive bacteria
Source organism and antibacterial activity spectrum	Archaeosins are the bacteriocins produced by archaea. They are known to have wider spectrum of activity across species and domains present in the extreme environments. (Atanasova, Pietiik, & Oksanen, 2013)	Gram negative bacteria produce bacteriocins which have narrow antibacterial activity spectrum.	Gram positive bacteria produces bacteriocins which have wide antibacterial activity spectrum against some food spoilage organism and are nontoxic to the non-target eukaryotic cells and are hence regarded as safe for food applications.
Identified bacteriocins	Halocin S8 from halobacteria, a short hydrophobic peptide with 36 amino acids is the first discovered archaeosin.	Colicins from <i>E. coli</i> , Klebicins of <i>Klebsiella pneumoniae</i> , marcescins of <i>Serratia marcescens</i> , alveicins of <i>Hafnia alvei</i> , cloacins of <i>Enterobacter cloacae</i> and pyocins of <i>Pseudomonads</i> and the representatives of gram-negative bacterial group.	Most of the bacteriocins are produced by Lactic acid bacteria which are rendered "GRAS" status. Nisin A by <i>Lactococcus lactis</i> , Cytolysin by <i>Enterococcus faecalis</i> , Pediocin by <i>Pediococcus acidilactici</i> , Lactococcin from <i>Lactococcus cremoris</i> and a vast repertoire of bacteriocins are produced by this group of bacteria.
Structure and mode of action	They are generally divided into two groups (i) Protein halocins (30–40 kDa) like H1 and H4 (Meseguer & Rodriguez Valera, 1985; Shand & Leyva, 2007) (ii) Microhalocins (smaller than 10 kDa) like H6/H7, R1, C8, S8 and U1 (Shand & Leyva, 2007) The halocin H6/H7 are shown to inhibit the growth by disrupting Na ⁺ /H ⁺ antiporter causing cell lysis. These archaeosins are produced in stationary phase. They are encoded in megaplasmids. (Meseguer & Rodriguez-Valera, 1985) The halocin H6/H7 are shown to inhibit the growth by disrupting Na ⁺ /H ⁺ antiporter causing cell lysis. These archaeosins are produced in stationary phase. They are encoded in megaplasmids. (Meseguer & Rodriguez-Valera, 1985) Protein halocins are generally more sensitive to environmental stress. Microhalocins have the ability to withstand low salt concentrations, heating, long-term storage. (Meseguer & Rodriguez-Valera, 1985; Pašić, Velikonja, & Ulinh, 2008; Shand & Leyva, 2007)	The bacteriocins have relatively larger structure. They are divided in to three types: (i) Microcins which are less than 20 kDa in size (ii) Colicin-like bacteriocins (CLBs) 20 to 90 kDa in size (Cascales et al. 2007) (iii) Tailocins which are high molecular weight bacteriocins with multisubunits resembling the tail like structure of bacteriophages. (Ghequire et al. 2014) The CLBs are composed of a receptor binding domain, a translocation domain and a cytotoxic domain. Thus, the bacteriocins are bound and imported in to cell membrane and exercising the cytotoxic activity by nucleases/pore formation. (Cascales et al. 2007)	They greatly differ in their structure and their mode of action. (See section 2)
Stability and other desirable characteristics		They are generally heat labile except for Microcin V produced by <i>E. coli</i>	They are generally heat stable and are functional at a wide range of pH.

Table 1. Main features of bacteriocins depending on different producer microorganisms (Johnson et al. 2018).

Among bacteriocins, those produced by Lactic acid bacteria (LAB) have attracted great interest, especially for their employment in food industry (Cotter et al. 2005). The effectivity of LAB bacteriocins is mainly due to electrostatic interactions between them and negatively charged phosphate groups on target cell membranes, leading to initial binding, pores forming and death of the cells, leading to autolysin activation to digest cellular wall (García-Bayona et al. 2017; Singh 2018).

Well-established bacteriocins ability to kill foodborne pathogenic bacteria and their safety for human health led to the discovery of a huge repertoire of bacteriocins and preservation strategies based on

bacteriocins incorporation into food matrixes (**Silva et al. 2018**). The first bacteriocin accepted by FDA as a safe bio-preservative agent is nisin, which is very effective to inhibit Gram-positive bacteria growth. Otherwise, nisin activity strongly depends on pH conditions in food matrix, since its activity increases with pH values decrease (**da Silva Malheiros et al. 2010**). Thus, from nisin discovery in 50' decade until nowadays, further bacteriocins have been discovered and validated as novel promising food additives. Bacteriocins commonly used in foods like dairy, meat and vegetable products, are lantibiotics nisin and lactacin, pediocin-like bacteriocins and enterocin AS-48. Bacteriocins can be added to food samples by *in situ* production by starter or protective cultures, as an ingredient of fermentation of a bacteriocin genic strain, and additives into a semi- or purified preparation (**Singh 2018**). This last bio-preservation procedure consists in the use of bacteriophages, that are defined as viruses that specifically infect and multiply in bacterial cells, and are usually harmless to humans, animals, and plants (**Bruessow and Kutter 2005**). Based on tails structure, bacteriophages can be classified in three families: (i) *Myoviridae* with contractile tail, (ii) *Siphoviridae* that contain long non contractile tail, and (iii) *Podoviridae* family characterized by an extremely short tail. Bacteriophages can be successfully used to reduce pathogen carriage in livestock farming and after slaughter or milking (**Singh 2018**). Bacteriophages have been found to be endowed with significant antimicrobial action towards *Salmonella* strains, *Campylobacter* and *E. coli*; furthermore, they are able to eradicate *Staphylococcus aureus* biofilm (**Fiorentin et al. 2005; Atterbury 2009; Azeredo and Sutherland 2008 and Mann 2008**). Some of the commercially available phage preparations have got approval from FDA. Among these, Listex and LMP 102 are used for ready-to-eat meat, and anti-*E. coli* and anti-*Salmonella* phage-based products are used to treat live animals prior to slaughtering (**Singh 2018**).

Many studies have proved the ability of essential oils, plant extracts or natural molecules from different organisms, such as animals, plants or insects, to inhibit food microbial contamination. As an example, some polysaccharides isolated from animals are endowed with antimicrobial activity. Among these, chitosan is isolated from the exoskeleton of crustaceans and arthropods; it is a biopolymer consisting of N-acetylglucosamine and glucosamine molecules

linked by β -1-4 glycosidic links, **(Fisoredman and Juneja 2010)**. This biopolymer is endowed with antifungal **(Ben-Shalom et al. 2003)** and antimicrobial properties towards many common food-borne pathogens. Moreover, chitosan is able to form biodegradable membranes that have been tested for their applicability in food packaging **(Sundaram et al. 2016)**. Many marine algae derivatives are promising novel antimicrobial agents with multiple applicability in pharmaceutical and food industry **(Shannon and Abu-Ghannam 2016)**. Indeed, algae are able to produce different molecules, such as phlorotannins, fatty acids, polysaccharides, peptides, and terpenes endowed with antimicrobial properties **(Shannon and Abu-Ghannam 2016)**. Moreover, some studies on different seaweed extracts highlighted their ability to counteract contaminations due to *Staphylococcus spp.*, *Salmonella spp.*, *Enterococcus faecalis* and *Pseudomonas aeruginosa* **(Shannon and Abu-Ghannam 2016)**. Moreover, plant polyphenols are promising molecules in the field of food preservation because of their antimicrobial and antioxidant properties. Edible and herbal plants/spices, such as oregano, cinnamon, clove, citrus, garlic, coriander, parsley, rosemary, lemongrass, sage and vanillin, have been employed alone or combined with other preservation techniques **(Bor et al. 2016)**. For instance, it has been reported that many plant extracts are endowed with antibacterial activity towards *Salmonella* and other *enterobacteriaceae* **(Nanasombat and Lohasupthawee 2005)**.

1.5 Host Defense Peptides (HDPs)

Naturally occurring the Host Defense Peptides (HDPs), first called AntiMicrobial Peptides (AMPs), have attracted considerable attention because of their wide range of properties. They represent a group of evolutionarily conserved molecules of the innate immune system, present in all complex living organisms. HDPs have been found to be endowed with a broad-spectrum antimicrobial activity, since they have been found to be effective on bacteria, viruses, fungi, and protozoa **(Zasloff 2002; Harris et al. 2013)**. Natural HDPs have a size ranging from 12 to 50 amino acids, are mostly cationic owing to the presence of a high content in lysine and arginine residues, and contain over 50% hydrophobic amino acids **(Zasloff 2002; Hancock and Le her 1998)**. HDPs are classified into four major classes based on their structures: β -sheet (for example,

human α and β defensins), α -helical (for example, LL-37, magainins and mellitin), loop peptides with one disulfide bridge (for example, bactenecin), and peptides enriched in specific amino acid, such as proline, tryptophan, histidine or glycine, without a well-defined structure (for example, indolicidin) (Okumura 2011) (Figure 5).

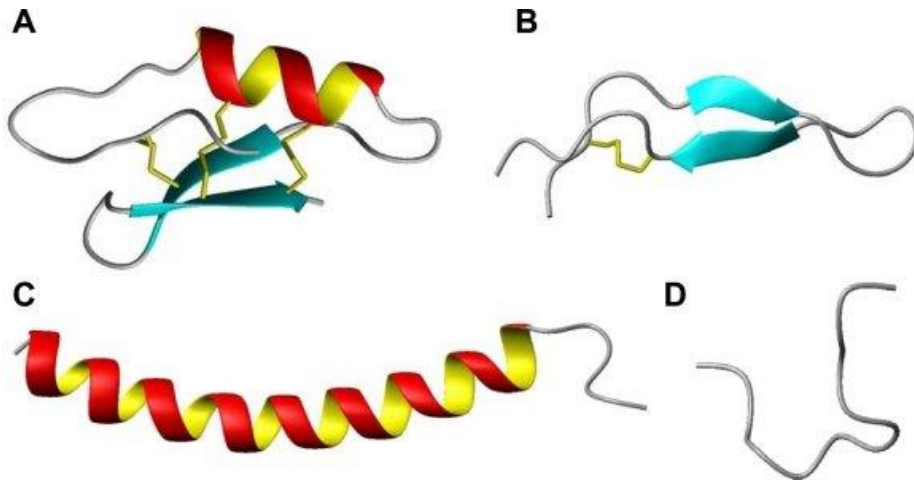


Figure 5. Schematic representation of different HDPs conformations. A) mixed or loop structure, B) β -sheet structure, C) α -helix structure and D) extended peptide structure (Jenssen 2009).

These properties are at the basis of HDPs ability to interact with bacterial membranes, and, in some cases, to penetrate cell membranes (Hancock and Sahl 2006; Zasloff 2009; Kumar, Kizhakkedathu and Straus 2018). In model systems, HDPs associate preferentially with negatively charged membranes of bacteria-like composition, but many peptides are also able to translocate into host cells. Several models have been proposed to explain HDPs interaction with bacterial membrane, such as *carpet model*, *barrel-stave model*, the *toroidal-pore model*, and the *detergent-type mechanism* (Hale and Hancock 2007) (Figure 6).

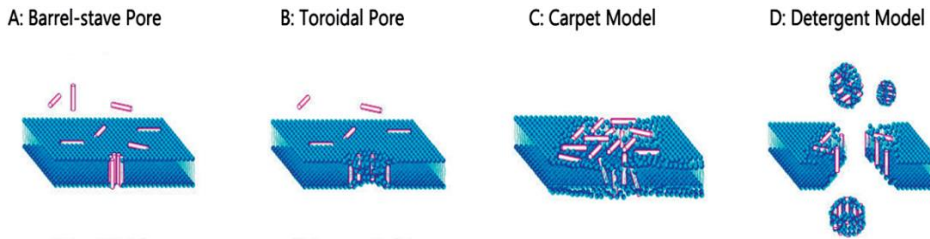


Figure 6. Schematic representation of HDPs mechanism of action (Zhang, Zhao, and Zheng 2014).

However, although the mechanism of action of HDPs direct antimicrobial activity against bacteria mainly involves their interaction with bacterial membrane, multiple additional targets have been identified, such as cell wall peptidoglycans, cytosolic RNA, proteins, or cytosolic enzymes/chaperones (Hale and Hancock 2007); (Fjell et al. 2012). Given to this broad range of targets, induction of resistance mechanisms in bacteria by treatment with HDP is improbable (Hilchie, Wuerth, and Hancock 2013). Moreover, it is becoming increasingly evident that these peptides are endowed with a wide range of biological activities, such as multispecies anti-biofilm properties, modulation of innate immune response, anticancer, analgesic, antioxidant and anti-inflammatory activities (Zasloff 2002; de la Fuente-Núñez et al. 2014; Boes et al. 2011).

1.6 Host defense peptides in food preservation

Many studies proved that HDPs are able to counteract microbial contamination and food spoilage. Indeed, they are active towards food-borne pathogens directly as antimicrobials or indirectly by exploiting different activities, such as anti-biofilm and immunomodulation. Besides their interesting mechanism of action and broad- spectrum activity, researchers have showed that HDPs are able to preserve food without altering qualities and the organoleptic properties. Pleurocidins are cationic mucus derived HDPs, isolated from the Atlantic flounders (Pundir et al. 2014). They have been found to be endowed with significant antimicrobial activity towards main foodborne pathogens, such as *Vibrio parahaemolyticus*, *L. monocytogenes*, *E. coli* O157:H7, *Saccharomyces cerevisiae*, and *Penicillium expansum* (Burrowes et al. 2006). Defensins from vertebrates, produced by mammalian phagocytes and epithelial cells of chickens, have been confirmed to

possess antimicrobial activity against bacteria, fungi, and viruses. Gallinacin-6, a defensin produced in chicken digestive tract, showed antimicrobial activity towards many foodborne pathogens, such as *E. coli*, *Salmonella*, *Staphylococcus aureus*, *Saccharomyces cerevisiae* and *Candida albicans* (**Van Dijk et al. 2007**). Milk is one of the main sources of antimicrobial peptides. Indeed, molecules like Casocidin, casein A and casein B, and lactoferrin are able to inhibit the growth of foodborne pathogens (**Khan et al. 2018**). Lactoferrin is present in different meat products, where it exploits its antimicrobial activity towards *Carnobacterium*, *L. monocytogenes*, *E. coli*, and *Klebsiella* (**Murdock et al. 2007**). Altogether, these findings indicate the huge potentialities of host defense peptides in food field, as novel biopreservatives and novel components in active packaging and surfaces.

1.6 Aims of the Thesis

The main goal of the present Thesis has been the characterization of host defense peptides, previously identify in the human Apolipoprotein B, in order to evaluate their applicability in the food industry as novel biopreservatives. ApoB derived peptides have been identify by a novel bioinformatic tool developed by Professor Eugenio Notomista (**Pane et al. 2018**). Peptides have been recombinantly produced by a cost-effective experimental procedure developed by our research group (**Gaglione et al. 2019**). ApoB derived peptides have been showed to be endowed with antimicrobial and anti-biofilm properties. Furthermore, they have been found to exert immunomodulatory and wound healing activity and they were found to be not toxic when tested on eukaryotic cell lines (**Gaglione et al. 2017**).

The first aim of the present Thesis, reported in **Chapter 2**, has been the characterization of the antimicrobial activity of ApoB derived peptides towards two selected *Salmonella* strains. Moreover, peptides' ability to affect *Salmonella* biofilm has been also investigated. Since one of the main features of novel antimicrobial and anti-biofilm agents in food industry is the stability and resistance to stress conditions, ApoB derived peptides activity has been analyzed upon peptides incubation at different temperature values and extreme pH values. Since, besides bacteria, also many species of fungi have been identified as responsible for food contamination, such as *Saccharomyces*, *Yarrowia*, *Zygosaccharomyces*,

Torulaspora, *Candida*, *Clyptococcus*, *Debaryomyces*, *Kluyveromyces* and *Trichosporon* (Viljoen and Greyling 1995), and increasing evidence of resistance development in fungi have been reported, the discovery of novel antifungal compounds has to be considered imperative. Based on this, the second aim of the present PhD Thesis has been the characterization of fungicidal effects of ApoB derived peptides towards the yeast *Candida albicans* and the filamentous fungus *Aspergillus niger*. These activities are described in **Chapter 3**. The third aim of the Thesis has been the evaluation of peptides safety and allergenicity. These activities are reported in **Chapter 4**. Finally, the fourth aim of the Thesis has been the development of chitosan surfaces functionalized with ApoB derived peptides, in order to prevent chicken meat spoilage and bacterial biofilm attachment to surfaces of industrial interest. These activities are reported in **Chapter 5**.

A general discussion on the main findings and conclusions derived from the present research work is reported in **Chapter 6**.

References

- Adedeji, W. A. 2016. "The treasure called antibiotics." *Annals of Ibadan postgraduate medicine* 14(2): 56–57.
- Alastruey-Izquierdo, A. et al. 2013. "Population-Based Survey of Filamentous Fungi and Antifungal Resistance in Spain (FILPOP Study)." *Antimicrobial Agents and Chemotherapy* 57(7): 3380–87.
- ANTIBIOTIC RESISTANCE THREATS in the United States. 2013.
- Atashgahi, Siavash et al. 2018. "Prospects for Harnessing Biocide Resistance for Bioremediation and Detoxification." *Science* 360(6390): 743–46.
- Atterbury, R. J. 2009. "Bacteriophage Biocontrol in Animals and Meat Products." *Microbial Biotechnology* 2(6): 601–12.
- Azeredo, J., and I. Sutherland. 2008. "The Use of Phages for the Removal of Infectious Biofilms." *Current Pharmaceutical Biotechnology* 9(4): 261–66.
- Al Bayssari, Charbel, Fouad Dabboussi, Monzer Hamze, and Jean Marc Rolain. 2015. "Emergence of Carbapenemase-producing *Pseudomonas Aeruginosa* and *Acinetobacter Baumannii* in Livestock Animals in Lebanon." *Journal of Antimicrobial Chemotherapy* 70(3): 950–51.
- Ben-Shalom, N. et al. 2003. "Controlling Gray Mould Caused by *Botrytis Cinerea* in Cucumber Plants by Means of Chitosan." *Crop Protection* 22(2): 285–90.
- Boes, Nelli et al. 2011. "Stringent Response Activates Quorum Sensing and Modulates Cell Density-Dependent Gene Expression In *Pseudomonas Aeruginosa* Stringent Response Activates Quorum Sensing and Modulates Cell

- Density-Dependent Gene Expression in *Pseudomonas Aeruginosa*." *Biosensors and Bioelectronics* 183(18): 5376–84.
- Bor, Tarik, Sulaiman O Aljaloud, Rabin Gyawali, and Salam A Ibrahim. 2016. "Chapter 26 - Antimicrobials from Herbs, Spices, and Plants A2 - Watson, Ronald Ross.": 551–78.
- Brown, Gordon D. et al. 2012. "Hidden Killers: Human Fungal Infections." *Science Translational Medicine* 4(165).
- "Bruessow and Kutter (2005) - Bacteriophage Ecology Group." p. 129-164.
- Burrowes, O. J., Hadjicharalambous C., Diamond G., and Tung-Ching LEE. 2006. "Evaluation of Antimicrobial Spectrum and Cytotoxic Activity of Pleurocinin for Food Applications." *Journal of Food Science* 69(3): 66–71.
- Ceri, H. et al. 1999. "The Calgary Biofilm Device: New Technology for Rapid Determination of Antibiotic Susceptibilities of Bacterial Biofilms." *Journal of Clinical Microbiology* 37(6): 1771–76.
- Chang, Qiuzhi et al. 2015. "Antibiotics in Agriculture and the Risk to Human Health: How Worried Should We Be?" *Evolutionary Applications* 8(3): 240–47.
- Cosgrove, Sara E. et al. 2003. "Comparison of Mortality Associated with Methicillin-Resistant and Methicillin-Susceptible *Staphylococcus Aureus* Bacteremia: A Meta-analysis" *Clinical Infectious Diseases* 36(1): 53–59.
- Cotter, Paul D, Colin Hill, and Paul R. Ross. 2005. "Bacteriocins: Developing Innate Immunity for Food." *Nature Reviews Microbiology* 3(10): 777–88.
- D'Costa, Vanessa M., Katherine M. McGrann, Donald W. Hughes, and Gerard D. Wright. 2006. "Sampling the Antibiotic Resistome." *Science* 311(5759): 374–77.
- Van Dijk, Albert et al. 2007. "The β -Defensin Gallinacin-6 Is Expressed in the Chicken Digestive Tract and Has Antimicrobial Activity against Food-Borne Pathogens." *Antimicrobial Agents and Chemotherapy* 51(3): 912–22.
- Dolan, John R et al. 2016. "Fiv046.Full." (June): 1–11.
- Ewnetu, Desalegne, and Adane Mihret. 2010. "Prevalence and Antimicrobial Resistance of *Campylobacter* Isolates from Humans and Chickens in Bahir Dar, Ethiopia." *Foodborne Pathogens and Disease* 7(6): 667–70.
- Florentin, L, ND Vieira, and W Barioni Júnior. 2005. "Use of Lytic Bacteriophages to Reduce *Salmonella* Enteritidis in Experimentally Contaminated Chicken Cuts." *Revista Brasileira de Ciência Avícola* 7(4): 255–60.
- Fischer, Jennie et al. 2012. "Escherichia Coli Producing VIM-1 Carbapenemase Isolated on a Pig Farm." *Journal of Antimicrobial Chemotherapy* 67(7): 1793–95.
- Fisher, Matthew C., Nichola J. Hawkins, Dominique Sanglard, and Sarah J. Gurr. 2018a. "Worldwide Emergence of Resistance to Antifungal Drugs Challenges Human Health and Food Security." *Science* 360(6390): 739–42.
- Fisher, Matthew C. 2018b. "Worldwide Emergence of Resistance to Antifungal Drugs Challenges Human Health and Food Security." *Science* 360(6390): 739–42.

- Fjell, Christopher D., Jan A. Hiss, Robert E.W. Hancock, and Gisbert Schneider. 2012. "Designing Antimicrobial Peptides: Form Follows Function." *Nature Reviews Drug Discovery* 11(1): 37–51.
- Flemming, Hans Curt, and Jost Wingender. 2010. "The Biofilm Matrix." *Nature Reviews Microbiology* 8(9): 623–33.
- Friedman, Mendel, and Vijay K. Juneja. 2010. "Review of Antimicrobial and Antioxidative Activities of Chitosans in Food." *Journal of Food Protection* 73(9): 1737–61.
- Gaglione, R. et al. 2017. "Novel Human Bioactive Peptides Identified in Apolipoprotein B: Evaluation of Their Therapeutic Potential." *Biochemical Pharmacology* 130.
- Gaglione, Rosa et al. 2019. "Cost-Effective Production of Recombinant Peptides in *Escherichia Coli*." *New Biotechnology* 51: 39–48.
- Galié, Serena et al. 2018. "Biofilms in the Food Industry: Health Aspects and Control Methods." *Frontiers in Microbiology* 9(MAY).
- García-Bayona, Leonor, Monica S. Guo, and Michael T. Laub. 2017. "Contact-Dependent Killing by *Caulobacter Crescentus* via Cell Surface-Associated, Glycine Zipper Proteins." *eLife* 6.
- Gebreyohannes, Gebreselema, Andrew Nyerere, Christine Bii, and Desta Berhe Sbhatu. 2019. "Challenges of Intervention, Treatment, and Antibiotic Resistance of Biofilm-Forming Microorganisms." *Heliyon* 5(8).
- Golkar, Zhabiz, Omar Bagasra, and Donald Gene Pace. 2014. "Bacteriophage Therapy: A Potential Solution for the Antibiotic Resistance Crisis." *Journal of Infection in Developing Countries* 8(2): 129–36.
- Gruber-Dorninger, Christiane, Barbara Novak, Veronika Nagl, and Franz Berthiller. 2016. "Emerging Mycotoxins: Beyond Traditionally Determined Food Contaminants. . *Agric. Food Chem.* 65:7052–7070.
- Hale, John D.F., and Robert E.W. Hancock. 2007. "Alternative Mechanisms of Action of Cationic Antimicrobial Peptides on Bacteria." *Expert Review of Anti-Infective Therapy* 5(6): 951–59.
- Hamamoto, H. et al. 2000. "Tandem Repeat of a Transcriptional Enhancer Upstream of the Sterol 14 α -Demethylase Gene (CYP51) in *Penicillium Digitatum*." *Applied and Environmental Microbiology* 66(8): 3421–26.
- Hancock, Robert E.W., and Robert Lehrer. 1998. "Cationic Peptides: A New Source of Antibiotics." *Trends in Biotechnology* 16(2): 82–88.
- Hancock, Robert E.W., and Hans Georg Sahl. 2006. "Antimicrobial and Host-Defense Peptides as New Anti-Infective Therapeutic Strategies." *Nature Biotechnology* 24(12): 1551–57.
- Harris, Frederick, Sarah R. Dennison, Jaipaul Singh, and David A. Phoenix. 2013. "On the Selectivity and Efficacy of Defense Peptides with Respect to Cancer Cells." *Medicinal Research Reviews* 33(1): 190–234.

- Hawkins, Nichola J. et al. 2014. "Paralog Re-Emergence: A Novel, Historically Contingent Mechanism in the Evolution of Antimicrobial Resistance." *Molecular Biology and Evolution* 31(7): 1793–1802.
- Healey, Kelley R., Cristina Jimenez Ortigosa, Erika Shor, and David S. Perlin. 2016. "Genetic Drivers of Multidrug Resistance in *Candida Glabrata*." *Frontiers in Microbiology* 7(DEC).
- Hilchie, Ashley L., Kelli Wuerth, and Robert E.W. Hancock. 2013. "Immune Modulation by Multifaceted Cationic Host Defense (Antimicrobial) Peptides." *Nature Chemical Biology* 9(12): 761–68.
- Ibrahim, Emad H. et al. 2000. "The Influence of Inadequate Antimicrobial Treatment of Bloodstream Infections on Patient Outcomes in the ICU Setting." *Chest* 118(1): 146–55.
- Iñiguez-Moreno, Maricarmen, Melesio Gutiérrez-Lomelí, Pedro Javier Guerrero-Medina, and María Guadalupe Avila-Novoa. 2018. "Biofilm Formation by *Staphylococcus Aureus* and *Salmonella* Spp. under Mono and Dual-Species Conditions and Their Sensitivity to Cetrimonium Bromide, Peracetic Acid and Sodium Hypochlorite." *Brazilian Journal of Microbiology* 49(2): 310–19.
- Jenssen, Håvard. 2009. "Therapeutic Approaches Using Host Defence Peptides to Tackle Herpes Virus Infections." *Viruses* 1(3): 939–64.
- Johnson, Eldin Maliyakkal et al. 2018. "Bacteriocins as Food Preservatives: Challenges and Emerging Horizons." *Critical Reviews in Food Science and Nutrition* 58(16): 2743–67.
- Khan, Muhammad Usman et al. 2018. "Role of Milk-Derived Antibacterial Peptides in Modern Food Biotechnology: Their Synthesis, Applications and Future Perspectives." *Biomolecules* 8(4).
- Kumar, Prashant, Jayachandran N. Kizhakkedathu, and Suzana K. Straus. 2018. "Antimicrobial Peptides: Diversity, Mechanism of Action and Strategies to Improve the Activity and Biocompatibility in Vivo." *Biomolecules* 8(1).
- de la Fuente-Núñez, César et al. 2014. "Broad-Spectrum Anti-Biofilm Peptide That Targets a Cellular Stress Response." *PLoS Pathogens* 10(5).
- Lavermicocca, Paola, Francesca Valerio, and Angelo Visconti. 2003. "Antifungal Activity of Phenyllactic Acid against Molds Isolated from Bakery Products." *Applied and Environmental Microbiology* 69(1): 634–40.
- Li, Bingyun, and Thomas J. Webster. 2018. "Bacteria Antibiotic Resistance: New Challenges and Opportunities for Implant-Associated Orthopedic Infections." *Journal of Orthopaedic Research* 36(1): 22–32.
- Lucas, John A., Nichola J. Hawkins, and Bart A. Fraaije. 2015. "The Evolution of Fungicide Resistance." *Advances in Applied Microbiology* 90: 29–92.
- Mann, Nicholas H. 2008. "The Potential of Phages to Prevent MRSA Infections." *Research in Microbiology* 159(5): 400–405.
- Marshall, Bonnie M., and Stuart B. Levy. 2011. "Food Animals and Antimicrobials: Impacts on Human Health." *Clinical Microbiology Reviews* 24(4): 718–33.

- Martínez, José L., Teresa M. Coque, and Fernando Baquero. 2015. "What Is a Resistance Gene? Ranking Risk in Resistomes." *Nature Reviews Microbiology* 13(2): 116–23.
- Moran, Gregory J. et al. 2006. "Methicillin-Resistant *S. Aureus* Infections among Patients in the Emergency Department." *New England Journal of Medicine* 355(7): 666–74.
- Murdock, C. A., J. Cleveland, K. R. Matthews, and Michael L. Chikindas. 2007. "The Synergistic Effect of Nisin and Lactoferrin on the Inhibition of *Listeria Monocytogenes* and *Escherichia Coli* O157:H7." *Letters in Applied Microbiology* 44(3): 255–61.
- Nanasombat, Suree, and Pana Lohasupthawee. 2005 "Antibacterial activity of crude ethanolic extracts and essential oils of spices against salmonellae and other enterobacteria". *Sci. Tech. J* 5(3) 527-538.
- Okumura, Kazuhiko. 2011. "Cathelicidins-Therapeutic Antimicrobial and Antitumor Host Defense Peptides for Oral Diseases." *Japanese Dental Science Review* 47(1): 67–81.
- Pane, Katia et al. 2018. "Identification of Novel Cryptic Multifunctional Antimicrobial Peptides from the Human Stomach Enabled by a Computational-Experimental Platform." *ACS Synthetic Biology* 7(9): 2105–15.
- Penesyan, Anahit, Michael Gillings, and Ian T. Paulsen. 2015. "Antibiotic Discovery: Combatting Bacterial Resistance in Cells and in Biofilm Communities." *Molecules* 20(4): 5286–98.
- Perry, Julie Ann, Erin Louise Westman, and Gerard D. Wright. 2014. "The Antibiotic Resistome: What's New?" *Current Opinion in Microbiology* 21: 45–50.
- Piddock, Laura J.V. 2012. "The Crisis of No New Antibiotics-What Is the Way Forward?" *The Lancet Infectious Diseases* 12(3): 249–53.
- Pitt, John I., and Ailsa D. Hocking. 2009. *Fungi and Food Spoilage*. Springer US.
- Price, Lance B. et al. 2012. "Staphylococcus Aureus CC398: Host Adaptation and Emergence of Methicillin Resistance in Livestock." *mBio* 3(1): 1–6.
- Pundir, P. et al. 2014. "Pleurocidin, a Novel Antimicrobial Peptide, Induces Human Mast Cell Activation through the FPRL1 Receptor." *Mucosal Immunology* 7(1): 177–87.
- Robbins, Nicole, Tavia Caplan, and Leah E. Cowen. 2017. "Molecular Evolution of Antifungal Drug Resistance." *Annual Review of Microbiology* 71(1): 753–75.
- Roberts, Rebecca R. et al. 2009. "Hospital and Societal Costs of Antimicrobial-Resistant Infections in a Chicago Teaching Hospital: Implications for Antibiotic Stewardship." *Clinical Infectious Diseases* 49(8): 1175–84.
- Sengupta, Saswati, Madhab K. Chattopadhyay, and Hans Peter Grossart. 2013. "The Multifaceted Roles of Antibiotics and Antibiotic Resistance in Nature." *Frontiers in Microbiology* 4(MAR).

- Shannon, Emer, and Nissreen Abu-Ghannam. 2016. "Antibacterial Derivatives of Marine Algae: An Overview of Pharmacological Mechanisms and Applications." *Marine Drugs* 14(4).
- Sharma, Divakar, Lama Misba, and Asad U. Khan. 2019. "Antibiotics versus Biofilm: An Emerging Battleground in Microbial Communities." *Antimicrobial Resistance and Infection Control* 8(1).
- Silva, Célia C.G., Sofia P.M. Silva, and Susana C. Ribeiro. 2018. "Application of Bacteriocins and Protective Cultures in Dairy Food Preservation." *Frontiers in Microbiology* 9(APR).
- da Silva Malheiros, Patrícia, Daniel Joner Daroit, and Adriano Brandelli. 2010. "Food Applications of Liposome-Encapsulated Antimicrobial Peptides." *Trends in Food Science and Technology* 21(6): 284–92.
- Silva, Maria Manuela, and Fernando Cebola Lidon. 2016. "Food Preservatives - An Overview on Applications and Side Effects." *Emirates Journal of Food and Agriculture* 28(6): 366–73.
- Singh, Pal. 2018. "Recent Approaches in Food Bio-Preservation-a Review." *Open Veterinary Journal* 8(1): 2226–4485.
- Solomon, Ethan B., Brendan A. Niemira, Gerald M. Sapers, and Bassam A. Annous. 2005. "Biofilm Formation, Cellulose Production, and Curli Biosynthesis by Salmonella Originating from Produce, Animal, and Clinical Sources." *Journal of Food Protection* 68(5): 906–12.
- Sommer, Morten O.A., Gautam Dantas, and George M. Church. 2009. "Functional Characterization of the Antibiotic Resistance Reservoir in the Human Microflora." *Science* 325(5944): 1128–31.
- Spellberg, Brad, and David N. Gilbert. 2014. "The Future of Antibiotics and Resistance: A Tribute to a Career of Leadership by John Bartlett." *Clinical Infectious Diseases* 59: S71–75.
- Sundaram, Jaya et al. 2016. "Antimicrobial and Physicochemical Characterization of Biodegradable, Nitric Oxide-Releasing Nanocellulose-Chitosan Packaging Membranes." *Journal of Agricultural and Food Chemistry* 64(25): 5260–66.
- Tanwar, Jyoti, Shrayanee Das, Zeeshan Fatima, and Saif Hameed. 2014. "Multidrug Resistance: An Emerging Crisis." *Interdisciplinary Perspectives on Infectious Diseases* 2014.
- The Open University. 2018. *Hygiene and Environmental Health Module: 8. Food Contamination and Spoilage*. Hygiene and Environmental Health Module: 8. Food Contamination and Spoilage: View as Single Page.
- Unosson, Erik. 2015. Doctor of Philosophy Thesis, Uppsala Universitet *Antibacterial Strategies for Titanium Biomaterials*.
- Vallet-Regí, María, Blanca González, and Isabel Izquierdo-Barba. 2019. "Nanomaterials as Promising Alternative in the Infection Treatment." *International Journal of Molecular Sciences* 20(15).

Viljoen, Bennie C., and Theunie Greyling. 1995. "Yeasts Associated with Cheddar and Gouda Making." *International Journal of Food Microbiology* 28(1): 79–88.

Zasloff, Michael. 2002. "Antimicrobial Peptides of Multicellular Organisms." *Nature* 415(6870): 389–95.

Zasloff, Michael C. 2009. "Mysteries That Still Remain." *Biochimica et Biophysica Acta - Biomembranes* 1788(8): 1693–94.

Zhang, Mingzhen, Jun Zhao, and Jie Zheng. 2014. "Molecular Understanding of a Potential Functional Link between Antimicrobial and Amyloid Peptides." *Soft Matter* 10(38): 7425–51.

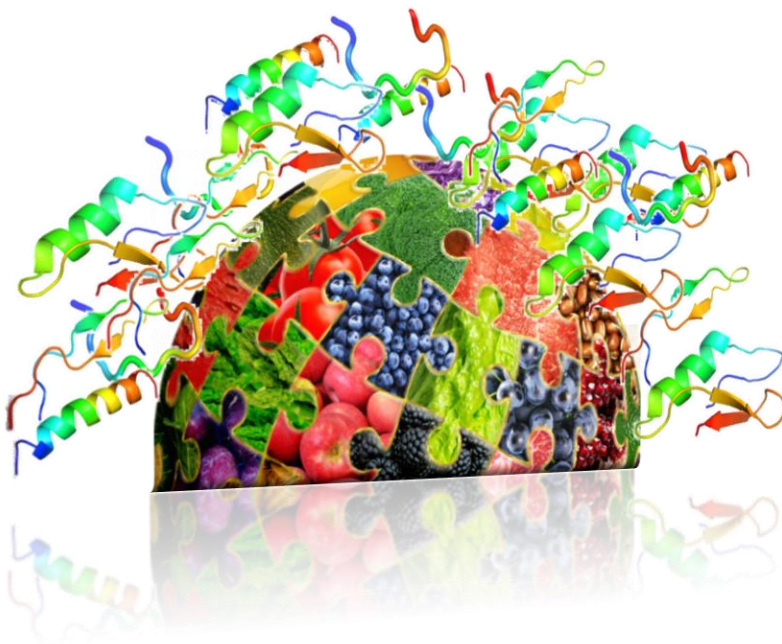
CHAPTER 2

ApoB derived peptides as novel antimicrobial and anti-biofilm agents towards *Salmonella* strains

Eliana Dell'Olmo

Department of Chemical Sciences, PhD in Biotechnology

University of Naples "Federico II"



1. Introduction

1.1 Food losses and microbial contamination

Today, food loss and waste are a major concern worldwide, since approximately one-third of all the food produced for human consumption is either lost or wasted (**Gustavsson, Cederberg, and Sonesson 2011**). Several reasons have been identified for this phenomenon. Among these, food spoilage associated to microbial contamination represents the main factor affecting organoleptic product quality (aspect, texture, taste, and aroma) (**Leyva Salas et al. 2017a**). Among foodstuff contaminants, resistant bacteria and fungi represent an emerging serious problem. Indeed, the emergence of antibiotic resistance (ABR) along the food chain is a major global public health issue, with several studies reporting the colonization and/or the infection of food animals and products by antibiotic-resistant strains, such as *Staphylococcus aureus* or *Salmonella* strains.

1.2 *Salmonella* strains outbreaks in food chain

Among of the foodborne pathogens, *Salmonella* causes about 1.35 million illnesses, 26,500 hospitalizations, and 420 deaths in the United States every year (**Scallan et al. 2011**). Bacteria belonging to *Salmonella* genera lead the insurgence of three types of diseases in humans: (i) noninvasive and nontyphoidal, (ii) invasive and nontyphoidal, and (iii) typhoidal fever Salmonellosis (**Kurtz, Goggins, and McLachlan 2017; Snider et al. 2014**). Moreover, *Salmonella* strains are widespread along the food chain and are able to contaminate different food samples, such as, raw meat, eggs, and fresh vegetables. Thus, the control of *Salmonella* contaminations is a milestone in the prevention of food spoilage. To this purpose, in the 1980' the World Health organization (WHO) proposed a global program to reduce the risk about *Salmonella* contamination (**World Health Organization 1981**). The program included: (i) control of *Salmonella* infections in food animals, (ii) the improvement of hygiene in the slaughter and further processes of raw meat, and (iii) and improvement in the education of food industry operators and consumers about good hygiene practices in food preparation (**Plym Forshell and Wierup 2006**). *Salmonellosis* can be treated only by using appropriate antibiotics (**Kelly 2011**), which in most cases belong to fluoroquinolones family. This put bacteria under an

evolutionary pressure that lead to the increase of resistant phenotypes (Maiti et al. 2014).

1.3 Development of novel antimicrobial and anti-biofilm agents

The dramatic situation of the antibiotic resistance in food chain highlighted the urgent need for novel alternative strategies that allow to preserve food and prevent infections in food animals. In this scenario, Host Defense Peptides (HDPs) have attracted great interest because of their ability to preserve food without altering its organoleptic properties. Recently, we described the identification of novel host defense peptides within precursor proteins by using a bioinformatic tool developed by Prof. Eugenio Notomista (Pane et al. 2018). We focused on a putative antimicrobial sequence identified in human Apolipoprotein B100. Consequently, a recombinant and cost-effective expression system (Gaglione et al. 2019) was set up to produce three versions of the identified sequence, here named r(P)ApoB^L^{Pro}, r(P)ApoB^S^{Pro} and r(P)ApoB^L^{Ala}; the last one presents an alanine instead of a proline in position seven of peptide sequence. ApoB derived peptides were found to be endowed with a wide range of activities, such as broad-spectrum antimicrobial activity, anti-biofilm activity, immunomodulatory and wound healing properties. Furthermore, they were found to have not toxic effects when tested on eukaryotic cell lines and on murine erythrocytes (Gaglione et al. 2017). Here, we analyze antimicrobial activity and anti-biofilm properties of ApoB derived peptides towards foodborne pathogens to evaluate their applicability as novel food biopreservatives. In particular, two *Salmonella* strains were selected as models of food contaminants, i.e. *Salmonella typhimurium* ATCC® 14028 and *Salmonella enteritidis* 706 RIVM. Antimicrobial activity of ApoB derived peptides has been tested by calculating Minimum Inhibitory Concentration (MIC₁₀₀) values, in order to determine the lowest peptide concentration able to completely inhibit bacterial growth. Moreover, Scanning Electron Microscopy (SEM) analyses have been performed to deepen and clarify ApoB derived peptides effects on bacteria morphology. Thermal and chemical stability of r(P)ApoB^L^{Pro}, r(P)ApoB^S^{Pro} and r(P)ApoB^L^{Ala} peptides has been also analyzed by determining peptides MIC₁₀₀ values upon incubation in specific conditions. Finally, anti-biofilm properties of ApoB derived peptides have been investigated by crystal violet assays and Confocal Laser Scanning Microscopy experiments.

2. Materials and methods

2.1 Materials

All the reagents were purchased from Sigma-Aldrich, Milan, Italy, unless differently specified.

2.2 Bacterial strains and growth conditions

Bacterial strains *Salmonella typhimurium* ATCC® 14028 and *Salmonella enteritidis* 706 RIVM were grown in Muller Hinton Broth (MHB, Becton Dickinson Difco, Franklin Lakes, NJ) and on Tryptic Soy Agar (TSA; Oxoid Ltd., Hampshire, UK). In all the experiments, bacteria were inoculated and grown overnight in MHB at 37°C. After about 24 h, bacteria were transferred into a fresh MHB tube and grown to mid-logarithmic phase.

2.3 Antimicrobial activity assay

To test the antimicrobial activity of ApoB derived peptides, bacteria were grown to mid-logarithmic phase in MHB at 37°C. Cells were then diluted to 2×10^6 CFU/mL in 0.5x Nutrient Broth (NB) (Difco, Becton Dickinson, Franklin Lakes, NJ) containing increasing amounts of peptides. In each case, starting from a peptide stock solution, two-fold serial dilutions were sequentially carried out, accordingly to broth microdilution method (**Wiegand, Hilpert, and Hancock 2008**). Following over-night incubation, MIC₁₀₀ values were determined as the lowest peptide concentration responsible for no visible bacterial growth. The assay was performed in triplicate.

2.4 Bactericidal activity assay

To study the bactericidal activity of ApoB derived peptides, the minimal bactericidal concentration (MBC) was determined by a colony count assay (**Wiegand, Hilpert, and Hancock 2008**). To this purpose, following the assay to determine MIC₁₀₀ values, bacterial aliquots were withdrawn from the wells with no visible bacterial growth, and serially diluted in 0.5x NB to be plated on TSA (Tryptic Soy Agar) plates and incubated at 37°C for 24 h. After incubation, bacterial colonies were counted, and the MBC was determined as the lowest concentration that caused >99.9% cell death with respect to the initial bacterial inoculum. The assay was performed in triplicate.

2.5 Scanning electron microscopy analyses

Bacterial cells in exponential growth phase were grown for 3 h in NB 0.5X in microfuge tubes in the absence or in the presence of ApoB derived peptides. Since high bacterial cell densities were required (2×10^8 CFU/mL) for the analysis, MIC₁₀₀ values were determined in these experimental conditions and found to be in the range 2.5-5 μ M. To perform scanning electron microscopy (SEM) analyses, *Salmonella typhimurium* ATCC® 14028 and *Salmonella enteritidis* 706 RIVM strains were incubated with 2.5 μ M peptides for 24 h at 37°C. Following incubation, bacterial cells were centrifuged at 10,000 rpm at 4°C and fixed in 2.5% glutaraldehyde. Following over-night incubation, bacterial cells were washed three times in distilled water (dH₂O) and then dehydrated with a graded ethanol series: 25% ethanol (1 \times 10 min); 50% ethanol (1 \times 10 min); 75% ethanol (1 \times 10 min); 95% ethanol (1 \times 10 min); 100% anhydrous ethanol (3 \times 30 min). Bacterial cells deposited onto glass substrate were first sputter coated with a thin layer of Au-Pd (Sputter Coater Denton Vacuum Desk V) to allow subsequent morphological characterization using a FEI Nova NanoSEM 450 at an accelerating voltage of 5 kV with Everhart Thornley Detector (ETD) and Lens Detector (TLD) at high magnification.

2.6 Effects of temperature and pH values on peptides stability

To test the effects of temperature on the antimicrobial activity of ApoB derived peptides, each peptide was heated at 28° and 60°C or stored at 4°C for 15 min and then the antimicrobial activity was assayed by MIC evaluation. In the same way, to assess the effects of pH values on peptides activity, ApoB derived peptides were solubilised in H₂O, and then the pH value was adjusted 6.0 or to 4.0 by adding 0.1 N HCl or to 9.0 by adding 0.1 M NH₃. Following pH variation, peptide solution was incubated for 15 min at room temperature, and then added to bacteria. To this purpose, cell cultures were grown to mid-logarithmic phase in 0.5X NB at 37°C, and then diluted to 2×10^6 CFU/mL in 0.5X NB (Difco, Becton Dickinson, Franklin Lakes, NJ) containing increasing amounts of peptides. In each case, starting from a peptide stock solution, two-fold serial dilutions were sequentially carried out, accordingly to broth microdilution method (**Wiegand, Hilpert, and Hancock 2008**). Following over-night incubation, MIC₁₀₀ values were determined as

the lowest peptide concentration responsible for no visible bacterial growth. The assay was performed in triplicate.

To assess the minimum bactericidal concentration, bacterial colonies were counted, and the MBC was defined as the lowest peptide concentration that caused >99.9% cell death with respect to the initial bacterial inoculum. The assay was performed in triplicate.

2.7 Anti-biofilm activity analyses

To test the anti-biofilm activity of ApoB derived peptides, bacteria were grown over-night in MHB (Becton Dickinson Difco, Franklin Lakes, NJ), and then diluted to 1×10^8 CFU/mL in 0.5X MHB medium (Li et al. 2013) containing increasing concentrations of peptides. As previously described, incubations were carried out for 48 h, in order to test peptides effects on biofilm formation. At the end of the incubation, crystal violet assays were performed. To do this, supernatant was removed from the wells, which were washed three times with sterile PBS prior to staining with 0.04% crystal violet for 20 min. Excess of dye was eliminated by three consecutive washes with sterile PBS. Finally, crystal violet was solubilised with 33% acetic acid prior to determination of samples optical absorbance at 600 nm by using an automatic plate reader (MicrobetaWallac 1420, Perkin Elmer, Waltham, MA, USA).

2.8 Analysis of static biofilm growth by confocal microscopy analyses

Bacterial biofilm was grown into chambered cover glass slides (Nunc Lab-Tek, ThermoFisher Scientific, Waltham, MA, USA) in 0.5 X MHB medium in static conditions at 37°C for 48 h. To do this, bacterial cells from an over-night culture were diluted to about 2×10^8 CFU/mL, and then seeded onto coverslips. Following bacterial biofilm formation for 48 h at 37°C, non-adherent bacteria were removed by gently washing samples with sterile phosphate buffer. Viability of cells embedded into biofilm structure was determined by sample staining with LIVE/DEAD® BacLight™ Bacterial Viability kit (Molecular Probes ThermoFisher Scientific, Waltham, MA, USA). Staining was performed accordingly to manufacturer instructions. Biofilm images were captured by using a confocal laser scanning microscopy (Zeiss LSM 710, Zeiss, Germany) and a 63x objective oil immersion system. Biofilm architecture was analysed by using the Zen Lite 2.3 software package. Each experiment was performed

in triplicate. Images are 2D-3D projections of biofilm structure obtained by confocal z-stacks using Zen Lite 2.3 software. All images were taken under identical conditions and represent the average of at least three different acquisition fields. Scale bar corresponds to 10 μm in all the cases. All images were taken under identical conditions. The experiments have been carried out in triplicate.

2.9 Statistical analyses

Statistical analyses were performed using a Student's t-Test. Significant differences were indicated as *($P < 0.05$), **($P < 0.01$) or ***($P < 0.001$).

3. Results

3.1 Antimicrobial activity of ApoB derived peptides towards *Salmonella* strains

It has been reported that in 2018 about 80% of total food production has been lost because of microbial contaminations and spoilage (**Food and Agriculture Organization of the United Nations, 2018**). On the other hand, the increased interest of consumers for natural food samples, obtained in the absence of pretreatments and chemical agents addition, forced the development of novel and more “*natural*” strategies to preserve food (**Wang et al. 2016**). In order to develop an effective biocompatible alternative, the antimicrobial activity of ApoB derived peptides has been tested towards *Salmonella typhimurium* ATCC® 14028 and *Salmonella enteritidis* RIVM 706 bacterial strains. Interestingly, r(P)ApoB^L^{Pro}, r(P)ApoB^S^{Pro} and r(P)ApoB^L^{Ala} were found to be endowed with a significant antimicrobial activity towards both *Salmonella typhimurium* ATCC® 14028 and *Salmonella enteritidis* RIVM 706 (Table 1). It has to be noticed that ApoB derived peptides are able to completely inhibit the growth of both *Salmonella* strains at very low concentrations.

Strains	MIC ₁₀₀ (μM)		
	r(P)ApoB _L ^{Pro}	r(P)ApoB _S ^{Pro}	r(P)ApoB _L ^{Ala}
<i>Salmonella typhimurium</i> ATCC® 14028	2.5	2.5	5
<i>Salmonella enteritidis</i> RIVM 706	5	5	5

Table 1. Minimum inhibitory concentration values determined for r(P)ApoB_L^{Pro}, r(P)ApoB_S^{Pro} and r(P)ApoB_L^{Ala} towards *Salmonella* strains.

3.2 Morphological analyses of *Salmonella* strains cells upon treatment with ApoB derived peptides

Host defense peptides are small molecules usually endowed with a net positive charge and high hydrophobicity. These features are at the basis of their mechanism of action and their ability to interact with negatively charged bacterial membranes (**Ebenhan et al. 2014**). Indeed, it is well known that HDPs generally exert their direct antimicrobial activity by disrupting bacterial membranes (**Haney, Straus, and Hancock 2019**). For these reasons, Scanning Electron Microscopy analyses have been carried out. To this purpose, r(P)ApoB_L^{Pro} and r(P)ApoB_S^{Pro} have been selected to treat both *Salmonella typhimurium* ATCC® 14028 and *Salmonella enteritidis* RIVM 706 strains. Peptides were used at a concentration of 2.5 μM for 24 h. Following incubation, scanning electron microscopy analyses highlighted the ability of ApoB derived peptides to interact with bacterial membranes. Indeed, upon treatment of *Salmonella* strains with r(P)ApoB_L^{Pro} and r(P)ApoB_S^{Pro}, membranes appeared corrugated and wrinkled with concomitant significant effects on cell viability (Figure 1 and Figure 2).

Salmonella typhimurium ATCC® 14028

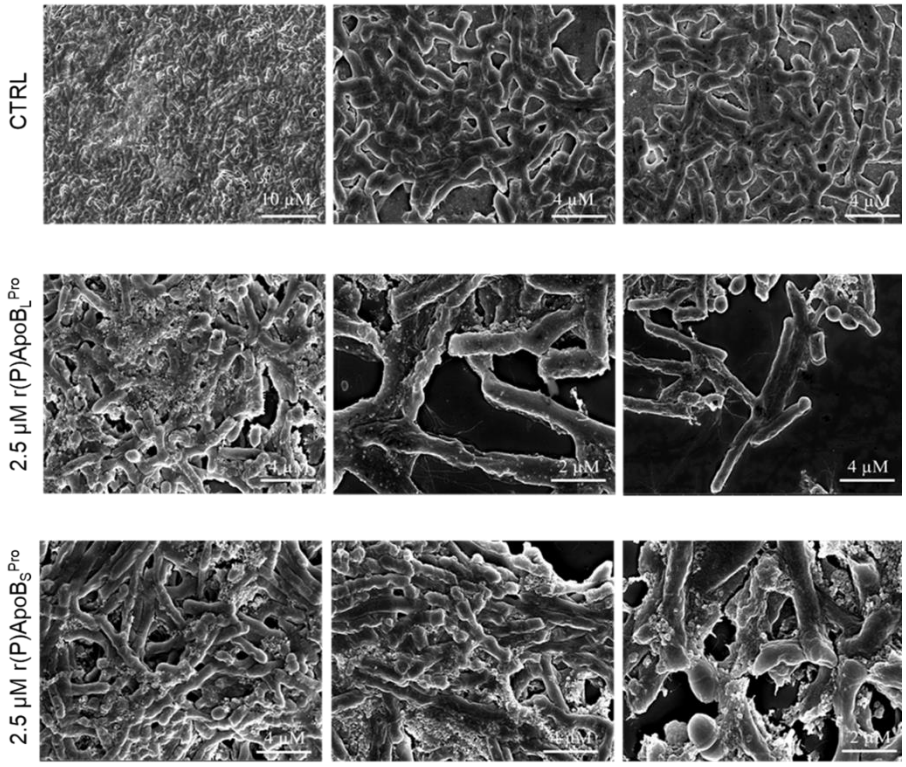


Figure 1. Scanning electron microscopy micrographs of *Salmonella typhimurium* ATCC® 14028 cells in the absence (first line) or in the presence of 2.5 μM r(P)ApoB_L^{Pro} (second line) or 2.5 μM r(P)ApoB_S^{Pro} (third line).

Salmonella enteritidis RIVM 706

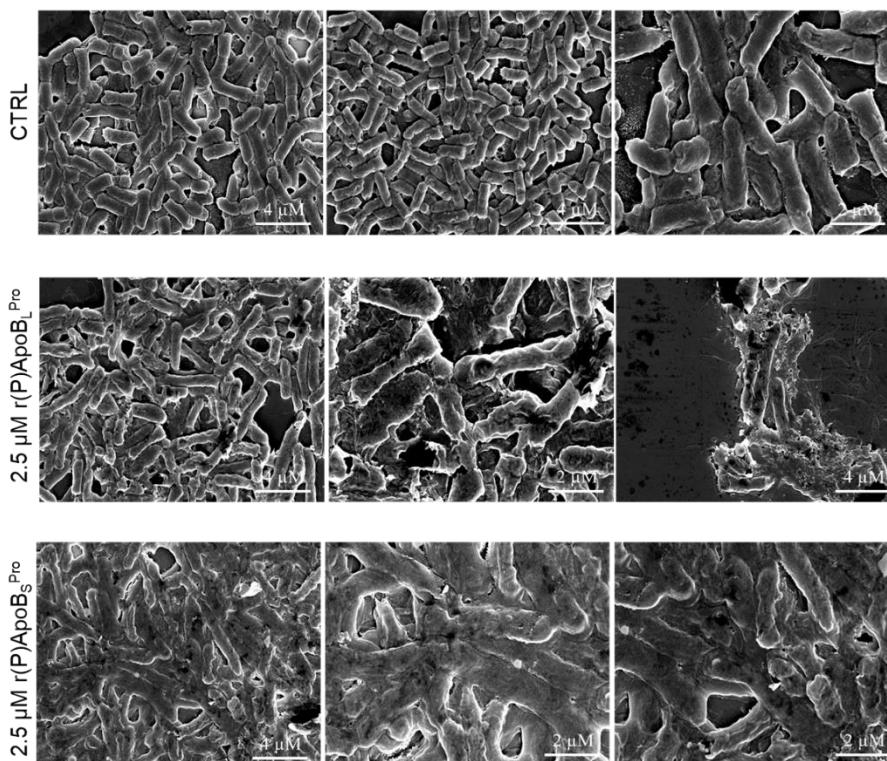


Figure 2. Scanning electron microscopy micrographs of *Salmonella enteritidis* RIVM 706 cells in the absence (first line) or in the presence of 2.5 μM r(P)ApoB^{Pro} (second line) or 2.5 μM r(P)ApoB_S^{Pro} (third line).

3.3 Thermal and chemical stability of ApoB derived peptides

Along production chain, food samples are subjected to several stress conditions, such as temperature variations and pH alteration. Hence, keeping antimicrobial activity of bio-preservative agents under common thermal processing and gastrointestinal tract conditions (pH, bile salt) is crucial. For this reason, the antimicrobial activity of ApoB derived peptides was investigated under different experimental conditions (**Assefa, Beyene, and Santhanam 2008**). To this purpose, the stability of ApoB derived peptides has been assessed upon incubation at different temperature values (4°, 28° and 60°C) and different pH values (4, 6 and 9) for 15 min. Surprisingly, r(P)ApoB^{Pro}, r(P)ApoB_S^{Pro} and r(P)ApoB_L^{Ala}

antimicrobial activity was found to be unchanged upon peptides incubation at different temperature values, suggesting that antimicrobial activity of peptides is not influenced by temperature variations (Table 2).

Strains	MIC ₁₀₀ values (μM)											
	r(P)ApoB _L ^{Pro}				r(P)ApoB _S ^{Pro}				r(P)ApoB _L ^{Ala}			
	CTRL	4°C	28 °C	60°C	CTRL	4°C	28°C	60°C	CTRL	4°C	28°C	60°C
<i>Salmonella typhimurium</i> ATCC®14028	2.5	2.5	2.5	2.5	2.5	2.5	5	5	5	5	5	5
<i>Salmonella enteritidis</i> RIVM 706	5.	5	2.5	2.5	5	5	10	10	5	5	5	5

Table2. MIC₁₀₀ values determined upon incubation of ApoB derived peptides at different temperatures.

Peptides antimicrobial activity was also tested at different pH values. In this case, no significant effects on antimicrobial activity were detected at pH 6.0 and 9.0, whereas significant effects were observed when peptides were incubated at pH 4.0 Indeed, in this experimental condition, MIC₁₀₀ values were found to increase of about 3-fold for all the peptides (Table 3).

Strains	MIC ₁₀₀ values (μM)											
	r(P)ApoB _L ^{Pro}				r(P)ApoB _S ^{Pro}				r(P)ApoB _L ^{Ala}			
	CTRL	pH 6	pH 4	pH 9	CTRL	pH 6	pH 4	pH 9	CTRL	pH 6	pH 4	pH 9
<i>Salmonella typhimurium</i> ATCC®14028	2.5	2.5	20	2.5	2.5	2.5	40	5	5	5	40	5
<i>Salmonella enteritidis</i> RIVM 706	5	5	20	2.5	5	5	40	10	5	5	40	5

Table3. MIC₁₀₀ values determined upon incubation of ApoB derived peptides upon incubation at different pH values.

Obtained results suggest that variation in pH values might provoke a variation of ApoB derived peptides net charge, with consequent negative effects on peptides ability to interact with bacterial membranes. Many strategies have been developed to overcome limits associated to peptide instability, such as peptides encapsulation in liposomes or lipid-based system (**Suleiman et al. 2019**). Researchers have also demonstrated the effectiveness of different types of nanoparticles to protect peptides from environmental stress conditions (**Tan et al. 2010**).

3.4 Anti-biofilm activity of ApoB derived peptides

Foodborne pathogens, such as *Salmonella* strains, are able to grow in very harsh conditions. This ability is due to their ability to form biofilm structures on different surfaces. Bacteria in biofilm matrix are more resistant to different stress conditions, such as lack of nutrients, osmolarity variations or antibiotic treatments (**MacKenzie et al. 2017**). Hence, the development of novel effective anti-biofilm agents to be employed in food industry is imperative. To this purpose, the effects of ApoB derived peptides on biofilm formation of both *Salmonella typhimurium* ATCC® 14028 and *Salmonella enteritidis* 706 RIVM strains have been investigated. Firstly, crystal violet assays have been performed upon treatment of bacterial biofilm with increasing concentration of r(P)ApoB_L^{Pro}, r(P)ApoB_S^{Pro} or r(P)ApoB_L^{Ala} for 48 h (Figure 3).

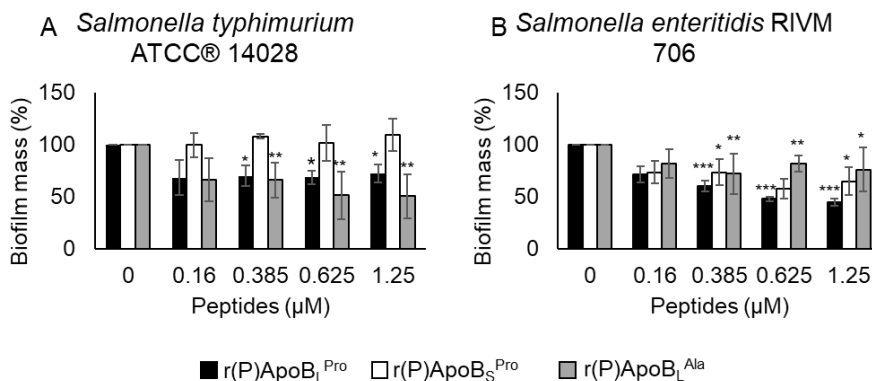


Figure 3. Anti-biofilm activity of r(P)ApoB_L^{Pro}, of r(P)ApoB_S^{Pro} and r(P)ApoB_L^{Ala} on *Salmonella typhimurium* ATCC® 14028 (A) and *Salmonella enteritidis* RIVM 706 (B). The biofilm mass has been evaluated by crystal violet assay upon the incubation with increasing concentrations of peptides for 48 h. The bars represent the mean of three independent experiments (\pm SD).

ApoB derived peptides were found to be able to reduce biofilm mass during formation stage. In particular, r(P)ApoB_L^{Pro} and r(P)ApoB_L^{Ala} were found to be able to counteract biofilm formation in the case of both *Salmonella typhimurium* ATCC® 14028 (A) and *Salmonella enteritidis* 706 RIVM (B) at sub-MIC concentration values. It has to be noticed that the shorter peptide r(P)ApoB_S^{Pro} was found to be more effective on *Salmonella typhimurium* ATCC® 14028 with

respect to *Salmonella enteritidis* RIVM 706 bacterial strain. Furthermore, to deeply characterize peptide anti-biofilm activity, confocal laser scanning microscopy analyses were performed. To this purpose, bacterial biofilm was incubated with r(P)ApoB_L^{Pro}, r(P)ApoB_S^{Pro} or r(P)ApoB_L^{Ala} peptides for 48 h, at 37° C in static conditions (Figure 4 and 5). Following incubation, samples were double stained (Syto9/PI mixture), in order to discriminate between live and dead bacterial cells embedded into biofilm structure. As shown in Figure 4 A and B, upon biofilm treatment with 0.625 µM r(P)ApoB_L^{Pro} peptide, biofilm architecture was found to be completely altered, with a significant decrease of biofilm thickness for both *Salmonella typhimurium* ATCC® 14028 and *Salmonella enteritidis* 706 RIVM strains.

Salmonella typhimurium ATCC® 14028

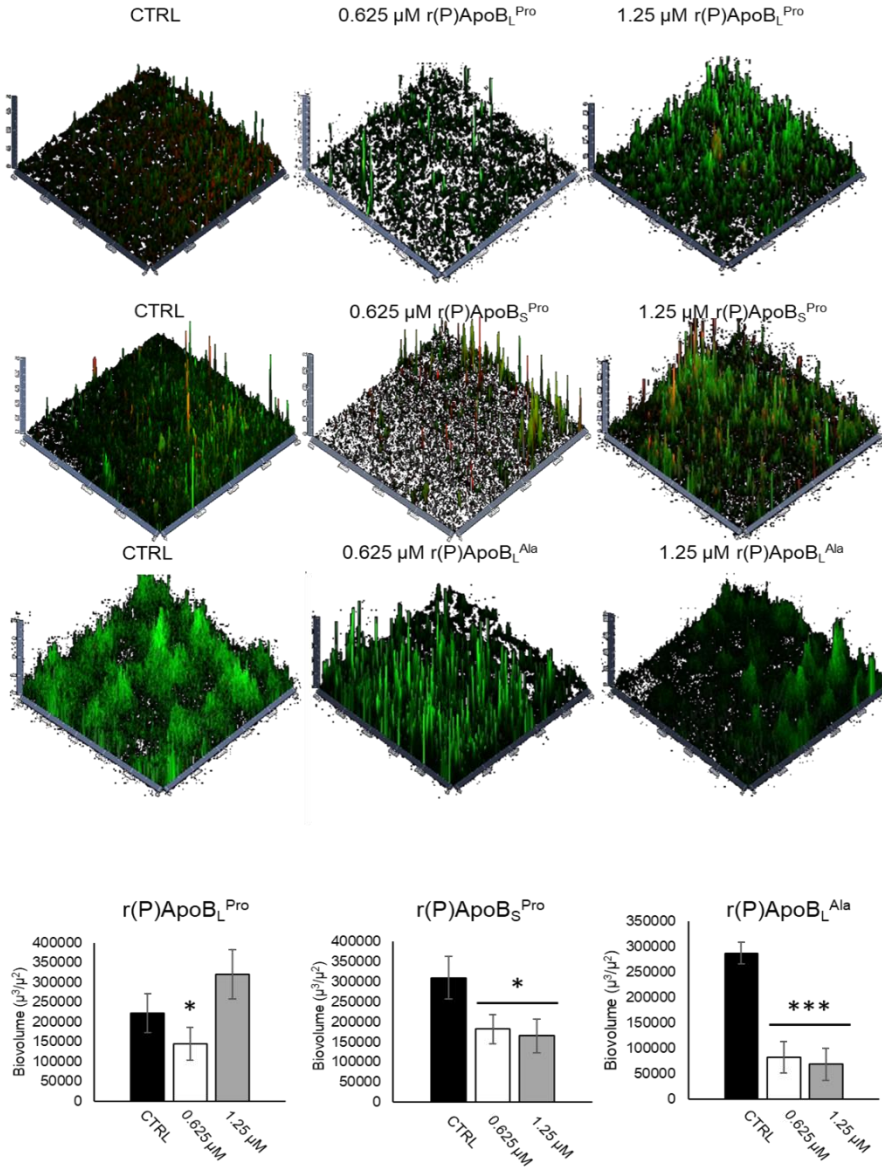


Figure 4. Confocal laser scanning microscopy analyses performed on *Salmonella typhimurium* ATCC® 14028. The images report the 2.5D reconstruction of biofilm matrix and the biofilm biovolume in the absence or in the presence of r(P)ApoB_L^{Pro}, r(P)ApoB_S^{Pro} or

r(P)ApoB_L^{Ala}. The graphs represent the mean of three different experiments.

Salmonella enteritidis RIVM 706

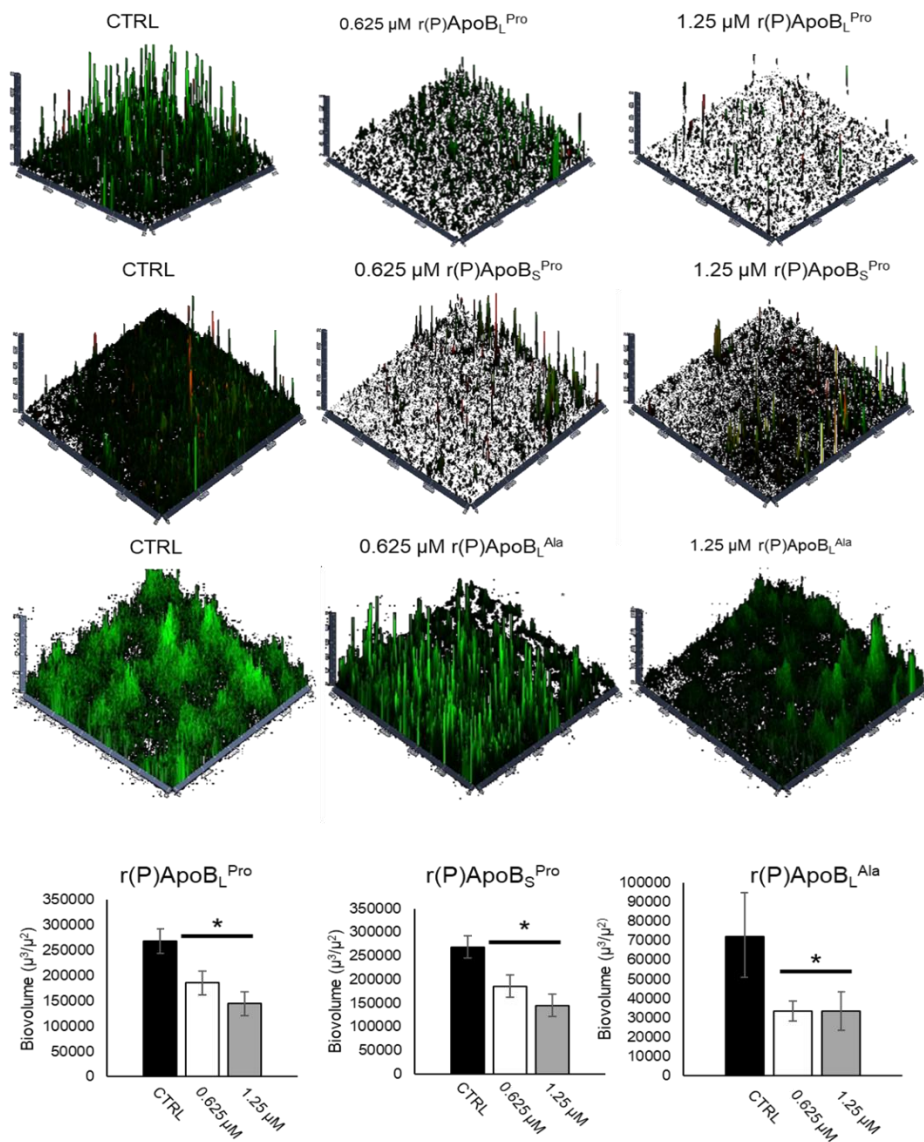


Figure 5. Confocal laser scanning microscopy analyses performed on *Salmonella enteritidis* RIVM 706. The images report the 2.5D reconstruction of biofilm matrix and the biofilm biovolume in the

absence or in the presence of r(P)ApoB_L^{Pro}, r(P)ApoB_S^{Pro} or r(P)ApoB_L^{Ala}. The graphs represent the mean of three different experiments.

Interestingly, r(P)ApoB_L^{Pro} peptide has been found to affect not only biofilm matrix, with a consequent reduction in biofilm thickness, but also to significantly reduce biofilm biovolume in the case of both *Salmonella typhimurium* ATCC® 14028 (A), and *Salmonella enteritidis* RIVM 706. On the other hand, r(P)ApoB_S^{Pro} peptide was found to exert strong anti-biofilm activities by affecting both biovolume and matrix structure at the lowest concentrations tested. It has to be noticed that no increase in cell death was detected. Finally, r(P)ApoB_L^{Ala} peptide has been found to be able to disrupt biofilm matrix in the case of both *Salmonella typhimurium* ATCC® 14028 (A) and *Salmonella enteritidis* RIVM 706 (B). Interestingly, this peptide has been found to be able to drastically reduce biovolume even at the lowest concentrations tested. Overall, obtained results highlight the ability of ApoB derived peptides to affect biofilm matrix without significantly altering cells viability.

4. Discussion

4.1 ApoB derived peptides as novel antimicrobial and anti-biofilm agents for food industry

Food loss and waste are major global issues that attracted great attention. It has been estimated that 1.3 million tonnes *per* year of total produced food have been lost or wasted (**Food losses and waste in the context of sustainable food systems A report by The High Level Panel of Experts on Food Security and Nutrition 2014**). Food loss and waste can occur at any stage of food chain production. Several reasons have been identified for this phenomenon. Among these, food spoilage associated to microbial contamination represents the main factor affecting organoleptic product quality (aspect, texture, taste, and aroma) (**Leyva Salas et al. 2017a**). In the last years, host defense peptides have attracted great interest because of their ability to prevent food contamination without altering food quality. Moreover, given to their features, such as the positive net charge (**Zasloff 2002; Hancock R. E. et al. 1998**) and the high content of hydrophobic residues, they are able to selectively interact with bacterial membranes. Moreover, because of their mechanism of action, HDPs generally do not lead to the

insurgence of resistance phenotype. The ApoB derived peptides have been showed a significant antimicrobial activity towards both *Salmonella typhimurium* ATCC® 14028 and *Salmonella enteritidis* RIVM 706. Moreover, scanning electron microscopy analyses emphasized the ability of r(P)ApoB^L^{Pro}, r(P)ApoB^S^{Pro} and r(P)ApoB^L^{Ala} to interact with bacterial membranes. It has been noticed that the mutation of a proline in an alanine residue in the sequence of the longer version of the peptides does not significantly affect the antimicrobial activity. Previously, zeta-potential measurements, performed on responsive and not responsive bacteria, showed that ApoB derived peptides are able to selectively neutralize the membrane potential of bacteria responsive to ApoB derived peptides antimicrobial activity **(Gaglione et al. 2019)**. Accordingly, isothermal titration calorimetry (ITC) experiments proved the ability of these peptides to selectively interact with lipopolysaccharides (LPS) on the membranes of responsive bacteria **(Gaglione et al. 2019)**. Similar mechanisms of action have been previously reported for well-known peptides, such as the chicken cathelicidin CATH-2, the human cathelicidin LL-37 **(Scheenstra et al. 2019)**. Furthermore, it is worthy to note that the most common peptide employed in food industry is a bacteriocin, Nisin A, which is the first peptide approved from FDA as a biopreservatives **(Gharsallaoui et al. 2016)**. This peptide showed a strong antimicrobial activity towards gram positive bacteria but not on gram negative ones; on the contrary, ApoB derived peptides are not only able to completely kill *Salmonella* strains, but they are also able to kill a broad-spectrum of gram negative and gram positive bacteria **(Gaglione et al. 2017)**. Interestingly, ApoB derived peptides have showed significant anti-biofilm activity towards both *Salmonella* strains. Indeed, r(P)ApoB^L^{Pro} peptide has been found to be able to significantly reduce the biofilm mass of both *Salmonella typhimurium* ATCC® 14028 and *Salmonella enteritidis* RIVM 706. These results have been also confirmed by confocal laser scanning microscopy experiments. On the contrary, r(P)ApoB^S^{Pro} peptide was found to be more effective in reducing biofilm formation of *Salmonella enteritidis* 706 RIVM with respect to *Salmonella typhimurium* ATCC® 14028. Surprisingly, when the anti-biofilm activity of the shorter peptide has been analysed by confocal laser scanning microscopy, biofilm matrix of both *Salmonella* strains was found to be disrupted. These observations highlight the ability of r(P)ApoB^S^{Pro} peptide to affect

biofilm integrity without influencing biofilm mass. In the case of r(P)ApoB_L^{Ala} peptide, reduction of biofilm mass has been observed for both *Salmonella* strains and has been confirmed by confocal laser scanning microscopy analyses. Anti-biofilm properties have been also demonstrated for several HDPs from different sources, such as gH625 peptide from amphibian secretions, human cathelicidins LL-37 and CATH-2 (**Galdiero et al. 2019; Dean, Bishop, and Van Hoek 2011**), or bacteriocins, such as nisin, lacticin Q, and nukacin ISK-1 (**Yasir, Willcox, and Dutta 2018**). Peptide gH625 has been tested on the biofilm of *Candida tropicalis*, *Serratia marcescens* and *Staphylococcus aureus* (de Alteriis et al. 2018), showing the ability to prevent biofilm formation and to eradicate preformed biofilm, even if at MIC values (de Alteriis et al. 2018). The well-known peptide LL-37 has been found to be effective on the biofilm of different *Staphylococcus aureus* strains, with a reduction of about 75% at concentration values close to MIC values (Haisma et al. 2014). On the basis of these evidences, host defence peptides represent good candidates for the development of anti-biofilm strategies in which the peptides affect biofilm matrix and conventional antibiotics kill planktonic cells embedded into biofilm matrix (Batoni et al. 2016). In this scenario, ApoB derived peptides represent a perfect alternative because of their effectiveness on biofilm as well as for their ability to synergistically act in combination with other substances (Gaglione et al. 2017).

4.2 Thermal and chemical stability of the ApoB derived peptides

Since HDPs to be employed in food industry have to be endowed with thermal stability and chemical resistance (**Sadeghi et al. 2018**), antimicrobial activity of r(P)ApoB_L^{Pro}, r(P)ApoB_S^{Pro} or r(P)ApoB_L^{Ala} peptides was also tested upon peptide incubation at different temperatures and pH values. Nowadays, thermal processing is one of the most used procedures to sterilize food samples. For this reason, thermal stability is one of the key features required for a novel bio-preservative. Surprisingly, ApoB derived peptides showed a strong thermal stability, since no significant variations of antimicrobial peptides activity have been observed upon peptides incubation at temperature values usually used to store food samples. An example is represented by nisin, a bacteriocin produced by *Lactococcus lactis subs.* It is the first bacteriocin

approved by Food and Drug administration as a food preservative **(Gharsallaoui et al. 2016)**. This bacteriocin has been widely tested for its stability, and it has been found to retain its antimicrobial activity even at very high temperature values, such as 120 °C **(Nostro et al. 2010)**. On the other hand, ApoB derived peptides incubation at different pH values highlighted a higher stability at basic pH values with respect to acidic pH values. Indeed, many evidences indicate that pH value is a key factor driving the interaction between peptides and bacterial membranes (Malik et al. 2016), thus modulating HDPs antimicrobial activity. Moreover, nisin antimicrobial activity has been found to strongly depend upon pH conditions. It is well known that nisin antimicrobial activity is highest at pH values around 2.0, whereas an increase in pH leads to a progressive loss of peptide activity and solubility **(Delves-Broughton 1990)**. Thus, ApoB derived peptides were found to retain their activity under different temperature and pH conditions, thus making them good candidates for food industry applications, as also indicated by their significant direct antimicrobial activity towards *Salmonella* strains, along with their effectiveness on bacterial biofilm at concentration values significantly lower than MIC values. Altogether, these findings indicate that ApoB derived peptides represent good candidates to develop novel strategies in food preservation and pose an important first step in the evaluation of ApoB derived peptides applicability as food biopreservatives.

References

- de Alteriis, E. et al. 2018. "Polymicrobial Antibiofilm Activity of the Membranotropic Peptide GH625 and Its Analogue." *Microbial Pathogenesis* 125: 189–95.
- Assefa, E. et al. 2008. "Effect of Temperature and PH on the Antimicrobial Activity of Inhibitory Substances Produced by Lactic Acid Bacteria Isolated from Ergo, an Ethiopian Traditional Fermented Milk."
- Batoni, G. et al. 2016. "Antimicrobial Peptides and Their Interaction with Biofilms of Medically Relevant Bacteria." *Biochimica et Biophysica Acta - Biomembranes* 1858(5): 1044–60.
- Dean, S. N., et al. 2011. "Susceptibility of *Pseudomonas Aeruginosa* Biofilm to Alpha-Helical Peptides: D-Enantiomer of LL-37." *Frontiers in Microbiology* 2(JULY).
- Delves-Broughton, J. 1990. "Nisin and Its Application as a Food Preservative." *International Journal of Dairy Technology* 43(3): 73–76.
- Ebenhan, T. et al. 2014. "Antimicrobial Peptides: Their Role as Infection-Selective Tracers for Molecular Imaging." *BioMed Research International* 2014.

Food Losses and Waste in the Context of Sustainable Food Systems A Report by The High Level Panel of Experts on Food Security and Nutrition. 2014.

Gaglione, R. et al. 2017. "Novel Human Bioactive Peptides Identified in Apolipoprotein B: Evaluation of Their Therapeutic Potential." *Biochemical Pharmacology* 130.

Gaglione, R. et al. 2019. "Cost-Effective Production of Recombinant Peptides in *Escherichia Coli*." *New Biotechnology* 51: 39–48.

Gaglione, R. et al. 2019. "Effects of Human Antimicrobial Cryptides Identified in Apolipoprotein B Depend on Specific Features of Bacterial Strains." *Scientific Reports* 9(1).

Galdiero, Emilia et al. 2019. "Biofilms: Novel Strategies Based on Antimicrobial Peptides." *Pharmaceutics* 11(7).

Gharsallaoui, A. et al. 2016. "Nisin as a Food Preservative: Part 1: Physicochemical Properties, Antimicrobial Activity, and Main Uses." *Critical Reviews in Food Science and Nutrition* 56(8): 1262–74.

Gustavsson, Jenny, Christel Cederberg, and Ulf Sonesson. 2011. *Global Food Losses and Food Waste*.

Haisma, Elisabeth M. et al. 2014. "LL-37-Derived Peptides Eradicate Multidrug-Resistant *Staphylococcus Aureus* from Thermally Wounded Human Skin Equivalents." *Antimicrobial Agents and Chemotherapy* 58(8): 4411–19.

Haney, Evan F. et al. 2019. "Reassessing the Host Defense Peptide Landscape." *Frontiers in Chemistry* 7(FEB).

Kelly P. 2011. "Diarrhoeal Disease." *Clinical Medicine, Journal of the Royal College of Physicians of London*: 11(5) 488-491.

Kurtz, Jonathan R. et al. 2017. "Salmonella Infection: Interplay between the Bacteria and Host Immune System." *Immunology Letters* 190: 42–50.

Leyva Salas, Marcia et al. 2017. "Antifungal Microbial Agents for Food Biopreservation—A Review." *Microorganisms* 5(3): 37.

Li, Junsheng et al. 2013. "Hydrophobic Liquid-Infused Porous Polymer Surfaces for Antibacterial Applications." *ACS Applied Materials and Interfaces* 5(14): 6704–11.

MacKenzie, Keith D., Melissa B. Palmer, Wolfgang L. Köster, and Aaron P. White. 2017. "Examining the Link between Biofilm Formation and the Ability of Pathogenic Salmonella Strains to Colonize Multiple Host Species." *Frontiers in Veterinary Science* 4(AUG).

Maiti, Soumitra et al. 2014. "Effective Control of Salmonella Infections by Employing Combinations of Recombinant Antimicrobial Human β -Defensins HBD-1 and HBD-2." *Antimicrobial Agents and Chemotherapy* 58(11): 6896–6903.

Malik, Erum et al. 2016. "PH Dependent Antimicrobial Peptides and Proteins, Their Mechanisms of Action and Potential as Therapeutic Agents." *Pharmaceutics* 9(4).

- Nostro, Antonia et al. 2010. "Control of Biofilm Formation by Poly-Ethylene-Co-Vinyl Acetate Films Incorporating Nisin." *Applied Microbiology and Biotechnology* 87(2): 729–37.
- Pane, Katia et al. 2018. "Identification of Novel Cryptic Multifunctional Antimicrobial Peptides from the Human Stomach Enabled by a Computational-Experimental Platform." *ACS Synthetic Biology* 7(9): 2105–15.
- Plym Forshell, L., and M. Wierup. 2006. "Salmonella Contamination: A Significant Challenge to the Global Marketing of Animal Food Products." *OIE Revue Scientifique et Technique* 25(2): 541–54.
- Sadeghi, Alireza et al. 2018. "Effects of Temperature, PH, and Bile Salt on Antimicrobial Activity of Bacteriocin-like Substances Obtained from Barley Sourdough LAB." *Comparative Clinical Pathology* 27(3): 611–19.
- Scallan, Elaine et al. 2011. "Foodborne Illness Acquired in the United States-Major Pathogens." *Emerging Infectious Diseases* 17(1): 7–15.
- Scheenstra, Maaikje R et al. 2019. "Cathelicidins PMAP-36, LL-37 and CATH-2 Are Similar Peptides with Different Modes of Action." *Scientific Reports* 9(1).
- Snider, Timothy A. et al. 2014. "Experimental Salmonellosis Challenge Model in Older Calves." *Veterinary Microbiology* 170(1–2): 65–72.
- Suleiman, Ehsan et al. 2019. "Electrostatically Driven Encapsulation of Hydrophilic, Non-Conformational Peptide Epitopes into Liposomes." *Pharmaceutics* 11(11).
- Tan, Mei Lin, P. F.M. Choong, and C. R. Dass. 2010. "Recent Developments in Liposomes, Microparticles and Nanoparticles for Protein and Peptide Drug Delivery." *Peptides* 31(1): 184–93.
- Wang, Shuai, Xiangfang Zeng, Qing Yang, and Shiyan Qiao. 2016. "Antimicrobial Peptides as Potential Alternatives to Antibiotics in Food Animal Industry." *International Journal of Molecular Sciences* 17(5).
- Wiegand, Irith, Kai Hilpert, and Robert E.W. Hancock. 2008. "Agar and Broth Dilution Methods to Determine the Minimal Inhibitory Concentration (MIC) of Antimicrobial Substances." *Nature Protocols* 3(2): 163–75.
- World Health Organization. 1981. Report of the WHO/WAVFH Round Table Conference on the Present Status of the Salmonella Problem (prevention and Control).
- Yasir, Muhammad, Mark Duncan Perry Willcox, and Debarun Dutta. 2018. "Action of Antimicrobial Peptides against Bacterial Biofilms." *Materials* 11(12).
- Zasloff, Michael. 2002. "Antimicrobial Peptides of Multicellular Organisms." *Nature* 415(6870): 389–95

CHAPTER 3

ApoB derived peptides as novel antifungal agents

Eliana Dell'Olmo

Department of Chemical Sciences, PhD in Biotechnology

University of Naples "Federico II"



1. Introduction

1.1 Fungal contamination along food chain

Massive food loss and waste are important global issues. Among causes, microbial contamination and spoilage represent key factors affecting food properties (**Leyva Salas et al. 2017b**). Among food pathogens, fungi play a key role because of their ability to contaminate food samples at any stage of production chain. Furthermore, fungi are able to grow in several environments and in harsh conditions (**Pitt and Hocking 2009b**). On the other hand, yeast microorganisms generally used as starter cultures in several processes, such as along cheese and bread production, as well as along wine and beer fermentation (**Lowes et al. 2000**), can act as spoilage agents in products as yoghurts, fresh fruits, juices and salads. Moreover, both yeasts and fungi are able to produce secondary metabolites, called mycocins and mycotoxins, respectively. While mycocins are usually harmless to humans, fungal mycotoxins can cause severe infections. Furthermore, microorganisms like fungi and yeasts can contaminate food at different stages. The main targets of fungal contaminations are: (i) the field, where water, soil, and air are natural fungal niches; (ii) raw materials, such as post-harvest crops, meats, and milk where fungal occurrence is related to food management during harvest or collecting, transportation, storage, and packaging, and (iii) during manufacturing of dairy, bakery, dry-ripened, and drink products (**Pitt and Hocking 2009b; Leyva Salas et al. 2017b**). Thus, prevention of fungal contamination in the food field is crucial.

1.2 Fungal resistance to conventional drugs

Since the 1980s, a significant increase in serious invasive fungal infections matched the rise in the number of highly susceptible people, mainly immunocompromised, such as elderly, transplanted subjects, cancer patients and premature infants, with consequent morbidity and mortality (**Brown et al. 2012**). *Candida* spp. and *Aspergillus* spp. represent the most common causes of fungal infections in humans (**Badiee and Hashemizadeh 2014; Alastruey-Izquierdo et al. 2013**). Furthermore, the narrow spectrum of possible antifungal treatments leads to the rapid rise of resistant fungal strains. Resistance in *Candida* and *Aspergillus* strains has become a global issue since the 1990's because of the

intensive use of triazoles (**Kontoyiannis and Lewis 2002**). Increase in resistance phenotype is exacerbated by a paucity of new antifungal agents characterized by unique mechanisms of action (**Oshero and Kontoyiannis 2017**).

1.3 Host defence peptides as antifungal agents

In this scenario, several HDPs have been tested for their antifungal properties. A great number of antifungal peptides have been identified as components of the innate immune response of invertebrates and vertebrates (**L. he Zhang and Chen 2006**). A marine metagenomic screening led to the identification of several peptides endowed with significant antifungal properties, such as heliomicin, juruin and tenecin-3 (**Ciociola et al. 2016**). In mammalian vertebrates, antifungal peptides are primarily produced by epithelial cells and neutrophils. Histatins, cathelicidins and defensins are the major group of mammalian antifungal peptides (**Ciociola et al. 2016**). Here, the antifungal activity of ApoB derived peptides towards the yeast *Candida albicans* ATCC 10231 and the filamentous fungus *Aspergillus niger* N402 has been investigated for the first time. Moreover, a novel form of r(P)ApoB^{Pro} has been designed with a cysteine instead of a proline residue at the N-terminus. The obtained peptide, here named r(C)ApoB^{Pro}, has been labelled with 5-Iodoacetamidofluorescein, thus obtaining a fluorescent version of the peptide. Peptide r(C)ApoB^{Pro} has been a precious tool to deepen the mechanism of action of ApoB derived peptides by live-imaging analyses on both *Candida albicans* ATCC 10231 and *Aspergillus niger* N402.

2. Materials and methods

2.1 Fungal strains and growth conditions

Cultures of *Candida albicans* ATCC 10231 were grown on Yeast Malt (YM-Sigma Aldrich; Y3752) agar plates. For all the experiments, yeasts were cultured at 30° C in 10 mL Yeast extract peptone dextrose broth (YPD) until mid-log phase was reached. Growth rate was monitored by measuring optical density (OD) values at 620 nm; mid-log phase was set at 2x10⁶ CFU/ml in 1/100 YM broth. In the case of Minimal fungicidal concentration (MFC) experiments, initial cell density was further analysed by plating a ten-fold dilution of culture in YM broth. *Aspergillus niger* N402 was grown at 30 °C in 20 mL of minimal medium (MM) (**de Vries et al., 2004**)

containing 2% glucose and 1.5% agar. Conidia used to inoculate cultures were harvested from 4-day-old colonies by using a buffer containing 0.8% NaCl and 0.005% Tween-80 (ST).

2.2 Expression and isolation of recombinant ApoB derived peptides

Expression and isolation of recombinant peptides was carried out as previously described (**Gaglione et al. 2017**). Peptide r(C)ApoB_L^{Pro} was obtained as described before (**Pane et al. 2018**).

2.3 Production of recombinant labelled peptide

r(C)ApoB_L^{Pro} was obtained by chemical hydrolysis of purified ONC-DCless-H6-(C)-ApoB_L^{Pro} fusion protein in a reducing buffer. Chimeric construct was expressed and purified as previously reported (**Pane et al. 2018**). Briefly, recombinant protein was expressed in *E. coli* BL21(DE3) strain as inclusion bodies, purified by immobilized metal affinity chromatography (IMAC), and dialyzed towards 0.1 M acetic acid. Chemical hydrolysis was carried out at 60 °C for 24 h at pH 2.0 (18 mM HCl). Peptide release was monitored by RP-HPLC on Europa Protein 300 C18 column using a linear gradient. r(C)ApoB_L^{Pro} peptide was then purified by column-free procedure based on different solubility of carrier and peptide at pH 7.0 (**Pane et al. 2018**). To this purpose, hydrolysis mixture was neutralized by adding diluted NH₃ for 5 min at 28 °C under nitrogen atmosphere. Insoluble fusion protein and carrier were then separated from soluble peptide by 10 min centrifugation at 18,000g at 4 °C. Soluble fraction was analyzed by RP-HPLC on Europa Protein 300 C18 column, in order to evaluate peptide purity. Supernatant, containing soluble peptide, was immediately incubated with 5-Iodoacetamidofluorescein (5-IAF) to label N-terminal cysteine residues as described below.

2.4 Labelling of purified peptide

r(C)ApoB_L^{Pro} peptide, purified by selective precipitation of carrier and fusion protein, was labelled by using thiol reactive fluorescent dye 5-Iodoacetamidofluorescein (5-IAF), in order to produce 5-IAF/r(C)ApoB_L^{Pro} labelled peptide. Purified r(C)ApoB_L^{Pro} peptide (9.6 mg, 60 µM final concentration) was incubated with 5-IAF (0.25 mM final concentration; 15 mM stock solution in dimethyl formamide) in 15 mM sodium phosphate buffer (NaP), pH 7.4, containing 2 M guanidine-HCl, for 2 h at 25 °C, in the dark under nitrogen

atmosphere. Molar ratio of 5-IAF over thiols was 4:1. r(C)ApoB_L^{Pro} labeling reaction was monitored by RP-HPLC on Europa Protein 300 C18 column (5 μm, 25 × 1) using gradient 1 (see “RP-HPLC analyses” section). To simplify RP-HPLC purification of the peptide, reaction was quenched by adding L-cysteine in a molar excess of 10:1 on 5-IAF, for 1 h at 37°C in the dark. Peptide was purified on Europa Protein 300 C18 column by using gradient 1. Purified 5-IAF/r(C)ApoB_L^{Pro} peptide was lyophilized and dissolved in water. Labelled peptide concentration was determined by using molar extinction coefficient reported in the literature (5-IAF: $\epsilon_{492\text{nm}} = 80,000\text{-}85,000 \text{ M}^{-1} \text{ cm}^{-1}$) and by BCA colorimetric assay. Purity of labelled peptide was evaluated by RP-HPLC on Europa Protein 300 C18 column (gradient 1).

2.5 RP-HPLC analyses

Reverse-phase high performance liquid chromatography (RP-HPLC) was carried out by using a Jasco LC-4000 system equipped with PU-4086 semipreparative pumps and an MD-4010 photo diode array detector. Europa Protein 300 C18 column (5 μm, 25 × 1) from Teknokroma (Barcelona, Spain) was used as RP-HPLC column. Solvents were 0.05% trifluoroacetic acid (TFA) in water (solvent A) and 0.05% TFA in acetonitrile (solvent B). Elution profiles were recorded by linear gradient 1 as follows:

gradient 1: from 5% to 25% solvent B in 10 min, from 25% to 35% solvent B in 30 min, from 35% to 50% solvent B in 10 min, from 50% to 100% solvent B in 10 min, isocratic elution at 100% solvent B for 10 min. The elution was monitored at 214 nm at a flow rate of 2 mL/min.

2.6 MFC Assay

Minimum fungicidal concentration (MFC) values of peptides were assessed by colony counting assays, as previously described (**Van Dijk et al. 2007**), with few modifications. Briefly, 50 μL of a 2x10⁶ CFU/mL cell suspension in 1/100 YM broth were incubated for 3 h at 37 °C with an equal volume of peptide (0-40 μM). Ten-fold dilutions in YM broth were then plated onto YP agar plates and incubated over-night at 37°C. Finally, colonies of surviving yeast cells were counted. The experiment has been performed in triplicate.

2.7 Killing kinetic studies

To kinetically analyse fungal killing by ApoB derived peptides, experiments on *Candida albicans* ATCC 10231 cells were performed. To this purpose, yeast cells grown overnight in YM medium were diluted in fresh YM medium, and then incubated at 37 °C until logarithmic phase of growth was reached. Yeasts were then diluted to 2×10^6 CFU/mL in a final volume of 500 μ L in 1/100 YM broth and mixed with the peptide (1:1 v/v). Increasing concentrations of peptide were analysed (ranging from 0 to 20 μ M). At defined time intervals, samples (20 μ L) were serially diluted (from 10- to 10,000-fold), and 100 μ L of each dilution was plated on YPD Agar. Following an incubation of 16 h at 37 °C, yeast colonies were counted. The experiment has been performed in triplicate.

2.8 PI uptake assay

Propidium iodide assay was performed as previously described (**Stone et al. 2003**) with some modifications. Briefly, 45 μ L of 1×10^7 CFU/mL of *Candida albicans* ATCC 10231 cells were plated into 96-well plates, treated with 45 μ L of peptides increasing concentrations (0-20 μ M), and incubated for 1 h at 37 °C. After that, 10 μ L of propidium iodide at a final concentration of 5 μ M were added. After 10 min of incubation, PI fluorescence was measured by using a microtiter plate reader (FLUOstar Omega, BMG LABTECH, Germany) at an excitation wavelength of 485 nm and an emission wavelength of 650 nm. The percentage of PI uptake was calculated as follow: $[F(\text{sample}) - F(\text{CTRL}) / F(100\%) - F(\text{CTRL})] \times 100$, where F(CTRL) is the fluorescence of untreated sample and F(100%) is the fluorescence of heat-treated samples (15 min at 95 °C). The experiment has been performed in quadruplicate.

2.9 ATP release assay

ATP released by cells exposed to peptides was measured by using ATP determination Kit from Molecular Probes (Life Sciences, Bleiswijk, The Netherlands). Briefly, a 1×10^7 CFU/mL *Candida albicans* ATCC 10231 suspension in 1:100 YM was incubated with increasing concentrations of each peptide for 10 and 60 min. Samples were then centrifuged for 1 min at $1,200 \times g$, and the supernatant was stored on ice for ATP determination as described by the manufacturer. ATP concentration in control samples was

found to be lower than 10 nM (data not shown). The experiment has been performed in triplicate.

2.10 Real-time localization of fluorescently labelled r(C)ApoB^{Pro}

Experiments were performed as previously described by Jang and co-workers with some modifications. In the case of all the experiments, 35 mm culture dishes (FluoroDish™, WPI, Sarasota, FL) were coated with 0.5 mg/mL Concanavalin A (Sigma-Aldrich; L7647) in water. A suspension (100 µL) of 1×10^7 CFU/mL *Candida albicans* ATCC 10231 in 1:100 YM medium was then added. Fluorescently labelled peptide (50 µL) was added in the medium containing propidium iodide (PI) 5 µM (Sigma-Aldrich; P4170). In the case of *Aspergillus niger* N402 hyphae, 100 µL of a solution of 1×10^7 spores/mL were incubated at 37 °C for 24 h in the presence of peptides. At defined time points (0, 16 and 24 h), analyses were performed. Confocal Images were acquired with a Leica SPE-II at the Centre for Cell Imaging (CCI)- Utrecht University, using 63x objective. A 488 nm argon laser and a 561 nm DPSS laser were used for simultaneous detection of 5-IAF-labelled peptide and PI, respectively. The experiment has been conducted in triplicate, by acquiring three different images for each sample.

2.11 Metabolic activity analyses

Aspergillus niger N402 metabolic activity was analysed by using cell proliferator reagent WST-1 (Roche Applied Science, Mannheim, Germany). Briefly, 45 µL of a 1×10^5 spores/mL suspension in MM or in 0.25X MM were incubated for 24 h at 37 °C with an equal volume of peptide (0-40 µM). In each well, 10 µL of WST-1 10 X was added. At defined time intervals, sample absorbance values were measured at 450 nm by using 650 nm as reference wavelength at a microtiter plate reader (FLUOstar Omega, BMG LABTECH, Germany). To investigate the effects of ApoB derived peptides on swollen spores, hyphae and mycelia, spores were previously incubated in MM containing 2% glucose for 6, 16 and 24 h, respectively. The experiment has been performed in quadruplicate, with triplicate determination.

2.12 Statistical analyses

Statistical analysis was performed using a Student's t-Test. Significant differences were indicated as *(P < 0.05), **(P < 0.01), ***(P < 0.001) or **** (P < 0.0001).

3. Results

3.1 Antifungal activity of r(P)ApoBL^{Pro}, r(P)ApoBS^{Pro} and r(P)ApoBL^{Ala} peptides

Many species of fungi and yeasts have been identified as responsible for food contamination, such as *Saccharomyces*, *Yarrowia*, *Zygosaccharomyces*, *Torulaspota*, *Candida*, *Clyptococcus*, *Debaryomyces*, *Kluyveromyces* and *Trichosporon* (Viljoen and Greyling 1995). Moreover, *Candida* species have been found to be responsible for human invasive and not invasive infections. Based on this and on the growing phenomenon of resistance development, the design of novel strategies to counteract yeast infections is very urgent. With the final aim to propose novel antifungal agents, ApoB derived peptides have been tested on fungi by firstly measuring minimum fungicidal concentrations towards *Candida albicans* ATCC 10231. Interestingly, all the peptides were found to be endowed with a significant antifungal activity by exerting significant effects at concentration values comprised in the range 5-20 μM (Figure 1).

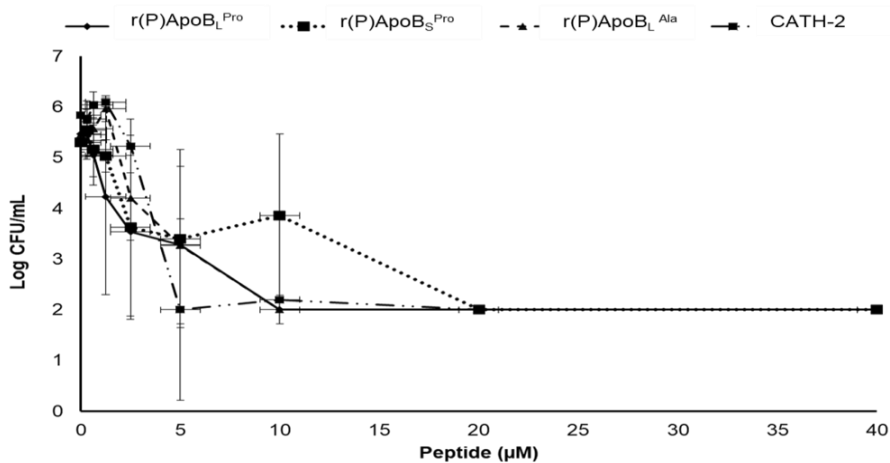


Figure 1. Antifungal activity of r(P)ApoBL^{Pro}, r(P)ApoBS^{Pro} and r(P)ApoBL^{Ala} peptides towards *Candida albicans* ATCC 10231. Minimum fungicidal concentration (MFC) values were assessed by

colony counting assays. Data represent means of three independent experiments (\pm SD). CATH-2 peptide was used as a positive control.

The chicken cathelicidin-2 was used as a positive control. In order to analyse peptides antifungal effects over time, kinetic killing curves were obtained by treating *Candida albicans* ATCC 10231 with increasing concentrations of each peptide and for different time intervals. As shown in Figure 2, at the highest peptide concentrations tested (5-10 μ M), *Candida albicans* ATCC 10231 was killed within 10 min, whereas, at lower concentration values (5 μ M), the same effects were observed after 180 min.

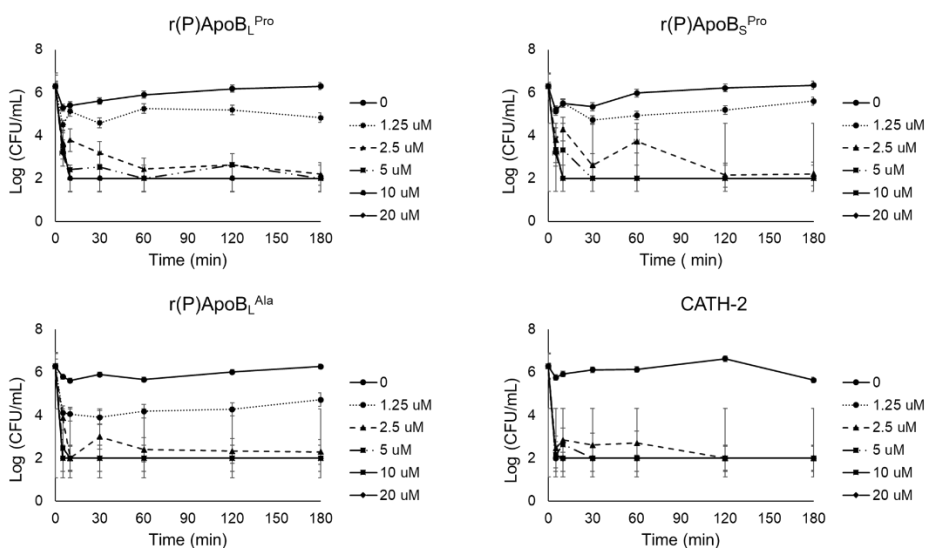


Figure 2. Time killing curves obtained by incubating *Candida albicans* ATCC 10231 cells with increasing concentrations of r(P)ApoB_L^{Pro}, r(P)ApoB_S^{Pro} and r(P)ApoB_L^{Ala} peptides for different time intervals. Data represent the mean (\pm SD) of at least three independent experiments, each one carried out with triplicate determinations. CATH-2 peptide was used as a positive control.

3.2 Peptide effects on yeast cells membranes

In order to analyse the mechanism of ApoB derived peptides fungicidal activity, propidium iodide uptake upon treatment with peptides was analysed. Propidium iodide is one of the dyes most commonly used to discriminate between live and dead cells, since it is able to selectively penetrate damaged cells. *Candida albicans* ATCC 10231 cells were treated with ApoB derived peptides at MFC

concentrations for 1 h. Interestingly, upon treatment of fungal cells with ApoB derived peptides, a significant increase of propidium iodide uptake was observed (Figure 3). This suggests that ApoB derived peptides effects on *Candida* cells are associated to membrane permeabilization induction.

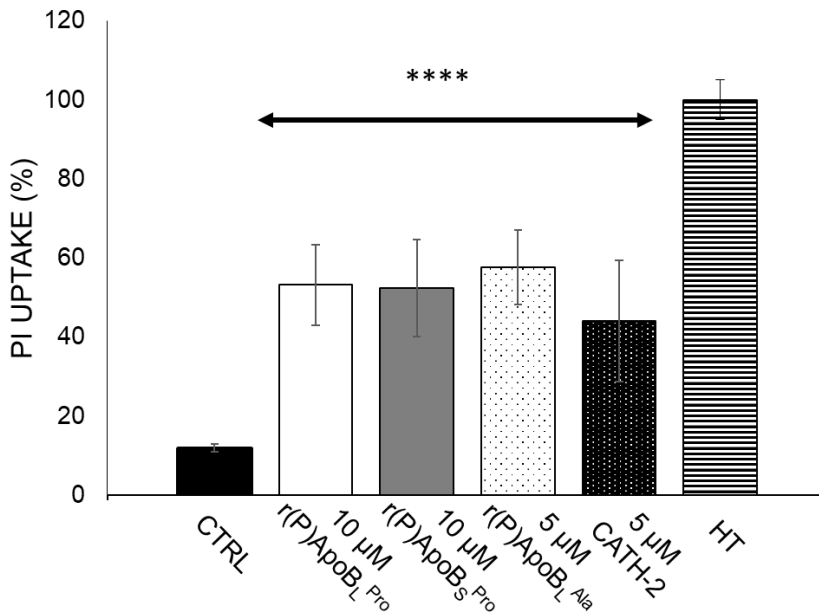


Figure 3. Propidium iodide (PI) influx in *Candida albicans* cells upon treatment with r(P)ApoBL^{Pro}, r(P)ApoBS^{Pro} and r(P)ApoBL^{Ala}. Heat treated (HT) *Candida albicans* ATCC 10231 cells have been used as positive control (dead cells). PI release was monitored by fluorimeter assays. The data represent the mean of three independent experiments (\pm SD), each one carried out in triplicate determination.

To support this finding, ApoB derived peptides effects on ATP leakage were analysed upon treatment of *Candida* cells with peptides for 10 and 60 min. Interestingly, it has been observed that r(P)ApoBL^{Pro}, r(P)ApoBS^{Pro} and r(P)ApoBL^{Ala} peptides are able to induce ATP release from *Candida albicans* cells after 10 min of incubation, with no further increase at 60 min, in agreement with peptide effects on propidium iodide uptake (Figure 4). Based on obtained results, it is possible to hypothesize a fast interaction between peptides and *C. albicans* cell membranes.

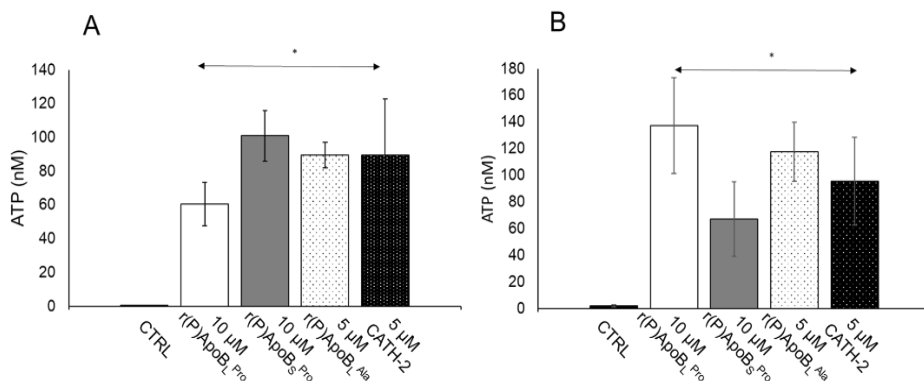


Figure 4. Peptide-induced ATP release. ATP concentrations in the culture medium are reported upon 10 (A) and 60 min (B) incubation with ApoB derived peptides. The graphs represent the data of three independent experiments (\pm SD), each one carried out in triplicate determinations.

3.3 Labelling of r(C)ApoB^LPro peptide

In order to produce a fluorescent version of r(P)ApoB^LPro peptide, a cysteine residue has been introduced instead of a proline at peptide N-terminus (**Pane et al. 2018**). Cysteine reactive residue has been then labelled with thiol-reactive probe 5-Iodoacetamidofluorescein (5'-IAF). Purification of labelled peptide has been allowed by the presence of an Asp-Cys dipeptide at the N-terminus of the peptide, useful to perform a selective acidic hydrolysis (**Pane et al. 2018**). This step allowed to separate the carrier protein from the peptide, which was then recovered by selective precipitation of the onconase carrier at pH 7.2. Peptide in the supernatant was then purified and analysed by RP-HPLC (Figure 5).

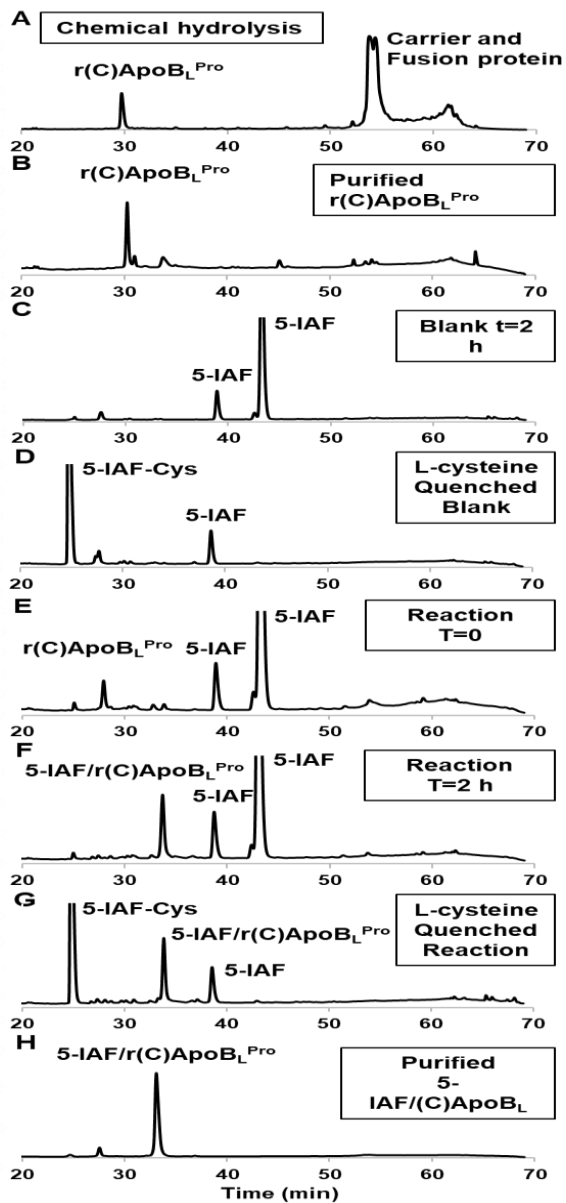


Figure 5. RP-HPLC analyses of the obtained IAF-r(C)ApoB_L^{Pro}.

3.4 Intracellular localization of ApoB derived peptides in *Candida albicans* cells

In order to further investigate the mechanism of action of ApoB derived peptides, live-imaging analyses were carried out. To this purpose, *Candida albicans* ATCC10231 cells were treated with

fluorescently labelled peptide r(C)ApoB_L^{Pro} at a concentration of 10 μ M for 30 min. Interestingly, fluorescent peptide immediately appears localized at fungal surface, with a progressive increase of fluorescence intensity over time. In agreement with this, a progressive uptake of propidium iodide was observed over time. This interestingly suggests that peptide interaction with yeast membranes is immediately responsible for a severe damage (Figure 6).

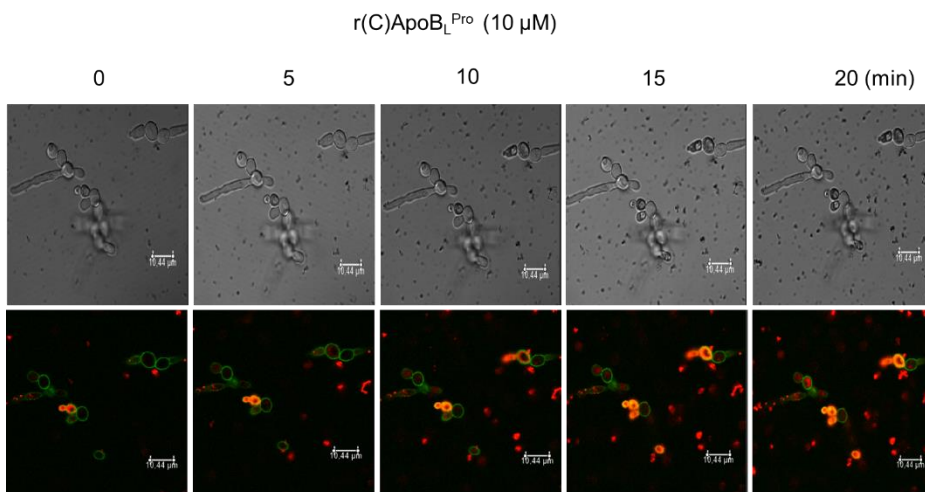


Figure 6. Analysis of intracellular localization of labelled r(C)ApoB_L^{Pro} peptide (green signal) and effects on propidium iodide (PI) uptake (red signal). The images are representative of at least three independent experiments. Scale bar 10 μ m.

3.5 ApoB derived peptides effects on *Aspergillus niger* N402

In order to deeply characterize the antifungal activity of ApoB derived peptides, experiments were performed on the filamentous fungus *Aspergillus niger* N402. To this purpose, metabolic activity of fungal spores in the absence or in the presence of increasing concentrations of peptides has been evaluated by performing WST-1 assays. Interestingly, r(P)ApoB_L^{Pro}, r(P)ApoB_S^{Pro} and r(P)ApoB_L^{Ala} peptides were found to be able to reduce *Aspergillus niger* N402 spores' metabolic activity in a concentration dependent manner (1.25-2.5 μ M) (Figure 7).

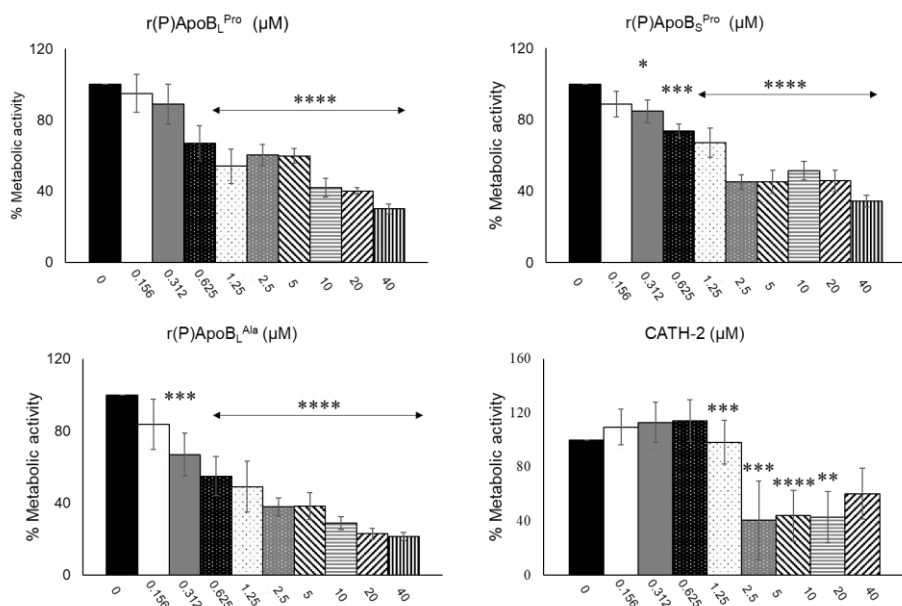


Figure 7. Effects of r(P)ApoBL^{Pro}, r(P)ApoBS^{Pro} and r(P)ApoBL^{Ala} on *Aspergillus niger* N402 spores' metabolic activity. WST-1 assay has been performed by incubating fungal spores with increasing concentrations of each peptide for 24 h. The data shown represent the mean of four independent experiments (\pm SD), each one carried out in triplicate determinations.

In the presence of unfavourable environmental conditions, filamentous fungi are forced to form spores. The switch from dormant spores to mycelia formation is associated to a defined sequence of events. During this process, fungi go through morphological changes associated to cell wall reorganization (**Wendland 2001**). On the basis of this peculiarity, experiments were performed to verify which stage of fungal growth was affected by treatment with ApoB derived peptides. Hence, swollen spores, germinating hyphae and branched mycelia were analysed. To analyse swollen spores, experiments were performed in complete MM for 6 h. Following incubation, increasing amounts of peptides were added and metabolic activity was analysed after 24 h (Figure 8). It was demonstrated that peptides are able to significantly affect swollen spores' metabolic activity. CATH-2 peptide was used as a positive control.

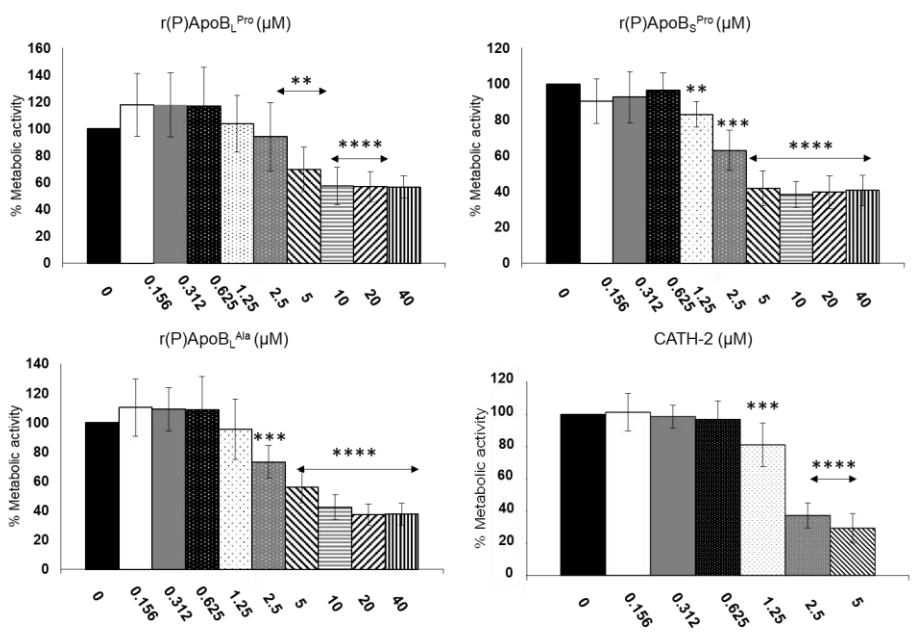


Figure 8. Effects of r(P)ApoB^{Pro}, r(P)ApoB_S^{Pro} and r(P)ApoB_L^{Ala} on *Aspergillus niger* N402 swollen spores. Metabolic activity was analyzed by incubating spores in MM for 6 h prior to peptide addition for 24 h. WST-1 assay was performed. The data shown represent the mean of four independent experiments (± SD), each one carried out in triplicate determinations.

Peptide effects on germinating hyphae were then analysed. To this purpose, *Aspergillus niger* N402 spores were incubated at least 16 h, in order to allow hyphae germination. ApoB derived peptides were then added for 24 h and WST-1 assay was performed at the end of the incubation. Interestingly, all the peptides have been found to significantly affect germinating hyphae metabolic activity even if stronger effects were observed at the highest peptide concentrations tested (Figure 9).

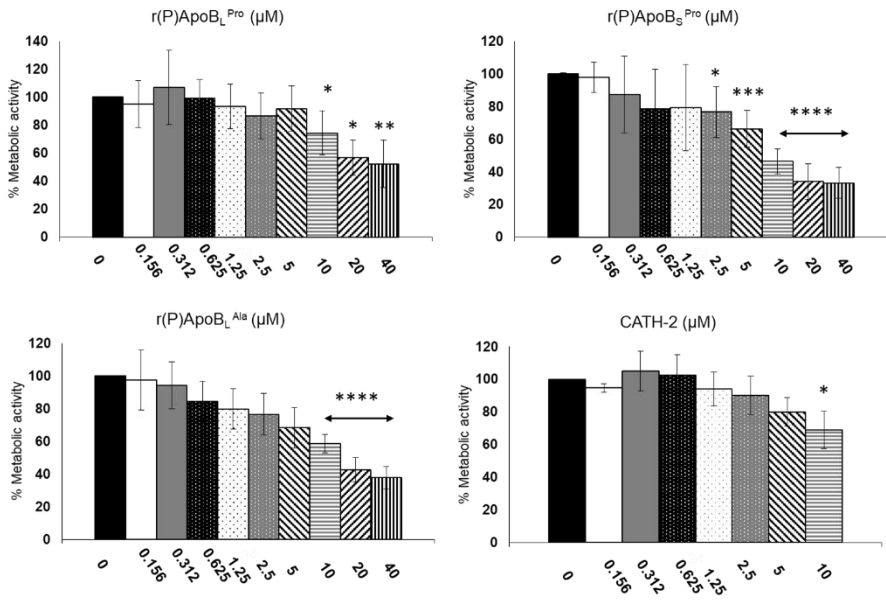


Figure 9. Effects of r(P)ApoB_L^{Pro}, r(P)ApoB_S^{Pro} and r(P)ApoB_L^{Ala} on *Aspergillus niger* N402 germinating hyphae. Spores were incubated in MM for 16 h prior to peptide addition for 24 h. WST-1 assay was performed. The data shown represent the mean of four independent experiments (± SD), each one carried out in triplicate determinations.

When branched mycelia were analysed, r(P)ApoB_L^{Pro} was found to be able to significantly reduce metabolic activity only at the highest concentration tested (40 μM), while CATH-2 control peptide, r(P)ApoB_S^{Pro} and r(P)ApoB_L^{Ala} were found to be ineffective (Figure 10).

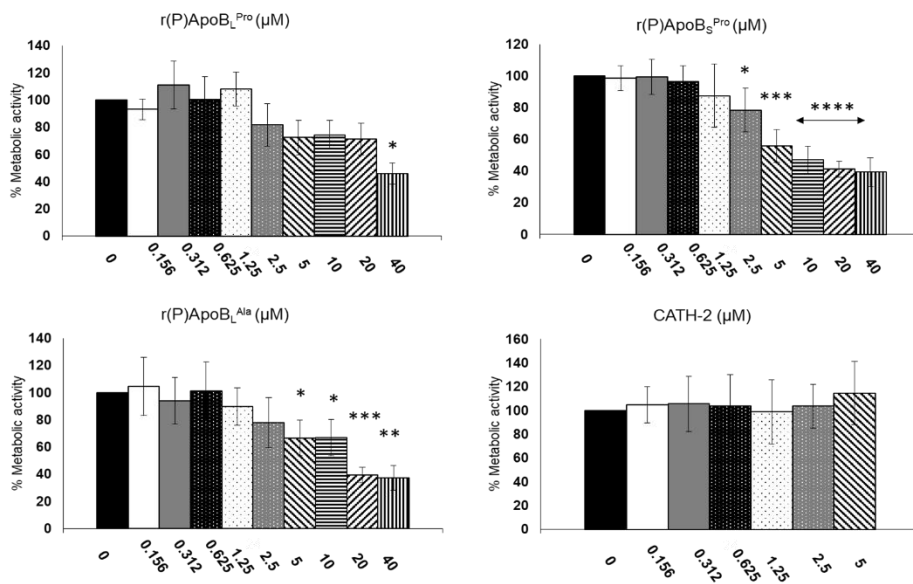


Figure 10. Effects of r(P)ApoB_L^{Pro}, r(P)ApoB_S^{Pro} and r(P)ApoB_L^{Ala} on *A. niger* N402 branched mycelium. Spores were incubated in MM for 24 h prior to peptide addition for further 24 h. WST-1 assay was performed. The data shown represent the mean of four independent experiments (\pm SD), each one carried out in triplicate determinations.

3.6 Analysis of fluorescently labelled r(C)ApoB_L^{Pro} internalization in fungal hyphae by live-imaging

In order to deeply characterize the effects of ApoB derived peptides on *Aspergillus niger* N402, fluorescently labelled peptide r(C)ApoB_L^{Pro} has been used to perform live-imaging analyses. To do this, *Aspergillus niger* spores have been incubated for 24 h in MM containing 10 μM peptide. Confocal laser scanning microscopy analyses, performed in real time, highlighted the ability of ApoB derived peptide to interact with swollen spores. Indeed, upon 16 h incubation, r(C)ApoB_L^{Pro} was found to accumulate into germinating spores, with a consequent accumulation into branched hyphae upon 24 h incubation (Figure 11).

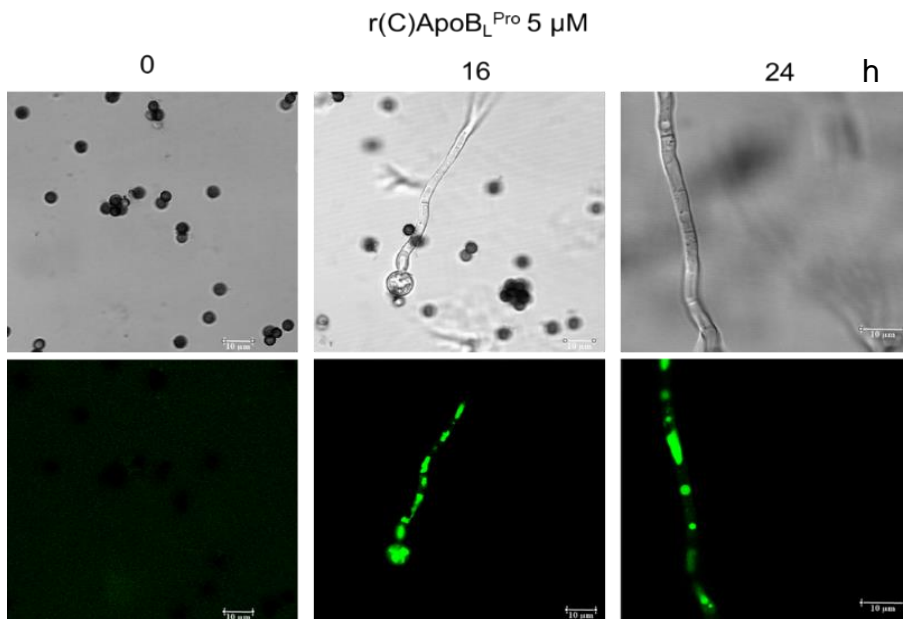


Figure 11. Localization of fluorescently labelled r(C)ApoB_L^{Pro} peptide in *Aspergillus niger* N402 hyphae. Images have been acquired at time 0 and after 16 and 24 h incubation. The images are representative of at least three independent experiments. Scale bar 10 μm.

4. Discussion

4.1 Antifungal activity of ApoB derived peptides towards yeasts

Yeasts and fungi are widespread organisms able to grow even in harsh conditions (Bahafid et al. 2017; Gulis and Bärlocher 2017). For this reason, microorganisms like fungi are able to contaminate food samples at any stage of the chain production. On the other hand, the intensive and increasing use of antifungals in agriculture, animal production and modern medicine leads to the fast development of resistant phenotypes (Kontoyiannis 2017). Along with antifungals misuse, the restricted number of effective antifungals raises up the resistance issue. Indeed, for the treatment of prolonged infections, azoles represent the only effective option treatment. For this reason, the isolation of *Aspergillus* triazole-resistant strains is a huge issue (Verweij et al. 2016). Also some *Candida spp.* strains have been found to be resistant to conventional antifungals (Healey et al. 2016; Lockhart et al. 2017). Hence, the

development of novel antifungal strategies based on novel effective molecules with peculiar mechanisms of action is imperative. In this scenario, host defence peptides play a key role because of their broad spectrum of activities and peculiar mechanisms of action (**Hancock and Le her 1998; Zasloff 2002; Brogden et al. 2003**). For this reason, the antifungal activity of ApoB derived peptides has been evaluated for the first time. Interestingly, r(P)ApoB^{L^{Pro}}, r(P)ApoB^{S^{Pro}} and r(P)ApoB^{L^{Ala}} peptides have been found to be endowed with significant fungicidal activity when tested on *Candida albicans* ATCC 10231. Moreover, ApoB derived peptides have been found to exploit their fungicidal action towards *Candida albicans* within 10 min of incubation at the MFC. Moreover, membrane-permeabilization assays highlighted an almost immediate interaction between ApoB derived peptides and *Candida albicans* cells, with a consequent damage and permeabilization of membranes. In all the cases, we observed similar effects for all the three peptides under test. Hence, fluorescently labelled r(C)ApoB^{L^{Pro}} peptide has been produced to deepen the mechanism of action of ApoB derived peptides antifungal activity. Interestingly, r(C)ApoB^{L^{Pro}} was immediately visualized on cell surfaces, with an almost concomitant uptake of propidium iodide into fungal cells. This phenomenon was found to progressively increase over-time. Similar observations have been reported for different host defence peptides, such as astacidin 1 identified in hemocyanin of the freshwater crayfish *Pacifastacus leniusculus*. This peptide was found to exert significant antifungal activity exploited through a pore-forming mechanism. Indeed, it has been reported that astacidin 1 peptide activity is mediated by disruption of *Candida albicans* cell membranes (**Choi and Lee 2014**). A similar mechanism of action has been also reported for CATH-2, LL-37 and histatin 5. These peptides have been found to be able to induce ATP leakage upon 5 min when tested on *Candida albicans* cells. Moreover, fluorescence microscopy analyses revealed that CATH-2 is able to immediately interact with *Candida albicans* cells, while LL-37 and Histatin 5 require about 3 min incubation prior to interaction with membranes (**Ordonez et al. 2014**). In this scenario, ApoB derived peptides behaviour appears in perfect agreement with previous findings. Altogether, obtained findings suggest ApoB derived peptides applicability in counteracting *Candida albicans* contaminations and infections.

4.2 Antifungal activity of ApoB derived peptides towards filamentous fungi

ApoB derived peptides have been also found to be able to affect metabolic activity of *Aspergillus niger* N402. Interestingly, analyses on swollen spores, germinating hyphae and branched mycelia highlighted that ApoB derived peptides are able to interact more efficiently with swollen spores and hyphae than with branched mycelia. These observations are in agreement with previous findings regarding the effects of Skh-AMP on *Aspergillus Famigatus*. Indeed, Skh-AMP was found to be able to affect spores' survival rate, even if at concentrations significantly higher than those required for ApoB derived peptides to exert significant effects. It has also to be noticed that, differently from Apo derived peptides, Skh-AMP was found to act on *Aspergillus* hyphae membranes more efficiently than on spores (**Khani et al. 2020**). This highlights the huge potentiality of ApoB derived peptides, that are able to act at lower concentration values and even on different fungal stages of growth. Finally, experiments performed by using fluorescently labelled r(C)ApoB^{Pro} peptide indicate an interaction of the peptide with swollen spores and its subsequent accumulation into hyphae. Plant defensins, extracted from chopea seeds, have been found to exert a good antifungal activity towards *Fusarium culmorum* even if MFC values on *Aspergillus* have been found to be higher than those reported for different antifungal peptides (**Schmidt, Arendt, and They 2019**), including ApoB derived peptides. Also chopea-thionin II has been found to be able to induce membrane permeabilization, confirming that the mechanism of action requires an initial interaction of the peptide with fungal cells, with consequent membrane permeabilization and cell lysis or, as here demonstrated for ApoB derived peptides, with consequent internalization into fungal swollen spores or germinating hyphae.

Altogether, obtained results suggest that ApoB derived peptides show significant effects on *Aspergillus niger*, and, even more importantly, they are endowed with additional properties with respect to previous identified antifungal peptides, such as lower MFC values and the ability to affect different stages of fungal growth.

References

- Alastruey-Izquierdo, A. et al. 2013. "Population-Based Survey of Filamentous Fungi and Antifungal Resistance in Spain (FILPOP Study)." *Antimicrobial Agents and Chemotherapy* 57(7): 3380–87.
- Badiee, Parisa, and Zahra Hashemizadeh. 2014. "Opportunistic Invasive Fungal Infections: Diagnosis & Clinical Management." *Indian Journal of Medical Research* 139(FEB): 195–204.
- Bahafid, Wifak et al. 2017. "Yeast Biomass: An Alternative for Bioremediation of Heavy Metals." In *Yeast - Industrial Applications*, InTech.
- Brogden, Kim A. et al. 2003. "Antimicrobial Peptides in Animals and Their Role in Host Defences." *International journal of antimicrobial agents* 22(5): 465–78. <http://www.ncbi.nlm.nih.gov/pubmed/14602364> (December 13, 2019).
- Brown, Gordon D. et al. 2012. "Hidden Killers: Human Fungal Infections." *Science Translational Medicine* 4(165).
- Choi, Hyemin, and Dong Gun Lee. 2014. "Antifungal Activity and Pore-Forming Mechanism of Astacidin 1 against *Candida Albicans*." *Biochimie* 105: 58–63.
- Van Dijk, Albert et al. 2007. "The β -Defensin Gallinacin-6 Is Expressed in the Chicken Digestive Tract and Has Antimicrobial Activity against Food-Borne Pathogens." *Antimicrobial Agents and Chemotherapy* 51(3): 912–22.
- Gaglione, Rosa et al. 2017. "Novel Human Bioactive Peptides Identified in Apolipoprotein B: Evaluation of Their Therapeutic Potential." *Biochemical Pharmacology* 130: 34–50.
- Gulis, Vladislav, and Felix Bärlocher. 2017. "Fungi: Biomass, Production, and Community Structure." In *Methods in Stream Ecology: Third Edition*, Elsevier Inc., 177–92.
- Hancock, Robert E.W., and Robert Lehrer. 1998. "Cationic Peptides: A New Source of Antibiotics." *Trends in Biotechnology* 16(2): 82–88.
- Healey, Kelley R. et al. 2016. "Prevalent Mutator Genotype Identified in Fungal Pathogen *Candida Glabrata* Promotes Multi-Drug Resistance." *Nature Communications* 7.
- Khani, Soghra et al. 2020. "Effects of the Antifungal Peptide Skh-AMP1 Derived from *Satureja Khuzistanica* on Cell Membrane Permeability, ROS Production, and Cell Morphology of *Conidia* and *Hyphae* of *Aspergillus Fumigatus*." *Peptides*.
- Kontoyiannis, Dimitrios P. 2017. "Antifungal Resistance: An Emerging Reality and a Global Challenge." *Journal of Infectious Diseases* 216: S431–35.
- Kontoyiannis, Dimitrios P., and Russell E. Lewis. 2002. "Antifungal Drug Resistance of Pathogenic Fungi." *Lancet* 359(9312): 1135–44.
- Leyva Salas, Marcia et al. 2017. "Antifungal Microbial Agents for Food Biopreservation—A Review." *Microorganisms* 5(3): 37. <http://www.mdpi.com/2076-2607/5/3/37> (December 7, 2019).

- Lockhart, Shawn R. et al. 2017. "Simultaneous Emergence of Multidrug-Resistant *Candida Auris* on 3 Continents Confirmed by Whole-Genome Sequencing and Epidemiological Analyses." *Clinical Infectious Diseases* 64(2): 134–40.
- Lowes, K. F. et al. 2000. "Prevention of Yeast Spoilage in Feed and Food by the Yeast Mycocin HMK." *Applied and Environmental Microbiology* 66(3): 1066–76.
- Ordonez, Soledad R. et al. 2014. "Fungicidal Mechanisms of Cathelicidins LL-37 and CATH-2 Revealed by Live-Cell Imaging." *Antimicrobial Agents and Chemotherapy* 58(4): 2240–48.
- Osherov, Nir, and Dimitrios P. Kontoyiannis. 2017. "The Anti-*Aspergillus* Drug Pipeline: Is the Glass Half Full or Empty?" In *Medical Mycology*, Oxford University Press, 118–24.
- Pane, Katia et al. 2018. "Chemical Cleavage of an Asp-Cys Sequence Allows Efficient Production of Recombinant Peptides with an N-Terminal Cysteine Residue." *Bioconjugate chemistry* 29(4): 1373–83.
- Pitt, John I., and Ailsa D. Hocking. 2009. "Introduction." In *Fungi and Food Spoilage*, Boston, MA: Springer US, 1–2.
- Schmidt, Marcus et al. 2019. "Isolation and Characterisation of the Antifungal Activity of the Cowpea Defensin Cp-Thionin II." *Food Microbiology* 82: 504–14.
- Tecla Ciociola et al. 2016. "Natural and Synthetic Peptides with Antifungal Activity." *Future Medicinal Chemistry*.
- Verweij, Paul E. et al. 2016. "Azole Resistance in *Aspergillus Fumigatus*: Can We Retain the Clinical Use of Mold-Active Antifungal Azoles?" *Clinical Infectious Diseases* 62(3): 362–68.
- Wendland, Jürgen. 2001. "Comparison of Morphogenetic Networks of Filamentous Fungi and Yeast." *Fungal Genetics and Biology* 34(2): 63–82.
- Zasloff, Michael. 2002. "Antimicrobial Peptides of Multicellular Organisms." *Nature* 415(6870): 389–95.
- Zhang, Li he, and Kaixian Chen. 2006. "Medicinal Chemistry." *Drug Discovery Today: Technologies* 3(3):

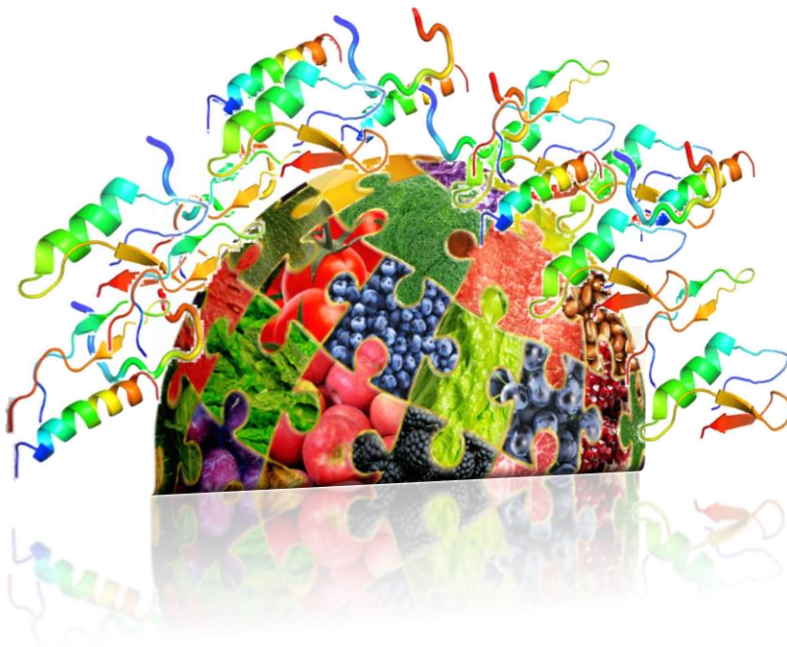
CHAPTER 4

Biocompatibility assessment of ApoB derived peptides

Eliana Dell'Olmo

Department of Chemical Sciences, PhD in Biotechnology

University of Naples "Federico II"



1. Introduction

1.1 Bio-preservation

Nowadays, main food additives and food preservatives are chemically defined substances. However, it has to be highlighted that synthetic food preservatives like nitrates, benzoates, sulphites, sorbates, and formaldehyde are known for their life-threatening side effects (**Kanta Das et al. 2014**). On the other hand, physical treatment, such as low temperature preservation, including freezing and refrigeration, or high temperature techniques like pasteurization, leads to the loss of organoleptic and nutrient features of foodstuff (**Singh 2018**). Hence, bio-preservation has gained great attention, since it represents the most reliable from 'farm to fork' concept. Indeed, in bio-preservation the antimicrobial potential of naturally occurring organisms and metabolites is exploited. Bio-preservation allows to preserve food samples by using natural compounds, such as animal-derived molecules (lysozyme, lactoferrin, and magainins), plant-derived products (phytoalexins, herbs, and spices) and microbial metabolites (bacteriocins, hydrogen peroxide, and organic acids) (**Lavermicocca et al. 2003**).

1.2 Biosafety evaluation of novel food additives

Several regulations impose that novel foods or novel food ingredients have to be legally approved before entering the market. Such regulations usually also require that these novel food ingredients have to be assessed for their safety (**Putten et al. 2011**). Safety assessment could be referred to different aspects, such as biocompatibility and allergy induction risks. Food allergy is a hypersensitivity reaction initiated by immunologic mechanisms in response to normally harmless food components. The prevalence ranges between 3 and 35% for self-reported allergies, and between 2 and 5% for reports based on objective measures, such as symptoms and sensitisation (**Rona et al. 2007**). In this scenario HDPs represent an attractive natural alternative as novel biopreservatives. Peptides as defensin and cathelicidin, normally produced in humans to play a key role in the immunomodulation, show a broad-spectrum antimicrobial activity in *in vitro* assays. In order to evaluate the safety of ApoB derived peptides as novel biopreservatives, experiments have been carried out on gastric and intestinal eukaryotic cell lines. Moreover, *in vitro* digestion analyses

have been performed and the pro-inflammatory potential of ApoB derived peptides has been also investigated.

2. Materials and methods

2.1 Chemicals and cell cultures

All the reagents were purchase from Sigma-Aldrich, unless differently specified. Gastric carcinoma cells SNU-1 (ATCC® CRL-5971™) and colon-rectal adenocarcinoma cells HT-29 (ATCC® HTB-38™) were from ATCC. Cells were cultured in Dulbecco's modified Eagle's medium or in RPMI 1640 supplemented with 10% fetal bovine serum (HyClone, GE Healthcare Lifescience, Chicago, IL) and antibiotics, in a 5% CO₂ humidified atmosphere at 37°C.

2.2 Biocompatibility assessment assays

Biocompatibility of r(P)ApoB_L^{Pro}, r(P)ApoB_S^{Pro} and r(P)ApoB_L^{Ala} on HT-29 and SNU-1 cells was determined by using the 3-(4,5-dimethylthiazol-2-yl)-2,5-diphenyltetrazolium bromide (MTT) assay. To this purpose, HT-29 and SNU-1 cells were plated into 96-well plates at a density of 5x10³ cells in 100 µL medium *per* well, and incubated overnight at 37°C. Afterwards, cells were treated with increasing concentrations (0 – 20 µM) of ApoB derived peptides for 24 h and 48 h at 37°C.

Following incubation, peptide-containing medium was removed, and 100 µL of MTT reagent, dissolved in DMEM without phenol red, were added to the cells (100 µL/well) at a final concentration of 0.5 mg/mL. After 4 h at 37°C, culture medium was removed, and the resulting formazan salts were dissolved by the addition of isopropanol containing 0.1 N HCl (100 µL/well). Absorbance values of blue formazan were determined at 570 nm using an automatic plate reader (Microbeta Wallac 1420, Perkin Elmer). In the case of SNU-1 cell line, upon treatment with peptides, plates were centrifuged at 1,000 rpm for 10 min. Following incubation, 50 µL of MTT solubilized in DMEM without phenol red were added to the cells. Upon 4 h at 37°C, DMSO in the molar ratio 1:5 with respect to the sample has been added to each well and incubated for 24 h at room temperature. Absorbance values of blue formazan were determined at 540 nm using an automatic plate reader (Microbeta Wallac 1420, Perkin Elmer). In all the cases, cell survival was expressed as the percentage of viable cells in the presence of the peptides, with respect to control cells grown in the absence of

peptide. The experiments have been carried out in triplicate, with triplicate determination.

2.3 *In silico* analyses to identify digestion sites in ApoB derived peptides sequence

Prediction of cutting sites for pepsin and trypsin enzyme has been performed by using “Peptide cutter tool” on ExPASy database as previously described (**Gasteiger et al. 2005**).

2.4 *In Vitro* Simulated Gastric Fluid (SGF) and Simulated Intestine Fluid (SIF) Assays

In vitro digestion of ApoB derived peptides has been performed as previously described (**Roesler and Rao 2001a**) with some modifications. Briefly, 100 μ L of r(P)ApoB_L^{Pro}, r(P)ApoB_S^{Pro} or r(P)ApoB_L^{Ala} have been tested in simulated gastric fluid (SGF) containing 0.32% (w/v) pepsin and 34 mM NaCl at pH 1.2 (**Astwood et al., 1996**), and in simulated intestinal fluid (SIF) containing 10 mg/mL trypsin in 50 mM KH₂PO₄ at pH 7.5 (**Roesler and Rao 2001b**). Preliminarily to the assay, both SGF and SIF mixtures have been pre-incubated at 37°C for 3 min in the absence of ApoB derived peptides. Peptides have been then added to SGF or SIF (1:1 v/v ratio and 1:20 v/v ratio, respectively) and the reaction mixtures have been subsequently incubated at 37°C for 0, 10, 30, 60, 120, and 180 min. The assay has been performed in duplicate for each experimental condition. Reactions have been stopped by adding 200 mM Na₂CO₃ (1:1 v/v ratio) and by heating at 100 °C for 3 min. Variations in r(P)ApoB_L^{Pro}, r(P)ApoB_S^{Pro} and r(P)ApoB_L^{Ala} levels upon incubation in SGF and SIF have been monitored by sodium dodecyl sulfate polyacrylamide-gel electrophoresis (SDS-PAGE, 18%) (**Laemmli, et al. 1970**) followed by densitometric analyses. Experiments have been carried out in duplicate.

2.5 ELISA assays

TNF- α levels have been determined by ELISA assay (DuoSet ELISA kits, R&D Systems, Minneapolis, MN) following the manufacturer’s instructions. Briefly, human THP-1 cells (2 x 10⁴ cells/well) were seeded into 96-well microtiter plates and grown to semi-confluency. After 24 h, culture medium was replaced with fresh medium containing peptides (5 or 20 μ M) and incubated for 24 h at 37°C. LPSs from *Escherichia coli* and *Pseudomonas aeruginosa* (1 μ g/mL) have been used as positive controls. In each

case, at the end of the incubation, culture supernatants have been collected, and centrifuged at 5,000 rpm for 3 min at room temperature, in order to remove cell debris. Samples have been then analyzed by reading absorbance values at 450 nm using 550 nm as a reference wavelength at an automatic plate reader (FLUOstar Omega, BMG LABTECH, Ortenberg, Germany). Experiments have been performed in duplicate, with quadruplicate determinations.

2.6 Statistical analyses

Statistical analysis was performed using a Student's t-Test. Significant differences were indicated as *($P < 0.05$), **($P < 0.01$) or ***($P < 0.001$).

3. Results

3.1 Evaluation of ApoB derived biocompatibility on gastrointestinal cells

One of the main features of novel food ingredients is their biocompatibility. This parameter has been evaluated by testing the toxicity of ApoB derived peptides towards SNU-1 and HT-29 cell lines, selected as models for stomach and intestine, respectively. To this purpose, eukaryotic cells have been incubated with increasing concentrations of r(P)ApoB^{L^{Pro}}, r(P)ApoB^{S^{Pro}} or r(P)ApoB^{L^{Ala}} for 24 and 48 h (Figure 1). Interestingly, ApoB derived peptides have been found to exert no toxic effects on both SNU-1 and HT-29 cells. These results let us to hypothesize that r(P)ApoB^{L^{Pro}}, r(P)ApoB^{S^{Pro}} and r(P)ApoB^{L^{Ala}} might be safe once they are ingested.

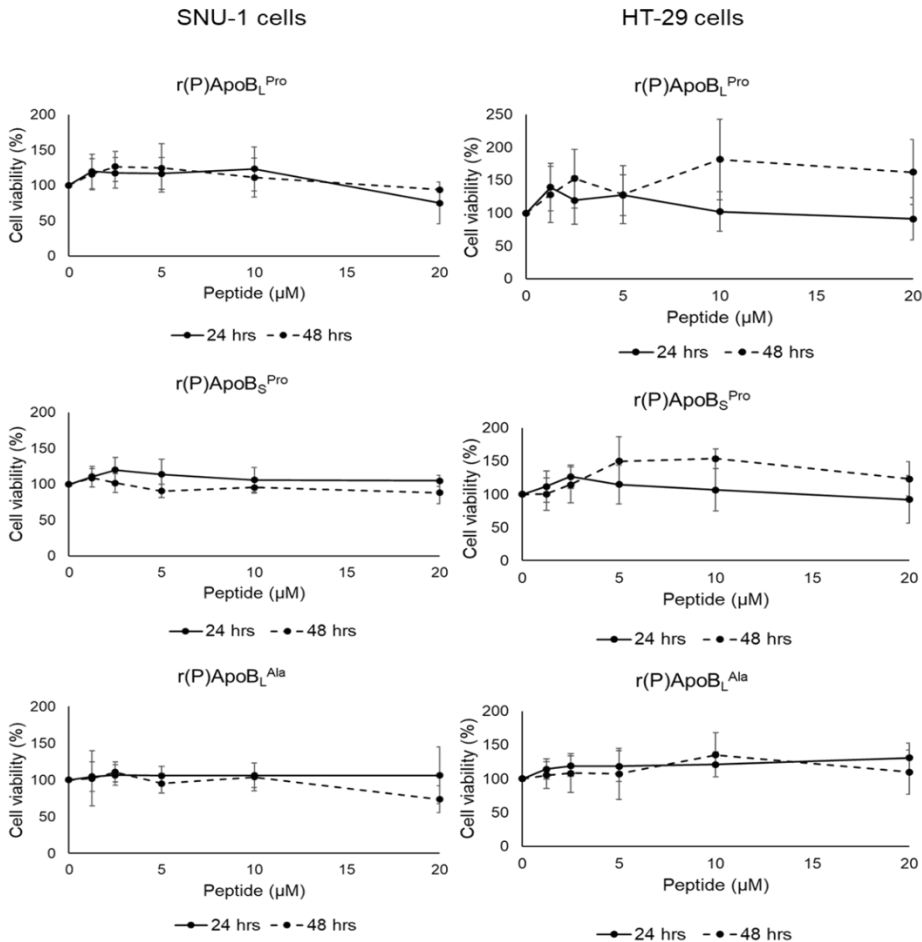


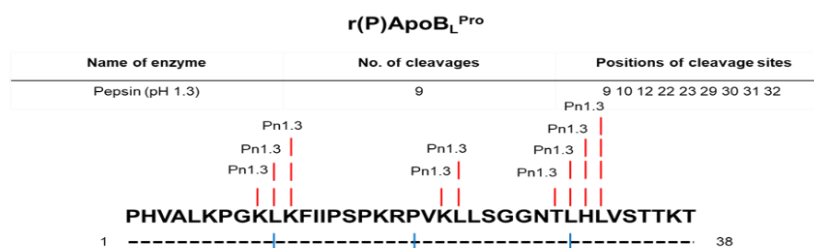
Figure 1. Effects of ApoB derived peptides on the viability of SNU-1 and HT-29 cell lines. MTT reduction assays were performed by treating cells with increasing concentrations (0-20 μM) of each peptide for 24 and 48 h. The data represent the mean of the values obtained in three different experiments, each one carried out in triplicate determinations.

3.2 *In silico* prediction of digestion sites in ApoB derived peptides sequence

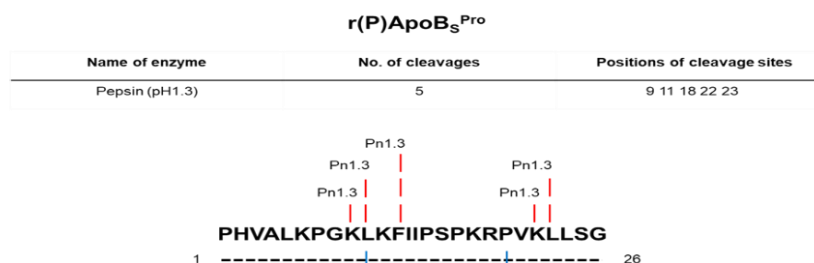
In order to investigate about ApoB derived peptides allergenic potential and their digestibility in the gastro-intestinal tract, *in silico* prediction of protease digestion sites has been carried out by using Peptide Cutter, a bioinformatic tool of ExPASy software. Pepsin and trypsin cleavage sites have been identified in all the peptides.

Interestingly, bioinformatic analyses allowed to identify a different number of cutting sites for r(P)ApoB_L^{Pro}, r(P)ApoB_S^{Pro} and r(P)ApoB_L^{Ala}. Indeed, it has been found that r(P)ApoB_L^{Pro} has 9 proteolytic sites recognized by pepsin enzyme while r(P)ApoB_L^{Ala} an additional site in correspondence of the substituted alanine (Figure 2, A-B-C). Peptide r(P)ApoB_S^{Pro}, instead, has only 5 cleavage sites recognized by pepsin enzyme, as expected on the basis of its shorter length.

A



B



C

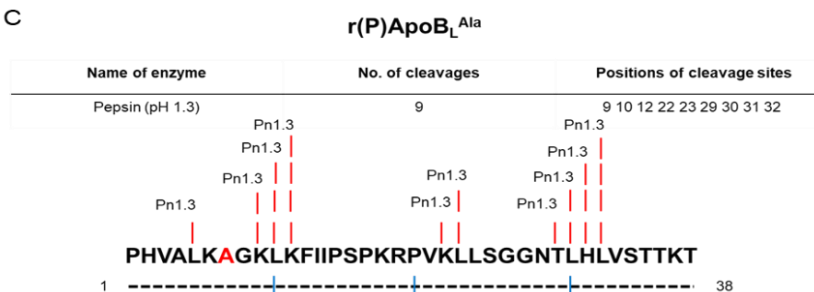
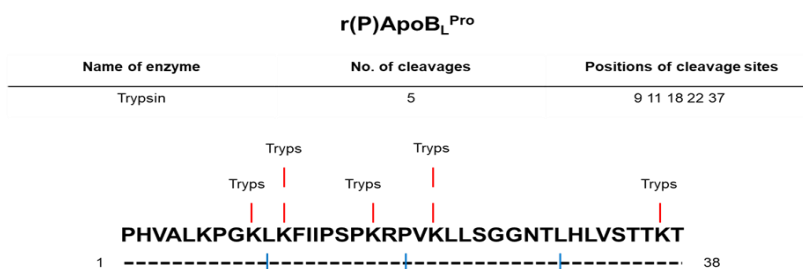


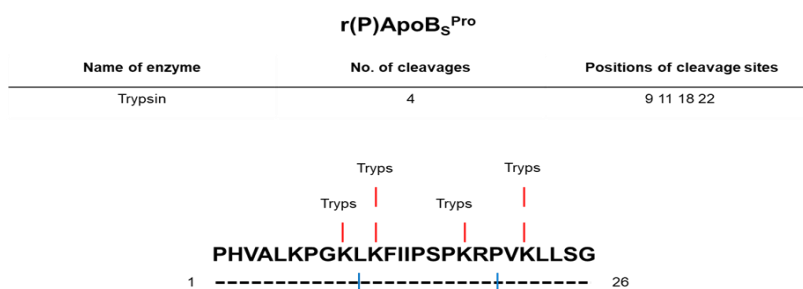
Figure 2. *In silico* identification of pepsin cleavage sites in ApoB derived peptides sequences. Analyses have been performed by using Peptide Cutter tool on ExSPAsy database. Tables show the total number and the position of each cleavage site in r(P)ApoB_L^{Pro} (A), r(P)ApoB_S^{Pro} (B) and r(P)ApoB_L^{Ala} (C).

Similar results have been obtained when trypsin cleavage sites have been identified in r(P)ApoB_L^{Pro}, r(P)ApoB_S^{Pro} and r(P)ApoB_L^{Ala}. Indeed, r(P)ApoB_L^{Ala} has been found to possess the highest number of cutting sites, whereas r(P)ApoB_S^{Pro} was found to present a lower number of cleavage sites (Figure 3, A-B-C).

A



B



C

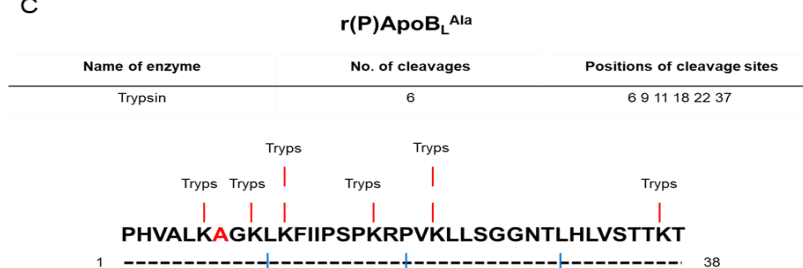


Figure 3. *In silico* identification of trypsin cleavage sites in ApoB derived peptides sequences. Analyses have been performed by using Peptide Cutter tool, on ExSPAsy database. Tables show the total number and the position of each cleavage site in r(P)ApoB_L^{Pro} (A), r(P)ApoB_S^{Pro} (B) and r(P)ApoB_L^{Ala} (C).

3.3 *In vitro* hydrolysis of ApoB derived peptides

Allergenic proteins or peptides are generally more resistant to proteases digestion than non-allergenic ones (**Anderson et al. 2006**). Thus, protein stability in the gastro-intestinal tract has been considered not only an indication of protein digestibility but also a proof of potential allergenic features (**Ekmay et al. 2017**). On the other hand, some proteins that are quickly degraded in the gastro-intestinal tract have been showed to induce allergy. This might be due to environmental conditions that can alter proteases activity (**Astwood et al. 1996**). Simulated Gastric Fluid (SGF) and Simulated Intestine Fluid (SIF) models are commonly used to preliminarily analyse allergenic potential of novel proteins or peptides to be employed in food preservation (**Williams et al. 2012**). For this reason, the stability of ApoB derived peptides in SGF and SIF have been tested by incubating peptides in a ratio of 1:1 and 1:20 in the case of pepsin and trypsin enzymes, respectively. Obtained mixtures have been incubated for 0, 10, 30, 60, 120 and 180 min. Afterwards, reactions have been stopped by adding 200 mM Na₂CO₃ for 3 min at 100 °C. SDS-page (18%) analyses have shown that r(P)ApoB^{L^{Pro}} is significantly degraded by pepsin within 10 min of incubation (about 50% protein degradation), and degradation was found to be even more pronounced (about 80% protein degradation) upon treatment with trypsin (Figure 4, A-B-C-D).

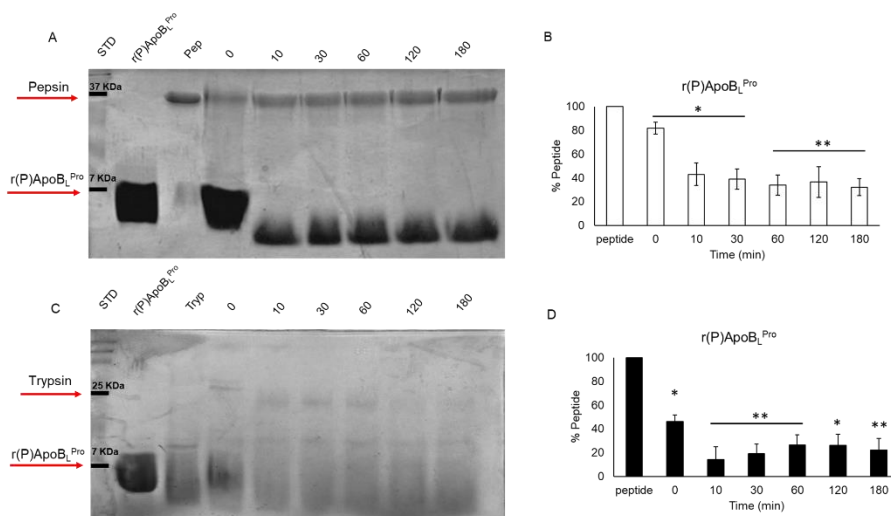


Figure 4. SDS-PAGE analyses of r(P)ApoB_L^{Pro} peptide hydrolysis in simulated gastric fluid (A) and simulated intestine fluid (C). Graphs reported in B and D have been obtained on the basis of protein bands intensity determined by densitometric analyses in the absence or in the presence of pepsin (B) or trypsin (D).

Peptide r(P)ApoB_S^{Pro} has been found to be more resistant to both pepsin and trypsin enzymes. Indeed, in SGF buffer only 50% of the peptide was found to be degraded and in SIF buffer the same percentage of degradation was observed even after 180 min of incubation (Figure 5, A-B-C-D).

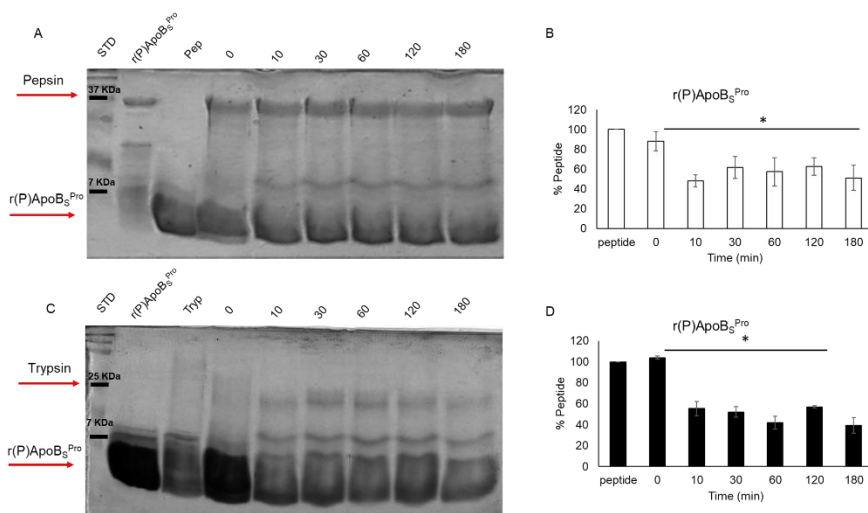


Figure 5. SDS-PAGE analyses of r(P)ApoB_S^{Pro} peptide hydrolysis in simulated gastric fluid (A) and simulated intestine fluid (C). Graphs reported in B and D have been obtained on the basis of protein bands intensity determined by densitometric analyses in the absence or in the presence of pepsin (B) or trypsin (D).

Regarding r(P)ApoB_L^{Ala} peptide, pepsin has been found to be able to degrade about 50 % of the peptide within 180 min of incubation. On the other hand, in SIF buffer, about 80% of the peptide has been degraded within 10 min of incubation (Figure 6).

Altogether, obtained results appear in agreement with bioinformatic predictions.

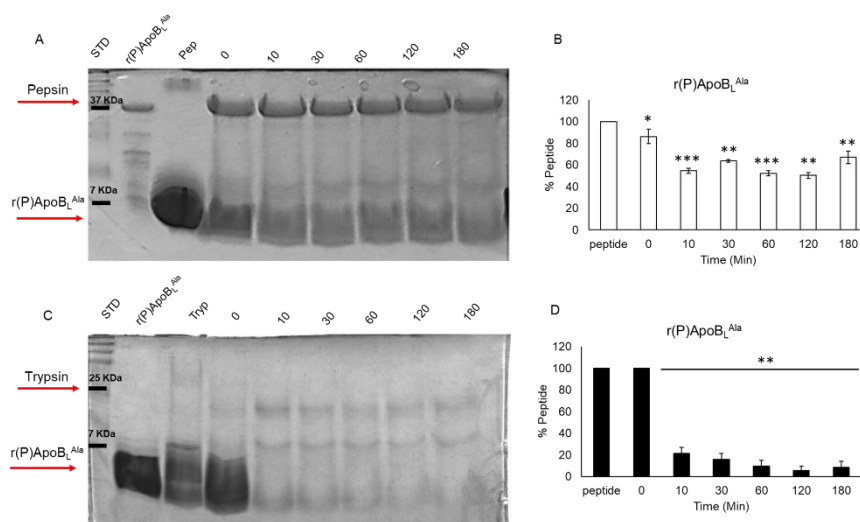


Figure 6. SDS-PAGE analyses of r(P)ApoB_L^{Ala} peptide hydrolysis in simulated gastric fluid (A) and simulated intestine fluid (C). Graphs reported in B and D have been obtained on the basis of protein bands intensity determined by densitometric analyses in the absence or in the presence of pepsin (B) or trypsin (D).

3.4 Analysis of pro-inflammatory activity of ApoB derived peptides

In the case of consumption of food of insufficient quality or in excessive quantity (**Food Insecurity Hunger United States 2006**), several negative effects are observed on human health, such as heart disease, diabetes, hypertension, hyperlipidemia, and poor mental health and depression (**Stuff et al. 2007; Pan et al. 2012; Gundersen and Ziliak 2015**). Immune-inflammatory pathways may represent a link between food insecurity and chronic diseases (**Bergmans et al. 2018a**). Indeed, it is well-known that the development of systemic inflammation can lead to the insurgence of many disorders, such as cancer, cardiovascular disease, and type II diabetes (**Coussens and Werb 2002; Mason and Libby 2015; Donath 2014**). Even if the correlation between such foods and an increased risk of inflammation has been established, few research works cover this field. The most common procedure to establish the inflammation risk associated to food samples, nutrients or bioactive compounds is the estimation of Dietary Inflammatory Index (DII), indicative of the ability of a defined diet to

induce or suppress inflammatory pathways (Cavicchia et al. 2009; Shivappa et al. 2014). DII provides information about the impact of food samples on different inflammation biomarkers, such as interleukin (IL)-1 β , IL-4, IL-6, IL-10, tumor necrosis factor α , and C-reactive protein (CRP) (Shivappa et al. 2014). This underlies the importance to evaluate the inflammatory potential of novel food additives and preservatives. Based on this, preliminary studies have been performed to evaluate the ability of ApoB derived peptides to induce inflammatory responses. To this purpose, TNF- α release has been monitored in THP-1 cells upon treatment with ApoB derived peptides (Figure 7). *E. coli* and *P. aeruginosa* LPSs have been used as positive controls. Interestingly, ApoB derived peptides have been found to have no effects on TNF- α release at both concentrations tested (5 and 20 μ M). Indeed, the amount of TNF- α produced upon stimulation with ApoB derived peptides is comparable to that observed in control untreated cells. Altogether, these observations support previous findings here described suggesting that ApoB derived peptides are safe molecules to be employed in food industry.

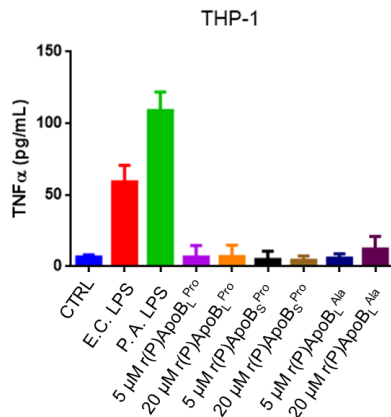


Figure 7. TNF- α production in THP-1 cells upon stimulation with 5 or 20 μ M r(P)ApoBL^{Pro}, r(P)ApoBS^{Pro} or r(P)ApoBL^{Ala}. The bars are representative of at least three independent experiments and the error is the standard deviation.

4. Discussion

4.1 Food safety assessment

Food safety has become one of the major issues worldwide. Increasing attention for “natural foods” along with the knowledge about side effects of chemical additives opened the way to the search of novel molecules to be employed as novel biopreservatives. However, when a novel food ingredient has to be released on the market, a careful evaluation of risk assessment is required (**Jain and Mathur 2015**). European Food Safety Authority recommends toxicological studies and dietary exposure assessment. Moreover, food preservatives along with food additives are under strict control of diverse government bodies. European Commission (EC) allows the introduction of a new food product or ingredient into the market only upon a careful evaluation of risk assessment conducted by European Food Safety Authority (EFSA). Within this risk assessment, EFSA reviews the dossier that is delivered by food business operator who requests authorisation for product of interest. In this occasion, health risks of the product are evaluated (**EC 2012/C 115/01 2012**). The main features of a novel food preservative are its biocompatibility and the absence of toxicological effects. Moreover, the assessment of the resistance to proteases is carried out and the evaluation of the immunogenic response is performed (**Neto et al. 2017**). Moreover, from 2011 EFSA recommends to test *in vitro* digestibility of novel food ingredients (**EFSA 2011**). One of the methods employed to study the digestibility of novel peptides and proteins in food industry is the evaluation of their resistance to pepsin and trypsin cleavage (**Thomas et al. 2004; Astwood et al. 1996**).

4.2 Biocompatibility assessment of ApoB derived peptides

Based on the regulations, ApoB derived peptides were here analyzed for their biocompatibility, digestibility, allergenic potential and inflammatory properties. To assess peptides biocompatibility, gastric and intestinal cell lines were analyzed. Interestingly, no toxic effects were exerted by peptides on SNU-1 and HT-29 cell lines in the experimental conditions tested. It has to be noticed that the substitution of a proline residue with an alanine in the longer peptide does not affect peptides biocompatibility. Since the introduction of novel peptides or protein-derived products in human diet might lead to the insurgence of allergy (**Verhoeckx et al. 2019**), allergenic risk

assessment is a key issue (**Verhoeckx et al. 2019**). For this reason, ApoB derived peptides sequences have been firstly analyzed by using a bioinformatic tool, such as Peptide cutter, to predict the presence of cutting sites recognized by pepsin and trypsin enzymes. Moreover, experiments have been carried out in simulated gastric fluid and simulated intestine fluid, in order to analyze the effects of the gastro-intestinal tract conditions on ApoB derived peptides stability. Interestingly, bioinformatic prediction highlighted that r(P)ApoB^{L^{Ala}} peptide presents the highest number of cleavage sites for both pepsin and trypsin enzymes, since an additional cutting site is acquired because of the substitution of a proline residue with an alanine. The short peptide r(P)ApoB^{S^{Pro}}, instead, appears to be the most stable because of its reduced length and the consequent absence of 4 cleavage sites present in the C-terminal region of the longer peptide r(P)ApoB^{L^{Pro}}. Bioinformatic predictions have been fully confirmed by *in vitro* digestion analyses. Indeed, only 50% r(P)ApoB^{S^{Pro}} was found to be degraded by pepsin and trypsin enzymes after 180 min incubation, whereas both r(P)ApoB^{L^{Pro}} and r(P)ApoB^{L^{Ala}} have been found to be completely hydrolyzed within 10 min incubation. Similar studies have been described for nisin peptide, and it has been reported that the peptide is completely digested only when it is incubated in the small intestine simulated fluid. Indeed, in oral and gastric digestion fluid, only 16% of total nisin has been found to be hydrolyzed (**Gough et al. 2017; Jarvis and Mahoney 1969**). These results suggest that once ApoB derived peptides are ingested for human consumption, they are immediately degraded, at a rate even higher than that described for peptides already in the market, thus representing good candidates for food preservation with no impact on human health.

4.3 ApoB derived peptides immunogenic response

Because of the well-established link between food and chronic inflammation, pro-inflammatory properties of ApoB derived peptides have been analyzed. In particular, TNF- α released by THP-1 cells upon treatment with ApoB derived peptides has been analyzed. Interestingly, peptides have been found to have no effects on TNF- α release, suggesting that they do not induce inflammatory responses. Hence, peptides appear not toxic for eukaryotic cell lines, are low stable in conditions simulating those of gastro-intestinal tract, and do not induce inflammatory reactions. Similar

features have been reported for nisin, a bacteriocin approved as a novel bio-preservative (**Elayaraja et al. 2014**). It has been reported that the main problems associated to HDPs human consumption are i) their toxicity, ii) immunogenicity, iii) drug resistance, iv) hemolytic activity and v) side effects (**Moravej et al. 2018**). As an example, Indolicidin has a broad spectrum antimicrobial activity, but also exerts haemolytic effects (**Mirski et al. 2017**). Although these peptides are small molecules and are endowed with no immunogenicity or less, putative immunogenicity is still a serious problem in peptide drug development. In a previous work, we already demonstrated that ApoB derived peptides have no haemolytic activity and are endowed with slight anti-inflammatory properties (**Gaglione et al. 2017**). Accordingly, ApoE derived peptides have been found to be able to bind to LPS molecules and consequently reduce expression levels of two cytokines, COX-2 and IL-8, suggesting a role in immunomodulation (**Zanfardino et al. 2018**). Similar results have been also obtained with ApoB derived peptides, suggesting that they are not only safe for human consumption, but they may have a beneficial effect on the immune-response. Altogether, obtained results suggest that ApoB derived peptides are promising novel biopreservatives to be employed in food industry.

References

- Anderson, Deverick J. et al. 2006. "Predictors of Mortality in Patients with Bloodstream Infection Due to Ceftazidime-Resistant *Klebsiella Pneumoniae*." *Antimicrobial Agents and Chemotherapy* 50(5): 1715–20.
- Astwood, James D. et al. 1996. "Stability of Food Allergens to Digestion in Vitro." *Nature Biotechnology* 14(10): 1269–73.
- Bergmans, Rachel S. et al. 2018. "Associations between Food Security Status and Dietary Inflammatory Potential within Lower-Income Adults from the United States National Health and Nutrition Examination Survey, Cycles 2007 to 2014." *Journal of the Academy of Nutrition and Dietetics* 118(6): 994–1005.
- Cavicchia, Philip P. et al. 2009. "A New Dietary Inflammatory Index Predicts Interval Changes in Serum High-Sensitivity." *J Nutr* 139(12): 2365–72.
- Coussens, Lisa M., and Zena Werb. 2002. "Inflammation and Cancer." *Nature* 420(6917): 860–67.
- Donath, Marc Y. 2014. "Targeting Inflammation in the Treatment of Type 2 Diabetes: Time to Start." *Nature Reviews Drug Discovery* 13(6): 465–76.
- EC 2012/C 115/01. 2012. "Commission Delegated Regulation (EU) No 244/2012 of 16 January 2012 Supplementing Directive 2010/31/EU of the European Parliament and of the Council on the Energy Performance of Buildings by

Establishing a Comparative Methodology Framework for Calculating.” Official Journal of the European Union: 28.

EFSA. 2011. “Guidance for Risk Assessment of Food and Feed from Genetically Modified Plants.” EFSA Journal 9(5): 2150. <http://doi.wiley.com/10.2903/j.efsa.2011.2150> (January 2, 2020).

Ekmay, Ricardo D. et al. 2017. “Allergenic Potential of Novel Proteins – What Can We Learn from Animal Production?” Regulatory Toxicology and Pharmacology 89: 240–43.

Elayaraja, Sivaramasamy et al. 2014. “Production, Purification and Characterization of Bacteriocin from *Lactobacillus Murinus* AU06 and Its Broad Antibacterial Spectrum.” Asian Pacific Journal of Tropical Biomedicine 4: S305–11.

Food Insecurity and Hunger in the United States. 2006. Food Insecurity and Hunger in the United States National Academies Press.

Gaglione, Rosa et al. 2017. “Novel Human Bioactive Peptides Identified in Apolipoprotein B: Evaluation of Their Therapeutic Potential.” Biochemical Pharmacology 130.

Gasteiger, Elisabeth et al. 2005. Protein Analysis Tools on the ExPASy Server 571 571 From: The Proteomics Protocols Handbook Protein Identification and Analysis Tools on the ExPASy Server.

Gough, Ronan et al. 2017. “Simulated Gastrointestinal Digestion of Nisin and Interaction between Nisin and Bile.” LWT - Food Science and Technology 86: 530–37.

Gundersen, Craig, and James P. Ziliak. 2015. “Food Insecurity and Health Outcomes.” Health Affairs 34(11): 1830–39.

Jain, Arushi, and Pulkit Mathur. 2015. “Evaluating Hazards Posed by Additives in Food: A Review of Studies Adopting a Risk Assessment Approach.” Current Research in Nutrition and Food Science 3(3): 243–55.

Jarvis, B., and R. R. Mahoney. 1969. “Inactivation of Nisin by Alpha-Chymotrypsin.” Journal of Dairy Science 52(9): 1448–50.

Kanta Das, Kamal et al. 2014. “Microbiological Analysis of Common Preservatives Used in Food Items and Demonstration of Their in Vitro Anti-Bacterial Activity Microbiological Analysis of Common Preservatives Used in Food Items and Demonstration of Their in Vitro Anti-Bacterial Activity Asian Pacific Journal of Tropical Disease.” Article in Asian Pacific Journal of Tropical Disease 4(6): 452–56.

Lavermicocca, Paola et al. 2003. “Antifungal Activity of Phenyllactic Acid against Molds Isolated from Bakery Products.” Applied and Environmental Microbiology 69(1): 634–40.

Mason, Justin C., and Peter Libby. 2015. “Cardiovascular Disease in Patients with Chronic Inflammation: Mechanisms Underlying Premature Cardiovascular Events in Rheumatologic Conditions.” European Heart Journal 36(8): 482–89.

- Mirski, Tomasz et al. 2017. "Utilisation of Peptides against Microbial Infections – a Review." *Annals of Agricultural and Environmental Medicine* 25(2): 205–10.
- Moravej, Hoda et al. 2018. "Antimicrobial Peptides: Features, Action, and Their Resistance Mechanisms in Bacteria." *Microbial Drug Resistance* 24(6): 747–67. <http://www.ncbi.nlm.nih.gov/pubmed/29957118> (February 28, 2020).
- Pan, Liping et al. 2012. "Food Insecurity Is Associated with Obesity among US Adults in 12 States." *Journal of the Academy of Nutrition and Dietetics* 112(9): 1403–9.
- Neto, Paula et al. 2017. "Effects of Food Additives on Immune Cells as Contributors to Body Weight Gain and Immune-Mediated Metabolic Dysregulation." *Frontiers in Immunology* 8(NOV).
- Putten, M. C.van et al. 2011. "Novel Foods and Allergy: Regulations and Risk-Benefit Assessment." *Food Control* 22(2): 143–57.
- Roesler, Keith R., and A. Gururaj Rao. 2001a. "Rapid Gastric Fluid Digestion and Biochemical Characterization of Engineered Proteins Enriched in Essential Amino Acids." *Journal of Agricultural and Food Chemistry* 49(7): 3443–51.
- Roesler, Keith R. et al. 2001b. "Rapid Gastric Fluid Digestion and Biochemical Characterization of Engineered Proteins Enriched in Essential Amino Acids." *Journal of Agricultural and Food Chemistry* 49(7): 3443–51.
- Rona, Roberto J et al. 2007. "The Prevalence of Food Allergy: A Meta-Analysis." *The Journal of allergy and clinical immunology* 120(3): 638–46.
- Shivappa, Nitin et al. 2014. "Designing and Developing a Literature-Derived, Population-Based Dietary Inflammatory Index." *Public Health Nutrition* 17(8): 1689–96.
- Singh, Veer Pal. 2018. "Recent Approaches in Food Bio-Preservation-A Review." *Open Veterinary Journal* 8(1): 104–11.
- Stuff, Janice E. et al. 2007. "Household Food Insecurity and Obesity, Chronic Disease, and Chronic Disease Risk Factors." *Journal of Hunger and Environmental Nutrition* 1(2): 43–62.
- Thomas, K. et al. 2004. "A Multi-Laboratory Evaluation of a Common in Vitro Pepsin Digestion Assay Protocol Used in Assessing the Safety of Novel Proteins." *Regulatory Toxicology and Pharmacology* 39(2): 87–98.
- Verhoeckx, Kitty et al. 2019. "The Relevance of a Digestibility Evaluation in the Allergenicity Risk Assessment of Novel Proteins. Opinion of a Joint Initiative of COST Action ImpARAS and COST Action INFOGEST." *Food and Chemical Toxicology* 129: 405–23.
- Williams, Hywel D. et al. 2012. "Toward the Establishment of Standardized in Vitro Tests for Lipid-Based Formulations. 2. the Effect of Bile Salt Concentration and Drug Loading on the Performance of Type I, II, IIIA, IIIB, and IV Formulations during in Vitro Digestion." *Molecular Pharmaceutics* 9(11): 3286–3300.
- Zanfardino, Anna et al. 2018. "Human Apolipoprotein E as a Reservoir of Cryptic Bioactive Peptides: The Case of ApoE 133-167." *Journal of Peptide Science*

CHAPTER 5

Design of novel ApoB peptides based active coatings for food industry applications

Eliana Dell'Olmo

Department of Chemical Sciences, PhD in Biotechnology

University of Naples "Federico II"



1. Introduction

1.1 Bacterial biofilm issues in food production

Foodborne pathogens are able to grow both as free-floating (planktonic) cells in a liquid aqueous phase and as interfaces or surfaces associated cells, because of their ability to adhere to different surfaces and to form biofilms **(Vreuls et al. 2010)**. Since bacteria in biofilm are embedded in a polymeric matrix with a protective function, they are more resistant to chemical and physical biocidal treatments **(Vreuls et al. 2010; Mah and O'Toole 2001; Stoodley et al. 2002; Gilbert, McBain, and Rickard 2003)**. Moreover, bacterial colonization is responsible for equipment corrosion, processing surface cross contamination, manufactured product contamination and spoilage **(Vreuls et al. 2010)**. The huge impact that food contamination and, consequently, foodborne illness have on economy and society requires the urgent development of alternative effective strategies to prevent bacterial attachment and growth **(Karam et al. 2013)**. Hence, the design of novel biopreservatives for food samples might be not enough to counteract contaminations. For this reason, among the main strategies adopted in food field, active packaging and the employment of antimicrobial surfaces have attracted great interest **(Coma 2008)**.

1.2 Active antimicrobial packaging

In the case of an active packaging, the product and the environment interact to prolong the shelf-life and to enhance food safety without altering qualities **(Suppakul et al. 2003)**. Different biopolymers, such as chitosan, have been proposed to set up novel biodegradable films and coatings. They have been selected for their properties comparable to those of commercialized plastic materials **(Harish Prashanth and Tharanathan 2007; Tharanathan and Kittur 2003)**. Chitosan is a polycationic polymer obtained from chitin recovery from shrimps and crabs through an alkaline deacetylation **(Rabea et al. 2003; López-Cervantes et al. 2007)**. This polymer is composed by glucosamine; hence, it is biocompatible, edible, and biodegradable. Moreover, it is also well-known for its antimicrobial and antifungal properties **(Raphaël and Meimandipour 2017)**. Many studies have been conducted to characterize the properties of chitosan edible films and coatings. Although chitosan has many

advantages, its antimicrobial activity is influenced by external factors, such as pH, molecular weight, grade of deacetylation, temperature and kind of food sample (**Batt 1992**). For this reason, several studies have been conducted to improve the antimicrobial features of chitosan, including the incorporation of antimicrobial substances and peptides in chitosan films (**Tin et al. 2009; Elsabee et al. 2008**).

1.3 Antimicrobial surfaces as a novel strategy to prevent biofilm attachment

It has been established that the first step in bacteria colonization is the adhesion of bacterial cells to a surface. For this reason, several strategies employed in food preservation aim to interfere with bacteria attachment. One of the main strategies is the coating of industrial surfaces with antimicrobial polymers or molecules. To this purpose, chitosan has been also used to develop antimicrobial surfaces, able to prevent adhesion of viable bacteria (**Campoccia et al. 2013; Banerjee et al. 2011; Siedenbiedel and Tiller 2012**). Through this PhD thesis, a coating solution based on chitosan (CH) functionalized with r(P)ApoB_L^{Pro} (CH-r(P)ApoB_L^{Pro}) has been developed. Obtained CH-r(P)ApoB_L^{Pro} coating has been characterized for its ability to prevent bacterial biofilm attachment of both *Salmonella typhimurium* ATCC[®] 14028 and *Salmonella enteritidis* 706 RIVM on different surfaces, such as polystyrene and more importantly the stainless steel (SS), which is commonly used for food industry equipment. Moreover, chitosan-based coatings have been tested for their ability to preserve chicken meat samples from microbial contaminations during 5 days of storage (CH-r(P)ApoB_L^{Pro}). To this purpose, a differential colony counting assay has been performed to discriminate between mesophilic and psychrophilic bacteria.

2. Materials and methods

2.1 Bacterial cells and growth conditions

Bacterial strains *Salmonella typhimurium* ATCC[®] 14028 and *Salmonella enteritidis* RIVM 706 were grown in Muller Hinton Broth (MHB, Becton Dickinson Difco, Franklin Lakes, NJ) or in 0.5X Nutrient broth (NB, Becton Dickinson Difco, Franklin Lakes, NJ) and on Tryptic Soy Agar (TSA; Oxoid Ltd., Hampshire, UK). In all the experiments, bacteria were inoculated and grown overnight in MHB

at 37°C. The next day, bacteria were diluted in fresh medium and grown to mid-logarithmic phase.

2.2 Preparation of film forming solutions

Chitosan (CH) stock solution (2%) was prepared by dissolving CH in 0.1 N HCl at room temperature under overnight constant stirring at 700 rpm (**Di Pierro et al. 2006; Sabbah et al. 2019**). Moreover, pectin (PEC) stock solution (4%) was prepared by dissolving PEC in Mill-Q water at room temperature under overnight constant stirring at 1,000 rpm (**Al-Asmar et al. 2018**). CH and PEC dipping solutions were diluted into Mill-Q water to obtain a concentration corresponding to 1.2%. pH value was adjusted to 4.5 by using NaOH 1 N. Final volume was set to 100 mL for all the solutions. r(P)ApoB_L^{Pro} peptide was added dropwise to CH and PEC at a final concentration of 5 µM under continuous stirring. Solution was then stirred for 1h before its use for dipping. Control samples were prepared in the same experimental conditions in the absence of the peptide. Dipping solutions were sterilized by exposure to UV light for 15 min. Film forming solutions have been prepared as describe above by using 0.6% chitosan and 2.5 µM r(P)ApoB_L^{Pro} peptide.

2.3 Surfaces functionalization

To functionalize plastic and glass, 150 µL of film forming solution were added and completely dried at 37°C in static conditions. Stainless steel plates 2-mm-thick were cut into pieces of 1 cm × 1 cm. Coupons were subsequently cleaned by ultrasonication for 10 min in the following solutions in a defined order: deionized water, acetone, ethanol, and deionized water. Once cleaned, coupons were activated by immersion in a piranha solution (H₂SO₄:H₂O₂, 3:1 v:v) for 30 min to produce a hydroxyl-enriched SS, or a SS-OH, surface (**Fan et al. 2005**). Finally, coupons were sterilized by exposure to UV light. To functionalize surfaces, 150 µL of chitosan itself or chitosan-r(P)ApoB_L^{Pro} film forming solution were added to the activated stainless-steel surface and desiccated completely at 37°C. Active biomaterial was then sterilized by exposure to UV light for 5 min.

2.4 Crystal violet assays

To test CH-r(P)ApoB_L^{Pro} film forming solution anti-biofilm activity, bacteria were grown over-night in MHB (Becton Dickinson Difco,

Franklin Lakes, NJ), and then diluted to 1×10^8 CFU/mL in 0.5X MHB medium. Cells were then plated into a 24 well plate containing functionalized surfaces. Assays were performed in static conditions at 37°C for 16 h. At the end of the incubation, crystal violet assays were performed as previously described. The experiment has been performed in triplicate.

2.5 Confocal laser scanning microscopy analyses

To assess the effects of the chitosan-r(P)ApoBL^{Pro} coating solution on biofilm attachment, Confocal Laser Scanning Microscopy analyses were performed. Bacterial biofilm was grown on functionalized glass cover-slips in 0.5X MHB medium, starting from a bacterial culture at a concentration of 2×10^8 CFU/mL, in static conditions at 37°C for 16 h. Upon incubation, non-adherent bacteria were removed by gently washing samples with sterile phosphate buffer. Viability of cells embedded into biofilm structure was determined by sample staining with LIVE/DEAD® BacLight™ Bacterial Viability kit (Molecular Probes ThermoFisher Scientific, Waltham, MA, USA). Staining was performed accordingly to manufacturer instructions. Biofilm images were captured by using a confocal laser scanning microscopy (Zeiss LSM 710, Zeiss, Germany) and a 63 X objective oil immersion system. Biofilm architecture was analysed by using the Zen Lite 2.3 software package. Each experiment was performed in triplicate. Images are 2.5D projections of biofilm structure obtained by confocal z-stack using Zen Lite 2.3 software. All images were taken under identical conditions and represent the average of at least three different acquisition fields. Scale bar corresponds to 10 μ m in all the cases. All images were taken under identical conditions.

2.6 Scanning electron microscopy analyses

To perform scanning electron microscopy (SEM) analyses, *Salmonella* cells from an over-night culture were diluted to about 2×10^8 CFU/mL, and then incubated into chamber wells containing stainless steel coupons treated with chitosan-r(P)ApoBL^{Pro} film forming solution, for 16 h at 37°C in static conditions. Following incubation, bacterial cells were fixed in 2.5% glutaraldehyde. Following over-night incubation, bacterial cells were washed three times in distilled water (dH₂O) and then dehydrated with a graded ethanol series: 25% ethanol (1×10min); 50% ethanol (1×10min);

75% ethanol (1×10min); 95% ethanol (1×10min); 100% anhydrous ethanol (3×30min). Bacterial cells deposited onto glass substrate were first sputter coated with a thin layer of Au-Pd (Sputter Coater Denton Vacuum Desk V) to allow subsequent morphological characterization using a FEI Nova NanoSEM 450 at an accelerating voltage of 5 kV with Everhart Tornley Detector (ETD) and Trough Lens Detector (TLD) at high magnification.

2.7 Chicken fillet coating and samples preparation

A defined amount of each sample of chicken meat (5 g each) was dipped in 1.2% chitosan (CH) or pectin film forming solution (PEC) with or without 5 μ M of r(P)ApoB_L^{Pro} (CH-r(P)ApoB_L^{Pro} or PEC-r(P)ApoB_L^{Pro}). In addition, chicken meat samples dipped in water in the presence or in the absence of r(P)ApoB_L^{Pro} peptide have been used as positive controls. Chicken samples have been dipped in each film forming solution for 30 sec. After that, samples have been dried under continuous flow at room temperature for 15 min. Finally, samples have been stored at 4 °C for 0, 3 and 5 days.

2.8 Determination of microbial load of stored chicken samples

Chicken meat samples have been aseptically transferred into a sterile plastic falcon tube and homogenized in 45 mL of 0.1% (w/v aqueous solution) sterile Buffered Peptone Water (BPW) for 1 min at room temperature. Once sample volume was adjusted to 50 mL, decimal serial dilutions were prepared in 0.1% BPW (1 mL of final volume), and 50 μ L of each dilution were inoculated into Plate count agar (PCA) growth medium for the total count (TVC) of viable bacteria. Therefore, each sample was plated on aerobic count plates and the incubation has been performed at 37°C for 24 h to count mesophilic bacteria and at 4° C for 4 days to count psychrophilic bacteria.

2.9 Statistical analyses

Statistical analysis was performed using a Student's t-Test. Significant differences were indicated as *(P < 0.05), **(P < 0.01) or ***(P < 0.001). In the case of the analysis of the significative variation between the samples CH with respect to CH-r(P)ApoB_L^{Pro}, one-way analysis of variance (ANOVA) has been performed. Statistical significance was accepted at p < 0.05 or p < 0.01.

3. Results

3.1 Analyses of anti-biofilm properties of r(P)ApoB_L^{Pro} based coating solutions

Here, it has been developed an active coating solution composed by chitosan functionalized with r(P)ApoB_L^{Pro}. The ability of this solution to prevent biofilm attachment has been here characterized. First of all, crystal violet assays have been performed on plastic (polystyrene) and on stainless steel coupons. To this purpose, polystyrene and stainless steel have been functionalized with 0.6% chitosan coating solution in the absence or in the presence of 2.5 μM r(P)ApoB_L^{Pro}. Not functionalized plastic and steel samples have been used as control samples. Interestingly, CH-r(P)ApoB_L^{Pro} has been found to be more efficient than chitosan itself to prevent bacterial biofilm attachment on plastic in the case of both *Salmonella typhimurium* ATCC® 14028 and *Salmonella enteritidis* RIVM 706. Indeed, a biofilm mass decrease of 80 % has been observed for *Salmonella typhimurium* ATCC® 14028 in the presence of CH-r(P)ApoB_L^{Pro} coating solution, whereas chitosan itself was found to have no significant effects. In the case of *Salmonella enteritidis* 706 RIVM, instead, chitosan itself was found to be effective, but an even more drastic reduction of biofilm biomass was observed in the presence of r(P)ApoB_L^{Pro} peptide (Figure 1).

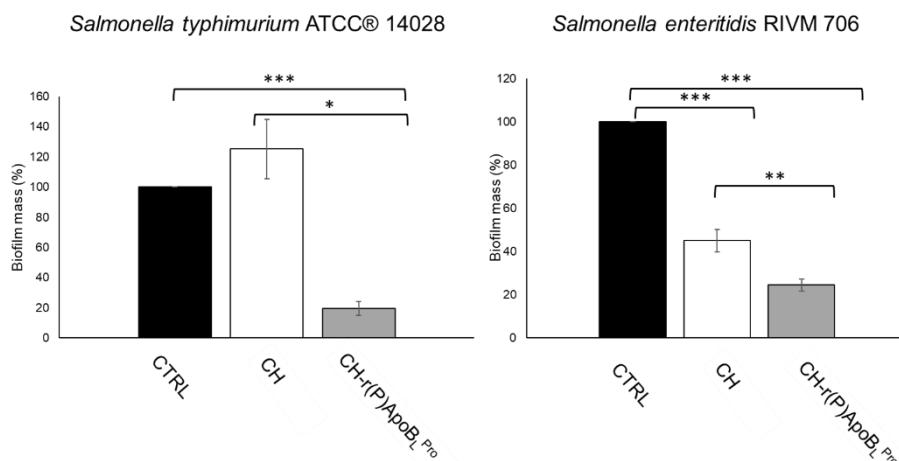


Figure 1. Crystal violet assays performed on functionalized polystyrene for *Salmonella typhimurium* ATCC® 14028 and *Salmonella enteritidis* RIVM 706. Histograms report the percentage

of biofilm mass for the control sample (black bar), for the surface functionalized with chitosan (white bar) and for chitosan functionalized with 2.5 μM r(P)ApoB_L^{Pro} (grey bar). The data represent the mean of three independent experiments ($\pm\text{SD}$), each one carried out in duplicate determination.

Similar results have been obtained when these novel coating solutions have been used to functionalize stainless steel coupons (Figure 2). In this case, chitosan solution appeared to be able to counteract bacterial attachment of *Salmonella typhimurium* ATCC® 14028 even if a stronger effect was observed in the presence of the peptide. On the other hand, in the case of *Salmonella enteritidis* RIVM 706, a severe reduction of biofilm attachment was observed in the presence of chitosan functionalized with r(P)ApoB_L^{Pro}, whereas chitosan itself was found to have no significant effects.

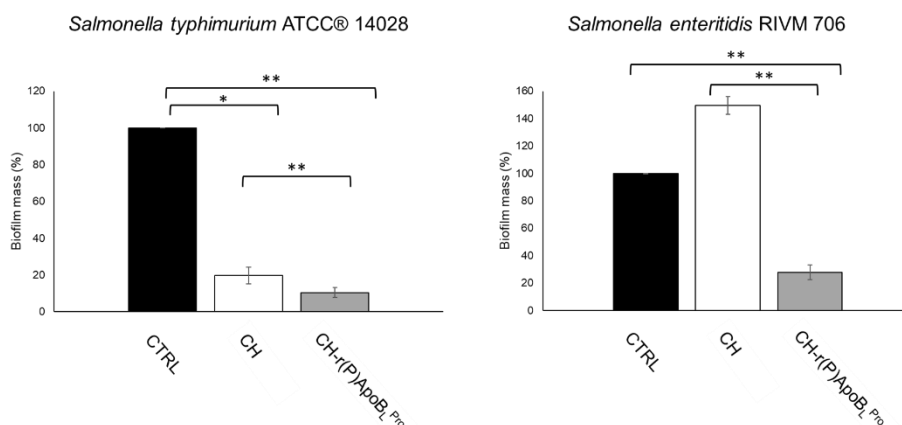


Figure 2. Crystal violet assays performed on functionalized stainless steel for *Salmonella typhimurium* ATCC® 14028 and *Salmonella enteritidis* RIVM 706. Histograms report the percentage of biofilm mass for the control sample (black bar), for the surface functionalized with chitosan (white bar) and for chitosan functionalized with 2.5 μM r(P)ApoB_L^{Pro} (grey bar). The data represent the mean of three independent experiments ($\pm\text{SD}$), each one carried out in duplicate determination.

3.2 Evaluation of CH-r(P)ApoB_L^{Pro} coating solution effects on static biofilm attachment

In order to further investigate anti-biofilm properties of designed coating solutions, glass cover slips have been functionalized with chitosan and CH-r(P)ApoB_L^{Pro} coating solutions to perform Confocal Laser Scanning Microscopy (CLSM) analyses. Interestingly, CH-r(P)ApoB_L^{Pro} coating solutions appear to strongly inhibit bacterial biofilm attachment in the case of both *Salmonella typhimurium* ATCC® 14028 and *Salmonella enteritidis* RIVM 706. In particular, *Salmonella typhimurium* ATCC® 14028 biofilm appears disrupted, many agglomerates are visible, most of the cells in planktonic form are alive, and biovolume appears significantly reduced (Figure 3). In the case of chitosan itself, instead, it is possible to observe an almost complete disruption of biofilm and a slight increase of biovolume (Figure 3).

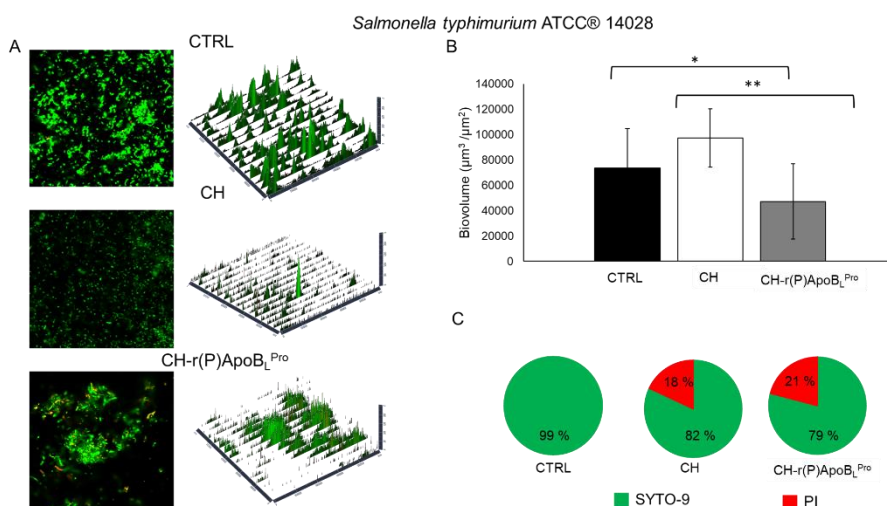


Figure 3. Confocal Laser Scanning Microscopy images of *Salmonella typhimurium* ATCC® 14028 biofilm attachment on not functionalized cover slips (black bar), cover slips functionalized with 0.6% chitosan (white bar) or functionalized with 0.6% chitosan containing 2.5 μM of r(P)ApoB_L^{Pro} (grey bar). Fluorescence images and 2.5D reconstructions of the biofilm matrix are reported (A). On the right side, biovolume (B) and viability analyses (C) are reported.

In the case of *Salmonella enteritidis* RIVM 706, biofilm appears drastically disrupted in the presence of CH itself and an even more dramatic effect is observed in the presence of r(P)ApoB_L^{Pro} (Figure 4).

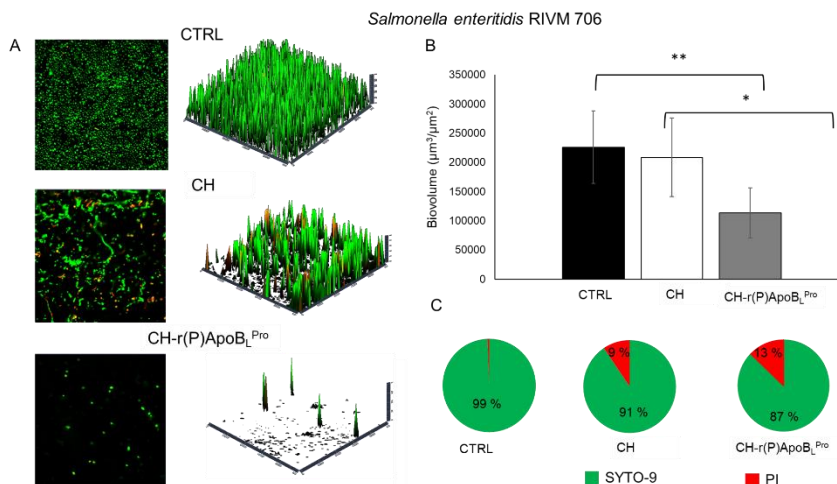


Figure 4. Confocal Laser Scanning Microscopy images of *Salmonella enteritidis* RIVM 706 biofilm attachment on not functionalized cover slips (black bar), cover slips functionalized with 0.6% chitosan (white bar) or functionalized with 0.6% chitosan containing 2.5 µM r(P)ApoB_L^{Pro} (grey bar). Fluorescence images and 2.5D reconstruction of biofilm matrix are reported (A). On the right side, biovolume (B) and viability analyses (C) are reported.

3.3 Scanning electron microscopy analyses

Stainless steel is the most common material employed in food industry equipment. The ability of foodborne pathogens to attach and colonize steel surfaces is a major issue in food safety, since bacteria in biofilm matrix cause persistent contaminations. For this reason, the ability of CH-r(P)ApoB_L^{Pro} solution to prevent bacterial attachment and biofilm formation has been evaluated by scanning electron microscopy (SEM) analyses. In the case of *Salmonella typhimurium* ATCC® 14028, bacterial biofilm attached on not functionalized stainless steel, cells appear turgid and with regular surfaces (Figure 5). In the case of chitosan itself, no significant effects on biofilm formation are evidenced. In the case of chitosan functionalized with the peptide CH-r(P)ApoB_L^{Pro}, significant drastic

effects on biofilm are evident, while single cells show a loss of electron dense material and corrugated surfaces.

Salmonella typhimurium ATCC® 14028

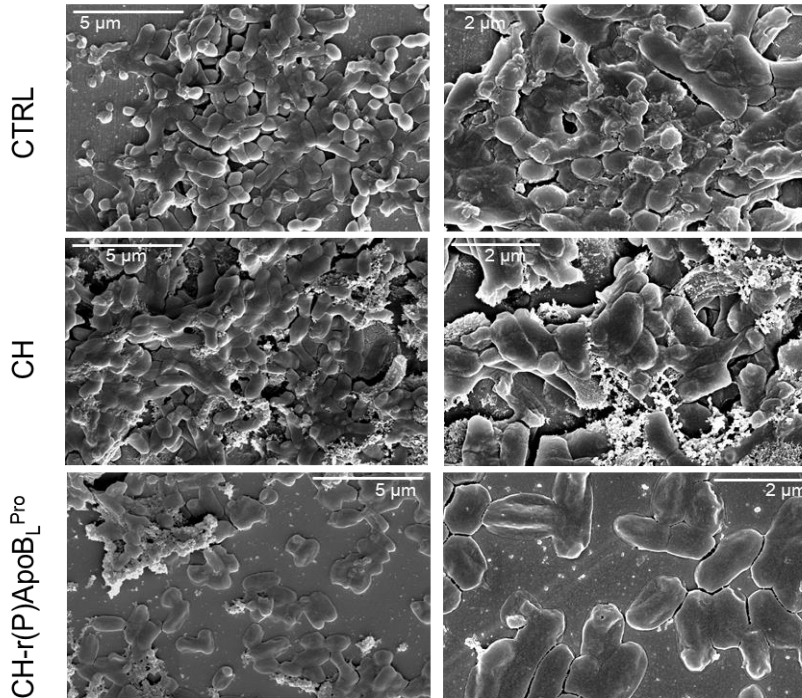


Figure 5. Scanning Electron Microscopy micrographs of *Salmonella typhimurium* ATCC® 14028. Images have been acquired at two different magnification: 25,000X (left side) and 50,000X (right side).

In the case of *Salmonella enteritidis* RIVM 706, a stronger effect was observed (Figure 6). Cells of the control sample appear turgid and able to form biofilm. In the presence of chitosan, strong effects on cell viability and a strong reduction in biofilm formation was detected (Figure 6, second line). In the presence of r(P)ApoBL^{Pro}, biofilm matrix appears thicker and cell surface appears even more corrugated than with chitosan alone (Figure 6, third line).

Salmonella enteritidis 706 RIVM

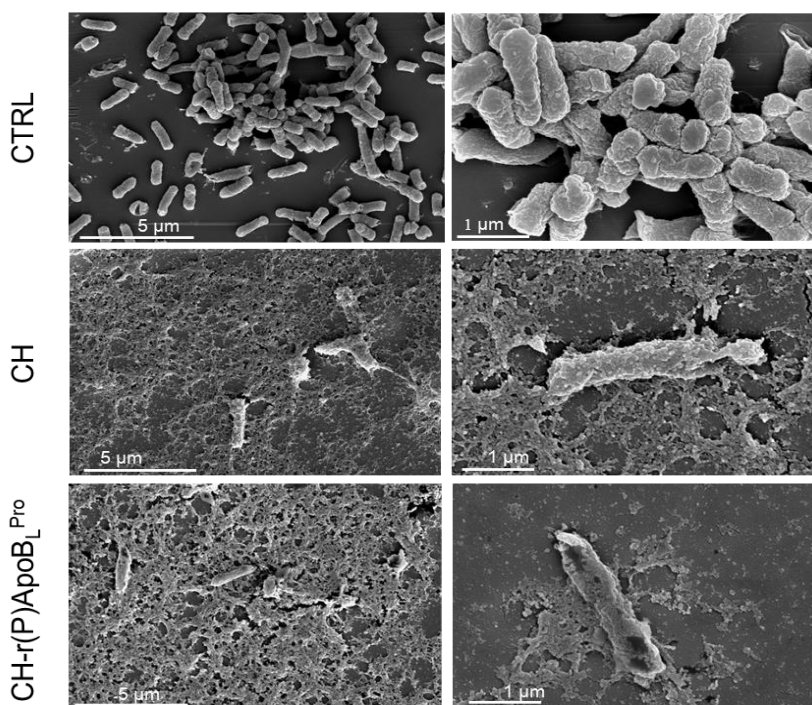


Figure 6. Scanning Electron Microscopy micrographs of *Salmonella enteritidis* RIVM 706. Images have been acquired at two different magnification: 25,000X (left side) and 80,000X (right side).

3.5 Effectiveness of CH-r(P)ApoBL^{Pro} in chicken meat storage

Meat is one of the most perishable of all industrially processed foods, since it contains enough nutrients to support the growth of microorganisms. Overall, chicken meat might be contaminated at several points along the food chain production. For this reason, CH and CH functionalized with 5 μ M r(P)ApoBL^{Pro} CH-r(P)ApoBL^{Pro} coating solutions have been checked for their ability to prevent chicken meat spoilage. For this reason, coating solutions have been used to coat chicken meat samples and content of mesophilic and psychrophilic bacteria has been evaluated during five days of storage. Pectin coating solution with or without the peptide has been used as a control, since it is well-known that this polymer is not endowed with antimicrobial properties. Moreover, chicken meat

samples treated with water containing or not r(P)ApoB_L^{Pro} have been used as prototype of uncoated samples. Interestingly, in the case of mesophilic bacteria analyses, upon 3 days of storage microbial load was found to be 1-Log lower with respect to control samples. Similar results were obtained also in the case of samples analysed upon a storage time of 5 days (Figure 7).

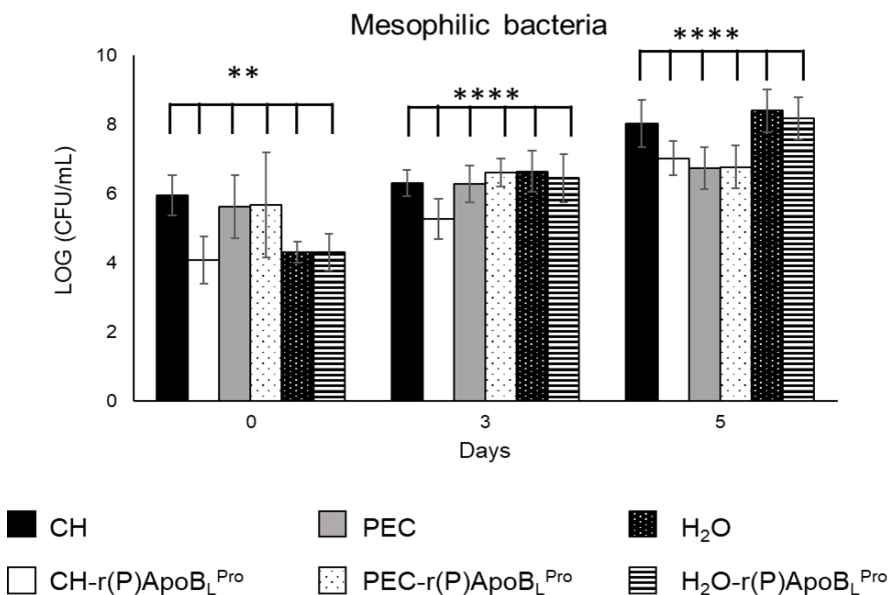


Figure 7. Total viable cells (TVC) of mesophilic bacteria were counted overtime for chicken meat samples coated with chitosan 1.2% (black bars), pectin 1.2% (grey bars) and H₂O (black dotted bars) in the absence or in the presence of 5 μM r(P)ApoB_L^{Pro} peptide.

Promising results have been obtained also in the case of psychrophilic bacteria (Figure 8). Notably, CH-r(P)ApoB_L^{Pro} keeps microbial load lower with respect to other systems during 5 days storage. Altogether, these results suggest that the designed coating solution is able to reduce the microbial load of chicken meat samples, thus opening interesting perspectives to its applicability in food preservation.

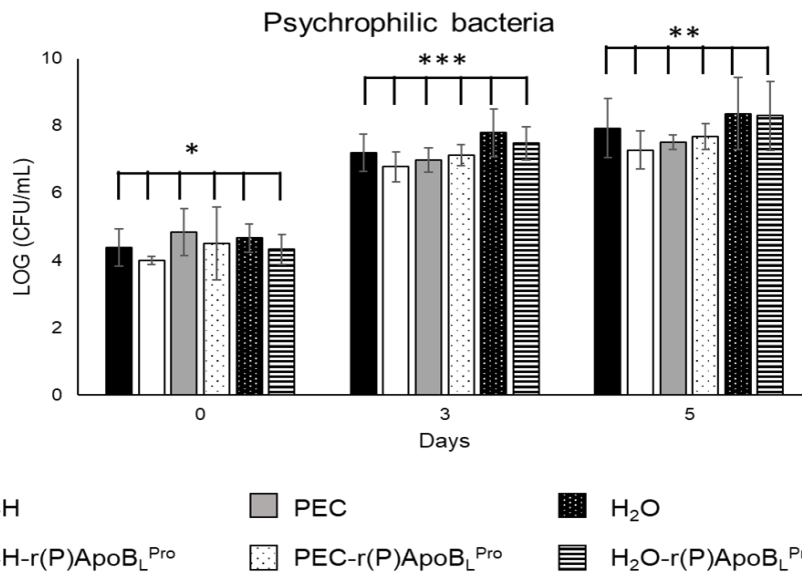


Figure 8. Total viable cells (TVC) of psychrophilic bacteria were counted overtime for chicken meat samples coated with chitosan 1.2% (black bars), pectin 1.2% (grey bars) and H₂O (black dotted bars) in the absence or in the presence of 5 μ M r(P)ApoB_L^{Pro} peptide.

4. Discussion

4.1 ApoB derived peptides in antimicrobial surfaces

Nowadays, it has been well established that the ability of many bacteria to adhere to surfaces and form biofilms is a huge economic and health issue (**Donlan 2002; Meyer 2003; Høiby et al. 2011**). Moreover, biofilm formation in industrial settings and equipment may have dramatic consequences, since resistant bacteria can easily spread along the food chain production. Mechanical removal of biofilms in industrial settings is effective even if expensive. Moreover, it is often a source of cellular debris dangerous for human health (**Swartjes et al. 2014**). An alternative to mechanical treatment is represented by antibiotics, but their misuse leads the insurgence of resistant bacteria. In this scenario, active packaging and antimicrobial surfaces have attracted great attention as promising effective alternatives to conventional antibiotics (**Campoccia et al. 2013; Banerjee et al. 2011; Siedenbiedel and Tiller 2012**). This strategy allowed not only to prevent biofilm

formation, but also to maintain bacteria in their planktonic form (**Swartjes et al. 2014**). Firstly, strategies have been based on the use of brushed polymers, such as polyethylene glycol (PEG), and it has been demonstrated their ability to decrease bacterial growth (**Nejadnik et al. 2008; Holmberg et al. 1993; Park et al. 1998**). Even if functionalized PEG surfaces were found to be endowed with antimicrobial activity, no complete prevention of biofilm attachment was observed (**Nejadnik et al. 2008**). In this context, antimicrobial coating formed by a biodegradable polymer functionalized with antimicrobial molecules is an attractive alternative. To this purpose, r(P)ApoB_L^{Pro} has been selected as a model peptide to set up novel coating solutions to be employed in food industry. Chitosan has been chosen as edible biopolymer endowed with well-known antimicrobial properties. Interestingly, the obtained CH-r(P)ApoB_L^{Pro} has been successfully applied to different surfaces. Indeed, when plastic surfaces have been functionalized with CH-r(P)ApoB_L^{Pro}, attachment of both *Salmonella typhimurium* ATCC® 14028 and *Salmonella enteritidis* RIVM 706 has been strongly inhibited. Moreover, confocal laser scanning microscopy analyses revealed that CH-r(P)ApoB_L^{Pro} is able to drastically reduce the number of bacterial cells adhering to stainless steel coupons with respect to both not functionalized and CH functionalized surfaces. This was demonstrated for *Salmonella typhimurium* ATCC® 14028 strain. In the case of *Salmonella enteritidis* RIVM 706, instead, even if CH itself was found to be effective in preventing attachment, membrane cells appear more damaged in the presence of the peptide. It has to be noticed that chitosan functionalization with r(P)ApoB_L^{Pro} has been carried out by electrostatic interactions, that is a cost-effective process with respect to more complicated strategies, such as covalent binding directly on the surface or the employment of a spacer (**Pinto et al. 2019**). Moreover, even when functionalization doesn't include a covalent bond formation, high concentrations of antimicrobial peptides are generally required. However, in the case of r(P)ApoB_L^{Pro}, good results have been obtained with a concentration of peptide very close to MIC value. These results suggest that CH-r(P)ApoB_L^{Pro} is a promising coating system to obtain effective antimicrobial surfaces.

4.2 ApoB derived peptides as components of active packaging

Even if the first requisite of a packaging system is to allow food transportation, the increasing demand for non-processed and high-quality food opened novel paths in food preservation. The main strategies are based on the set up and employment of novel antimicrobial edible packaging systems. Experiments have been conducted to test the effectiveness of CH-r(P)ApoB_L^{Pro} in the preservation of chicken meat samples. To this purpose, chicken samples have been treated with CH or CH-r(P)ApoB_L^{Pro} coating solutions and microbial load has been determined upon storage. Pectin films and water in the presence or in the absence of the peptide have been used as control samples. Obtained coating system CH-r(P)ApoB_L^{Pro} was found to be able to control microbial load in chicken meat until 5 days storage at 4 °C. It is worthy to note that chitosan is a biodegradable polymer as well as edible. In a previous work, the bacteriocin sonorensin has been used to set up biodegradable films based on the low density polyethylene polymer (**Chopra et al. 2015**). To this purpose, the concentration of the peptide has been increased about 10 fold with respect to MIC value, thus obtaining a very strong effect on the biofilm of *Staphylococcus aureus* and on chicken meat directly (**Chopra et al. 2015**). The system here developed is cheaper than the ones set up for sonorensin and, even more importantly, chitosan could be eaten by humans without risks. Altogether, these findings underlie the huge potential of CH-r(P)ApoB_L^{Pro} as a novel active packaging system to be employed in food industry.

References

- Al-Asmar, Asmaa et al. 2018. "Hydrocolloid-Based Coatings Are Effective at Reducing Acrylamide and Oil Content of French Fries." *Coatings* 8(4): 147.
- Banerjee, Indrani et al. 2011. "Antifouling Coatings: Recent Developments in the Design of Surfaces That Prevent Fouling by Proteins, Bacteria, and Marine Organisms." *Advanced Materials* 23(6): 690–718.
- Batt, Carl. 1992. "Book Review." *Food Microbiology* 9(1): 85.
- Campoccia, Davide et al. 2013. "A Review of the Biomaterials Technologies for Infection-Resistant Surfaces." *Biomaterials* 34(34): 8533–54.
- Chopra, Lipsy et al. 2015. "Sonorensin: A New Bacteriocin with Potential of an Anti-Biofilm Agent and a Food Biopreservative." *Scientific Reports* 5: 1–13.
- Coma, Véronique. 2008. "Bioactive Packaging Technologies for Extended Shelf Life of Meat-Based Products." *Meat Science* 78(1–2): 90–103.

- Donlan, Rodney M. 2002. "Biofilms: Microbial Life on Surfaces." *Emerging Infectious Diseases* 8(9): 881–90.
- Elsabee, Maher Z. et al. 2008. "Surface Modification of Polypropylene Films by Chitosan and Chitosan/Pectin Multilayer." *Carbohydrate Polymers* 71(2): 187–95.
- Fan, Xiaowu et al. 2005. "Biomimetic Anchor for Surface-Initiated Polymerization from Metal Substrates." *Journal of the American Chemical Society* 127(45): 15843–47.
- Gilbert, P., A. J. McBain, and A. H. Rickard. 2003. "Formation of Microbial Biofilm in Hygienic Situations: A Problem of Control." In *International Biodeterioration and Biodegradation*, Elsevier Ltd, 245–48.
- Harish Prashanth, K. V., and R. N. Tharanathan. 2007. "Chitin/Chitosan: Modifications and Their Unlimited Application Potential-an Overview." *Trends in Food Science and Technology* 18(3): 117–31.
- Høiby, Niels et al. 2011. "The Clinical Impact of Bacterial Biofilms." In *International Journal of Oral Science*, , 55–65.
- Holmberg, Krister et al. 1993. "Effects on Protein Adsorption, Bacterial Adhesion and Contact Angle of Grafting PEG Chains to Polystyrene." *Journal of Adhesion Science and Technology* 7(6): 503–17.
- Karam, Layal et al. 2013. "Study of Surface Interactions between Peptides, Materials and Bacteria for Setting up Antimicrobial Surfaces and Active Food Packaging." *J. Mater. Environ. Sci* 4(5): 798–821.
- López-Cervantes, J., D. I. Sánchez-Machado, and K. E. Delgado-Rosas. 2007. "Quantitation of Glucosamine from Shrimp Waste Using HPLC." *Journal of Chromatographic Science* 45(4): 195–99.
- Mah, Thien Fah C, and George A. O'Toole. 2001. "Mechanisms of Biofilm Resistance to Antimicrobial Agents." *Trends in Microbiology* 9(1): 34–39.
- Meyer, Bernhard. 2003. "Approaches to Prevention, Removal and Killing of Biofilms." In *International Biodeterioration and Biodegradation*, Elsevier Ltd, 249–53.
- Nejadnik, M. Reza, Henny C. van der Mei, Willem Norde, and Henk J. Busscher. 2008. "Bacterial Adhesion and Growth on a Polymer Brush-Coating." *Biomaterials* 29(30): 4117–21.
- Park, K D et al. 1998. "Bacterial Adhesion on PEG Modified Polyurethane Surfaces." *Biomaterials* 19(7–9): 851–59.
- Di Pierro, Prospero et al. 2006. "Chitosan–Whey Protein Edible Films Produced in the Absence or Presence of Transglutaminase: Analysis of Their Mechanical and Barrier Properties." *Biomacromolecules* 7(3): 744–49.
- Pinto, Ingrid Batista et al. 2019. "Utilization of Antimicrobial Peptides, Analogues and Mimics in Creating Antimicrobial Surfaces and Bio-Materials." *Biochemical Engineering Journal* 150: 107237.

- Rabea, Entsar I. et al. 2003. "Chitosan as Antimicrobial Agent: Applications and Mode of Action." *Biomacromolecules* 4(6): 1457–65.
- Raphaël, Kana Jean, and Amir Meimandipour. 2017. "Antimicrobial Activity of Chitosan Film Forming Solution Enriched with Essential Oils; an in Vitro Assay." *Iranian Journal of Biotechnology* 15(2): 111–19.
- Sabbah, Mohammed et al. 2019. "Development and Properties of New Chitosan-Based Films Plasticized with Spermidine and/or Glycerol." *Food Hydrocolloids* 87: 245–52.
- Siedenbiedel, Felix, and Joerg C. Tiller. 2012. "Antimicrobial Polymers in Solution and on Surfaces: Overview and Functional Principles." *Polymers* 4(1): 46–71.
- Stoodley, P., K. Sauer, D. G. Davies, and J. W. Costerton. 2002. "Biofilms as Complex Differentiated Communities." *Annual Review of Microbiology* 56(1): 187–209.
- Suppakul, P., J. Miltz, K. Sonneveld, and S.W. Bigger. 2003. "Active Packaging Technologies with an Emphasis on Antimicrobial Packaging and Its Applications." *Journal of Food Science* 68(2): 408–20.
- Swartjes, J.J.T.M. et al. 2014. "Current Developments in Antimicrobial Surface Coatings for Biomedical Applications." *Current Medicinal Chemistry* 22(18): 2116–29.
- Tharanathan, Rudrapatnam N., and Farooqahmed S. Kittur. 2003. "Chitin - The Undisputed Biomolecule of Great Potential." *Critical Reviews in Food Science and Nutrition* 43(1): 61–87.
- Tin, San, Kishore R. Sakharkar, Chu Sing Lim, and Meena K. Sakharkar. 2009. "Activity of Chitosans in Combination with Antibiotics in *Pseudomonas Aeruginosa*." *International Journal of Biological Sciences* 5(2): 153–60.
- Vreuls, C. et al. 2010. "Biomolecules in Multilayer Film for Antimicrobial and Easy-Cleaning Stainless Steel Surface Applications." *Biofouling* 26(6): 645–56.

CHAPTER 6

General discussion and concluding remarks

Eliana Dell'Olmo

Department of Chemical Sciences, PhD in Biotechnology

University of Naples "Federico II"



The overuse and misuse of conventional antibiotics in several fields is responsible for the fast emergence of bacteria no longer responsive to a panel of antimicrobial therapy (**Rydlo et al. 2006**). In the 2004, Mayrhofer and co-workers presented a study on 5 major foodborne pathogens, isolated from different meat samples. They demonstrated that *enterobacteriaceae* were highly resistant to a wide range of antimicrobials with different resistance phenotypes (**Mayrhofer et al. 2004**). Resistance rise of in foodborne pathogens has been considered from WHO as one of the main public health concerns (**Samson 2004; Holyoak et al. 1996; Lin et al. 1996; Park et al. 1996; WHO 2000**). Indeed, it has been reported that *Salmonella* infections cause 35% of hospitalization for food poisoning in United States (**Scallan et al. 2011**). Indeed, children and immunocompromised patients are more sensible to *Salmonella* infections with dramatic consequences for their health (**Maiti et al. 2014**). Moreover, in immunocompromised subjects *Salmonella* infections lead to the insurgence of life-threatening disorders, such as intestinal perforation, internal bleeding, neurological damage, and hypotensive shock (**Crump et al. 2004**) (**Stuart and Pullen 1946**). These microorganisms are also able to adhere to different surfaces and form biofilms (**Galié et al. 2018**). *Salmonella* is able to adhere to stainless steel, the material commonly used in food industry equipment, but is also capable to form biofilm on meat and other food samples, thus causing cross-contamination between food batches (**Galié et al. 2018; Wang et al. 2013**). To counteract the spread of resistant foodborne pathogens, many strategies have been developed. Food thermal processing is a procedure largely employed. It implies food exposure to temperatures comprised between 60 - 100 °C for several seconds to min. During this treatment, thermal energy is transferred to food in large amounts, with possible undesired organoleptic and nutritional effects. Moreover, synthetic food preservatives like nitrates, benzoates, sulphites, sorbates, and formaldehyde are also known for their life-threatening side effects (**Kanta Das et al. 2014**). Modifications of food organoleptic properties along with the increasing demand for mild-processed food samples opened the way for novel preservation techniques, such as bio-preservation (**Rydlo et al. 2006; Singh 2018; Bañón et al. 2007**). Bio-preservation is based on the use of natural compounds, including animal-derived systems (lysozyme, lactoferrin, and magainins), plant-derived products (phytoalexins,

herbs, and spices), and microbial metabolites (bacteriocins, hydrogen peroxide, and organic acids) (**Lavermicocca et al. 2003**). In this scenario, naturally occurring Host Defence Peptides (HDPs), first called Anti-Microbial Peptides (AMPs), have attracted considerable attention, since they are not harmful, and have the ability to preserve food without altering its quality (**Wang et al. 2016**). Bacteriocins peptides, produced by lactic acid bacteria, have been considered for years a promising class of molecules to be employed in food preservation (**Jung et al. 2016; Rydlo et al. 2006**). Indeed, they have several advantages, such as their broad-spectrum antibacterial activity (**Cleveland et al. 2001; Chen and Hoover 2003**). Nisin, a bacteriocin produced by *Lactococcus lactis*, has been approved by FDA as a novel bio-preservative. It is heat-stable, harmless and effective on Gram-positive bacteria, such as *Listeria monocytogenes* (**Santos et al. 2018**). On the other hand, beyond to be ineffective towards Gram-negative bacteria, its antimicrobial activity is strongly dependent from pH values. Indeed, at neutral pH nisin antibacterial activity is strongly compromised (**Jozala, Novaes, and Pessoa 2015**). For this reason, alternative peptides have been tested for their ability to preserve food. In this context, the present PhD thesis aimed to test novel host defence peptides, identified in human apolipoprotein B (**Pane et al. 2018; Gaglione et al. 2017**), for their effectiveness against foodborne pathogens, such as *Salmonella* strains. In the **Chapter 2**, it is reported that ApoB derived peptides are endowed with significant antimicrobial activity towards both *Salmonella typhimurium* ATCC® 14028 and *Salmonella enteritidis* 706 RIVM. Scanning electron microscopy analyses proved the ability of peptides to interact with bacterial membranes and to kill bacteria. ApoB derived peptides have been found to be able to affect *Salmonella* biofilm at sub-MIC concentration values. Indeed, confocal laser scanning microscopy analyses highlighted the ability of peptides to disrupt biofilm matrix and to affect its thickness. No increase in cell death has been, instead, observed. Obtained results highlighted that ApoB derived peptides are able to detach bacteria from surfaces without killing planktonic cells. This observation opens interesting perspectives to the employment of ApoB derived peptides in combination with other antimicrobial substances. For instance, to overcome nisin high selectivity towards gram positive bacteria, many combinations with natural substances, such as cinnamon (**Yuste and Fung 2004**) or chelating agents like

EDTA (**Schved et al. 1994**), have been developed. Moreover, peptides were found to be stable at temperatures of interest for industrial and storage processes (4, 28 and 60°C), with no significant effects on their antimicrobial activity. Moreover, when ApoB derived peptides have been tested for their chemical stability, significant effects on peptides antimicrobial activity have been found at pH 4.0, whereas no variation have been reported at pH 9.0. This is probably due to fact that peptides net charge, secondary structure, binding properties, and cytotoxic activity are affected by variations in pH value (**Rydlo et al. 2006**). The thermal stability of peptides allows to combine anti-biofilm properties of ApoB derived peptides with mild thermal processing in which the organoleptic properties of food samples are not affected. Similar strategies have been employed with nisin peptide, in order to counteract *E. coli* (**Lee et al. 2002**) and *Salmonella enteritidis* contaminations (**Esteban et al. 2013**). Besides bacteria, fungal contamination is also responsible for food spoilage, with consequences on economy and human health (**They et al. 2019**). Fungi are able to colonize a wide range of food samples because of their ability to grow in different environmental conditions (**Booth and Stratford 2003; Stratford et al. 2013; Pitt and Hocking 2009**), and to produce mycotoxins (**Oliveira et al. 2012**). One of the main problems associated with fungal contamination is the narrow spectrum of antifungal agents, with a consequent rapid insurgence of resistant fungal strains (**Lucas, Hawkins, and Fraaije 2015**). Fungi have been found to develop resistance to conventional antifungals, such as azoles (**Hawkins et al. 2014**), but also against some preservatives as propionic and sorbic acid used in bakery industry. In this scenario, natural antifungal peptides have attracted great interest. While many AMPs were found to inhibit the growth of bacteria and fungi, some peptides, including histatins or bacterial lipopeptides, specifically target fungi (**Matejuk et al. 2010**). Despite structural and sequence diversity, antifungal peptides present similar features, including small size and presence of cationic and hydrophobic residues (**They et al. 2019**). In **Chapter 3**, ApoB derived peptides antifungal properties have been investigated. Interestingly, r(P)ApoB^L^{Pro}, r(P)ApoB^S^{Pro} and r(P)ApoB^L^{Ala} were found to be able to kill *Candida albicans* ATCC 10231 upon only 10 min of incubation. Similar results have been obtained with control peptides CATH-2 and LL-37 (**Ordonez et al. 2014**). Propidium iodide influx assay and ATP-

leakage assay suggested a fast interaction between ApoB derived peptides and *Candida* cells. These results have been confirmed by real-time tracking of fluorescently labelled peptide r(C)ApoB_L^{Pro}. Indeed, it has been observed that the peptide immediately localizes on *Candida* cell surfaces, with consequent membrane damage and PI influx. A similar mechanism of action has been described for cathelicidins, even if their use has been limited by their haemolytic effects (**They et al. 2019; Chen and Hoover 2003**). Similar results have been also described for human defensin Histatin 5. This peptide is active against several *Candida* species, including foodborne strains. ATP-leakage assay and calcein release experiments confirmed an interaction with the membranes and with the mitochondria (**Puri and Edgerton 2014**). Further experiments may be performed in the future to deepen the mechanism of action of ApoB derived peptides. In **Chapter 3**, ApoB derived peptides have been found to be able to slow down metabolic activity of *Aspergillus niger* N402. Moreover, experiments performed on swollen spores, germinating hyphae and branched mycelia highlighted a preferential interaction of peptides with swollen spores and germinating hyphae. This suggests that fungal growth phase and consequent differences in cell wall composition and metabolic activity influence *Aspergillus niger* N402 susceptibility to peptides. Moreover, live-imaging experiments confirmed that fluorescently labelled peptide is internalized into swollen spores with consequent accumulation in hyphae. A similar mechanism of action has been observed also for Pf2, an albumin derived from *Passiflora edulis* able to inhibit conidial germination and hyphae elongation (**Meneguetti et al. 2017**). For both fungal strains, further experiments will be carried out to better clarify cellular targets of ApoB derived peptides. This will allow to create novel combinations with conventional antibiotics or with proper drug delivery systems to overcome fungal resistance phenotype. However, Pf2 cannot be used as food preservatives because of its allergenicity (**Moreno and Clemente 2008**). For this reason, in **Chapter 4**, potential side effects of ApoB derived peptides have been evaluated. Firstly, toxic effects have been studied on stomach and intestine derived cell lines, SNU-1 and HT-29, respectively. Interestingly, no toxic effects have been reported even at high peptide concentrations. By using a bioinformatic tool (**Gasteiger et al. 2005**), cleavage sites recognized by pepsin and trypsin enzymes have been predicted in peptides

sequences. Preliminary analyses revealed that r(P)ApoB_S^{Pro} is the most stable among ApoB derived peptides because of its shorter length. These results have been confirmed by *in vitro* digestion experiments conducted in Simulated gastric fluid and in Simulated intestine fluid (**Vermaak et al. 2009**), in the presence of pepsin and trypsin, respectively. Obtained results confirmed the greater stability of the shorter peptide that was found to be half degraded upon 180 min incubation. Longer peptides, instead, were found to be completely digested upon 10 min incubation in the case of both pepsin and trypsin enzymes. This is indicative of the absence of allergenic effects induced by ingestion of ApoB derived peptides, since they should be rapidly digested by gastric and intestinal processes. Indeed, proteins or peptides that are rapidly degraded into small peptides and amino acids can be considered less allergenic, since they are not able to resist to acidic conditions of digestive system (**Farias et al. 2015; Xu et al. 2009; Mathur et al. 2015**). These results pave the way to future studies. Firstly, experiments will be carried out to identify naturally occurring peptides released from human apolipoprotein B and, even more interestingly, different peptides will be probably identified in diverse physiological conditions. Secondly, chemically modified analogues will be developed in order to increase peptides stability to proteases. Finally, since it is well-established a link between food insecurity and inflammation (**Bergmans et al. 2018b**), preliminary studies on the pro-inflammatory potential of ApoB derived peptides have been carried out. To this purpose, the levels of tumour necrosis factor TNF- α secretion have been determined in THP-1 cells upon 24 h incubation with peptides. It has been demonstrated that ApoB derived peptides do not activate pro-inflammatory responses in human monocytes THP-1. Finally, in **Chapter 5**, the setup of novel antimicrobial surfaces and active packaging has been carried out. Antimicrobial surfaces are an alternative strategy to prevent biofilm attachment and formation (**Campoccia et al. 2013; Banerjee, Pangule, and Kane 2011; Siedenbiedel and Tiller 2012**). This is achieved not only by preventing biofilm adhesion, but also by maintaining bacteria in their planktonic form, more susceptible to antimicrobial treatments (**Swartjes et al. 2014**). Chitosan has been selected as a biodegradable and biocompatible polymer (**Anitha et al. 2014**) to be functionalized with r(P)ApoB_L^{Pro} peptide. Firstly, we

have obtained antimicrobial surfaces by using CH-r(P)ApoB_L^{Pro} solution to coat polystyrene and stainless steel, materials commonly used in food industry. Afterwards, the effects of obtained surfaces on *Salmonella typhimurium* ATCC® 14028 and *Salmonella enteritidis* RIVM 706 adhesion were analysed. Crystal violet assays showed that functionalized surfaces are able to prevent the adhesion of both *Salmonella typhimurium* ATCC® 14028 and *Salmonella enteritidis* RIVM 706. To further investigate the properties of CH-r(P)ApoB_L^{Pro}, confocal laser scanning microscopy and scanning electron microscopy analyses have been carried out. These analyses confirmed the ability of functionalized chitosan to prevent bacteria adhesion. In the case of *Salmonella typhimurium* ATCC® 14028, a drastic cell death has been also evidenced. Chitosan itself was found to be able to prevent the attachment of *Salmonella enteritidis* RIVM 706. However, in the presence of the peptide, more severe membranes damages were observed. CH-r(P)ApoB_L^{Pro} solution was also used to coat chicken samples, in order to prevent meat spoilage. Active packaging is an innovative approach to maintain or prolong the shelf-life of food products while ensuring their quality, safety, and integrity (Yildirim et al. 2018). As affirmed in European regulation (EC) No 450/2009, active packaging comprises packaging systems that interact with food samples in such a way as to “deliberately” incorporate components that would be released or absorbed into or from the packaged food or the environment surrounding the food” (European Committie 2009). Active packaging can be loaded with antimicrobial substances, such as HDPs. The addition of active substances, through the use of AP instead of direct addition to food, may decrease the amount of required substances (Yildirim et al. 2018). For this reason, CH-r(P)ApoB_L^{Pro} has been used to store chicken meat for 5 days at 4 °C. Obtained results indicate that it is able to efficiently control microbial load in stored samples. Active packaging systems functionalized with antimicrobial peptides are very advantageous, since they allow to preserve peptides from food matrix and from adverse conditions. Further experiments could be aimed at understanding the kinetic of peptides release from antimicrobial coatings and surfaces, but also at improving the effectiveness towards food-borne pathogens. Moreover, it has been highlighted that r(P)ApoB_L^{Pro} and r(P)ApoB_L^{Ala} peptides exert similar effects. Ongoing experiments are aimed at understanding if peptides are

different from a chemical-physical point of view. In particular, experiments performed in the presence of the LPS highlighted that r(P)ApoB_L^{Pro} is able to form fibrillar structure that are not visible in the case of r(P)ApoB_L^{Ala}, thus suggesting that the two peptides might act through different mechanisms of action. In conclusion, ApoB derived peptides have been found to be endowed with significant antimicrobial and anti-biofilm activities towards both *Salmonella typhimurium* ATCC® 14028 and *Salmonella enteritidis* RIVM 706 strains. Moreover, strong antifungal activities have been also demonstrated for ApoB derived peptides, which have been found to be safe, not allergenic, and characterized by high digestibility. These peptides have been also found to efficiently work in active packaging systems, what opens interesting perspectives to their applicability in food industry applications.

References

- Anitha, A. et al. 2014. "Chitin and Chitosan in Selected Biomedical Applications." *Progress in Polymer Science* 39(9): 1644–67.
- Banerjee, Indrani, Ravindra C. Pangule, and Ravi S. Kane. 2011. "Antifouling Coatings: Recent Developments in the Design of Surfaces That Prevent Fouling by Proteins, Bacteria, and Marine Organisms." *Advanced Materials* 23(6): 690–718.
- Bañón, Sancho et al. 2007. "Ascorbate, Green Tea and Grape Seed Extracts Increase the Shelf Life of Low Sulphite Beef Patties." *Meat Science* 77(4): 626–33.
- Bergmans, Rachel S. et al. 2018. "Associations between Food Security Status and Dietary Inflammatory Potential within Lower-Income Adults from the United States National Health and Nutrition Examination Survey, Cycles 2007 to 2014." *Journal of the Academy of Nutrition and Dietetics*.
- Booth, I. R., and M. Stratford. 2003. "Acidulants and Low PH." In *Food Preservatives*, Springer US, 25–47.
- Campoccia, Davide et al. 2013. "A Review of the Biomaterials Technologies for Infection-Resistant Surfaces." *Biomaterials* 34(34): 8533–54.
- Cleveland, Jennifer et al. 2001. "Bacteriocins: Safe, Natural Antimicrobials for Food Preservation." *International Journal of Food Microbiology* 71(1): 1–20.
- Crump, John A. et al. 2004. "The Global Burden of Typhoid Fever." *Bulletin of the World Health Organization* 82(5): 346–53.
- Esteban, María Dolores, Arantxa Aznar, Pablo S. Fernández, and Alfredo Palop. 2013. "Combined Effect of Nisin, Carvacrol and a Previous Thermal Treatment on the Growth of *Salmonella Enteritidis* and *Salmonella Senftenberg*." *Food Science and Technology International* 19(4): 357–64.

- European Committie. 2009. "Food Contact Materials | Food Safety."
- Farias, Davi Felipe et al. 2015. "Food Safety Assessment of Cry8Ka5 Mutant Protein Using Cry1Ac as a Control Bt Protein." *Food and Chemical Toxicology* 81: 81–91.
- Gaglione, Rosa et al. 2017. "Novel Human Bioactive Peptides Identified in Apolipoprotein B: Evaluation of Their Therapeutic Potential." *Biochemical Pharmacology* 130: 34–50.
- Galié, Serena et al. 2018. "Biofilms in the Food Industry: Health Aspects and Control Methods." *Frontiers in Microbiology* 9(MAY).
- Gasteiger, Elisabeth et al. 2005. Protein Analysis Tools on the ExPASy Server 571 571 From: *The Proteomics Protocols Handbook Protein Identification and Analysis Tools on the ExPASy Server*.
- H. Chen, and D.G. Hoover. 2003. "Bacteriocins and Their Food Applications." *Comprehensive Reviews in Food Science and Food Safety* 2(3): 82–100.
- Hawkins, Nichola J. et al. 2014. "Paralog Re-Emergence: A Novel, Historically Contingent Mechanism in the Evolution of Antimicrobial Resistance." *Molecular Biology and Evolution* 31(7): 1793–1802.
- Holyoak, C. D. et al. 1996. "Activity of the Plasma Membrane H⁺-ATPase and Optimal Glycolytic Flux Are Required for Rapid Adaptation and Growth of *Saccharomyces Cerevisiae* in the Presence of the Weak-Acid Preservative Sorbic Acid." *Applied and Environmental Microbiology* 62(9): 3158–64.
- Jozala, Angela Faustino, Leticia Celia de Lencastre Novaes, and Adalberto Pessoa. 2015. "Nisin." In *Concepts, Compounds and the Alternatives of Antibacterials*, InTech.
- Jung, Yongmoon et al. 2016. "Novel Biotechnological Applications of Bacteriocins: A Review." *Food Control* 49(2): 128–41.
- Kanta Das, Kamal et al. 2014. "Microbiological Analysis of Common Preservatives Used in Food Items and Demonstration of Their in Vitro Anti-Bacterial Activity Microbiological Analysis of Common Preservatives Used in Food Items and Demonstration of Their in Vitro Anti-Bacterial Activity *Asian Pacific Journal of Tropical Disease*." Article in *Asian Pacific Journal of Tropical Disease* 4(6): 452–56.
- Lavermicocca, Paola, Francesca Valerio, and Angelo Visconti. 2003. "Antifungal Activity of Phenyllactic Acid against Molds Isolated from Bakery Products." *Applied and Environmental Microbiology* 69(1): 634–40.
- Lee, Jeong-In, Hu-Jang Lee, and Mun-Han Lee. 2002. "Synergistic Effect of Nisin and Heat Treatment on the Growth of *Escherichia Coli* O157:H7." *Journal of food protection* 65(2): 408–10.
- Lin, Jyhshiu et al. 1996. "Mechanisms of Acid Resistance in Enterohemorrhagic *Escherichia Coli*." *Applied and Environmental Microbiology* 62(9): 3094–3100.

- Lucas, John A. et al. 2015. "The Evolution of Fungicide Resistance." *Advances in Applied Microbiology* 90: 29–92.
- Maiti, Soumitra et al. 2014. "Effective Control of Salmonella Infections by Employing Combinations of Recombinant Antimicrobial Human β -Defensins HBD-1 and HBD-2." *Antimicrobial Agents and Chemotherapy* 58(11): 6896–6903.
- Matejuk, A. et al. 2010. "Peptide-Based Antifungal Therapies against Emerging Infections." *Drugs of the Future* 35(3): 197–217.
- Mathur, Chandni et al. 2015. "Lack of Detectable Allergenicity in Genetically Modified Maize Containing 'Cry' Proteins as Compared to Native Maize Based on In Silico & In Vitro Analysis" ed. Manoj Prasad. *PLOS ONE* 10(2): e0117340.
- Mayrhofer, Sigrid et al. 2004. "Antimicrobial Resistance Profile of Five Major Food-Borne Pathogens Isolated from Beef, Pork and Poultry." *International Journal of Food Microbiology* 97(1): 23–29.
- Meneguetti, Beatriz T. et al. 2017. "Antimicrobial Peptides from Fruits and Their Potential Use as Biotechnological Tools-A Review and Outlook." *Frontiers in Microbiology* 7(JAN).
- Moreno, F. Javier, and Alfonso Clemente. 2008. "2S Albumin Storage Proteins: What Makes Them Food Allergens?" *The Open Biochemistry Journal* 2: 16–28.
- Oliveira, Pedro M. et al. 2012. "Fundamental Study on the Influence of Fusarium Infection on Quality and Ultrastructure of Barley Malt." *International Journal of Food Microbiology* 156(1): 32–43.
- Ordóñez, Soledad R. et al. 2014. "Fungicidal Mechanisms of Cathelicidins LL-37 and CATH-2 Revealed by Live-Cell Imaging." *Antimicrobial Agents and Chemotherapy* 58(4): 2240–48.
- Pane, Katia et al. 2018. "Identification of Novel Cryptic Multifunctional Antimicrobial Peptides from the Human Stomach Enabled by a Computational-Experimental Platform." *ACS Synthetic Biology* 7(9): 2105–15.
- Park, Yong Keun et al. 1996. "Internal PH Crisis, Lysine Decarboxylase and the Acid Tolerance Response of Salmonella Typhimurium." *Molecular Microbiology* 20(3): 605–11.
- Pitt, John I., and Ailsa D. Hocking. 2009. *Fungi and Food Spoilage*. Springer US.
- Puri, Sumant, and Mira Edgerton. 2014. "How Does It Kill?: Understanding the Candidacidal Mechanism of Salivary Histatin 5." *Eukaryotic Cell* 13(8): 958–64.
- Rydlo, Tali et al. 2006. "Eukaryotic Antimicrobial Peptides: Promises and Premises in Food Safety." *Journal of Food Science* 71(9): R125–35.
- Samson, R.A. 2004. *Introduction to Food- and Airborne Fungi.*
- Santos, Johnson C.P. et al. 2018. "Nisin and Other Antimicrobial Peptides: Production, Mechanisms of Action, and Application in Active Food Packaging." *Innovative Food Science and Emerging Technologies* 48: 179–94.

- Scallan, Elaine et al. 2011. "Foodborne Illness Acquired in the United States-Major Pathogens." *Emerging Infectious Diseases* 17(1): 7–15.
- Schved, F., Y. Henis, and B. J. Juven. 1994. "Response of Spheroplasts and Chelator-Permeabilized Cells of Gram-Negative Bacteria to the Action of the Bacteriocins Pediocin SJ-1 and Nisin." *International Journal of Food Microbiology* 21(4): 305–14.
- Siedenbiedel, Felix, and Joerg C. Tiller. 2012. "Antimicrobial Polymers in Solution and on Surfaces: Overview and Functional Principles." *Polymers* 4(1): 46–71.
- Singh, Veer Pal. 2018. "Recent Approaches in Food Bio-Preservation-A Review." *Open Veterinary Journal* 8(1): 104–11.
- Stratford, Malcolm et al. 2013. "Extreme Resistance to Weak-Acid Preservatives in the Spoilage Yeast *Zygosaccharomyces Bailii*." *International Journal of Food Microbiology* 166(1): 126–34.
- Stuart, Byron M., and Roscoe L. Pullen. 1946. "Typhoid: Clinical Analysis of Three Hundred and Sixty Cases." *Archives of Internal Medicine* 78(6): 629–61.
- Swartjes, J.J.T.M. et al. 2014. "Current Developments in Antimicrobial Surface Coatings for Biomedical Applications." *Current Medicinal Chemistry* 22(18): 2116–29.
- Thery, Thibaut et al. 2019. "Natural Antifungal Peptides/Proteins as Model for Novel Food Preservatives." *Comprehensive Reviews in Food Science and Food Safety* 18(5): 1327–60.
- Vermaak, I., A. M. Viljoen et al. 2009. "The Effect of Simulated Gastrointestinal Conditions on the Antimicrobial Activity and Chemical Composition of Indigenous South African Plant Extracts." *South African Journal of Botany* 75(3): 594–99.
- Wang, Huhu et al. 2013. "Biofilm Formation of Salmonella Serotypes in Simulated Meat Processing Environments and Its Relationship to Cell Characteristics." *Journal of Food Protection* 76(10): 1784–89.
- Wang, Shuai et al. 2016. "Antimicrobial Peptides as Potential Alternatives to Antibiotics in Food Animal Industry." *International Journal of Molecular Sciences* 17(5).
- WHO. 2000. THE USE OF ESSENTIAL DRUGS Ninth Report of the WHO Expert Committee (Including the Revised Model List of Essential Drugs).
- Xu, Wentao et al. 2009. "Safety Assessment of Cry1Ab/Ac Fusion Protein." *Food and Chemical Toxicology* 47(7): 1459–65.
- Yildirim, Selçuk et al. 2018. "Active Packaging Applications for Food." *Comprehensive Reviews in Food Science and Food Safety* 17(1): 165–99.
- Yuste, J., and D. Y.C. Fung. 2004. "Inactivation of Salmonella Typhimurium and Escherichia Coli O157:H7 in Apple Juice by a Combination of Nisin and Cinnamon." *Journal of Food Protection* 67(2): 371–7

ABBREVIATIONS:

MRSA: methicillin-resistant *Staphylococcus aureus*; **VRE:** vancomycin-resistant enterococci; **HDPs:** host defence peptides; **AMPs:** antimicrobial peptides; **LPS:** lipopolysaccharide; **ApoB:** Apolipoprotein B; **MIC:** minimal inhibitory concentration; **MBC:** Minimal bactericidal concentration; **TSA:** Tryptic Soy Agar; **MHB:** Muller Hinton Broth; **NB:** Nutrient Broth; **SD:** standard deviation; **SDS:** sodium dodecyl sulfate; **FIC:** fractional inhibitory concentration; **CATH-2:** cathelicidin-2; **ONC:** onconase; **PBS:** phosphate-buffered saline; **CFU:** colony forming unit; **CLSM:** Confocal Laser Scanning Microscopy **SEM:** Scanning Electron Microscopy; **YPD:** yeast extract peptone dextrose; **YMB:** yeast malt broth; **MM:** minimal medium; **MFC:** minimal fungicidal concentration; **TKC:** time killing curve; **PI:** Propidium iodide; **ATP:** adenosine triphosphate; **LB:** Luria-Bertani; **IMAC:** ion metal affinity chromatography; **5'IAF:** 5-iodoacetamidofluorescein; **TFA:** trifluoroacetic acid; **MTT:** 3-(4,5-dimethylthiazol-2-yl)- 2,5-diphenyltetrazolium bromide; **SGF:** simulated gastric fluid; **SIF:** simulated intestine fluid; **TNF- α :** tumor necrosis factor; **AP:** active packaging; **AS:** antimicrobial surface; **CH:** chitosan; **PEC:** pectin; **TVC:** total viable count

LIST OF PUBLICATIONS:

1. Sabbah M., Di Pierro P., **Dell'Olmo E.**, Arciello A., Porta R. Improved shelf-life of Nabulsi cheese wrapped with hydrocolloid films. (Food hydrocolloids. 96 (2019) 1-716).
2. Sabbah M., Di Pierro P., Cammarota M., **Dell'Olmo E.**, Arciello A., Porta R. Development and properties of new chitosan-based films plasticized with spermidine and/or glycerol. (Food Hydrocolloids.87 (2019) 245–252)
3. **Dell'Olmo E.**, Gaglione R., Pane K., Sorbo S., Basile A., Esposito S., Arciello A. Fighting Multidrug Resistance with a fruit extract: anti-cancer and anti-biofilm activities of *Feijoa sellowiana* (Natural Product Research. 2019 May; doi 10.1080/14786419.2019.1624961.)
4. Gaglione R., Cesaro A., **Dell'Olmo E.**, Della Ventura B., Casillo A., Di Girolamo R., Velotta R., Notomista E., Veldhuizen E.J.A., Corsaro M.M., De Rosa C., Arciello A. Effects of human antimicrobial cryptides identified in apolipoprotein B depend on specific features of bacterial strains. (Scientific Report. 2019 Apr 30;9(1):6728)
5. Gaglione R., Pane K., **Dell'Olmo E.**, Pizzo E., Olivieri G., Notomista E., Arciello A. Cost-effective production of host defence peptides in *Escherichia coli*. (New BIOTECHNOLOGY. 2019 Jul 25;51:39-48)
6. Zanfardino A., Bosso A., Gallo G., Pistorio V., Di Napoli M., Gaglione R., **Dell'Olmo E.**, Varcamonti M., Notomista E., Arciello A., Pizzo E. Human Apolipoprotein E as a reservoir of cryptic bioactive peptides: the case of ApoE 133-167 (J Pept Sci. 2018 Jul;24(7):e3095)
7. Gaglione R., Pirone L., Farina B., Fusco S., Smaldone G., Aulitto M., **Dell'Olmo E.**, Roschetto E., Del Gatto A., Fattorusso R., Notomista E., Zaccaro L. Arciello A., Pedone E and Contursi P. Insights into the anticancer properties of

the first antimicrobial peptide from Archaea. (BBA – General Subjects 2017 Sep; 1861(9):2155-2164)

8. Gaglione R., **Dell’Olmo E.**, Bosso A., Chino M., Pane K., Ascione., Itri F., Caserta S., Amoresano A., Lombardi A., Haagsman H. P., Piccoli R., Pizzo E., Veldhuizen J. A. E., Notomista E., Arciello A. Novel human bioactive peptides identified in apolipoprotein B: evaluation of their therapeutic potential. (Biochemical Pharmacology 2017 Apr 15; 130:34-50)

LIST OF COMMUNICATIONS

- I. **BioID&A**, **BI**Otechnology **I**dentify and **A**pplications. Member of the organizing committee on the Industrial Biotechnology. (Complesso Universitario di Monte Sant’Angelo, Napoli, 28 Ottobre 2018)
- II. Gaglione R., Pane K., Itri F., Bosso A., **Dell’Olmo E.**, Cafaro V., Pizzo E., Veldhuizen E. J. A., Piccoli R., Notomista E., Arciello A. Novel cryptic cationic antimicrobial peptides from human ApoB. (15th Naples Workshop on bioactive peptides. Peptides: recent developments and future directions. 23-25 Giugno 2016, Napoli)
- III. Gaglione R., Pane K., **Dell’Olmo E.**, Bosso A., Chino M., Itri F., Cafaro V., Pizzo E., Veldhuizen E.J. A., Lombardi A., Piccoli R., Notomista E., Arciello A. Novel human antimicrobial peptides from ApoB are endowed with promising anti-inflammatory properties. (XIV Congress of the Italian Federation of Life Sciences (FISV), 20-23 Settembre 2016, Università di Roma “Sapienza”)
- IV. Rosa Gaglione, **Eliana Dell’Olmo**, Andrea Bosso, Katia Pane, Bartolomeo Della Ventura, Rocco Di Girolamo, Finizia Auriemma, Elio Pizzo, Renata Piccoli, Edwin J.A. Veldhuizen, Eugenio Notomista, Angela Arciello. **Novel human bioactive peptides identified in Apolipoprotein B**. 59th Congress of the Italian Society of Biochemistry and Molecular Biology (SIB).
- V. “Superbugs” Strumento di intervento nell’era post-biotica. (Giuseppe Dossetti Association, 14 Giugno 2017, Roma)
- VI. Gaglione R., **Dell’Olmo E.**, Bosso A., Pane K., Della Ventura B., Di Girolamo R., Auriemma F., Pizzo E., Piccoli R., Notomista E., Veldhuizen E. J. A., Arciello A.. **Human cryptic Host Defence Peptides identified in Apolipoprotein B: analysis of their antimicrobial, anti-biofilm and immunomodulatory properties**. (IMAP 2017, 7th International Meeting on Antimicrobial Peptides, Copenhagen, Agosto 25-27, 2017)
- VII. Gaglione R., **Dell’Olmo E.**, Cesaro A., Della Ventura B., Casillo A., Di Girolamo R., Notomista E., Pizzo E., Corsaro M., Auriemma F., Arciello A. **Novel insights into the mechanism of action of human cryptides identified in apolipoprotein B** (IMAP 2018, 8th International Meeting on Antimicrobial Peptides Edinburgh, UK, September 2 – 4, 2018)
- VIII. C. Valeria L. Giosafatto, Angela Arciello, **Eliana Dell’Olmo**, B. E. Garcia-Almendarez, Renata Piccoli, Raffaele Porta. **Bioactive protein-based**

- films containing an antimicrobial apolipoprotein B fragment.** XV Congresso della Federazione Italiana Scienze della Vita (FISV 2018).
- IX. **Dell’Olmo E.**, Gaglione R., Giosafatto V. L. C., Di Girolamo R., Cesaro A., Piccoli R., Notomista E., Veldhuizen E. J. A., Porta R., Arciello A. **Human apolipoprotein B: an unpredictable and promising source of novel food preservatives.** 2nd Workshop of Società Italiana Biochimici (Sib)
- X. **Dell’Olmo E.**, Gaglione R., Giosafatto C.VL., Sabbah M., Di Girolamo R., Cesaro A., Renata Piccoli, Eugenio Notomista, Edwin J.A Veldhuizen, Raffaele Porta, Angela Arciello. **Human apolipoprotein B: an unpredictable and promising source of novel food preservatives.** (AntiMic 2019, Second International Symposium on natural antimicrobials, Lille, FR July 2-4, 2019)

EXPERIENCE IN FOREIGN LABORATORIES

Visiting period at the Department of Infectious Diseases and Immunology, Division Molecular Host Defence, Faculty of Veterinary Medicine, Utrecht University, The Netherlands, from 1st May 2018 to 1st November 2018. The work was carried out in the lab of Professor Henk Prof. Haagsman.

ACKNOWLEDGMENTS

So, here we are... this is the end of the exciting life path that the PhD was and it's time to look back (just for few minutes) in the past three years and say thanks to all the people that participated at this journey.

I would like to first say thank you to Prof. Renata Piccoli for allow me to be part of your research group in my Master thesis and then of this PhD school. A big thanks to my supervisor, Prof. Angela Arciello, you have been the first person who believed in me and gave me the chance to be part of the PhD school in Biotechnology, allowing to my biggest dream come true. It has not been always easy to understand each other but finally we made a great job together!!! I am also very grateful to Angela for her scientific advice and knowledge and many insightful discussions and suggestions. Thanks mostly to support all my crazy ideas during this PhD course and to be so supporting in realizing my objectives. I will never thank you enough to allowing me to grow as a scientist and also as a person.

I would also thanks Dr. Rosa Gaglione, for being so supportive during these years. Thanks to your advices, enthusiasm and passion, you made these last three years easier for me. But I would say thank you Rosa, also for the emotional support, you have always been there in my hard moment, encouraging me to keep going and believing in myself.

Thanks to all the wonderful FIB group!! Daria, Angelica, Luigi, Davide and Maria, without anyone of you the lab should be different. Thanks for the funniest moments, the coffee breaks and also to be a support in my bad days, so thanks to be so amazing!! Thanks all the students that came in our lab, I learn something from each of you and everyone leave an indelible sign in our lab. Special thanks to the best student that a PhD student would have, Martina! You have been an amazing right-hand woman during my last year, without you I wouldn't achieve all the results that we have. Above all, thanks to teaching me the train theory!

I also so grateful to my Dutch research group, I have been left there a piece of my heart. Thanks Edwin, you are the amazing supervisor and the funniest and smart person I will never know. You made my visit period full of knowledge and thanks to your experience and your advices my experience in foreign lab have been less hard!! Thanks to Hank, you are the kind of scientist that I would like to be in the future. I will never forget our work meeting, full of questions, advises and observations. Our science discussions will remain one of the most stimulant things that I have done. Thanks to all the people in the MHB group: Melanie, Maikee, Lianci, Roel and Albert. You have been so welcoming, supportive, funny people that you always have a special spot in my heart and memories.

How I could forget my Italian family in the Netherlands!! Thank you Benedetta for our chats, trips, bike rides, lunches, dinners, drinks and so much more. You have been and always will be a wonderful friend!! Thanks Riccardo, for all our coffee break, our discussion on scientific topics and for all the beers that we shared!! Thank you both of you, for the support and for the friendship, those six months have not been the same without you!!

Thanks to Paola and Giovanni, you not only are amazing colleagues but also two wonderful friends, without you I couldn't never survive to these three years. Thank

for to be supportive in the bad moment but also for the smile and the funny moments, that we have spent together. We have shared the fears, the deadlines, the stress and now I'm looking forward to share with both of you the end of PhD. I'm so proud of you, I couldn't ask for best friends!! Thanks to Carla, you have been the first person I met at the university, in the Biotechnology faculty. We have shared so many moments together that I can't list them here. Thanks for sharing the exams pressure, anxiety, lazy days and bad days with me.

A big thanks goes to all my friends, that encourage me during the PhD, for believe in me, to be always right my side when I need them at most. I will never be the "Dottoressa" without you!!

I reserve one of the mines biggest thanks to my family. They were, are and will be the most passionate support that I could ever have. Thanks to my mom, the strongest woman that I know, to grow me in the ideal that: impossible is nothing. Thanks to my dad, because also if he does not understand my passion in science, he always believes in me and encourage me. Thanks to my grandmother, to have been my second mum and to be so proud of me, also when I don't deserve it.

Finally, I want to say thank you to my favourite person in all the world, my missed puzzle piece, my milestones and the love of my life, Stefano. I don't know if it is better to say thank you for all the things that you have done for me, to allow me to reach this achievement or maybe It's better to say sorry, for the tears, the anger, the anxiety, for the absence in some moments, for all the times in which I put my job first. Thank you to be "My Person", my future and my landmark and mostly you are mine happy place, for ever and ever.

"In life we must never resign ourselves to mediocrity, but we must get out of that "grey zone" in which everything is habit and passive resignation. We must cultivate the courage to rebel"

Rita Levi Montalcini

RINGRAZIAMENTI

Quindi eccoci... sono arrivata alla fine di questo eccitante percorso di vita che è stato il corso di dottorato. È arrivato il tempo di guardare in dietro (solo per pochi minuti) e ringraziare tutte le persone che hanno partecipato a questo viaggio.

Prima di tutto voglio ringraziare la Prof. Renata Piccoli, per avermi permesso di essere parte del suo gruppo di ricerca durante la tesi magistrale e poi di questa scuola di dottorato. Un grande grazie va al mio tutor, la Prof.ssa Angela Arciello per essere stata la prima a credere in me e che mi ha dato la possibilità di far parte della scuola di dottorato in Biotecnologie, facendo diventare realtà uno dei miei più grandi sogni. Non è sempre stato facile capirsi ma alla fine abbiamo fatto un gran bel lavoro insieme!!! Angela ti sono inoltre molto grata per tutti i consigli scientifici, per la tua conoscenza e per tutte le chiacchierate e suggerimenti. Soprattutto Grazie per aver supportato tutte le mie pazze idee durante tutti e tre gli anni e per aver partecipato attivamente alla realizzazione dei miei obiettivi. Ma il grazie più importante è: Grazie Angela per avermi permesso di crescere come scienziato ma anche come persona.

Voglio anche ringraziare la Dott.ssa Rosa Gaglione, per essere stata di grande supporto durante questi anni- Grazie ai tuoi consigli, al tuo entusiasmo e alla tua passione, hai reso questi tre anni un po' più facili. Ma voglio ringraziarti, anche per il supporto emotivo, sei sempre stata al mio fianco nei momenti difficili, incoraggiandomi ad andare avanti e a credere in me stessa.

Grazie a tutto il meraviglioso Gruppo FIB!! Daria, Angelica, Luigi, Davide e Maria, senza ognuno di voi il laboratorio non sarebbe lo stesso. Grazie per tutti i momenti divertenti, le pause caffè e anche per il vostro supporto nei giorni no, praticamente grazie per essere così fantastici!! Grazie a tutti gli studenti che sono passati nel nostro laboratorio, ho imparato tanto da ognuno di voi e avete lasciato un segno indelebile nel nostro gruppo. Un grazie speciale va alla migliore studentessa che un dottorando possa avere, Martina! Sei stata un braccio destro magnifico durante quest'ultimo anno, senza di te non avrei potuto raggiungere tutti i risultati che abbiamo. Ma soprattutto grazie per avermi insegnato la teoria del treno!!

Sono inoltre immensamente grata al mio gruppo di ricerca olandese, ho lasciato un pezzo del mio cuore lì. Grazie Edwin, sei stato un tutor eccezionale e la persona più divertente e intelligente che abbia mai conosciuto. Hai reso il mio periodo all'estero pieno di conoscenza e grazie alla tua esperienza e ai tuoi suggerimenti la mia esperienza all'estero è stata un po' meno ardua. Grazie Hank, tu sei il tipo di scienziato che vorrei diventare in futuro. Non potrò mai dimenticare i nostri work meeting, pieni di suggerimenti, consigli e osservazioni. Le nostre chiacchierate scientifiche sono una delle cose più stimolanti fatte nella mia vita. Grazie a tutti i componenti del gruppo MHB: Melanie, Maikee, Lianci, Roel e Albert. Siete stati così accoglienti, incoraggianti, divertenti che avrete sempre un posto speciale nel mio cuore e nei miei ricordi.

Come potrei dimenticare la mia famiglia italiana in Olanda!! Grazie Benedetta per le nostre chiacchierate, le gite, le passeggiate in bicicletta, i pranzi, le cene, i drink e molto altro. Sei stata e sarai per sempre un'ottima amica!! Grazie a Riccardo, per le pause caffè, per le chiacchierate scientifiche e per tutte le birre che abbiamo condiviso. Grazie ad entrambi per il supporto e l'amicizia, quei sei mesi non sarebbero stati gli stessi senza di voi.

Grazie a Paola e Giovanni, non solo per essere colleghi fantastici ma anche per essere amici straordinari, senza di voi non sarei sopravvissuta a questi tre anni. Grazie per essere così incoraggianti nei momenti difficili ma anche per i sorrisi e i momenti divertenti che abbiamo passato insieme. Abbiamo condiviso lacrime, scadenze, stress e ora non vedo l'ora di condividere con voi anche la fine del PhD. Sono così orgogliosa di voi, non avrei potuto chiedere due amici migliori! Grazie Carla, sei stata la prima persona che ho conosciuto all'università, alla facoltà di biotecnologie. Abbiamo condiviso così tanti momenti insieme che è impossibile elencarli qui. Grazie per aver condiviso la pressione per gli esami, l'ansia e giorni di pigrizia e di disperazione con me!

Grazie a tutti i miei amici, per avermi incoraggiato durante il dottorato, per aver creduto in me e per essere sempre stati al mio fianco quando avevo più bisogno di voi. Non sarei mai diventata la vostra "Dottoressa" senza di voi!!

Ho riservato uno dei miei grazie più grandi alla mia famiglia. Loro erano, sono e saranno i miei "fan" più appassionati. Grazie a mia madre, la donna più forte che io conosca, per avermi cresciuta nell'ideale che: niente è impossibile. Grazie a mio padre. Perché anche non capendo la mia passione per la scienza, ha sempre creduto in me e mi ha sempre incoraggiato. Grazie, a mia nonna, per essere stata una seconda mamma per me e per essere così orgogliosa di me anche quando non lo merito!!

In fine voglio ringraziare la persona che preferisco al mondo, il mio pezzo mancante del puzzle, la mia roccia e l'amore della mia vita, Stefano. Non so se è più giusto ringraziarti per tutte le cose che hai fatto per me, per farmi raggiungere questo obiettivo; forse è più giusto scusarmi per tutte le lacrime, la rabbia, l'ansia e per l'assenza a cui in certi momenti, hai dovuto rassegnarti. Grazie per essere la mia Persona, il mio futuro e il mio punto di riferimento ma soprattutto per essere la mia isola felice ora e per sempre.

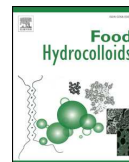
"Nella vita non bisogna mai rassegnarsi, arrendersi alla mediocrità, bensì uscire da quella "zona grigia" in cui tutto è abitudine e rassegnazione passiva. Bisogna coltivare il coraggio di ribellarsi"

Rita Levi Montalcini



Contents lists available at ScienceDirect

Food Hydrocolloids

journal homepage: www.elsevier.com/locate/foodhyd

Improved shelf-life of Nabulsi cheese wrapped with hydrocolloid films

 Mohammed Sabbah^{a,b}, Prospero Di Pierro^{a,*}, Eliana Dell'Olmo^a, Angela Arciello^a, Raffaele Porta^a
^a Department of Chemical Sciences, University of Naples "Federico II", Complesso Universitario di Monte Sant' Angelo, Via Cintia 21, 80126, Naples, Italy

^b Department of Nutrition and Food Technology, An-Najah National University, P.O. Box: 7 Nablus, Palestine


ARTICLE INFO

Keywords:

 Nabulsi cheese
 Edible film
 Shelf-life
 Wrapping
 Chitosan
 Bitter vetch proteins

ABSTRACT

Chitosan- and bitter vetch protein-based films were prepared, characterized and applied as wrapping films of Nabulsi cheese, to improve the shelf-life of such dairy product widely consumed in the Middle East. Unsalted cheese wrapped with these hydrocolloid films was found to maintain the pH value of the fresh product during storage, whereas the pH of unwrapped samples was shown to progressively decrease. These findings were confirmed by the decrease in titratable acidity detected in the wrapped unsalted cheeses at 9th day of storage. Conversely, no effect was observed at different storage times in the weight loss of wrapped samples, compared to the unwrapped ones, stored both in the absence and presence of salts. However, chitosan films proved to be the most effective wrapping material in hindering microorganism growth in unsalted cheese. Hardness, chewiness and gumminess of the wrapped unsalted samples increased during storage, whereas no significant difference in springiness was observed between the wrapped and unwrapped cheeses, except for the protein-wrapped salted samples in which the springiness was observed to decrease slightly from the 3rd day onward. The proposed wrapping is suggested as an innovative packaging system of Nabulsi cheese to preserve over time its quality without brining.

1. Introduction

The use of polymeric packages for food preservation has increased considerably over recent decades and, due to the shortage of petroleum resources and waste management issues, the research interest is switching from synthetic oil-based materials to non-environmentally harmful biopolymers (Grujić, Vujadinović, & Savanović, 2017). Moreover, biodegradable plastics exhibit a more diversified chemical nature and structure, providing, thus, numerous opportunities to tailor the properties of the packaging material to specific foods. In particular, the use of biopolymers such as proteins and polysaccharides derived from renewable agro-resources is in agreement with the increasing consumer demands for safe and non-polluting materials. As a consequence, these biomacromolecules are increasingly being investigated as food contact film components alternatives to conventional polymers obtained from oil derivatives. These hydrocolloid edible films can be, in fact, specially suitable for food coating or wrapping, as well as for separation of different food portions. However, although "bio-plastics" is a rising market capturing that of plastics at a growth rate of 30% annually (Reddy, Vivekanandhan, Misra, Bhatia, & Mohanty, 2013), some drawbacks, such as the marked hydrophilicity and the quite poor mechanical and

barrier properties, still limit a wide commercial application of these materials. Therefore, few bio-based materials currently have commercial use in the food packaging sector with the exception of the cellulose-based ones. Among the most promising biopolymers chitosan (CH), a deacetylated chitin derivative, is known to possess effective antimicrobial properties against a variety of fungi, yeasts and bacteria and is able to produce biodegradable/edible films potentially useful as main component of packaging biomaterials for food shelf-life improvements (Elsabee & Abdou, 2013). Furthermore, numerous plant proteins attracted attention as biodegradable raw polymers for food packaging development, due to their ability to form three-dimensional macromolecular networks strengthened by hydrogen bonds, hydrophobic interactions, as well as by covalent (isopeptide and disulfide) links (Wihodo & Moraru, 2013; Zink, Wyrobnik, Prinz, & Schmid, 2016). But, since both polysaccharide- and protein-based materials are low moisture barriers, their use as food coating or wrapping components has been so far rather limited (Pascall & Lin, 2013). Nevertheless, different strategies have been designed to overcome these drawbacks, including blending, cross-linking and grafting biopolymers on various nanoparticles, with the intention of replacing mostly the polyethylene (PE)-based films still widely used for different purposes (Song & Zheng,

* Corresponding author. Department of Chemical Sciences, University of Naples "Federico II", Complesso Universitario di Monte Sant' Angelo, Via Cintia 21, 80126, Napoli, Italy.

E-mail addresses: mohammed.sabbah@unina.it (M. Sabbah), prospero.dipierro@unina.it (P. Di Pierro), eliana.dellolmo@unina.it (E. Dell'Olmo), anarciello@unina.it (A. Arciello), raffaele.porta@unina.it (R. Porta).

<https://doi.org/10.1016/j.foodhyd.2019.05.010>

Received 9 February 2019; Received in revised form 2 May 2019; Accepted 6 May 2019

Available online 06 May 2019

0268-005X/ © 2019 Published by Elsevier Ltd.

2014).

The cheese industry is one of the most important sectors where polysaccharide and protein-based materials have a good opportunity for application and CH is without any doubt one of the best candidates to formulate edible coatings for different fresh, semi-hard and hard cheese, being able to prevent the growth of moulds, yeasts and several bacteria (Costa, Maciela, Teixeira, Vicente, & Cerqueira, 2018). In fact, based on its antimicrobial activity and film forming capacity, CH-based coatings were tested in the last ten years on several types of dairy products aiming at a decrease of microbiological growth and, thus, at an extension of their shelf-life (Beigomohammadi et al., 2016; Cano; Bonilla & Sobral, 2018; Di Pierro, Sorrentino, Mariniello, Giosafatto, & Porta, 2011; El-Sisi, El-Sattar, Gapr, & Kamaly, 2015; Cano Embuena et al., 2016; Ramos et al., 2012; Romero, Borneo, Passalacqua, & Aguirre, 2016; Santonicola, Ibarra, Sendon, Mercogliano, & Quiros, 2017). Furthermore, among plants containing high protein amounts in their seeds, bitter vetch (BV, *Vicia ervilia*) was recently proposed as renewable resource to obtain an effective matrix of protein-based films (Arabestani et al., 2016; Arabestani, Kadivar, Shahedi, Goli, & Porta, 2013; Fernandez-Bats, Di Pierro, Villalonga-Santana, Garcia-Almendarez, & Porta, 2018; Porta, Di Pierro, Roviello, & Sabbah, 2017; Porta et al., 2016, 2015; Sabbah et al., 2017). Therefore, the packaging by biodegradable films, focusing mainly on their antimicrobial and/or antioxidant activities, represents an intriguing possibility to extend the shelf-life also of Nabulsi cheese (NC), the most popular and economically important cheese consumed in the Middle East, and to contribute to its safety and quality. NC is a semihard unfermented cheese manufactured by renneting unpasteurized milk from cow, sheep or goat, or their mixtures, without using starter culture (Carić, 1999; Tamime & Robinson, 1991, pp. 125–139; Yamani, Al-Nabulsi, Haddadin, & Robinson, 1998). The obtained pressed curd is usually boiled in brine solution (20% NaCl, w/v) and finally stored at room temperature immersed in it (Humeid, Tukan, & Yamani, 1990; Mazahreh, Quasem, Al-Shawabkeh, & Afaneh, 2009; Yamani, Tukan, & Abu-Tayeh, 1997). NC is generally consumed, either as it is or as ingredient of some traditional salty or sweet foods, after partial or complete salt removal by soaking in water the stored product at least for 12 h (Mazahreh et al., 2009). Since the increasing demand for ready-to-eat/use NC requires preservative innovative methodologies, alternative to the NC storage under brine solution, the under vacuum wrapping of NC with both CH- and bitter vetch protein concentrate (BVPC)-based films was investigated. In fact, preservation of NC strictly depends thus far on its immersion in salt concentrated solutions (Humeid et al., 1990) and, in spite of this treatment, undesirable changes -such as discolouration and textural problems, bitterness and off-flavour production-occur when NC is stored in large cans (Mazahreh et al., 2009; Yamani et al., 1997). Therefore, NC with a prolonged shelf-life, but not brined, would be of special interest because it could be consumed from people with health problems related to salt consumption, as well as be component of various sweet confectioneries.

2. Materials and methods

2.1. Materials

BV seeds were purchased from a local market in Gallicchio (PZ), Italy. CH (mean molar mass of 3.7×10^4 g/mol) with a degree of 9.0% N-acetylation, was a gift from Prof. R.A.A. Muzzarelli (University of Ancona, Italy). PE and Mater-Bi (S 301) were from local market shopping bags, Naples, Italy. Glycerol (GLY) (about 87%) was from the Merck Chemical Company (Darmstadt, Germany). Fresh cow milk and fine dry salt were purchased from local market, Naples, Italy, and all other chemicals and solvents used in this study were analytical grade commercial products.

2.2. Hydrocolloid film preparation

BVPC was prepared from the BV seeds as previously described by Sabbah et al. (2017). 1% BVPC solution was prepared in distilled water adjusting the pH to 12.0 by 1.0 N NaOH addition under stirring to completely solubilize BV proteins. An aliquot (40 mL, containing 400 mg BV proteins) of the obtained solution was then brought to pH 8.0 by 1.0 N HCl and GLY was added as plasticizer, under constant stirring, up to reach a final concentration of 50% (w/w hydrocolloid mass). BVPC film forming solution (FFS) final volume was adjusted to 50 mL by adding distilled water. Conversely, 0.75% CH solution was prepared in distilled water adjusting the pH to 4.5 by 1.0 N HCl addition under stirring to completely solubilize CH. An aliquot (40 mL, containing 300 mg CH) of the obtained solution was added with GLY, under constant stirring, up to reach a final concentration of 30% (w/w hydrocolloid mass) of plasticizer. CH FFS final volume was adjusted to 50 mL by adding distilled water. The selected GLY concentrations were those previously demonstrated to be optimal to obtain handleable films (Porta et al., 2017; Sabbah et al., 2019). The prepared FFSs were casted onto 8 cm diameter polystyrene Petri dishes (8 mg BV protein/cm² and 6 mg CH/cm², respectively) and dried into a climatic chamber for 48 h at 25 °C and 45% RH. The obtained films were conditioned in an environmental chamber at 25 °C and 50% RH for 2 h, by placing them into a desiccator over a saturated solution of Mg(NO₃)₂·6H₂O, before being tested.

2.3. Film characteristics

The heat sealability of the different materials was examined by cutting all film samples into strips of 5 × 2.5 cm, and one strip was placed onto another one of the same sample (Fig. 1). All the samples were previously conditioned at 25 °C and 50 ± 5% RH for 48 h and few drops of distilled water were dispersed onto the sealing areas (0.3 cm) before inserting the two strips into an automatic heat sealer (Magic Vac® Axolute Mod: P0608ED, Italy). Sealing temperature, dwell time and pressure were automatically assessed and the resulting welds were

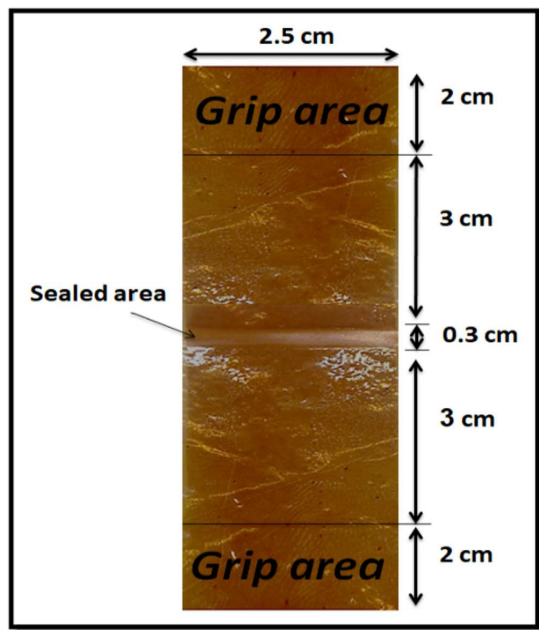


Fig. 1. Visualization of the film heat-sealing procedure.

analyzed according to ASTM E88-07a (ASTM, 2007) with an Instron universal testing instrument model no. 5543A (Instron Engineering Corp., Norwood, MA, USA). The seal strength (N/m) was calculated by dividing the maximum peak force to the film width.

Transparency test was carried out according to Tonyali, Cikrikci, and Oztop (2018) by evaluating film opacity dividing the absorbance at 600 nm for the film thickness (mm).

Film permeabilities to O₂, CO₂ and water vapor were measured in triplicate for each film at 25 °C and 50% RH by using a Total Perm apparatus (ExtraSolution s.r.l., Pisa, Italy) (ASTM D3985-05, 2010; ASTM F2476-13, 2013; ASTM F1249-13, 2013).

Film tensile strength, elongation at break, and Young's module were determined in six specimens for each sample (1 kN load and 5 mm/min speed) as previously reported by using an Instron universal testing instrument model No. 5543A (Instron Engineering Corp., Norwood, MA, USA) (ASTM D882-97, 1997).

Film thickness measurements were performed in six different points of each film with a digital micrometer (DC-516, sensitivity 0.1 µm).

2.4. NC preparation

Unsalted (UNC) and salted (SNC) NC were prepared from fresh cow milk as previously described by Al-Dabbas, Saleh, Abu-Ghoush, Al-Ismail, and Osaili (2014) with the following modifications: 5 L of fresh milk were tempered to 35 °C and rennet was added; after 60 min the curd was cut and settled for 15 min and, then, transferred into cheesecloth inside a perforated square stainless steel frame (20 × 20 × 2 cm); the curd was then pressed with 25 Kg weight for 2 h and the cheese cut into small blocks (2 × 2 × 2 cm) by using a stainless steel cheese slicer. Dry salt (2.5%, w/w of cheese) was dispersed onto the surface of the half of the cheese blocks to prepare SNC samples.

2.5. NC wrapping

CH and BVPC films (7.5 × 9.5 cm) were used to wrap both UNC and SNC samples after their equilibration for 2 days at 50 ± 5% RH and 23 ± 2 °C in an environmental chamber. The two types of films were heat-sealed by three sides giving rise to an open bag in which each cheese block was placed. Then, vacuum was applied to discard all air inside the bag and also the fourth side of the films was heat-sealed under vacuum by using an automated heat sealer, described above, equipped with a vacuum pump (60 cm/Hg – 0.80 bar/11.6 PSI). All the wrapped cheese samples were finally stored at 4 °C for different times. PE films of same dimensions were used as control wrapping material, whereas unwrapped UNC and SNC samples were also prepared and used as controls (Fig. 2). All the wrapped and unwrapped samples were stored in a refrigerator at 4 °C and finally analyzed after 3, 6 and 9 days.

2.6. NC chemical analysis

NC fat content was determined according to the standard method (AOAC, 1990) by analyzing, in triplicate, 1.0 g of fresh NC, whereas protein content was assessed, according to AOAC 2001.14 (2002), by Kjeldahl method with a conversion factor of 6.38.

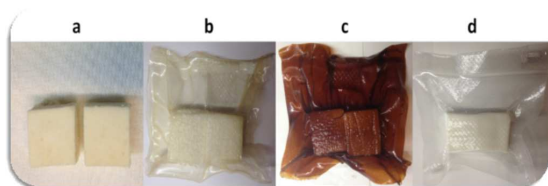


Fig. 2. UNC samples unwrapped (a) or wrapped with CH (b), BVPC (c) and PE (d) films before their storage.

For pH measurements, carried out using a digital pH meter model 211 (Hanna instruments, PBI International), the NC samples (10 g) were first homogenized, at the maximum speed for 5 min, in 100 mL of distilled water by an Ultra-Turrax T8 homogenizer (IKA-WerkeGmbH, Staufen, Germany). Then, after stirring for 15 min, the homogenates were centrifuged at 2500 × g for 10 min and the obtained supernatants were filtered through both cotton lint and paper filter and their pH values finally determined (AOAC, 1990).

NC titratable acidity (TA) was measured according to Di Piero et al. (2011). Cheese samples (10 g) were added to 50 mL of distilled water at 40 °C and homogenized for 5 min at the maximum speed. After centrifugation at 3000 × g for 10 min, the supernatants were filtered and 5 drops of phenolphthalein (1% in ethanol) were added to 25 mL of each sample. TA values were determined by adding 0.1 N NaOH until the solutions became pink and were expressed as milliequivalent/100 g.

2.7. NC weight loss

NC samples were individually weighed on an automatic analytical balance (ORMA s.r.l. BCA310 S. Milano) with a precision of ± 0.0001 g at the beginning and at the different times of storage (3, 6, 9 days), and the percentage weight loss from the initial cheese weight was calculated by the following equation:

$$\text{weight loss (\%)} = \frac{W1 - W2}{W1} \times 100 \quad (1)$$

where W1 is the cheese initial weight and W2 is the cheese weight after storage. Three experiments with each NC sample were performed.

2.8. NC texture profile analysis

Unwrapped and wrapped NC samples were analyzed, as previously described by Gutiérrez-Méndez, Trancoso-Reyes, and Leal-Ramos (2013) and Rossi Marquez et al. (2017), by using an Instron universal testing instrument model no. 5543A (Instron Engineering Corp., Norwood, MA, USA) with a 2.0 kN load cell in compression mode with a cylindrical probe (55 mm in diameter). Eight cylindrical sections (1.5 cm diameter and about 2 cm height) of each sample were compressed by 60% deformation two times using a crosshead speed of 1.0 mm/s. Hardness, chewiness, gumminess and springiness were calculated by using Bluehill 3.0 software. The maximum force of the first compression peak was the hardness, whereas the cohesiveness describes how well a food retains its form between the 1st and 2nd compression, and springiness is defined as the rate at which a deformed cheese returns to its original height between the first and second compression. Chewiness, defined as the total amount of energy needed to chew cheese to a state ready for swallowing, was calculated by multiplying the hardness × cohesiveness × springiness. Finally gumminess, defined as the energy needed to disintegrate the cheese until it is ready to swallow, was calculated by multiplying the hardness × cohesiveness (Joshi, Jhala, Muthukumarappan, Acharya, & Mistry, 2004).

2.9. Microbiological analysis

Each sample of NC (5 g) was aseptically transferred into a sterile plastic falcon tube and homogenized in 45 mL of 0.1% (w/v aqueous solution) sterile Buffered Peptone Water (BPW) for 2 min at room temperature by using an Ultra-Turrax T8 homogenizer and sample volume was adjusted to 50 mL. Decimal serial dilutions were then prepared in 0.1% BWP (1.0 mL final volume) and 100 µL of each diluted solution were inoculated into plate count agar growth medium. More in detail, each diluted solution was plated, in triplicate, on an aerobic count plate for 48 h at room temperature, and mesophilic microorganisms were counted at the end of the incubation.

Table 1
Properties of fresh milk and fresh NC.

Properties	Fresh milk	Fresh NC
Fat (%)	3.6 ^a	20.2 ± 2.3
Protein (%)	3.4 ^a	15.2 ± 2.6
pH	6.61 ± 0.03	6.92 ± 0.07
TA (meq/100g)	0.13 ± 0.01	0.10 ± 0.01

^a Reported in the packaging label of the milk bottle.

2.10. Statistical analysis

JMP software 10.0 (SAS Institute, Cary, NC, USA) was used for all statistical analyses. The data were subjected to analysis of variance, and the means were compared using the Tukey-Kramer HSD test. Differences were considered to be significant at $p < 0.05$.

3. Results and discussion

It is well known that many undesirable changes, such as discoloration, off-flavor production, slime and gas formation, as well as increase in bitterness, may occur to the NC produced by traditional methods during its storage (Mazaherh et al., 2009; Yamani et al., 1997). Since NC chemical composition varies considerably depending on several factors, i.e. source of milk, different conditions of cheese production, seasonal variations, animal feeding, degree of curd pressing and whey drainage (Al-Dabbas et al., 2014), the main characteristics of cow fresh milk used and NC samples prepared for packaging experiments are reported in Table 1. The obtained NC chemical composition resulted in agreement with that previously reported by Al-Dabbas et al. (2014).

Due to their mechanical and barrier properties, CH- and BVPC-based films plasticized with GLY were selected as wrapping materials to try to improve the shelf-life of both UNC and SNC samples (Porta et al., 2017; Sabbah et al., 2019). The main physicochemical and functional properties of the prepared hydrocolloid films are itemized in Table 2 in comparison to those of biodegradable (Mater-Bi) and non-biodegradable (PE) commercial materials. Since heat-sealing is the most widespread method used in food packaging industry in welding synthetic polymer films in order to wrap and preserve foods, the seal strength of the produced CH- and BVPC-based films was analyzed. Table 2 reports that, whereas BVPC-based films showed a significantly lower seal strength in comparison with the other materials analyzed, GLY-plasticized CH films exhibited a seal strength similar to that of both commercial materials tested, as well as to that of other GLY-plasticized polysaccharide-based films previously examined (Farhan & Hani, 2017). Furthermore, the opacity of both CH- and BVPC-based films was observed to be significantly lower than that of the commercial materials, even though the colour of BVPC films was markedly brown and that of CH films slightly yellowish. Then, a possible utilization of these materials as wrappings to prevent cheese spoilage during storage was, thus, investigated, and all the wrapped and unwrapped UNC and SNC

Table 2
Properties of GLY-plasticized CH- and BVPC-based films compared to those of commercial materials.

Film properties	BVPC	CH	PE	Mater-Bi
Seal strength (N/m)	33.4 ± 4.6 ^a	196.4 ± 8.5 ^b	205.5 ± 7.1 ^b	201.5 ± 6.6 ^b
Opacity (mm ⁻¹)	4.8 ± 0.8 ^a	1.3 ± 0.6 ^b	16.9 ± 0.6 ^c	59.8 ± 3.7 ^d
CO ₂ permeability (cm ³ mm m ⁻² day ⁻¹ kPa ⁻¹)	3.0 ± 0.2 ^a	0.7 ± 0.1 ^b	10.9 ± 1.5 ^c	5.2 ± 0.1 ^d
O ₂ permeability (cm ³ mm m ⁻² day ⁻¹ kPa ⁻¹)	1.9 ± 0.1 ^a	0.11 ± 0.02 ^b	3.2 ± 0.6 ^c	0.7 ± 0.1 ^d
Water vapor permeability (cm ³ mm m ⁻² day ⁻¹ kPa ⁻¹)	0.050 ± 0.001a	0.300 ± 0.03b	0.0002 ± 0.00001c	0.040 ± 0.003a
Tensile strength (MPa)	1.6 ± 0.4 ^a	10.2 ± 0.4 ^b	13.1 ± 1.4 ^b	18.4 ± 2.7 ^c
Elongation at break (%)	35.1 ± 3.4 ^a	109.8 ± 5.5 ^b	501.9 ± 43.3 ^c	317.9 ± 35.9 ^d
Young's module (MPa)	30.7 ± 0.6 ^a	27.7 ± 2.9 ^a	75.2 ± 2.7 ^b	42.9 ± 0.8 ^c
Thickness (μm)	107.9 ± 1.8 ^a	84.7 ± 4.1 ^b	36.2 ± 1.7 ^c	16.0 ± 1.3 ^d

All results are reported as mean ± standard deviation. Values within each row with different letters are significantly different ($p < 0.05$).

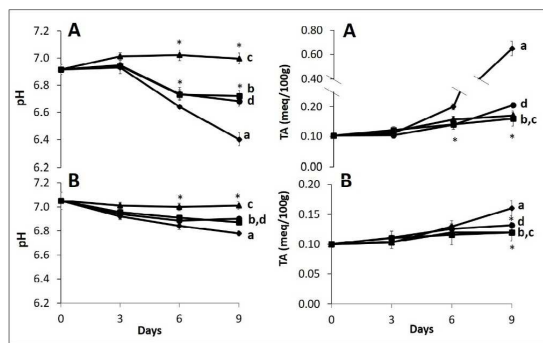


Fig. 3. Effect of wrapping with CH (b), BVPC (c) or PE (d) films on the pH and TA of UNC (A) and SNC (B) samples at different storage times; unwrapped sample (a). *Significantly different values compared to the unwrapped NC samples ($p < 0.05$).

samples were analyzed after 3, 6 and 9 days for both pH and TA changes, as well as for cheese weight loss. No further storage times were investigated because NC is traditionally considered, and usually consumed, as a fresh cheese; moreover, the spoilage of the unwrapped UNC was observed to be extremely advanced at the days following the 9th day. Fig. 3A (left panel) shows that the pH value of both wrapped and unwrapped UNC was around 7.0 and that BVPC wrapping was effective to maintain such pH value until day 9th, whereas the pH of unwrapped cheese progressively decreased to 6.7 and 6.4 at day 6th and 9th, respectively. A similar, even though lower, effect was observed by analyzing the UNC wrapped with either CH or PE films. Conversely, Fig. 3B (left panel) indicates that the pH values of all the SNC samples, both wrapped and unwrapped, did not significantly vary, confirming that salt addition was effective in preserving NC during storage. These findings are in line with NC TA measurements. In fact, only the TA values of unwrapped samples of UNC were found to significantly increase after the 9th day of storage, whereas TA values of all SNC samples, both wrapped and unwrapped, as well as those of wrapped UNC, exhibited TA values similar to the ones of all samples measured at time 0 (Fig. 3A and B, right panels).

Furthermore, the evaluation of the weight loss of all the NC samples indicated that only PE wrapping hindered almost completely the weight loss of both UNC and SNC during their storage, probably as a consequence of the strong water vapor barrier effect exerted by the PE-based material, whereas all the CH and BVPC wrapped NC samples, as well as the unwrapped ones, lost weight in a similar way (about 40% at 9th day) (Fig. 4).

The prevention of microbial contaminations is one of the main parameters to evaluate the effectiveness of preservative packaging of foods and, in particular, of dairy products. Therefore, the effect of UNC and SNC wrapping by different hydrocolloid materials on the growth

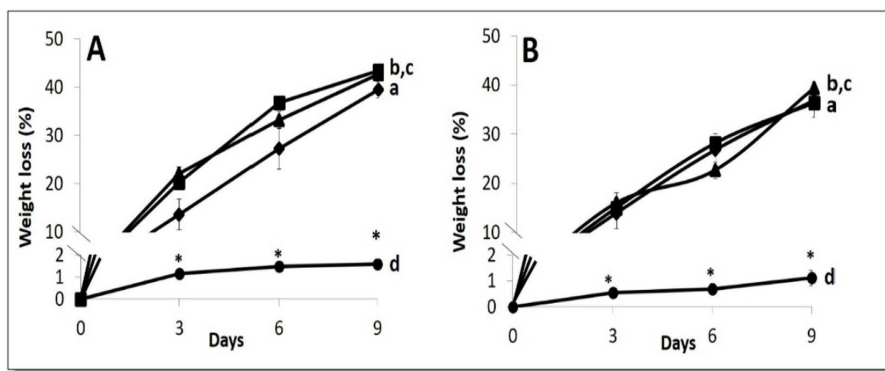


Fig. 4. Effect of wrapping with CH (b), BVPC (c) or PE (d) films on the weight loss of UNC (A) and SNC (B) samples at different storage times; unwrapped sample (a). *Significantly different values compared to the unwrapped cheese samples ($p < 0.05$).

Table 3
Effect of CH, BVPC or PE wrapping of UNC and SNC samples onto development of mesophilic bacteria.

Storage (days)	Sample wrapping	Mesophilic bacteria (CFU/mL)	
		UNC	SNC
0 (controls)	unwrapped	4.64 ± 0.18	3.33 ± 0.57
	CH-wrapped	4.65 ± 0.19	3.34 ± 0.59
	BVPC-wrapped	4.63 ± 0.17	3.32 ± 0.58
	PE-wrapped	4.62 ± 0.19	3.33 ± 0.60
9	unwrapped	10.37 ± 0.08 ^a	8.11 ± 0.53
	CH-wrapped	7.86 ± 0.12 ^b	7.72 ± 1.40
	BVPC-wrapped	8.95 ± 0.01 ^c	8.08 ± 0.51
	PE-wrapped	9.38 ± 0.12 ^d	8.28 ± 0.87

All results are reported as mean ± standard deviation. Values with different letters within UNC column at 9 days are significantly different ($p < 0.05$).

and survival of total aerobic mesophilic microorganisms has been evaluated. Table 3 shows that, unlike UNC, no significant differences were detected between SNC unwrapped samples and those wrapped with CH, BVPC or PE films after 9 days storage. Conversely, among the different wrapping materials, CH film proved to be the most effective by hindering microorganism growth in UNC samples similarly to the NC

preservation under salts, probably because of the well known CH antimicrobial property (Elsabee & Abdou, 2013; Santonicola et al., 2017). Moreover, it is worthy to note that both CH- and BVPC-based wrappings showed to be able to counteract UNC spoilage more effectively than the wrapping based on PE, the traditional material used to pack NC in preventing microbial contaminations during storage.

Finally, wrapped and unwrapped NCs were analyzed by the texture profile analysis, the most broadly used instrumental measurement for cheese texture evaluation (Gutiérrez-Méndez et al., 2013). Although caution is urged in the interpretation of the obtained results by varying the percentage of deformation with parallel plates and the crosshead speed values (Rosenthal, 2010), the data reported in Fig. 5A would indicate that both hardness and chewiness of UNC samples wrapped with CH- and BVPC-based biomaterials progressively increased during storage. One possible explanation of these phenomena might be related to the high water loss (Hassan, Frank, & Elsoda, 2004; Youssef, EL-Sayed, EL-Sayed, Salama, & Dufresne, 2016) which could be reverted, as well as NC texture properties, by soaking the wrapped product in water before use, a procedure normally performed to eliminate the excess of salt from the cheese stored in brine solution. However, since the unwrapped samples showed a weight loss extent very similar to that observed in the CH- and BVPC-wrapped samples, we hypothesize an additional influence of the hydrocolloid films on the cheese textural

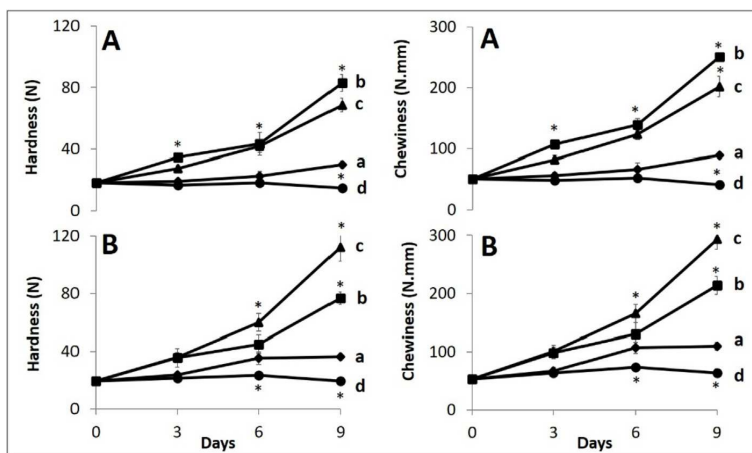


Fig. 5. Effect of wrapping with CH (b), BVPC (c) or PE (d) films on the hardness and chewiness of UNC (A) and SNC (B) samples at different storage times; unwrapped sample (a). *Significantly different values compared to the unwrapped cheese samples ($p < 0.05$).

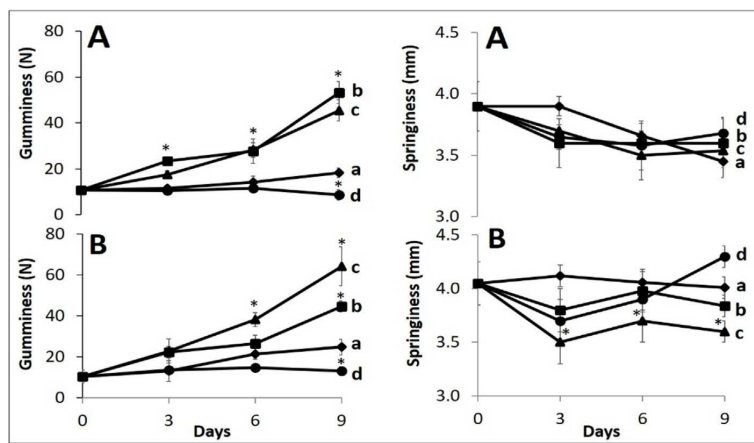


Fig. 6. Effect of wrapping with CH (b), BVPC (c) or PE (d) films on the gumminess and springiness of UNC (A) and SNC (B) samples at different storage times; unwrapped sample (a). *Significantly different values compared to the unwrapped cheese samples ($p < 0.05$).

characteristics, other than that related to the water loss and probably due to their gas barrier properties. Furthermore, the increase in the hardness and chewiness resulted more marked when SNC samples wrapped with BVPC film were examined (Fig. 5B), thus suggesting that salt addition had some additional compacting effect(s), other than that of the water loss, on the structure of the NC specifically wrapped with the protein-based material. Fig. 5 clearly indicates also that both UNC and SNC samples wrapped with PE showed a significantly lower hardness and chewiness at 9th days of storage with respect not only to the CH and BVPC wrapped samples, but also with respect to the unwrapped samples. This effect was probably due to the extremely high water vapor barrier properties own of the oil-derived wrapping material, and to the consequent increase of enzymatic hydrolysis of α -casein by the proteolytic enzymes (Akan & Kinik, 2018).

NC gumminess, the energy needed to disintegrate a semi-solid food until it becomes ready for swallowing, and springiness, the rate at which a deformed sample returns to its original shape, were finally determined (Nateghi et al., 2012). The gumminess both of UNC and SNC samples wrapped with either CH- or BVPC-based materials significantly increased with the storage time with respect to the unwrapped samples, as well as with respect to the PE-wrapped ones (Fig. 6). Conversely, no significant difference in springiness was observed during storage between all the wrapped and unwrapped NC samples, except for the BVPC-wrapped SNC samples, the springiness of which slightly but significantly decreased since the 3th day onwards.

In conclusion, our findings demonstrate that NC wrapping with hydrocolloid films, both polysaccharide- and protein-based, has effects similar to those deriving from NC brining in preventing lowering of pH, increase of TA and aerobic mesophilic microorganism growth and development, all phenomena occurring during the storage of such dairy product. At the same time, an increase in the cheese hardness, chewiness and gumminess of both salted and unsalted NC, wrapped with the analyzed hydrocolloid films, was observed. In addition, such preserving methodology seems to be able to hinder cheese spoilage without preventing its weight loss and, probably, without significantly modifying the regular cheese ripening. In fact, same results cannot be reached by the traditional cheese wrapping with an oil-derived plastic material, such as PE, because of its well known powerful barrier properties toward water vapor. Therefore, due to the well-known short shelf-life of NC, also under refrigeration, the reported hydrocolloid film wrapping would allow to preserve the quality of the dairy product during storage without any prior addition of salts. In fact, the only way used still today by the industry to market NC is its storage in plastic/glass jars or cans

containing high concentrations of brine solution. Consequently, NC is usually consumed as it is or after partial removal of salts by soaking it in water at least for 12 h. UNC with a prolonged shelf-life, because wrapped in a hydrocolloid wrapping, might be, thus, particularly required for several arabian confectioneries, such kunafeh and other sweet cakes. As well as people at high risk of developing health problems related to salt consumption, such as patients with elevated blood pressure and/or diabetes, might consume UNC appropriately stored in the proposed packaging.

4. Conclusions

The possible future industrial production of an innovative dairy product derived from NC wrapped with the described hydrocolloid edible films is suggested. This product would present the advantages to increase the shelf-life of the fresh cheese avoiding any postprocess contamination without brining and, consequently, enhancing the possible demand for a cheese more healthy and ready-to-eat. Moreover, CH or BVPC wrappings are suggested as possible preservative packaging materials for fresh dairy products.

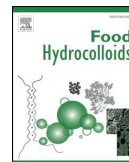
Acknowledgments

This work was financially supported by the Italian Ministry of Agricultural, Food and Forestry Policies (CUP: J57G17000190001) (to R.P. & A.A.). We are grateful to Maria Fenderico for her helpful assistance.

References

- Akan, E., & Kinik, O. (2018). Properties of Turkish white cheese. *Mljekarstvo*, 68, 46–56.
- Al-Dabbas, M. M., Saleh, M., Abu-Ghoush, H. M., Al-Ismaïl, K., & Osaili, T. (2014). Influence of storage, brine concentration and in-container heat treatment on the stability of white brined Nabulsi cheese. *International Journal of Dairy Technology*, 67, 427–436.
- AOAC (1990). *Official method*, 933.05. Fat in cheese.
- AOAC (2002). *Official Method*, 2001. 14. Determination of nitrogen (total) in cheese Kjeldahl method.
- Arabestani, A., Kadivar, M., Shahedi, M., Goli, S. A. H., & Porta, R. (2013). Properties of a new protein film from bitter vetch (*Vicia ervilia*) and effect of CaCl_2 on its hydrophobicity. *International Journal of Biological Macromolecules*, 57, 118–123.
- Arabestani, A., Kadivar, M., Amoresano, A., Illiano, A., Di Pierro, P., & Porta, R. (2016). Bitter vetch (*Vicia ervilia*) seed protein concentrate as possible source for production of bilayered films and biodegradable containers. *Food Hydrocolloids*, 60, 232–242.
- ASTM D3985-05 (2010). *Standard test method for oxygen gas transmission rate through plastic film and sheeting using a colorimetric sensor*. West Conshohocken, PA, USA: ASTM international.

- ASTM D882-97 (1997). *Standard test method for tensile properties of thin plastic sheeting*. Philadelphia, PA, USA: ASTM.
- ASTM E88-07a (2007). Standard test method for seal strength of flexible barrier materials. F 88-07. *Annual book of American standard testing methods* (pp. 768–777). Philadelphia, PA: American Society for Testing and Materials.
- ASTM F1249-13 (2013). *Standard test method for water vapor transmission rate through plastic film and sheeting using a modulated infrared sensor*. West Conshohocken, PA, USA: ASTM International.
- ASTM F2476-13 (2013). *Standard test method for the determination of carbon dioxide gas transmission rate (CO₂ TR) through barrier materials using an infrared detector*. West Conshohocken, PA, USA: ASTM International.
- Beigmohammadi, F., Peighambaroust, S. H., Hesari, J., Azadmard-Damirchi, S., Peighambaroust, S. J., & Khosrowshahi, N. K. (2016). Antibacterial properties of LDPE nanocomposite films in packaging of UF cheese. *Lebensmittel-Wissenschaft und -Technologie- Food Science and Technology*, 65, 106–111.
- Bonilla, J., & Sobral, P. G. A. (2018). Gelatin-chitosan edible film activated with Boldo extract for improving microbiological and antioxidant stability of sliced Prato cheese. *International Journal of Food Science and Technology*. <https://doi.org/10.1111/ijfs.14032>.
- Cano Embuena, A. I., Chafer Nacher, M., Chiralat Boix, A., Molina Pons, M. P., Borrás Llopis, M., Beltran Martínez, M. C., et al. (2016). Quality of goat's milk cheese as affected by coating with edible chitosan-essential oil films. *International Journal of Dairy Technology*, 70, 68–76.
- Caric, M. (1999). Ripened cheese varieties native to the balkan countries. In P. F. Fox (Ed.). *Cheese: Chemistry, physics and microbiology*. Boston, MA: Springer.
- Costa, M. J., Maciela, L. C., Teixeira, J. A., Vicente, A. A., & Cerqueira, M. A. (2018). Use of edible films and coatings in cheese preservation: Opportunities and challenges. *Food Research International*, 107, 84–92.
- Di Piero, P., Sorrentino, A., Mariniello, L., Giosafatto, C. V. L., & Porta, R. (2011). Chitosan/ whey protein film as active coating to extend Ricotta cheese shelf-life. *Lebensmittel-Wissenschaft und -Technologie- Food Science and Technology*, 44, 2324–2327.
- El-Sisi, A. S., El-Sattar, A., Gapr, M., & Kamaly, K. M. (2015). Use of chitosan as an edible coating in RAS cheese. *Bioline*, 3, 564–570.
- Elsabee, M. Z., & Abdou, E. S. (2013). Chitosan based edible films and coatings: A review. *Materials Science and Engineering: C*, 33, 1819.
- Farhan, A., & Hani, N. M. (2017). Characterization of edible packaging films based on semi-refined kappa-carrageenan plasticized with glycerol and sorbitol. *Food Hydrocolloids*, 64, 48–58.
- Fernandez-Bats, I., Di Piero, P., Villalonga-Santana, R., Garcia-Almendarez, B., & Porta, R. (2018). Bioactive mesoporous silica nanocomposite films obtained from native and transglutaminase-crosslinked bitter vetch proteins. *Food Hydrocolloids*, 82, 106–115 2018.
- Grujić, R., Vujanović, D., & Savanović, D. (2017). Biopolymers as food packaging materials. In E. Pellicer, D. Nikolic, J. Sort, M. Baró, F. Zivic, & N. Grujovic, (Eds.). *Advances in applications of industrial biomaterials* (pp. 139–160). Springer Int. Publishing.
- Gutiérrez-Méndez, N., Trancoso-Reyes, N., & Leal-Ramos, Y. M. Y. (2013). Texture profile analysis of fresh cheese and Chihuahua cheese using miniature cheese models. *TECNOCENCIA Chihuahua*, 7, 65–74.
- Hassan, A. N., Frank, J. F., & Elsoda, M. (2004). Microstructure and rheology of an acid-coagulated cheese (Karish) made with an exopolysaccharide-producing *Streptococcus thermophilus* strain and its exopolysaccharide non-producing genetic variant. *Journal of Dairy Research*, 71, 120–166.
- Humeid, M. A., Tukan, S. K., & Yamani, M. I. (1990). In-bag steaming of white brined cheese as a method for preservation. *Milchwissenschaft*, 45, 513–516.
- Joshi, N. S., Jhala, R. P., Muthukumarappan, K., Acharya, M. R., & Mistry, V. V. (2004). Textural and rheological properties of processed cheese. *International Journal of Food Properties*, 7, 519–530.
- Mazahreh, A. S., Quasem, J. M., Al-Shawabkeh, A. F., & Afaneh, I. A. (2009). The effect of adjusting pH on stretchability and meltability to white brined Nabulsi cheese. *American Journal of Applied Sciences*, 6, 543–550.
- Nateghi, L., Roohinejad, S., Totosaus, A., Mirhosseini, H., Shuhaimi, M., Meimandipour, A., et al. (2012). Optimization of textural properties and formulation of reduced fat Cheddar cheeses containing fat replacers. *Journal of Food Agriculture and Environment*, 10, 46–54.
- Pascall, M. A., & Lin, S. J. (2013). The application of edible polymeric films and coatings in the food industry. *Journal of Food Processing & Technology*, 4, 1000–1116.
- Porta, R., Di Piero, P., Rossi-Marquez, G., Mariniello, L., Kadivar, M., & Arabestani, A. (2015). Microstructure and properties of bitter vetch (*Vicia ervilia*) protein films reinforced by microbial transglutaminase. *Food Hydrocolloids*, 50, 102–107.
- Porta, R., Di Piero, P., Roviello, V., & Sabbah, M. (2017). Tuning the functional properties of bitter vetch (*Vicia ervilia*) protein films grafted with spermidine. *International Journal of Molecular Sciences*, 18, 2658–2669.
- Porta, R., Di Piero, P., Sabbah, M., Regalado Gonzales, C., Mariniello, L., Kadivar, M., et al. (2016). Blend films of pectin and bitter vetch (*Vicia ervilia*) proteins: Properties and effect of transglutaminase. *Innovative Food Science & Emerging Technologies*, 36, 245–251.
- Ramos, Ó. L., Pereira, J. O., Silva, S. I., Fernandes, J. C., Franco, M. I., Lopes-da-Silva, J. A., et al. (2012). Evaluation of antimicrobial edible coatings from a whey protein isolate base to improve the shelf life of cheese. *Journal of Dairy Science*, 95, 6282–6292.
- Reddy, M. M., Vivekanandhan, S., Misra, M., Bhatia, S. K., & Mohanty, A. K. (2013). Biobased plastics and bionanocomposites: Current status and future opportunities. *Progress in Polymer Science*, 38, 1653–1689.
- Romero, V., Borneo, R., Passalacqua, N., & Aguirre, A. (2016). Biodegradable films obtained from triticale (*x Triticosecale Witt- mack*) flour activated with natamycin for cheese packaging. *Food Packaging and Shelf Life*, 10, 54–59.
- Rossi Marquez, G., Di Piero, P., Mariniello, L., Esposito, M., Giosafatto, C. V. L., & Porta, R. (2017). Fresh-cut fruit and vegetable coatings by transglutaminase-crosslinked whey protein/pectin edible films. *Lebensmittel-Wissenschaft und -Technologie- Food Science and Technology*, 75, 124–130.
- Sabbah, M., Di Piero, P., Cammarota, M., Dell'Olmo, E., Arciello, A., & Porta, R. (2019). Development and properties of new chitosan-based films plasticized with spermidine and/or glycerol. *Food Hydrocolloids*, 87, 245–252.
- Sabbah, M., di Piero, P., Giosafatto, C. V. L., Esposito, M., Mariniello, L., Regalado-Gonzales, C., et al. (2017). Plasticizing effects of polyamines in protein-based films. *International Journal of Molecular Sciences*, 18, 1026–1035.
- Santonicola, S., Ibarra, V. G., Sendon, R., Mercogliano, R., & Quiros, A. R. B. (2017). Antimicrobial films based on chitosan and methylcellulose containing natamycin for active packaging applications. *Coatings*, 7(177), 1–10.
- Song, Y., & Zheng, Q. (2014). Ecomaterials based on food proteins and polysaccharides. *Polymer Reviews*, 54, 514–571.
- Tamime, A. Y., & Robinson, R. K. (1991). *Feta and related cheeses*. Cambridge, UK: Abington Hall.
- Tonyali, B., Cikriki, S., & Oztop, M. H. (2018). Physicochemical and microstructural characterization of gum tragacanth added whey protein based films. *Food Research International*, 105, 1–9.
- Wihodo, M., & Moraru, C. I. (2013). Physical and chemical methods used to enhance the structure and mechanical properties of protein films: A review. *Journal of Food Engineering*, 114, 292–302.
- Yamani, M. I., Al-Nabulsi, A. A., Haddadin, M. S., & Robinson, R. K. (1998). The isolation of salt tolerant bacteria from ovine and bovine milks for use in the production of Nabulsi cheese. *International Journal of Dairy Technology*, 51, 86–89.
- Yamani, M. I., Tukan, S. K., & Abu-Tayeh, S. J. (1997). Microbiological quality of kunafa and the development of a hazard analysis critical control point (HACCP) plan for its production. *Dairy, Food, and Environmental Sanitation*, 17, 638–643.
- Youssef, A. M., EL-Sayed, S. M., EL-Sayed, H. S., Salama, H. H., & Dufresne, A. (2016). Enhancement of Egyptian soft white cheese shelf life using a novel chitosan/carboxymethyl cellulose/zinc oxide bionanocomposite film. *Carbohydrate Polymers*, 151, 9–19.
- Zink, J., Wyrobnik, T., Prinz, T., & Schmid, M. (2016). Physical, chemical and biochemical modifications of protein-based films and coatings: An extensive review. *International Journal of Molecular Sciences*, 17, 1376–1421.



Development and properties of new chitosan-based films plasticized with spermidine and/or glycerol



Mohammed Sabbah^{a,b}, Prospero Di Piero^{a,*}, Marcella Cammarota^c, Eliana Dell'Olmo^a, Angela Arciello^a, Raffaele Porta^a

^a Department of Chemical Sciences, University of Naples "Federico II", Complesso Universitario di Montesantangelo, Via Cintia 21, 80126, Naples, Italy

^b Department of Nutrition and Food Technology, An-Najah National University, P.O. Box: 7, Nablus, Palestine

^c Department of Experimental Medicine, Section of Biotechnology and Molecular Biology, University of Campania "Luigi Vanvitelli", Via De Crecchio 7, 80138, Naples, Italy

ARTICLE INFO

Keywords:

Chitosan
Spermidine
Glycerol
Edible films
Plasticizer
Food coating

ABSTRACT

Different chitosan solutions were characterized by evaluating zeta potential and particle size, in the absence or presence of spermidine and/or glycerol, and the physicochemical, morphological and antimicrobial properties of the derived films were determined. An increase of film tensile strength and elongation at break was observed by increasing chitosan amounts, whereas only tensile strength and Young's modulus values were revealed higher at all chitosan concentrations when spermidine was absent. Spermidine-containing films were always more extensible exhibiting an elongation at break even higher than that of glycerol-plasticized films. The concurrent presence of appropriate concentrations of spermidine and glycerol further enhanced the extensibility and plasticity of the biomaterial, conferring to it the ability to be heat-sealed, as well as similar permeability in comparison with Viscofan NDX, widely commercialized as protein-based food casing. Finally, all the prepared films exhibited a clear antimicrobial activity, thus representing credible candidates as food preservative coatings and/or wrappings.

1. Introduction

Chitin is the second most abundant biopolymer occurring in nature after cellulose and chitinous waste, mainly produced from sea food processing (crustacean shells), still represents a major environmental issue (Arbia, Arbia, Adour, & Amrane, 2013).

Chitin is not soluble in common solvents, mostly due to its highly crystalline structure, and this property strongly limits the possible re-use of the polysaccharide. Nevertheless, one possible recycling of chitin rich wastes involves the chemical conversion of chitin in chitosan (CH), a random copolymer formed by D-glucosamine and N-acetyl-D-glucosamine units, by alkaline deacetylation at high temperatures (Muxika, Etxabide, Uranga, Guerrero, & de la Caba, 2017). Although various factors (e.g. chitin source, alkali concentration, deacetylation temperature and time) may affect its properties, CH (pKa, 6.3) is easily dissolved in acidic solutions, i.e. when its free amino groups are fully protonated (Aljawish, Chevalot, Jasniewski, Scher, & Muniglia, 2015; Babu, O'Connor, & Seeram, 2013; Kaur & Dhillon, 2014; Van den Broek,

Knoop, Kappen, & Boeriu, 2015).

The unique physicochemical and biological features of CH make it worthy in regard to various biomedical, pharmaceutical and agricultural applications. Moreover, because of CH broad antibacterial and antifungal properties, CH-based edible films may be promoted as promising "new economy" bio-based plastics (Spierling et al., 2018) also for food coating and protection in addition to the protein-based biomaterials (Han, Yu, & Wang, 2018). In fact, although CH-based films exhibit weak mechanical properties, as well as unsatisfying water vapor (WV) barrier features, they remain the most promising ones among the various hydrocolloid biomaterials so far proposed, because they are biodegradable, biocompatible, non-toxic and obtainable in large quantities from waste products of seafood industries (crustacean shells) (Elsabee & Abdou, 2013; Mayachiew & Devahastin, 2008; Van der Broek et al., 2015). In addition, CH has been considered as a GRAS (Generally Recognized As Safe) food additive for both consumers and the environment (FDA, 2012).

Several advantages have been demonstrated when different food

* Corresponding author. Department of Chemical Sciences, University of Naples "Federico II", Complesso Universitario di Montesantangelo, via Cintia 21, 80126, Napoli, Italy.

E-mail addresses: mohammed.sabbah@unina.it (M. Sabbah), prospero.dipiero@unina.it (P. Di Piero), marcella.cammarota@unicampania.it (M. Cammarota), eliana.dellolmo@unina.it (E. Dell'Olmo), anarciel@unina.it (A. Arciello), raffaele.porta@unina.it (R. Porta).

<https://doi.org/10.1016/j.foodhyd.2018.08.008>

Received 28 May 2018; Received in revised form 3 August 2018; Accepted 4 August 2018

Available online 06 August 2018

0268-005X/ © 2018 Elsevier Ltd. All rights reserved.

products were CH-coated. CH was shown to be able to form a semi-permeable layer on the surface of various fruits and vegetables, and to delay the rate of respiration and their ripening by reducing food moisture and weight loss (Alvarez, Ponce, & Moreira, 2013; Chofer, Sanchez-Gonzalez, Gonzalez-Martinez, & Chiralt, 2012; Gol, Patel, & Rao, 2013; Sun et al., 2014). Moreover, edible CH films have also been used as carriers releasing different bioactive agents like essential oils, as well as antimicrobials and/or antioxidants (Acevedo-Fani, Salvia-Trujillo, Rojas-Graü, & Martín-Belloso, 2015; Avila-Sosa et al., 2012), and to protect fish, red meat, poultry and their processed products, with the aim to decrease color changes, lipid oxidation, growth of pathogenic and spoilage bacteria and to extend product shelf life (Chamanara, Shabanpour, Khomeiri, & Gorgin, 2013; Gómez-Estaca, De Lacey, López-Caballero, Gómez-Guillén, & Montero, 2010; Samelis, 2006).

Many different attempts have been made to improve mechanical, barrier and functionality properties of CH films by blending CH film forming solution (FFS) with other biopolymers like proteins (Baron, Pérez, Salcedo, Córdoba, & Sobral, 2017; Di Piero et al., 2007, 2006; Escamilla-García et al., 2017). A further way to modify the physico-chemical characteristics of the hydrocolloid edible films, and for a subsequent breakthrough in their applications, is the addition of appropriate concentrations of a suitable plasticizer. Generally, plasticizers are added to both synthetic and bio-based polymeric materials to decrease the intermolecular forces along the polymer chains, impart flexibility and lower the glass transition temperature (Mekkonen, Mussone, Khalil, & Bressler, 2013; Vieira, Altenhofen da Silva, Oliveira dos Santos, & Beppu, 2011). Our recent studies have shown that aliphatic polyamines, in particular the triamine spermidine (SPD), are able to influence the morphological, mechanical and barrier properties of pectin- and protein-based films (Esposito et al., 2016; Porta, Di Piero, Roviello, & Sabbah, 2017). In addition, the combination of different concentrations of both SPD and glycerol (GLY) may give rise to protein-based biomaterials possessing a wide spectrum of functional characteristics (Porta et al., 2017; Sabbah et al., 2017). Since Chanphai and Tajmir-Riahi (2016) recently reported the conjugation of CH nanoparticles with biogenic polyamines SPD and spermine in aqueous solution, we were stimulated to analyze the physicochemical and biological properties of CH-based films by incorporating various SPD and GLY proportions into the host polysaccharide matrix. Based on the present investigation, it is expected that the addition of both plasticizers to polymeric matrix can bring about improved features of the CH films in such a way that a new polysaccharide-based biomaterial can represent a valid alternative to gelatin-based films, such as the well commercialized Viscofan (www.viscofan.com) widely used for food wrapping. In fact, gelatin is one of the most controversial of kosher and halal food ingredients and it seems advisable to replace it according to the religion-based dietary restrictions of Muslim and Jewish consumers and the consequent negative impact in their marketplace (Regenstein, Chaudry, & Regenstein, 2003).

2. Materials and methods

2.1. Materials

CH (mean molar mass of 3.7×10^4 g/mol) with a degree of 9.0% *N*-acetylation, was a gift from Prof. R.A.A. Muzzarelli (University of Ancona, Italy). The mean molar mass of CH was determined by a viscometric method, as previously described (Costa, Teixeira, Delpech, Sousa & Costa, 2015), by dissolving 0.2 g of CH in 10 mL of 0.1 M acetic acid, containing 0.2 M sodium chloride, and obtaining five different dilutions of the original solution. The degree of *N*-acetylation was determined by the first derivative ultraviolet spectrophotometric method, as described by Muzzarelli and Rocchetti (1985), based on recording of the first derivative of the CH UV spectra at 202 nm by using a standard curve obtained by varying *N*-acetylglucosamine concentrations. Citrus

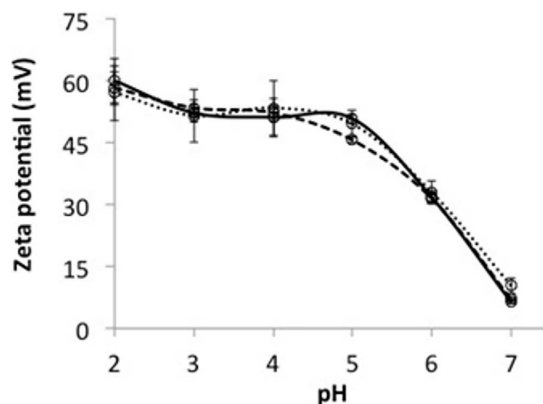


Fig. 1. Effect of either 5 mM SPD and/or 25 mM GLY on zeta potential of 0.2% CH FFSs measured at different pH values. The different FFSs contained only CH (solid line), CH + SPD (point line), CH + GLY (dashed line). The results are expressed as mean \pm standard deviation. Further experimental details are given in sections 2.2 and 2.5.

peel low-methylated (7.0%) pectin (Aglupectin USP) was purchased from Silvateam srl (San Michele Mondovì, CN, Italy). Viscofan NDX edible casings were from Naturin Viscofan GmbH (Tajonar-Navarra, Spain). GLY (about 87%) was supplied from the Merck Chemical Company (Darmstadt, Germany), whereas SPD was from Sigma Chemical Company (St. Louis, MO, USA). All other chemicals were analytical grade.

2.2. Titration of CH FFSs

Zeta potential values of different CH solutions (0.2% CH containing or not 5 mM SPD and/or 25 mM GLY) were determined by a Zetasizer Nano-ZSP (Malvern[®], Worcestershire, UK) equipped with an automatic titrator unit (MPT-2). The device was equipped with a helium-neon laser of 4 mW output power operating at the fixed wavelength of 633 nm (wavelength of laser red emission). The instrument software programmer calculated the zeta potential through the electrophoretic mobility by applying a voltage of 200 mV using the Henry equation. CH FFSs were prepared at pH 2.0 by using 1.0 N HCl and then the titration was carried out from pH 2.0 to pH 7.0 by adding 1.0, 0.5, and 0.1 N NaOH as titrant solutions under constant stirring at 25 °C. Zeta potential values were measured at each pH in triplicate.

2.3. CH FFS and film preparation

CH stock solution (2%) was prepared by dissolving the polysaccharide in 0.1 N HCl at room temperature under overnight constant stirring at 700 rpm (Di Piero et al., 2006). FFSs and films were obtained at pH 4.5 by using CH (0.1–0.6%) mixed or not with different concentrations of SPD (2–10 mM; 5–24%, w/w with respect to maximal CH concentration used) and/or GLY (2–40 mM; 3–60%, w/w with respect to maximal CH concentration used). All FFSs were characterized for their zeta potential, Z-average and conductivity by a Zetasizer Nano-ZSP as described above. FFSs were then poured onto polystyrene plates (1 mL \times cm²), most experiments being performed by using 8 cm diameter polystyrene Petri dishes. FFSs were allowed to dry in an adjusted environmental chamber at 25 °C and 45% RH for 48 h and, finally, the dried films were peeled from the casting surface and stored at 25 °C and 50% RH.

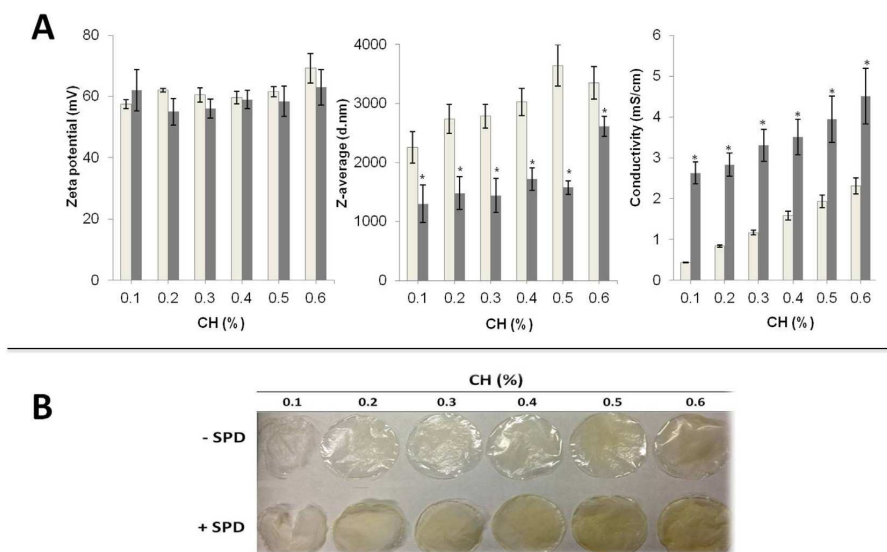


Fig. 2. Zeta potential, Z-average and conductivity values of FFSs prepared at pH 4.5 with different CH concentrations in the absence (light bars) or presence (grey bars) of 5 mM SPD (panel A), and the images of the derived films (panel B). The results are expressed as mean ± standard deviation. *Values significantly different compared to the ones obtained at the same CH concentration in the absence of SPD (p < 0.05). Further experimental details are given in sections 2.2–2.5.

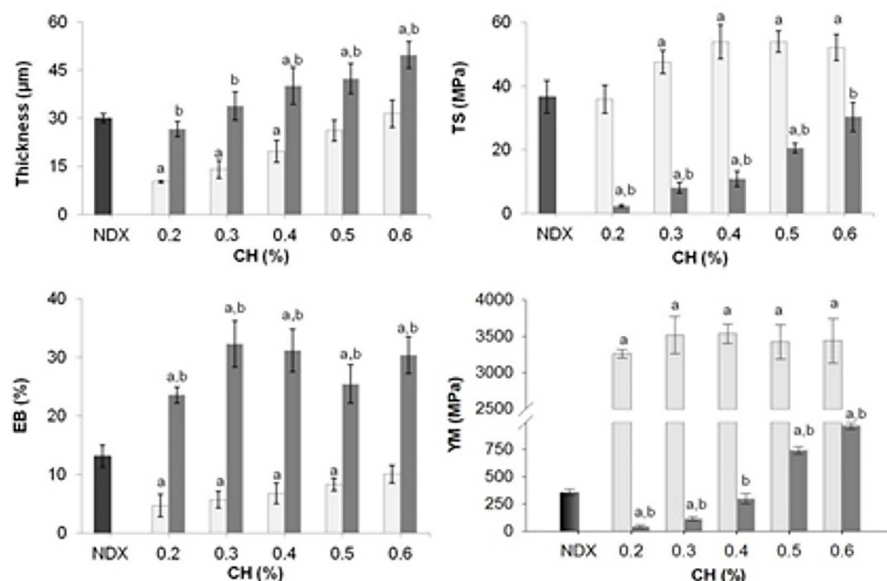


Fig. 3. Effect of different CH concentrations on thickness and mechanical properties of films prepared in the absence (light bars) or presence (grey bars) of 5 mM SPD. The results are expressed as mean ± standard deviation. The values significantly different from those obtained by analyzing Viscofan NDX (black bars) are indicated by “a”, whereas the values indicated by “b” were significantly different from those obtained at the same CH concentration but in the absence of SPD. Further experimental details are given in sections 2.3–2.5.

2.4. Film characterization

All films, cut into 1 cm × 8 cm strips by using a sharp scissor, were conditioned at 25 °C and 50% RH for 2 h by placing them into a desiccator over a saturated solution of Mg(NO₃)₂·6 H₂O before being tested. Film thickness was measured in six different points with a micrometer (Electronic digital micrometer, DC-516, sensitivity 0.001 mm

and their tensile strength (TS), elongation at break (EB) and Young's modulus (YM) were determined on five specimens of each sample (5 cm gage length, 1 kN load and 1 mm/5 min speed) by using an Instron universal testing instrument model no. 5543A (Instron Engineering Corp., Norwood, MA, USA). One specimen of each sample (1 × 30 cm strip) was always prepared and analyzed with a specimen gage length of 25 cm (ASTM D882-97, 1997) to confirm the data obtained with

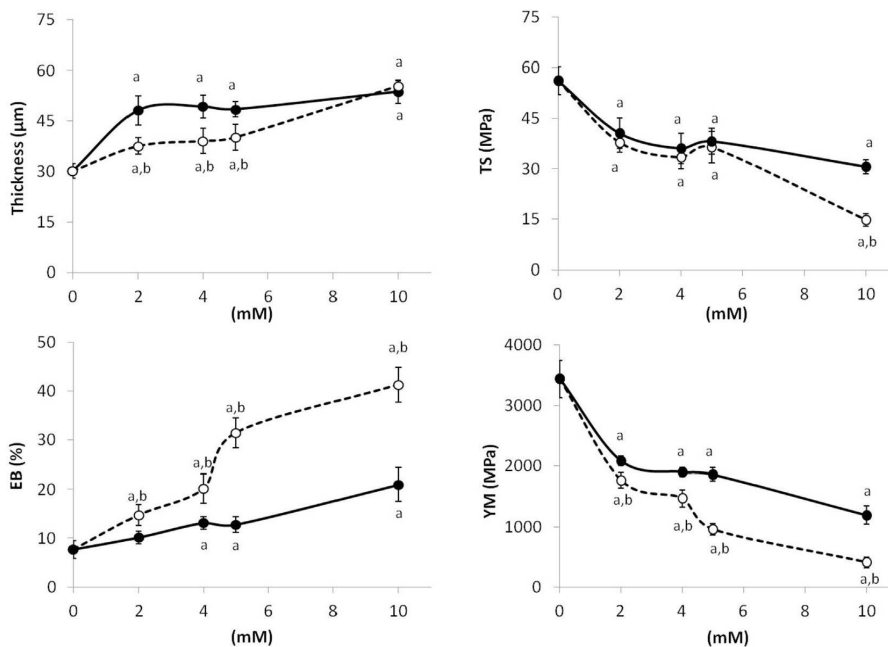


Fig. 4. Effect of different concentrations of SPD (dashed line) and GLY (solid line) on the mechanical properties of 0.6% CH films. The results are expressed as mean ± standard deviation. The values significantly different from those obtained with films made by only CH were indicated by “a”, whereas the values of the SPD-containing films indicated by “b” were significantly different from those obtained with films prepared in the presence of GLY. Further experimental details are given in sections 2.3–2.5.

Table 1
Effect of different concentrations of GLY on the mechanical properties of 0.6% CH films containing different amounts of SPD.

Addition		Thickness (μm)	TS (MPa)	EB (%)	YM (MPa)
SPD	GLY				
mM					
-	-	31.50 ± 4.23	52.19 ± 4.15	10.07 ± 2.53	3438.10 ± 506.30
-	10	53.71 ± 3.46	30.57 ± 2.04	20.95 ± 3.43	1194.38 ± 150.87
-	20	76.00 ± 5.30	15.60 ± 2.21	73.10 ± 3.48	146.30 ± 10.00
-	30	84.67 ± 4.04	10.20 ± 0.38	109.97 ± 5.51	27.70 ± 2.94
-	40	91.00 ± 3.60	10.12 ± 2.24	136.04 ± 8.15	19.24 ± 2.67
1	-	36.70 ± 3.25	46.06 ± 5.23	12.19 ± 2.07	2114.01 ± 206.86
1	10	39.33 ± 3.79	25.78 ± 3.26	25.38 ± 0.24	1191.72 ± 46.35
1	20	48.00 ± 1.00	20.08 ± 3.18	73.10 ± 3.40	143.11 ± 22.04
1	30	74.67 ± 2.52	18.12 ± 2.40	139.33 ± 8.40	42.46 ± 4.33
1	40	92.30 ± 3.60	11.41 ± 2.42	134.60 ± 8.07	19.06 ± 1.14
2	-	37.60 ± 4.51	37.80 ± 2.90	14.73 ± 3.13	1874.03 ± 186.30
2	10	34.67 ± 3.51	30.63 ± 0.38	42.33 ± 2.72	1613.10 ± 19.03
2	20	57.34 ± 2.52	31.09 ± 1.69	116.78 ± 7.91	195.97 ± 62.86
2	30	74.34 ± 2.08	16.74 ± 1.46	113.46 ± 2.44	69.56 ± 1.65
2	40	95.30 ± 3.50	7.80 ± 1.52	113.02 ± 5.30	29.52 ± 3.72
5	-	49.83 ± 4.21	30.33 ± 4.50	30.35 ± 3.53	965.36 ± 36.56
5	10	52.00 ± 2.65	28.92 ± 1.99	101.32 ± 6.04	221.73 ± 2.57
5	20	76.33 ± 3.51	8.97 ± 2.65	118.34 ± 17.22	36.90 ± 5.00
5	30	86.00 ± 3.61	7.86 ± 2.50	109.70 ± 10.21	26.44 ± 3.25
5	40	97.70 ± 2.50	7.80 ± 1.52	117.70 ± 16.14	20.76 ± 2.16
10	-	55.33 ± 1.53	14.68 ± 0.92	41.36 ± 3.57	412.00 ± 90.00
10	10	71.00 ± 3.61	13.53 ± 1.32	111.12 ± 4.88	48.28 ± 2.42
10	20	82.33 ± 3.79	5.95 ± 0.41	109.80 ± 4.61	31.61 ± 3.54
10	30	90.30 ± 2.50	5.76 ± 0.57	113.57 ± 10.42	27.78 ± 3.94
10	40	102.00 ± 4.40	5.03 ± 0.75	109.09 ± 9.75	20.84 ± 1.92

The results are expressed as mean ± standard deviation. Further experimental details are given in sections 2.3–2.5.

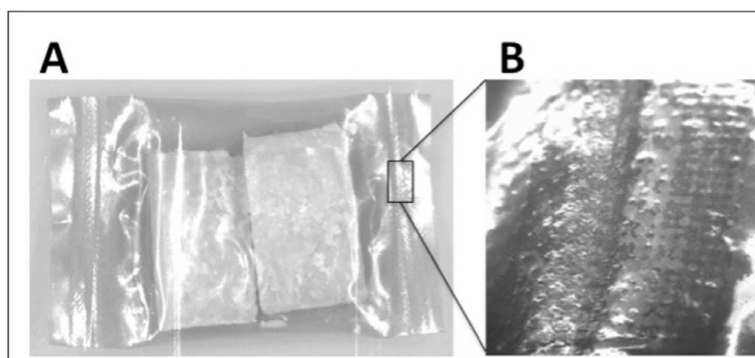


Fig. 5. Food wrapping by a heat-sealed CH film containing 5 mM SPD and 25 mM GLY (panel A), and the magnification (50 \times) under optical microscope of the film heat-welding (panel B).

Table 2

Gas and WV permeability of 0.6% CH films prepared at pH 4.5 in the presence of 5 mM SPD and/or 25 mM GLY.

Film	Permeability (cm ³ mm ⁻² day ⁻¹ kPa ⁻¹)		
	CO ₂	O ₂	WV
Viscofan NDX	3.71 \pm 0.16 ^b	0.03 \pm 0.01 ^b	0.08 \pm 0.01
CH film	15.81 \pm 2.06 ^a	14.33 \pm 0.29 ^a	0.05 \pm 0.02
CH film + SPD	2.84 \pm 0.01 ^{ab}	3.67 \pm 0.01 ^{ab}	0.17 \pm 0.01 ^{ab}
CH film + GLY	0.71 \pm 0.07 ^{ab}	0.11 \pm 0.02 ^{ab}	0.28 \pm 0.02 ^{ab}
CH film + SPD + GLY	2.40 \pm 0.13 ^{ab}	0.05 \pm 0.01 ^{ab}	0.37 \pm 0.01 ^{ab}

Significantly different values compared to those observed analyzing Viscofan NDX (^a) and to those observed analyzing CH film obtained in the absence of plasticizers (^b). Further experimental details are given in sections 2.3–2.5.

1 \times 8 cm film strips.

To determine film permeabilities to O₂ (ASTM D3985-05, 2010), CO₂ (ASTM F2476-13, 2013) and WV (ASTM F1249-13, 2013) aluminum masks were used with the aim to reduce the film test area to 5 cm². The measurements were carried out in triplicate at 25 $^{\circ}$ C and 50% RH by using a TotalPerm apparatus (Extra Solution s.r.l., Pisa, Italy).

CH films surface and cross section ultrastructure was analyzed by using a Scanning Electron Microscope (SEM). Films were cutted using scissors, mounted on stub and sputter-coated with platinum-palladium (Denton Vacuum Desk V), before observation with Supra 40 ZEISS (EHT = 5.00 kV, detector inlens). To test CH film ability to be heat-sealed, a routine device to thermo-weld polyethylene film strips was purchased from Cytinet Medical (Milano, Italy) (C.A. 50 Hz. 200–250 V) and utilized by subjecting double layers of CH films containing different GLY concentrations to a pressure at high temperatures for 10 s. The thermo-sealed film strips were analyzed by an optical microscope at 50 \times magnification.

To evaluate the antimicrobial activity of CH films, *Salmonella typhimurium* ATCC 14028 was grown in Tryptic Soy Broth (TSB, Becton Dickinson Difco, Franklin Lakes, NJ) and on Tryptic Soy Agar (TSA; Oxoid Ltd., Hampshire, UK). In all the experiments, bacteria were inoculated and grown overnight in TSB at 37 $^{\circ}$ C and, the day after, were transferred into a fresh TSB tube and grown to mid-logarithmic phase. Bacterial cells were then diluted in TSB to approximately 2 \times 10⁷ CFU/mL and inoculated by surface streaking into TSA plates using a swab. A 1 cm² strip of CH film, containing or not 5 mM SPD and/or 25 mM GLY, was finally placed onto the center of the inoculated plate and pressed to ensure full contact with the agar surface. Plates were incubated at 37 $^{\circ}$ C for 24 h and the presence or absence of bacterial growth under the film was evaluated. Parallel experiments by testing the antimicrobial

activities of pectin-based films, prepared as previously described (Esposito et al., 2016) in the absence or presence of 5 mM SPD and/or 25 mM GLY, were carried out. Negative controls were carried out by placing pectin and CH films in contact with the agar surface in the absence of bacterial cells.

2.5. Statistical analysis

JMP software 10.0 (SAS Institute, Cary, NC, USA) was used for all statistical analyses. One-way ANOVA and the least significant difference (LSD) test for mean comparisons were used. Differences at $p < 0.05$ were considered significant and are indicated with different letters.

3. Results and discussion

Since the ability of the aliphatic triamine SPD to act as plasticizer of pectin-based films (Esposito et al., 2016), as well as of protein-based films (Porta et al., 2017; Sabbah et al., 2017), has been recently demonstrated, we were stimulated to investigate the effects of SPD on the properties of CH-based films. Therefore, preliminary experiments aimed to find adequate conditions for the development of stable FFSs were carried out by determining the zeta potential of CH aqueous solutions, containing or not either SPD or GLY, as a function of pH using an apparatus capable of separating by microelectrophoresis and measuring dynamic light scattering. The zeta potential of 0.2% CH solutions, prepared both in the absence and presence of 5 mM SPD and/or 25 mM GLY, showed a value ranging from +60 mV to +50 mV between pH 2.0 and 5.0 (Fig. 1). The value was found to progressively decrease with further increases of pH and approach to CH pKa, up to +10 mV at pH 7.0. These findings clearly indicated that neither the polyamine, even though positively charged, nor GLY influenced the zeta potential and the stability of CH solution.

Moreover, FFSs containing lower or higher CH concentrations (0.1–0.6%), prepared at pH 4.5 both in the absence and presence of 5 mM SPD, were found to have significantly different zeta potential values (all higher than +50 mV) (Fig. 2, panel A). Conversely, the same panel shows that the Z-average values increased in parallel with the enhancement of CH concentration and FFS conductivity. However, SPD containing CH FFS samples always showed markedly lower Z-average values (< 3000 dnm), probably due to their higher conductivity (Sabbah et al., 2016). Finally, handleable films were formed starting from 0.2% CH and their yellowish color was more intense by both increasing CH concentration and, mostly, in the presence of SPD (Fig. 2, panel B).

Fig. 3 shows the effects of CH concentration on the thickness and

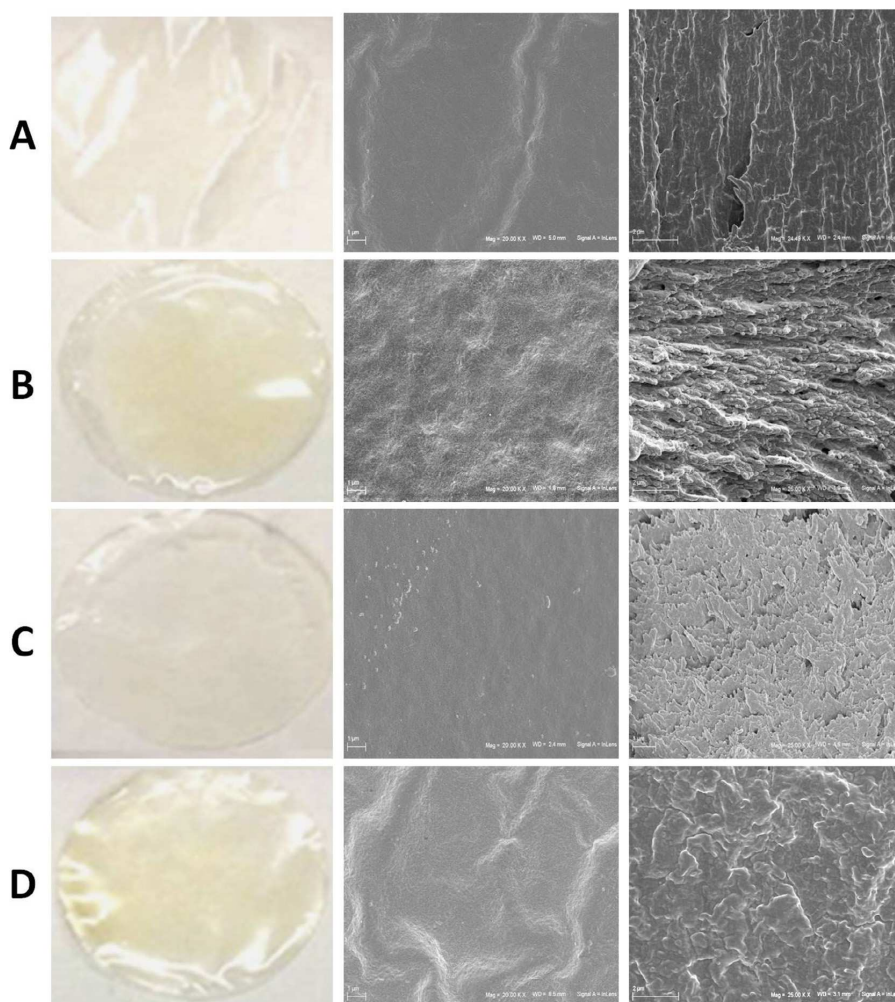


Fig. 6. Film images (left) and SEM micrographs of the film surfaces (20,000 \times magnification, center) and cross sections (25,000 \times magnification, right) obtained with 0.6% CH films prepared in the absence of plasticizers (A) and in the presence of either 25.0 mM GLY (B), 5.0 mM SPD (C) or both (D). The images shown were chosen as the most representative of each sample. Further experimental details are given in sections 2.3–2.5.

mechanical properties of the films prepared in the absence and presence of 5 mM SPD, in comparison with those detected by using a commercial biomaterial widely used for meat casing (Viscofan NDX). Increasing CH amounts were found to determine a parallel increase in film thickness, TS and EB both in the absence and presence of SPD, whereas the EB values were found much higher, and YM much lower, at all CH concentrations when films were prepared in the presence of SPD.

Therefore, the polyamine was confirmed to act as plasticizer not only in anionic polysaccharide (pectin) based films, as previously reported by Esposito et al. (2016), but also in cationic polysaccharide (CH) based ones, being able to increase their EB and reducing both TS and YM. Since also SPD is positively charged under the experimental conditions used to prepare CH FFSs, the plasticizing effect of the polyamine may be explained only by assuming the formation of non-ionic interactions between CH and SPD during FFS drying. This conclusion is supported by spectroscopic, thermodynamics and docking experiments recently reported by Chanphai and Tajmir-Riahi (2016), indicating the occurrence of hydrophobic and H-bonding interactions

between the polyamine and CH nanoparticles. However, regardless of any other consideration, it is worthy to note that by adding the polyamine to the FFS, and by varying CH concentration, it is possible to prepare a polysaccharide-based material possessing mechanical properties very similar to those exhibited by Viscofan NDX, a widely commercialized protein-based casing.

To compare SPD effects on the mechanical properties of the CH-based films with respect to those determined by another well known plasticizer, i.e. GLY, we measured the TS, EB and YM values, as well as the thickness, of the CH films containing different concentrations of either SPD or GLY (Fig. 4).

Our findings indicate that SPD-containing CH films were always more extensible, exhibiting a higher EB than that of CH films plasticized by GLY. Conversely, they showed a similar TS, but lower thickness and YM, exhibiting thus also a major elasticity with respect to the GLY-containing films.

Finally, we investigated the mechanical properties of CH films containing different concentrations of both SPD and GLY. Table 1 shows

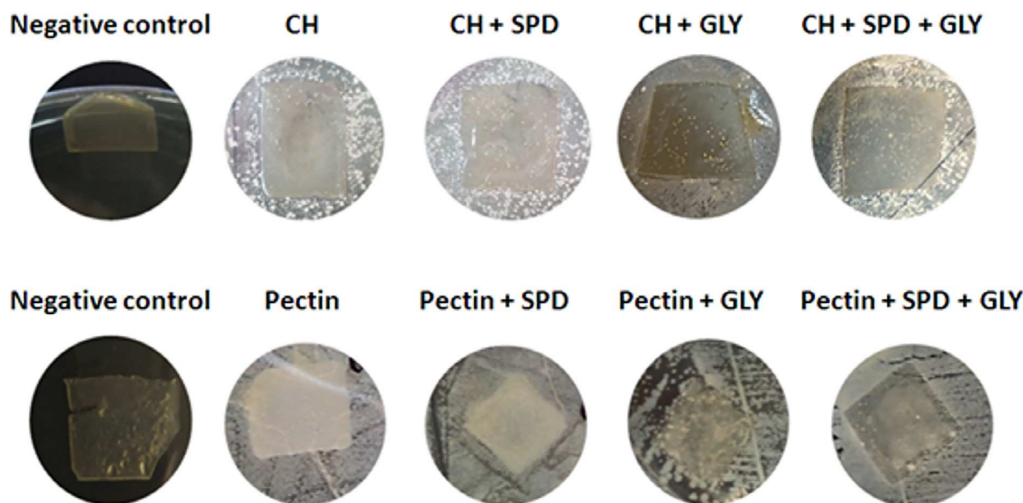


Fig. 7. Antimicrobial activity of CH and pectin films prepared in the absence or presence of 5 mM SPD and/or 25 mM GLY. The biological effect was evaluated on *Salmonella typhimurium* ATCC 14028 foodborne pathogenic bacterium by analyzing the growth of bacterial cells in direct contact with the film. CH and pectin negative controls were obtained in the absence of bacterial cells. Further experimental details are given in sections 2.3–2.5.

that the concomitant presence of increasing concentrations of both SPD and GLY significantly enhanced film EB as well as their thickness. More in particular, it seemed sufficient to blend at least 5.0 mM SPD with 10.0 mM GLY to reach a film EB three times higher than that observed with films containing only 5.0 mM SPD. Moreover, to obtain a similar so high EB value with lower SPD concentrations, higher amounts of GLY were needed (20 mM GLY with 2 mM SPD or 30 mM GLY with 1.0 mM SPD).

Conversely, very marked reductions of TS and YM values of the CH films were detected only when GLY was both present in the FFS. In particular, very low YM values began to be observed by mixing 5.0 mM SPD with only 10 mM GLY. Therefore, the obtained CH films blended with both SPD and GLY resulted to possess a capacity to withstand loads tending to elongate not much lower than that of Viscofan NDX but with an ultimate elongation and elasticity markedly improved with respect to those of the widely commercialized biomaterial (see Fig. 3).

Furthermore, we investigated the ability of the CH films, prepared in the absence or presence of different SPD and/or GLY concentrations, to be heat-sealed. Our results indicate that only the films containing at least 25 mM GLY, prepared both in the absence and presence of SPD, were able to be heat-sealed (Fig. 5). Therefore, we decided to continue our studies by analyzing the morphological features, as well as the barrier and antimicrobial properties, of 0.6% CH films obtained in the presence of SPD and/or GLY at concentrations of 5 and 25 mM, respectively.

Also the permeability tests of the CH films blended with SPD and GLY indicated interesting features of the new biomaterials. In fact, Table 2 reports that whereas the CH films obtained in the absence of plasticizers showed, with respect to Viscofan NDX, barrier properties toward O₂ and CO₂ markedly lower but similar WV permeability, CH films blended with both SPD and GLY exhibited similar gas barrier effect but increased WV permeability. Therefore, once again, SPD and/or GLY addition may represent a useful strategy to give rise to different edible films specifically tailored for desired applications.

Surface and cross-sectional morphology of the selected CH films, prepared in the absence or presence of SPD and/or GLY are illustrated in Fig. 6. According to the SEM images it seems that SPD contributes to maintain the film surface structure of the original CH matrix (Fig. 6 C, left), whereas GLY increases film surface roughness (Fig. 6 B, left). Furthermore, film cross section analyses indicate that, even though all

matrices have ordered structures, GLY and SPD alone give rise to fibrous-like and exfoliated layers (Fig. 6 B and C, right), respectively, whereas the concomitant presence of both SPD and GLY generates amorphous structures (Fig. 6 D, right).

Finally, the antimicrobial activity of the selected CH films was assayed on *Salmonella typhimurium* strain by placing small pieces of each film into the center of the inoculated plate in full contact with the agar surface (Sagoo, Board, & Roller, 2002). By analyzing the agar surface in contact with the film after 24 h at 37 °C we observed that the CH film itself exhibited an evident antimicrobial activity that was not influenced by the presence of SPD and/or GLY. Neither the controls carried out without microorganism inoculation nor the films prepared with a different polysaccharide, such as pectin, showed inhibitory effects on the bacterial cell growth similar to those exhibited by all the CH-based films (Fig. 7).

4. Conclusions

The results reported in the present study open new possibilities in the applications of bio-based materials derived from CH and, as a consequence, in chitin waste recycling. CH-based films prepared in the presence of SPD and GLY were shown to possess noteworthy mechanical and permeability properties compared to the films obtained with CH alone. The plasticized films are able to be thermo-sealed and retain the well known antimicrobial CH features. The use of these new biomaterials as alternative to Viscofan, a well known and commercialized edible casing, as well as in coatings and wrappings of selected food products, is suggested.

Acknowledgements

This work was supported by the Italian Ministries of Foreign Affairs and International Cooperation (IV Programma Quadro di Cooperazione Italia/Messico, 2017, (CUP: E62D15002620001)) (to P.D.) and of Agricultural, Food and Forestry Policies (CUP: J57G17000190001) (to R.P. & A.A.). We are grateful to Mrs. Maria Fenderico for her helpful assistance.

References

- Acevedo-Fani, A., Salvia-Trujillo, L., Rojas-Graü, M. A., & Martín-Belloso, O. (2015). Edible films from essential-oil-loaded nanoemulsions: Physicochemical characterization and antimicrobial properties. *Food Hydrocolloids*, *47*, 168–177.
- Aljawish, A., Chevalot, I., Jasniowski, J., Scher, J., & Muniglia, L. (2015). Enzymatic synthesis of chitosan derivatives and their potential applications. *Journal of Molecular Catalysis B: Enzymatic*, *112*, 25–39.
- Alvarez, M. V., Ponce, A. G., & Moreira, M. d. R. (2013). Antimicrobial efficiency of chitosan coating enriched with bioactive compounds to improve the safety of fresh cut broccoli. *LWT-Food Science and Technology*, *50*, 78–87.
- Arbia, W., Arbia, L., Adour, L., & Amrane, A. (2013). Extraction from crustacean shells using biological methods – a review. *Food Technology and Biotechnology*, *51*, 12–25.
- ASTM D3985-05 (2010). *ASTM International. West Conshohocken, PA: Standard test method for oxygen gas transmission rate through plastic film and sheeting using a colorimetric sensor.*
- ASTM D882-97 (1997). *Annual book of ASTM standards. Philadelphia, PA: Standard test method for tensile properties of thin plastic sheeting.*
- ASTM F1249-13 (2013). *ASTM International. West Conshohocken, PA: Standard test method for water vapor transmission rate through plastic film and sheeting using a modulated infrared sensor.*
- ASTM F2476-13 (2013). *ASTM International. West Conshohocken, PA: Standard test method for the determination of carbon dioxide gas transmission rate (CO₂ TR) through barrier materials using an infrared detector.*
- Avila-Sosa, R., Palou, E., Munguía, M. T. J., Nevárez-Moorillón, G. V., Cruz, A. R. N., & López-Malo, A. (2012). Antifungal activity by vapor contact of essential oils added to amaranth, chitosan, or starch edible films. *International Journal of Food Microbiology*, *153*, 66–72.
- Babu, R., O'Connor, K., & Seeram, R. (2013). Current progress on bio-based polymers and their future trends. *Progress in Biomaterials*, *2*, 1–16.
- Baron, R. D., Pérez, L. L., Salcedo, J. M., Córdoba, L. P., Sobral, P. J., & do, A. (2017). Production and characterization of films based on blends of chitosan from blue crab (*Callinectes sapidus*) waste and pectin from Orange (*Citrus sinensis* Osbeck) peel. *International Journal of Biological Macromolecules*, *98*, 676–683.
- Chamanara, V., Shabanpour, B., Khomeiri, M., & Gorgin, S. (2013). Shelf-life extension of fish samples by using enriched chitosan coating with thyme essential oil. *Journal of Aquatic Food Product Technology*, *22*, 3–10.
- Chanphai, P., & Tajmir-Riahi, H. A. (2016). Conjugation of chitosan nanoparticles with biogenic and synthetic polyamines: A delivery tool for antitumor polyamine analogues. *Carbohydrate Polymers*, *152*, 665–671.
- Chofer, M., Sanchez-Gonzalez, L., Gonzalez-Martinez, C., & Chiralt, A. (2012). Fungal decay and shelf life of oranges coated with chitosan and bergamot, thyme, and tea tree essential oils. *Journal of Food Science*, *77*, E182–E187.
- Costa, C. N., Teixeira, V. G., Delpach, M. C., Souza, J. V. S., & Costa, M. A. S. (2015). Viscometric study of chitosan solutions in acetic acid/sodium acetate and acetic acid/sodium chloride. *Carbohydrate Polymers*, *133*, 245–250.
- Di Piero, P., Chico, B., Villalonga, R., Mariniello, L., Damiao, A. E., Masi, P., et al. (2006). Chitosan-why protein edible films produced in the absence or presence of transglutaminase: Analysis of their mechanical and barrier properties. *Biomacromolecules*, *7*, 744–749.
- Di Piero, P., Chico, B., Villalonga, R., Mariniello, L., Masi, P., & Porta, R. (2007). Transglutaminase-catalyzed preparation of chitosan-ovalbumin films. *Enzyme and Microbial Technology*, *40*, 437–441.
- Elsabee, M. Z., & Abdou, E. S. (2013). Chitosan based edible films and coatings: A review. *Materials Science and Engineering C*, *33*, 1819–1841.
- Escamilla-García, M., Calderón-Domínguez, G., Chanona-Pérez, J. J., Mendoza-Madrugal, A. G., Di Piero, P., García-Almendárez, B. E., et al. (2017). Physical, structural, barrier, and antifungal characterization of chitosan–zein edible films with added essential oils. *International Journal of Molecular Sciences*, *18*, 2370–2384.
- Esposito, M., Di Piero, P., Regalado-Gonzales, C., Mariniello, L., Giosafatto, C. V. L., & Porta, R. (2016). Polyamines as new cationic plasticizers for pectin-based edible films. *Carbohydrate Polymers*, *153*, 222–228.
- FDA (2012). *Generally recognized as Safe (GRAS) notice inventory*. Silver Spring, MD: U.S. Food and Drug Administration.
- Gol, N. B., Patel, P. R., & Rao, T. R. (2013). Improvement of quality and shelf-life of strawberries with edible coatings enriched with chitosan. *Postharvest Biology and Technology*, *85*, 185–195.
- Gómez-Estaca, J., De Lacey, A. L., López-Caballero, M., Gómez-Guillén, M., & Montero, P. (2010). Biodegradable gelatin–chitosan films incorporated with essential oils as antimicrobial agents for fish preservation. *Food Microbiology*, *27*, 889–896.
- Han, Y., Yu, M., & Wang, L. (2018). Bio-based films prepared with soybean by-products and pine (*Pinus densiflora*) bark extract. *Journal of Cleaner Production*. <https://doi.org/10.1016/j.jclepro.2018.03.115>.
- Kaur, S., & Dhillon, G. S. (2014). The versatile biopolymer chitosan: Potential sources, evaluation of extraction methods and applications. *Critical Reviews in Microbiology*, *40*, 155–175.
- Mayachiew, P., & Devahastin, S. (2008). Comparative evaluation of physical properties of edible chitosan films prepared by different drying methods. *Drying Technology*, *26*, 176–185.
- Mekonnen, T., Mussone, P., Khalil, H., & Bressler, D. (2013). Progress in bio-based plastics and plasticizing modifications. *Journal of Materials Chemistry A*, *1*, 13379–13398.
- Muxika, A., Etxabide, A., Uranga, J., Guerrero, P., & de la Caba, K. (2017). Chitosan as a bioactive polymer: Processing, properties and applications. *International Journal of Biological Macromolecules*, *105*, 1358–1368.
- Muzzarelli, R. A. A., & Rocchetti, R. (1985). Determination of the degree of acetylation of chitosans by first derivative ultraviolet spectrometry. *Carbohydrate Polymers*, *5*, 461–472.
- Porta, R., Di Piero, P., Roviello, V., & Sabbah, M. (2017). Tuning the functional properties of bitter vetch (*Vicia ervilia*) protein films grafted with spermidine. *International Journal of Molecular Sciences*, *18*, 2658–2669.
- Regenstein, J. M., Chaudry, M. M., & Regenstein, C. E. (2003). The kosher and halal food laws. *Comprehensive Reviews in Food Science and Food Safety*, *2*, 111–127.
- Sabbah, M., Di Piero, P., Esposito, M., Giosafatto, C. V. L., Mariniello, L., & Porta, R. (2016). Stabilization of charged polysaccharide film forming solution by sodium chloride: Nanoparticle Z-average and zeta-potential monitoring. *Journal of Biotechnology & Biomaterials*, *6*, e128. <https://doi.org/10.4172/2155-952X.1000e128>.
- Sabbah, M., Di Piero, P., Giosafatto, C. V. L., Esposito, M., Mariniello, L., Regalado-Gonzales, C., et al. (2017). Plasticizing effects of polyamines in protein-based films. *International Journal of Molecular Sciences*, *18*, 1026–1035.
- Sagoo, S., Board, R., & Roller, S. (2002). Chitosan inhibits growth of spoilage microorganisms in chilled pork products. *Food Microbiology*, *19*, 175–182.
- Samelis, J. (2006). Managing microbial spoilage in the meat industry. In C. D. W. Blackburn (Ed.), *Food spoilage microorganisms* (pp. 213–286). Boca Raton: CRS Press LLC.
- Spierling, S., Knupffer, E., Behnsen, H., Mudersbach, M., Krieg, H., Springer, S., et al. (2018). Bio-based plastics- A review of environmental, social and economic impact assessments. *Journal of Cleaner Production*, *185*, 476–491.
- Sun, X., Narciso, J., Wang, Z., Ference, C., Bai, J., & Zhou, K. (2014). Effects of chitosan-essential oil coatings on safety and quality of fresh blueberries. *Journal of Food Science*, *79*, M955–M960.
- Van den Broek, L. A. M., Knoop, R. J. I., Kappen, F. H. J., & Boeriu, C. G. (2015). Chitosan films and blends for packaging material. *Carbohydrate Polymers*, *116*, 237–242.
- Vieira, M. G. A., Altenhofen da Silva, M., Oliveira dos Santos, L., & Beppu, M. M. (2011). Natural-based plasticizers and biopolymer films: A review. *European Polymer Journal*, *47*, 254–263. www.viscofan.com, Accessed date: 4 April 2018.



Natural Product Research

Formerly Natural Product Letters

ISSN: 1478-6419 (Print) 1478-6427 (Online) Journal homepage: <https://www.tandfonline.com/loi/gnpl20>

Fighting multidrug resistance with a fruit extract: anti-cancer and anti-biofilm activities of *Acca sellowiana*

Eliana Dell'Olmo, Rosa Gaglione, Katia Pane, Sergio Sorbo, Adriana Basile, Sergio Esposito & Angela Arciello

To cite this article: Eliana Dell'Olmo, Rosa Gaglione, Katia Pane, Sergio Sorbo, Adriana Basile, Sergio Esposito & Angela Arciello (2019): Fighting multidrug resistance with a fruit extract: anti-cancer and anti-biofilm activities of *Acca sellowiana*, Natural Product Research, DOI: [10.1080/14786419.2019.1624961](https://doi.org/10.1080/14786419.2019.1624961)

To link to this article: <https://doi.org/10.1080/14786419.2019.1624961>



View supplementary material [↗](#)



Published online: 07 Jun 2019.



Submit your article to this journal [↗](#)



View Crossmark data [↗](#)

SHORT COMMUNICATION



Fighting multidrug resistance with a fruit extract: anti-cancer and anti-biofilm activities of *Acca sellowiana*

Eliana Dell'Olmo^{a*}, Rosa Gaglione^{a*}, Katia Pane^b, Sergio Sorbo^c, Adriana Basile^d, Sergio Esposito^d and Angela Arciello^{a,e}

^aDepartment of Chemical Sciences, University of Naples Federico II, Naples, Italy; ^bIRCCS SDN, Naples, Italy; ^cCeSMA, Microscopy Section, University of Naples Federico II, Naples, Italy; ^dDepartment of Biology, University of Naples Federico II, Naples, Italy; ^eIstituto Nazionale di Biostrutture e Biosistemi (INBB), Rome, Italy

ABSTRACT

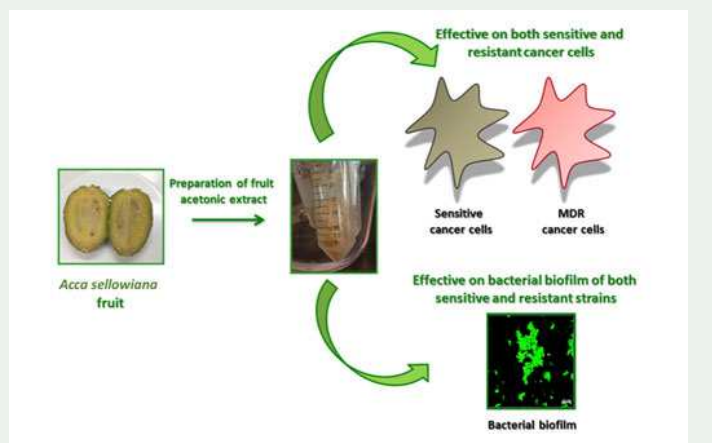
In this study, the efficacy of *Acca sellowiana* fruit acetonetic extract on human MDR cancer cells was tested for the first time, and it was demonstrated that the fruit extract is effective on both sensitive and resistant tumor cells. The effects of *A. sellowiana* extract on bacterial biofilm were also examined for the first time. By crystal violet assays and confocal microscopy analyses, it was demonstrated that the plant extract is able to strongly inhibit biofilm formation of both sensitive and resistant bacterial strains. Furthermore, antimicrobial activity assays and TEM analyses clearly demonstrated the effectiveness of plant extract on planktonic bacterial cells in both sensitive and resistant strains. Altogether, these findings intriguingly expand the panel of activities of *A. sellowiana* fruit extract with respect to previous reports, and open interesting perspectives to its therapeutic applications.

ARTICLE HISTORY

Received 26 February 2019
Accepted 23 May 2019

KEYWORDS

Fruit extract; antibiotic resistance; multidrug resistant tumor cells; bacterial biofilm



CONTACT Sergio Esposito ✉ sergio.esposito@unina.it Department of Biology, University of Naples Federico II, Via Cintia 4, 80126, Naples, Italy; Adriana Basile ✉ adbasile@unina.it Department of Biology, University of Naples Federico II, Via Cintia 4, 80126, Naples, Italy

*These authors equally contributed to the work.

 Supplemental data for this article can be accessed at <https://doi.org/10.1080/14786419.2019.1624961>

1. Introduction

It has been estimated that 11% of the 252 drugs considered as basic and essential by the World Health Organization (WHO) are exclusively of flowering plant origin (Cragg and Newman 2013). Some of these are efficient anticancer agents, while others are effective against bacterial biofilm (Hughes and Webber 2017). Among biofilm forming bacteria, *Pseudomonas aeruginosa* is greatly responsible for the persistence of chronic infections. Moreover, hospital isolates frequently develop multidrug-resistance (MDR) phenotype (Alonso et al. 1999). The occurrence of MDR phenotype is also one of the main obstacles to the successful chemotherapeutic treatment of cancer (Gillet and Gottesman 2010). In this scenario, herbal medicines might offer alternative and effective treatment options to counteract MDR phenotype. Among medicinal plants, *Acca sellowiana* (sin. *Feijoa sellowiana* Berg.) attracted great attention. It is an evergreen shrub or a small tree belonging to *Mirtaceae*, well acclimated in California, Florida, and Italy (Romero Rodriguez et al. 1992). *A. sellowiana* leaves, stem and the different components of the fruits are endowed with antibacterial activity (Shaw et al. 1989). Moreover, *A. sellowiana* fruit acetic extract is endowed with anti-oxidant, anti-inflammatory, and anticancer properties (Basile et al. 2010; Bontempo et al. 2007; Rossi et al. 2007; Piscopo et al. 2018).

In the present study, we analyze for the first time the effects of *A. sellowiana* fruit acetic extract on bacterial biofilm and its efficacy on MDR phenotype in cancer and bacterial infections.

2. Results and discussion

2.1. Effects of *A. sellowiana* acetic extract on normal and cancer eukaryotic cells

Cytotoxicity assays were performed on non-malignant BALB/c 3T3 murine cell line (Supplementary Figure S1A) and on its malignant counterpart, i.e. virus-transformed SVT2 mouse fibroblasts (Supplementary Figure S1B), as well as on human primary renal cortical epithelial (HRCE) cells (Supplementary Figure S1C) and on transformed human embryonic kidney HEK-293 cells (Supplementary Figure S1D). In all the cases, a time- and dose-dependent inhibition of cell viability was observed. Interestingly, extract was found to be more cytotoxic on cancer cells with respect to non-transformed cells (Supplementary Figure S1). Indeed, IC_{50} values at 48 hrs were found to be significantly lower for cancer cells (2.5 and 1 mg/mL for SVT2 and HEK-293 cells, respectively) with respect to untransformed cells (4.5 and 2.5 mg/mL for BALB/c 3T3 and HRCE cells, respectively), which is indicative of a certain selectivity of *A. sellowiana* extract toxicity towards transformed cancer cells.

2.2. *A. sellowiana* acetic extract efficacy towards multidrug resistant tumor cells

We also analyzed *A. sellowiana* extract effects on lineage-derived human MDR (KB-C1 and KB-A1) and their parental drug sensitive KB-3-1 cancer cell line and found that the

extract effectively inhibits proliferation of KB-3-1 cells and its MDR derivatives in a dose- and time-dependent manner (Supplementary Figure S2). IC₅₀ values at 72 hrs were found to be 1.75 mg/mL for KB-3-1 sensitive cells and 2 mg/mL for both KB-C1 and KB-A1 resistant cells, thus clearly indicating that *A. sellowiana* extract is equally effective on both sensitive and resistant KB tumor cells. These results open attractive perspectives to therapeutic potential of *A. sellowiana* extract.

2.3. Anti-biofilm activity of *A. sellowiana* acetonic extract

We tested *A. sellowiana* extract antimicrobial activity on *P. aeruginosa* PAO1 strain and found a significant effect with a MIC₁₀₀ (Minimum Inhibitory Concentration) value of about 2 mg/mL, and a Minimum Bactericidal Concentration (MBC) value of about 4 mg/mL (Table S1). We also performed transmission electron microscopy (TEM) analyses of *P. aeruginosa* PAO1 cells in the presence of 8 mg/mL *A. sellowiana* extract (Supplementary Figure S3B). As shown in Supplementary Figure S3, upon treatment with fruit extract, morphological changes appear evident, with large electron-clear regions in the bacterium protoplasm (Supplementary Figure S3B). Fruit extract anti-biofilm properties were also evaluated by testing its effects on different stages of biofilm formation, as previously described (Gaglione et al. 2017). By crystal violet assays, we found a significant dose-dependent inhibition of biofilm attachment and formation (Supplementary Figure S3C), and about 25% reduction of mature preformed biofilm (Supplementary Figure S3C). *A. sellowiana* extract anti-biofilm activity was also evaluated by confocal microscopy analyses by incubating bacterial cells with 0.5 mg/mL fruit extract for 24 hrs at 37 °C in static conditions. A double staining (Syto9/PI mixture) allowed to discriminate between live and dead cells embedded into biofilm structure. Treatment with fruit extract induced a dramatic decrease of cell cohesion, whereas no significant increase in cell death was observed (Supplementary Figure S3D).

2.4. *A. sellowiana* acetonic extract efficacy towards MDR bacterial biofilm

The antimicrobial activity of *A. sellowiana* extract was also tested on methicillin-resistant *Staphylococcus aureus* (MRSA WKZ-2). MIC₁₀₀ and MBC values were found to be 0.5 and >8 mg/mL, respectively (Table S1). TEM analyses revealed that, upon treatment of bacterial cells with fruit extract (8 mg/mL), significant morphological changes appear, with remarkable electron-light regions in the centre of bacteria and a marked accumulation of electron-dense material on the external face of outer membranes (Supplementary Figure S4B). Fruit extract anti-biofilm properties were also tested by crystal violet assays. A significant effect on biofilm formation (66% inhibition) was observed upon treatment with 0.6 mg/mL *A. sellowiana* extract for 24 hrs (Supplementary Figure S4C).

Effects on biofilm formation were also tested by confocal microscopy analyses performed upon incubation with fruit extract (6 mg/mL) for 24 hrs at 37 °C in static conditions. A dramatic decrease of cell cohesion was observed (Supplementary Figure S4D, left panels). These observations interestingly expand the panel of activities of *A. sellowiana* fruit extract.

4. Conclusion

The most active compound in *A.sellowiana* extract is flavone; this molecule is known for its anticancer and antibacterial activity (Bontempo et al. 2007; Basile et al 2010). Therefore, data here presented open interesting perspectives to future applications of *A. sellowiana* derived compounds in biomedical field for the successful treatment of MDR cancers and bacterial infections.

Disclosure statement

No potential conflict of interest was reported by the authors.

Funding

This research was partially supported by PROSIT s.n.c Spin Off "Isolation, identification and characterization of the bioactive principles of *Feijoa sellowiana*" admitted to financing with Rectoral Decree number 1954 of June 3, 2014.

References

- Alonso A, Campanario E, Martínez JL. 1999. Emergence of multidrug-resistant mutants is increased under antibiotic selective pressure in *Pseudomonas aeruginosa*. *Microbiology*. 145(10):2857–2862.
- Basile A, Botta B, Bruno M, Rigano D, Sorbo S, Conte B, Rosselli S, Senatore F. 2010. Effects of air pollution on production of essential oil in *Feijoa sellowiana* Berg. grown in the 'Italian triangle of death'. *Int J Environ Health*. 4(2/3):250–259.
- Bontempo P, Mita L, Miceli M, Doto A, Nebbioso A, De Bellis F, Conte M, Minichiello A, Manzo F, Carafa V, et al. 2007. *Feijoa sellowiana* derived natural Flavone exerts anti-cancer action displaying HDAC inhibitory activities. *Int J Biochem Cell Biol*. 39(10):1902–1914.
- Cragg GM, Newman DJ. 2013. Natural products: a continuing source of novel drug leads. *Biochim Biophys Acta*. 1830(6):3670–3695.
- Gillet JP, Gottesman MM. 2010. Mechanisms of multidrug resistance in cancer. *Methods Mol Biol*. 596:47–76.
- Gaglione R, Dell'Olmo E, Bosso A, Chino M, Pane K, Ascione F, Itri F, Caserta S, Amoresano A, Lombardi A, et al. 2017. Novel human bioactive peptides identified in Apolipoprotein B: Evaluation of their therapeutic potential. *Biochem Pharmacol*. 130:34–50.
- Hughes G, Webber MA. 2017. Novel approaches to the treatment of bacterial biofilm infections. *Br J Pharmacol*. 174(14):2237–2246.
- Romero Rodriguez MA, Vazquez Oderiz ML, Lopez Hernandez J, Simal Lozano J. 1992. Determination of vitamin C and organic acids in various fruits by HPLC. *J Chromatogr Sci*. 30(11):433–437.
- Piscopo M, Tenore GC, Notariale R, Maresca V, Maisto M, de Ruberto F, Heydari M, Sorbo S, Basile A. 2018. Antimicrobial and antioxidant activity of proteins from *Feijoa sellowiana* Berg. fruit before and after in vitro gastrointestinal digestion. *Nat Prod Res*.
- Rossi A, Rigano D, Pergola C, Formisano C, Basile A, Bramanti P, Senatore F, Sautebin L. 2007. Inhibition of inducible nitric oxide synthase expression by an acetonic extract from *Feijoa sellowiana* Berg. *J Agric Food Chem*. 55(13):5053–5061.
- Shaw GJ, Allen JM, Yates MK. 1989. Volatile flavour constituents in the skin oil from *Feijoa sellowiana*. *Phytochemistry*. 28(5):1529–1530.

SCIENTIFIC REPORTS

OPEN

Effects of human antimicrobial cryptides identified in apolipoprotein B depend on specific features of bacterial strains

Rosa Gaglione¹, Angela Cesaro¹, Eliana Dell'Olmo¹, Bartolomeo Della Ventura², Angela Casillo¹, Rocco Di Girolamo¹, Raffaele Velotta², Eugenio Notomista³, Edwin J. A. Veldhuizen⁴, Maria Michela Corsaro¹, Claudio De Rosa¹ & Angela Arciello^{1,5}

Cationic Host Defense Peptides (HDPs) are endowed with a broad variety of activities, including direct antimicrobial properties and modulatory roles in the innate immune response. Even if it has been widely demonstrated that bacterial membrane represents the main target of peptide antimicrobial activity, the molecular mechanisms underlying membrane perturbation by HDPs have not been fully clarified yet. Recently, two cryptic HDPs have been identified in human apolipoprotein B and found to be endowed with a broad-spectrum antimicrobial activity, and with anti-biofilm, wound healing and immunomodulatory properties. Moreover, ApoB derived HDPs are able to synergistically act in combination with conventional antibiotics, while being not toxic for eukaryotic cells. Here, by using a multidisciplinary approach, including time killing curves, Zeta potential measurements, membrane permeabilization assays, electron microscopy analyses, and isothermal titration calorimetry studies, the antimicrobial effects of ApoB cryptides have been analysed on bacterial strains either susceptible or resistant to peptide toxicity. Intriguingly, it emerged that even if electrostatic interactions between negatively charged bacterial membranes and positively charged HDPs play a key role in mediating peptide toxicity, they are strongly influenced by the composition of negatively charged bacterial surfaces and by defined extracellular microenvironments.

Antimicrobial peptides (AMPs) are effectors of the innate immune system in a wide variety of species from the plant and animal kingdoms, including humans¹. Although structurally different, most of these peptides fold into amphiphilic structures due to their short size (<50 amino acid residues), net positive charge and high content of hydrophobic residues². Their activity against a wide range of microorganisms combined with their unique property of displaying few to no resistance effects³ allowed AMPs to gain great attention as promising and effective alternatives to conventional antibiotics, also against strains resistant to approved antibacterial agents⁴. Since these peptides are also able to modulate the immune response of host organisms, their efficiency is considerably enhanced. Because of this extension of functionalities, they have been more properly named “host defence peptides” (HDPs)^{5,6}. The key features that make HDPs antimicrobial are their cationic nature, their ability to bind to bacterial membranes and to adopt specific secondary structures in membrane environments⁷, an essential prerequisite to their attachment and insertion into bacterial membranes. HDPs have been found to kill bacteria by first associating with their negatively charged cell surfaces and subsequently disrupt their cell membranes *via* mechanisms that involve membrane thinning, formation of transient pores, or disruption of lipid matrix, which impairs barrier function of bacterial membranes⁸. Some HDPs are also able to pass through the lipid bilayer of the membrane to act on intracellular targets⁸. Furthermore, some HDPs preferentially attack septating bacterial cells where peptides have been found to be associated to the septum and the curved regions of the outer membrane⁹. Since most HDPs target the bacterial plasma membrane directly rather than through specific protein receptors¹⁰,

¹Department of Chemical Sciences, University of Naples Federico II, 80126, Naples, Italy. ²Department of Physics, University of Naples Federico II, 80126, Naples, Italy. ³Department of Biology, University of Naples Federico II, 80126, Naples, Italy. ⁴Department of Infectious Diseases and Immunology, Division Molecular Host Defence, Faculty of Veterinary Medicine, Utrecht University, Utrecht, The Netherlands. ⁵Istituto Nazionale di Biostruttura e Biosistemi (INBB), Rome, Italy. Correspondence and requests for materials should be addressed to A.A. (email: anarciel@unina.it)

membrane phospholipid composition and net charge also play a key role in determining peptides antimicrobial activity¹¹. Indeed, these parameters vary not only from bacterium to bacterium, but also as a response to changing environments¹² and exposure to antimicrobial agents¹³. Peptide concentration also represents a further key parameter, with maximal antimicrobial activity reached only at peptide concentrations exceeding a threshold value¹⁴. Indeed, upon an initial electrostatic interaction between positively charged peptide molecules and negatively charged lipids, peptides reach an appropriate local concentration, allowing their penetration into the hydrophobic core of the bilayer^{15,16}. Membrane bilayer thickness also appears to have an effect on the ability of a peptide to bind to the membrane and, consequently, on the ability of a lipid bilayer to induce peptide secondary structures^{17,18}. However, despite decades of research, novel structural and dynamic features of membrane-associated HDPs are continuously being discovered¹⁹ and the exact molecular mechanism underlying HDPs ability to perturb bacterial membranes still remains controversial. Here, we analyse the antimicrobial activity of two recently characterized HDPs²⁰, identified in human apolipoprotein B by using a bioinformatics method developed by our research group^{21–25}. It has been reported that several eukaryotic proteins, with functions not necessarily related to host defence, act as sources of “cryptic” bioactive peptides released upon proteolytic processing by bacterial and/or host proteases^{26–28}. The two novel bioactive peptides analysed in the present study represent two variants of the HDP identified in human apolipoprotein B (residues 887–922), *i.e.* peptides ApoB887–923 and ApoB887–911. These two HDPs, recombinantly produced in bacterial cells, have been here named r(P)ApoB_L and r(P)ApoB_S because of the presence of a Pro residue becoming the N-terminus of the peptides released by the acidic cleavage of an Asp-Pro bond²⁰. The primary structure of the two ApoB derived HDPs is reported in Fig. S1. Both recombinant peptides have been found to be endowed with antimicrobial, anti-biofilm, wound healing and immunomodulatory properties²⁰. On the other hand, they have been found to be neither toxic for mammalian cells nor hemolytic towards murine red blood cells. Interestingly, ApoB derived peptides were also found to exert significant synergistic effects in combination with either conventional antibiotics or EDTA²⁰. Noteworthy, bacterial strains found to be not responsive to ApoB derived peptides, such as *S. aureus* strains and *P. aeruginosa* ATCC 27853, appeared highly susceptible to selected combinations of peptides and antibiotics or EDTA²⁰, thus opening interesting perspectives to the development of successful combination therapy approaches, that have a very low potential to induce resistance phenotype. Since the definition of the molecular bases of ApoB derived peptides biological activities could greatly contribute to the rational design of effective combinatorial therapeutic approaches, in the present paper, time killing curves, Zeta potential measurements, membrane permeabilization assays, isothermal titration calorimetry studies and morphological analyses by electron microscopy have been performed.

Results

Killing kinetics studies. It has been previously reported that ApoB derived peptides are effective on *B. globigii* TNO BM013 and *P. aeruginosa* PAO1 bacterial strains²⁰, as shown in Table S1. Here, in order to analyse the kinetic of peptides bactericidal activity, we obtained kinetic killing curves by treating bacterial cells with increasing concentrations of either r(P)ApoB_L or r(P)ApoB_S for different time intervals (0–180 min). The two bacterial strains have been selected as a prototype of Gram-positive (*B. globigii* TNO BM013) and Gram-negative (*P. aeruginosa* PAO1) strains susceptible to antimicrobial ApoB derived peptides. In all the experiments, chicken cathelicidin-2 (CATH-2), a known antimicrobial peptide from chicken²⁹, was tested as a positive control (Fig. 1E,F). To perform the analyses, following the incubation with peptides, control and treated samples were serially diluted and plated on agar, in order to count bacterial colonies³⁰. As reported in Fig. 1A,C, at the highest peptide concentrations tested (10–20 μM), *B. globigii* TNO BM013 cells were killed within 10–30 min. At the lowest peptide concentrations (1.25–2.5 μM), instead, the same effect was obtained within 120 min (Fig. 1A,C). When peptides were tested on *P. aeruginosa* PAO1, bacterial cells were killed within 30 minutes at the highest peptide concentrations tested (10–20 μM), and within 120–180 minutes at lower peptide concentrations (2.5–5 μM) (Fig. 1B,D). In the case of CATH-2 control peptide, all the curves obtained appear perfectly superimposable, since all peptide concentrations tested were found to have the same effects. As a consequence, only the curves corresponding to the highest peptide concentration tested (20 μM) appear visible (Fig. 1E,F).

Zeta potential measurements of bacterial cells upon treatment with peptides. To evaluate ApoB derived peptides effects on bacterial membrane surface, Zeta potential (ζ) measurements were carried out. First of all, ζ values of control bacterial cells were determined over time (0–180 min) in NB 0.5X medium, in order to obtain the electrostatic potential at the shear plane of the bacteria in solution (Fig. S2). It was found that ζ did not vary throughout the incubation time in the case of all the strains tested, thus indicating their high stability. In detail, the average potential of untreated *B. globigii* TNO BM013, *S. aureus* MRSA WKZ-2, *P. aeruginosa* PAO1 and *P. aeruginosa* ATCC 27853 strains were found to be -33 ± 3 , -28 ± 3 , -23 ± 2 , and -11 ± 2 mV, respectively (Fig. S2 and Table 1). The different values obtained for the various bacterial strains might be due to differences in membrane composition. Bacterial strains susceptible to antimicrobial ApoB derived peptides, *i.e.* *B. globigii* TNO BM013 and *P. aeruginosa* PAO1, were exposed to r(P)ApoB_L or r(P)ApoB_S at a concentration corresponding to their MIC values (Table S1). Upon treatment with each peptide, ζ was recorded at regular time intervals for 180 min. All the recorded ζ values are reported in Fig. S3. Values corresponding to the time point necessary to obtain complete cell death of treated bacterial cells on agar plates (30 min) have been reported for *B. globigii* TNO BM013 and *P. aeruginosa* PAO1 (both of them susceptible to antimicrobial peptides) in Fig. 2A,C, respectively. In Fig. 2B,D, instead, ζ values measured at the highest peptide concentration tested (40 μM) for *S. aureus* MRSA WKZ-2 and *P. aeruginosa* ATCC 27853 (both of them non-susceptible to antimicrobial peptides) are reported. Upon incubation of *B. globigii* TNO BM013 with r(P)ApoB_L or r(P)ApoB_S, ζ was found to shift from -33 ± 3 mV to -11 ± 3 and -19 ± 3 mV, respectively (Fig. 2A and Table 1). This is indicative of the occurrence of electrostatic interactions between positively charged peptides and negatively charged bacterial

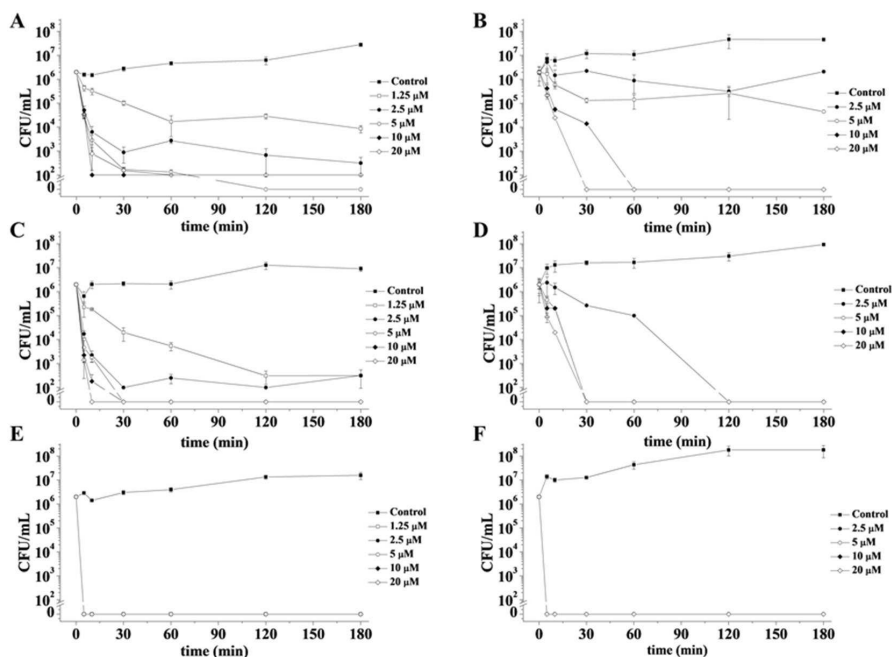


Figure 1. Time killing curves obtained by incubating *B. globigii* TNO BM013 (A,C,E) and *P. aeruginosa* PAO1 (B,D,F) strains with increasing concentrations of r(P)ApoB_L (A,B), r(P)ApoB_S (C,D) and CATH-2 (E,F) peptides for different lengths of time. Data represent the mean (\pm standard deviation, SD) of at least three independent experiments, each one carried out with triplicate determinations. For all the experimental points, * $p < 0.05$, ** $p < 0.01$, or *** $p < 0.001$ were obtained for control versus treated samples.

	SAMPLE	Z-POTENTIAL \pm DS (mV)
<i>B. globigii</i> TNO BM013	Cells t_0	-33 ± 3
	Cells $t_{30 \text{ min}}$	-29 ± 2
	Cells + r(P)ApoB _L $t_{30 \text{ min}}$	-11 ± 3
	Cells + r(P)ApoB _S $t_{30 \text{ min}}$	-19 ± 3
<i>P. aeruginosa</i> PAO1	Cells t_0	-23 ± 2
	Cells $t_{30 \text{ min}}$	-23 ± 2
	Cells + r(P)ApoB _L $t_{30 \text{ min}}$	-19 ± 3
	Cells + r(P)ApoB _S $t_{30 \text{ min}}$	-17 ± 3
<i>S. aureus</i> MRSA WKZ-2	Cells t_0	-28 ± 3
	Cells $t_{30 \text{ min}}$	-26 ± 2
	Cells + r(P)ApoB _L $t_{30 \text{ min}}$	-4 ± 3
	Cells + r(P)ApoB _S $t_{30 \text{ min}}$	-4 ± 3
<i>P. aeruginosa</i> ATCC 27853	Cells t_0	-11 ± 2
	Cells $t_{30 \text{ min}}$	-10 ± 2
	Cells + r(P)ApoB _L $t_{30 \text{ min}}$	-3 ± 2
	Cells + r(P)ApoB _S $t_{30 \text{ min}}$	-3 ± 2
Peptides alone	r(P)ApoB _L	-3 ± 1
	r(P)ApoB _S	-3 ± 1

Table 1. Zeta-potential values recorded for bacterial cells at time 0 and upon 30 min in the absence or in the presence of ApoB derived peptides; zeta-potential values of each peptide in solution are also reported.

surfaces, which leads to a partial neutralization of bacterial surface charge. A similar behavior was also observed in the case of Gram-negative *P. aeruginosa* PAO1 bacterial strain upon treatment with r(P)ApoB_L or r(P)ApoB_S, since also in this case ζ shifted towards more positive values (Fig. 2C and Table 1). It is worth to highlight that,

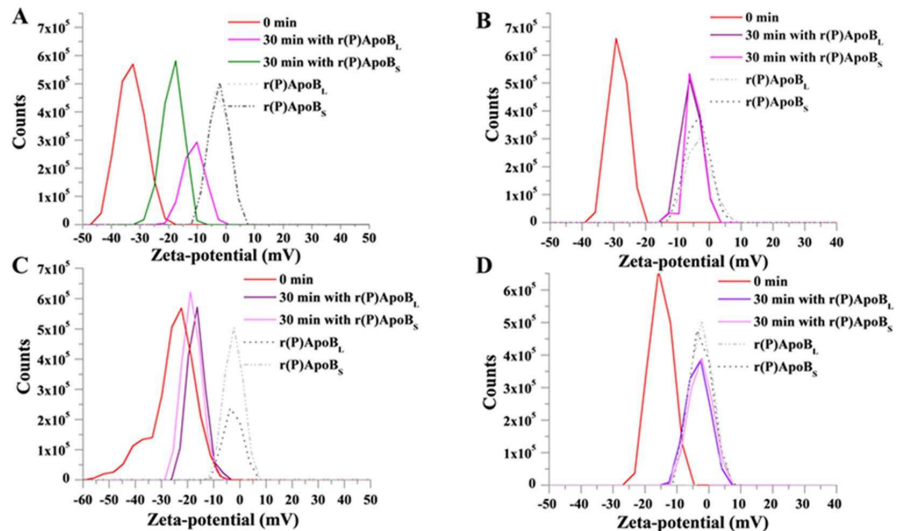


Figure 2. ApoB derived peptides effects on the Zeta potential of treated bacterial cells. Zeta potential values of *B. globigii* TNO BM013 (A) and *P. aeruginosa* PAO1 (C) bacterial strains were determined upon treatment with r(P)ApoB_L or r(P)ApoB_S peptides at a concentration corresponding to MIC₁₀₀ values. Zeta potential values of bacterial strains not responsive to antimicrobial ApoB derived peptides, i.e. *S. aureus* MRSA WKZ-2 (B) and *P. aeruginosa* ATCC 27853 (D), were determined upon treatment with peptides at the highest concentration tested (40 μM) for 180 min. Dashed curves represent the Zeta potential values of ApoB derived peptides alone in bacterial culture medium (NB 0.5X). In the case of *B. globigii* TNO BM013 (A) and *P. aeruginosa* PAO1 (C) bacterial strains, a positive ζ shift is indicative of an interaction between bacterial cells and peptides. On the contrary, in the case of *S. aureus* MRSA WKZ-2 (B) and *P. aeruginosa* ATCC 27853 (D) bacterial strains, signals recorded upon treatment with peptides (continuous lines) are almost completely superimposable to those recorded for free peptide in culture medium at 40 μM (dashed lines), thus indicating absence of interactions between bacterial cells and peptides. Data represent the average of at least three independent experiments.

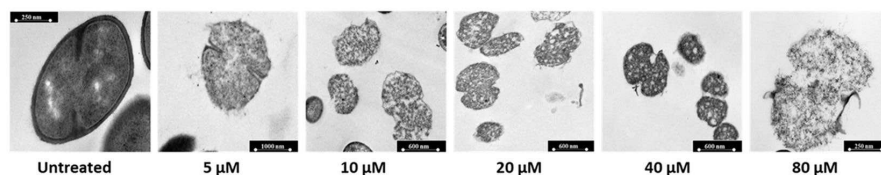
in the case of *B. globigii* TNO BM013 bacterial strain, a larger ζ shift was observed with respect to *P. aeruginosa* PAO1, as expected on the basis of its higher sensitivity to peptide toxicity. On the contrary, in the case of bacterial strains non-responsive to antimicrobial ApoB derived peptides, obtained signals were found to be almost completely superimposable to those recorded for the free peptide in solution at the same concentration (Fig. 2B,D, dashed lines), thus clearly indicating that only the signal attributable to the free peptide in solution was measured (Fig. 2B,D, dashed lines). This indicates that, in the case of non-responsive bacterial strains, no electrostatic interactions occur between bacterial surfaces and antimicrobial peptides. It is presumable that some extracellular factors or bacterial membrane composition might interfere with electrostatic interactions between negatively charged bacterial surfaces and positively charged peptides, and this ultimately makes peptides ineffective.

Membrane permeabilization assays. To evaluate the effect of ApoB derived peptides on bacterial membrane permeability, N-Phenyl-1-naphthylamine (NPN) fluorescent probe was used. As expected, NPN uptake was found to be negligible for untreated bacterial cells, characterized by intact cell surface (Table 2 and Fig. S4A,B). The spectrofluorometric assay was also performed upon treatment of bacterial strains with ApoB derived peptides for 30 min at 37 °C. Incubation time was selected on the basis of time killing curve data (Fig. 1). *B. globigii* TNO BM013 and *P. aeruginosa* PAO1 responsive strains were treated with peptide concentrations corresponding to previously determined MIC₁₀₀ values²⁰, reported in Table S1, whereas non responsive *S. aureus* MRSA WKZ-2 and *P. aeruginosa* ATCC 27853 strains were treated with 40 μM peptides for 30 min at 37 °C. As shown in Table 2, NPN uptake factor was found to be 1.4 ± 0.9 for control *P. aeruginosa* PAO1 cells, and increased to 8.9 ± 1.2 and 11.1 ± 2.0 upon treatment with r(P)ApoB_L and r(P)ApoB_S, respectively (Table 2). Similar results were obtained when responsive Gram-positive *B. globigii* TNO BM013 strain was tested. Indeed, NPN uptake factor was found to be 4.1 ± 0.9 for control cells and 7.8 ± 1.1 or 7.6 ± 1.0 for cells treated with r(P)ApoB_L and r(P)ApoB_S, respectively (Table 2). On the other hand, no significant variation in NPN uptake was detected when non responsive bacterial cells were treated with ApoB derived peptides (Table 2). As a positive control, bacterial strains under test were treated with increasing concentrations of polycationic antibiotic colistin (0.25–4 μg/mL) or glycopeptide antibiotic vancomycin (0.00156–0.250 μg/mL). In both cases, following treatment, NPN uptake was found to increase in a concentration dependent manner (Fig. S4A,B). Indeed, both antibiotics, although with different mechanisms, have been reported to ultimately cause membrane permeabilization^{31,32}. Altogether, obtained results confirm the crucial role played by bacterial membrane as main target of ApoB derived peptides antimicrobial activity.

	Samples	NPN uptake factor \pm SD
<i>B. globigii</i> TNO BM013	Cells	4.1 \pm 0.9
	Cells + r(P)ApoB _L t _{30 min}	7.8 \pm 1.1
	Cells + r(P)ApoB _S t _{30 min}	7.6 \pm 1.0
<i>P. aeruginosa</i> PAO1	Cells t ₀	1.4 \pm 0.9
	Cells + r(P)ApoB _L t _{30 min}	8.9 \pm 1.2
	Cells + r(P)ApoB _S t _{30 min}	11.1 \pm 2.0
<i>S. aureus</i> MRSA WKZ-2	Cells t ₀	1.6 \pm 0.5
	Cells + r(P)ApoB _L t _{30 min}	0.7 \pm 0.1
	Cells + r(P)ApoB _S t _{30 min}	1.2 \pm 0.1
<i>P. aeruginosa</i> ATCC 27853	Cells t ₀	0.2 \pm 0.1
	Cells + r(P)ApoB _L t _{30 min}	0.3 \pm 0.1
	Cells + r(P)ApoB _S t _{30 min}	0.5 \pm 0.1

Table 2. NPN uptake factors determined upon incubation of bacterial cells in the presence or in the absence of ApoB derived peptides. Data represent the average of at least three independent experiments.

A



B

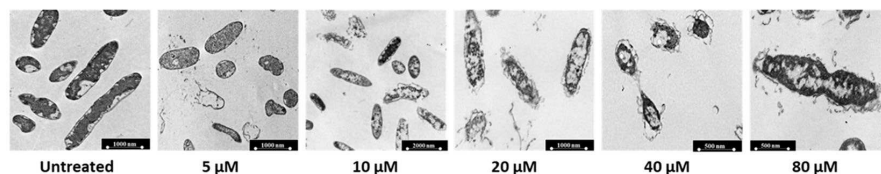


Figure 3. Morphological analyses of *B. globigii* TNO BM013 (A) and *P. aeruginosa* PAO1 (B) cells by TEM. Representative images are shown upon treatment of bacterial cells with increasing concentrations (0–80 μ M) of r(P)ApoB_L peptide. A total of 60 cells were analysed for each peptide concentration in two independent experiments. Bars 250, 500 or 1,000 nm.

Morphological alterations induced by ApoB derived peptides. To evaluate morphological alterations of bacterial strains susceptible to antimicrobial ApoB derived peptides, transmission electron microscopy (TEM) analyses were performed. In the case of control bacterial cells, intact membranes, a homogeneous intracellular distribution of DNA and ribosomes rich areas were observed (dark areas in Fig. 3). When bacterial cells were, instead, treated with increasing concentrations of r(P)ApoB_L peptide, a progressive detachment of cell wall and cell lysis was observed in the case of Gram-positive *B. globigii* TNO BM013 (Fig. 3A). Similarly, in the case of Gram-negative *P. aeruginosa* PAO1, a progressive wrinkling of outer membrane, dissociation of membrane fragments, permeabilization of outer and inner membranes and the leakage of electron dense material was detected (Fig. 3B). Moreover, in both cases, a complete alteration of intracellular morphology, with a decrease of cytoplasm density, was evaluated at the highest peptide concentrations tested (Fig. 3). Similar results were obtained when *B. globigii* TNO BM013 and *P. aeruginosa* PAO1 strains were treated with r(P)ApoB_S peptide at a concentration of 5 and 20 μ M, respectively (Fig. 4A,B). It is noteworthy that significant morphological alterations were already detected when peptides were tested at sub-MIC concentrations.

Furthermore, to analyse the surface of responsive bacterial cells upon treatment with antimicrobial ApoB derived peptides, scanning electron microscopy (SEM) analyses were also performed. In the absence of peptides, bacterial cells displayed smooth and intact surfaces (Figs 5 and 6). Preliminary occurrence of biofilm extracellular matrix formation was also detected in the case of control *P. aeruginosa* PAO1 cells (Figs 5B and 6B). When bacterial cells were, instead, treated with peptides, bacterial surfaces appeared corrugated with some dimples,

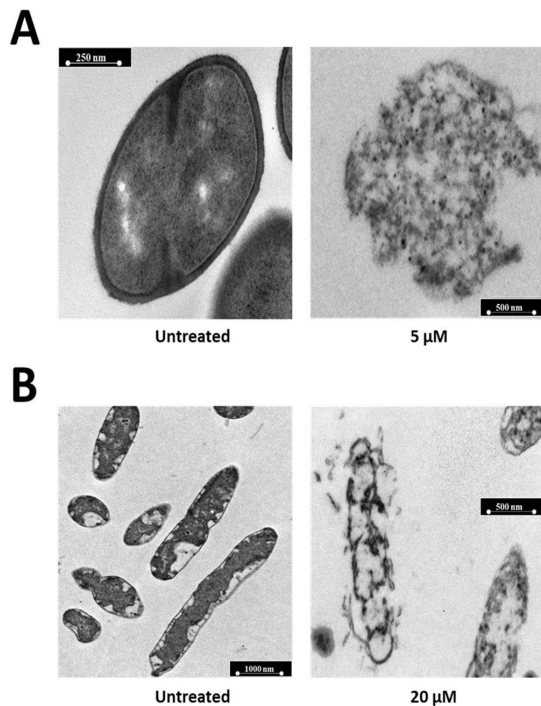


Figure 4. Morphological analyses of *B. globigii* TNO BM013 (A) and *P. aeruginosa* PAO1 (B) cells by TEM. Representative images are shown upon treatment of bacterial cells with r(P)ApoB₅ concentrations corresponding to sub-MIC values (5 μM and 20 μM for *B. globigii* TNO BM013 and *P. aeruginosa* PAO1 cells, respectively). A total of 60 cells were analysed for each sample in two independent experiments. Bars 250, 500 or 1,000 nm.

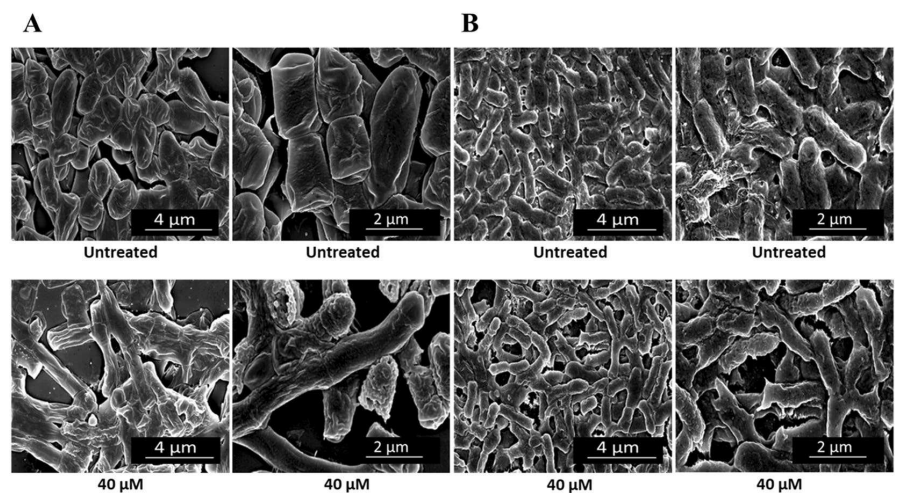


Figure 5. Morphological analyses of *B. globigii* TNO BM013 (A) and *P. aeruginosa* PAO1 (B) cells by SEM. Representative images are shown upon treatment of bacterial cells with 40 μM r(P)ApoB₅. A total of 60 cells were analysed for each sample in two independent experiments. Bars 2 or 4 μm.

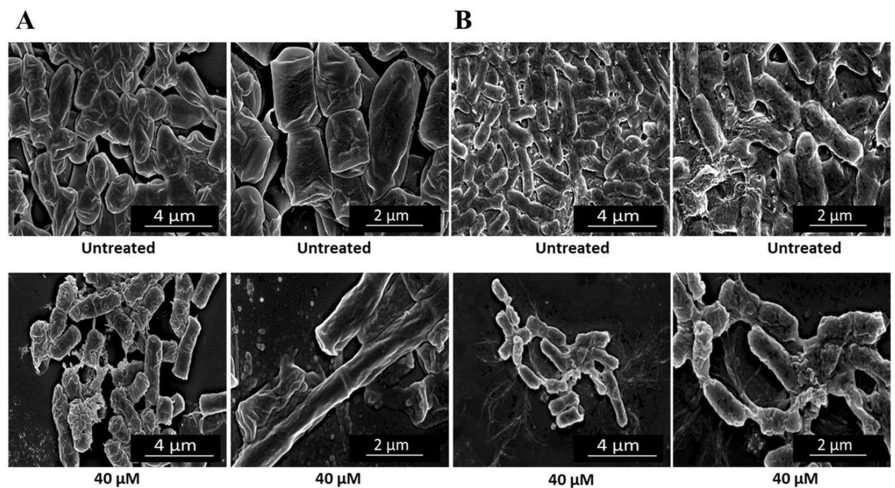


Figure 6. Morphological analyses of *B. globigii* TNO BM013 (A) and *P. aeruginosa* PAO1 (B) cells by SEM. Representative images are shown upon treatment of bacterial cells with 40 μ M r(P)ApoB₅. A total of 60 cells were analysed for each sample in two independent experiments. Bars 2 or 4 μ m.

both in the case of *B. globigii* TNO BM013 and *P. aeruginosa* PAO1 strains (Figs 5 and 6). Even more interesting is the evidence that the treatment of *B. globigii* TNO BM013 cells with ApoB derived peptides induces cells to grow as long filaments (Figs 5A and 6A), probably as a consequence of septation block, thus strongly suggesting that these peptides act by ultimately inhibiting cell division. To monitor this phenomenon, experiments were also performed by incubating *B. globigii* TNO BM013 cells with increasing concentrations of either r(P)ApoB_L or r(P)ApoB_S peptide. Obtained results, reported in Figs S5 and S6, clearly indicate that both peptides induce a septation block even at concentrations significantly lower than MIC₁₀₀ value. Moreover, obtained results support the evidence that peptides effects strongly depend on the features of bacterial strains under test. Indeed, when *P. aeruginosa* PAO1 cells were treated with 40 μ M r(P)ApoB_L (Fig. 5B) or 40 μ M r(P)ApoB_S peptide (Fig. 6B), no evidence of cell division block was detected. However, in both cases, a significantly lower cell density, indicative of a massive cell death, was revealed (Figs 5B and 6B). Moreover, in the case of all the treated samples, cell surfaces appeared irregular, corrugated, and withered (Figs 5 and 6), with some dimples and signs of cytoplasm leakage especially in the case of *P. aeruginosa* PAO1 strain (Figs 5B and 6B).

Analysis of lipopolysaccharides (LPSs) isolated from *P. aeruginosa* ATCC 27853 and *P. aeruginosa* PAO1 bacterial strains.

We previously demonstrated, by Far UV-CD analyses, that r(P)ApoB_L peptide gradually assumes a defined structure in the presence of increasing concentrations of LPS, what suggests a direct binding of this peptide to LPS³⁰. Here, to investigate the role played by LPS molecules in the efficacy or the inefficacy of ApoB derived peptides on Gram-negative bacterial strains, we extracted LPS molecules from *P. aeruginosa* ATCC 27853 and *P. aeruginosa* PAO1 bacteria. Afterwards, we analysed the interaction between ApoB derived peptides and the two purified LPS fractions by isothermal titration calorimetry (ITC) experiments. As shown in Fig. 7A, r(P)ApoB_L and r(P)ApoB_S peptides appear to bind to LPS molecules extracted from the two bacterial strains in a very similar fashion. Binding reactions were found to be all endothermic, thus indicating that they are driven by entropy rather than enthalpy. In the case of the binding of r(P)ApoB_L peptide to the LPS extracted from *P. aeruginosa* PAO1, a dissociation constant (Kd) of 3.6×10^{-6} M was determined, with an entropy (ΔS) of 269 J/mol and a positive enthalpy (ΔH) of 51.1 KJ/mol (Table S2). Similar spectra and binding parameters were also obtained in the case of the interaction of r(P)ApoB_S peptide with LPS molecules extracted from *P. aeruginosa* PAO1 bacterial strain (Fig. 7A and Table S2). No significant differences were detected when the binding of both ApoB derived peptides to LPS molecules extracted from *P. aeruginosa* ATCC 27853 strain was analysed (Fig. 7A and Table S2). Altogether, obtained data indicate that both ApoB derived peptides are able to directly interact with LPS molecules extracted from the two bacterial strains, with no major differences in the binding of peptides to LPS molecules extracted from *P. aeruginosa* susceptible and not responsive bacterial strains (Fig. 7A and Table S2), at least in *in vitro* experiments and in the experimental conditions tested. To deepen on the role that LPS molecules might play in determining the different susceptibility of Gram-negative bacterial strains to ApoB derived peptides toxicity, we also performed a preliminary characterization of LPS molecules extracted from *P. aeruginosa* ATCC 27853 and *P. aeruginosa* PAO1 bacterial strains. To this purpose, LPSs extracted from dried bacterial cells by the PCP method were analysed by 14% DOC-PAGE electrophoresis and visualized by silver nitrate staining, that revealed a smooth LPS for both strains. Smooth LPS extracted from *E. coli* O55:B5 was used as a standard (data not shown). To define the glycosyl compositions of the intact LPSs, acetylated methyl glycosides were analysed by GC-MS. The monosaccharides were identified from their EI mass spectra and from

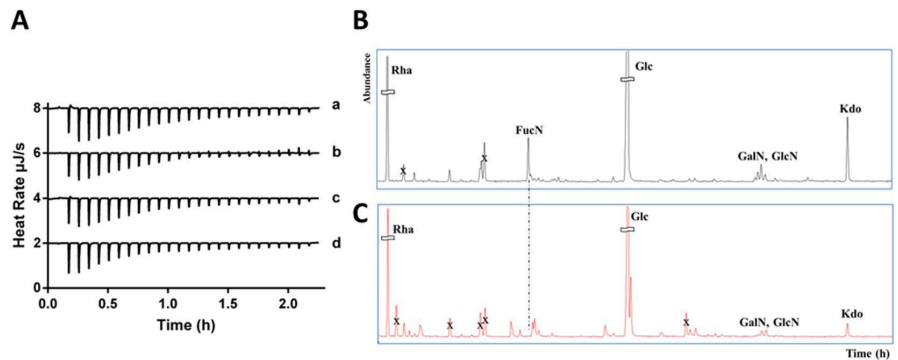


Figure 7. Analysis of the binding between ApoB derived peptides and LPSs extracted from *P. aeruginosa* PAO1 and *P. aeruginosa* ATCC 27853 bacterial strains by isothermal titration calorimetry (ITC) (A). The negative peaks indicate heat requirement for binding (endothermic), and are indicative of an entropy-driven binding reaction. (a) Binding of r(P)ApoB₁ peptide to LPS from *P. aeruginosa* PAO1; (b) binding of r(P)ApoB₁ peptide to LPS from *P. aeruginosa* ATCC 27853; (c) binding of r(P)ApoB₅ peptide to LPS from *P. aeruginosa* PAO1; (d) binding of r(P)ApoB₅ peptide to LPS from *P. aeruginosa* ATCC 27853. Chromatograms of acetylated methyl glycosides of LPSs extracted from *P. aeruginosa* PAO1 (B), and from *P. aeruginosa* ATCC 27853 (C).

their GC column retention time by comparison with authentic standards. For both LPSs, rhamnose (Rha), glucose (Glc), 2-amino-2-deoxy-D-galactopyranose (GalN), 2-amino-2-deoxy-D-glucopyranose (GlcN), and 3-deoxy-D-manno-oct-2-ulosonic acid (Kdo) were found to be present (Fig. 7B,C). The occurrence of heptoses was displayed only upon a de-phosphorylation reaction obtained by HF treatment (data not shown). It is important to highlight the selective presence of 2-amino-2,6-dideoxy-D-galactopyranose (FucN) in *P. aeruginosa* PAO1 LPS, as indicated by the chromatogram (Fig. 7B). It is noteworthy that the majority of *P. aeruginosa* strains have been reported to co-express two chemically and distinct forms of LPS O-antigens: (i) a serotype containing the O-antigen B-band and (ii) a common antigen referred to as O-antigen A-band. The chemical structure of the A-band from most of the sero-types was shown to be a linear α -D-rhamnan³³; instead, the chemical structure of the B-band was reported to contain two derivatives of the 2,3-diamino-2,3-dideoxy-D-mannuronic acid (Man2N3NA) and FucN³⁴. Our results suggest the absence of the B-band in the case of *P. aeruginosa* ATCC 27853 strain. This feature might be responsible for the different response of the two Gram-negative strains under test to ApoB derived peptides.

Discussion

The healthcare burden associated to the increasing emergence of microorganisms resistant to multiple antimicrobial compounds has accelerated in recent years, and alternative weapons are urgently needed. However, despite huge efforts, the discovery, development, manufacture and marketing of new antibiotics has significantly slowed down in the past 30 years, whereas the clinical and economic impact of resistance is alarmingly rising. Although the scientific difficulty in identifying novel antibiotics may be increasing, as microbes become resistant to an ever-increasing array of treatments and, concomitantly, the identification of novel targets is challenging, the main explanation is that investments made by large pharmaceutical companies did not lead to profitable products³⁵. In this scenario, naturally occurring Host Defense Peptides (HDPs) are gaining great attention. Indeed, being essential constituents of innate immunity, they represent promising lead structures to develop antibiotics against Gram-negative and Gram-positive bacteria, including strains resistant to approved antibacterial agents⁴. We recently characterized novel human HDPs identified by a bioinformatics approach in human ApoB^{20,21}, and demonstrated that the two recombinant ApoB derived HDPs are endowed with a broad-spectrum anti-microbial activity, and with anti-biofilm, wound healing and immunomodulatory properties²⁰. On the other hand, they have been found to be neither toxic nor hemolytic towards eukaryotic cells, what opens interesting perspectives to their therapeutic applicability²⁰. However, it should be emphasized that ApoB derived AMPs were found to be antimicrobial towards four out of eight strains tested, i.e. *E. coli* ATCC 25922, *P. aeruginosa* PAO1, *B. globigii* TNO BM013, and *B. licheniformis* ATCC 21424, with MIC₁₀₀ values comprised between 1.25 and 20 μ M, indicating that they are effective on both Gram-negative and Gram-positive bacterial strains²⁰. On the other hand, they were found to be ineffective towards *P. aeruginosa* ATCC 27853, methicillin-resistant *S. aureus* (MRSA WKZ-2), and *S. aureus* ATCC 29213²⁰. However, when peptides were tested in combination with conventional antibiotics or EDTA, remarkable synergistic effects were detected²⁰. Indeed, bacterial strains found to be not responsive to ApoB derived AMPs toxicity, such as *S. aureus* strains and *P. aeruginosa* ATCC 27853, were found to be highly susceptible to combinations of ApoB derived peptides with antibiotics or EDTA²⁰. This paves the way to the development of successful combination therapy approaches, that have a very low potential to induce resistance phenotype. Since the definition of the molecular bases of ApoB derived peptides antimicrobial activity could be crucial for the design of effective combinatorial therapeutic approaches, the mechanism of action of the two ApoB derived AMPs has been here investigated by selecting four bacterial strains as prototypes of Gram-positive and

Gram-negative strains susceptible or resistant to antimicrobial ApoB derived peptides. First of all, we analysed the kinetic of peptides bactericidal activity, and demonstrated that, at the highest peptide concentrations tested (10–20 μM), susceptible bacterial cells (*B. globigii* TNO BM013 and *P. aeruginosa* PAO1 cells) were killed within a very short time interval, i.e. 30 min. This evidence is in perfect agreement with data collected by measuring Zeta potential values upon incubation of susceptible bacterial cells with ApoB derived peptides tested at concentrations corresponding to previously determined MIC_{100} values. Indeed, in all the cases, a significant increase of Zeta potential values was detected, what is indicative of the occurrence of electrostatic interactions between positively charged peptides and negatively charged bacterial surfaces, with a consequent neutralization of bacterial surface. Interestingly, a greater variation in Zeta potential values was detected in the case of the strain characterized by the highest sensitivity to peptide toxicity, i.e. *B. globigii* TNO BM013. This might be indicative of a higher electrostatic affinity between cationic peptides and negatively charged bacterial surface. Indeed, it has been reported that bacterial membrane surface neutralization is a key event mediating the anti-microbial activity of several peptides³⁶, with Zeta potential alteration generally preceding membrane permeabilization leading to cell death³⁶. In perfect agreement with this finding, a significant increase of NPN uptake factor was selectively detected upon treatment of susceptible bacterial strains with ApoB derived peptides, thus strongly supporting the evidence that Zeta potential increase precedes membrane permeabilization, and confirming the crucial role played by bacterial membrane as main target of ApoB derived peptides antimicrobial activity. Moreover, in the case of *B. globigii* TNO BM013 susceptible bacterial strain, Zeta potential increase and membrane permeabilization is also accompanied by a septation block, as indicated by electron microscopy analyses performed at different time intervals and upon treatment with increasing ApoB derived peptides concentrations. These findings are in perfect agreement with a recent report indicating that *E. coli* treatment with antimicrobial peptides causes cells to filament through a division block controlled by the PhoQ/PhoP signaling pathway³⁷. Bacterial cell filamentation, here observed by electron microscopy analyses, might be a result of DNA replication inhibition, SOS induction, chromosome segregation, or failure of septation process³⁸. It has been previously reported that treatment of *E. coli* with the antimicrobial peptide microcin J25 causes cells to filament, with a consequent inhibition of cell division processes through a non-SOS-dependent mechanism mediating a bacteriostatic mode of action³⁹. Similarly, *E. coli* cells treated with dipterocin showed a significantly elongated morphology, indicating that this peptide may affect cell targets involved in cell division to induce cell death, as suggested by its selective activity on actively growing *E. coli* cells⁴⁰. Also human defensin 5 (HD5) was found to induce extensive cell elongation, with a consequent disruption of cell division events⁴¹. Interestingly, in agreement with our findings, such treatment outcomes were observed only upon treatment of Gram-negative bacteria with HD5, thus suggesting a common inhibitory activity depending on specific features of bacterial strains under test. Also in the case of ApoB derived peptides, effects appear to strongly depend on specific properties of analysed bacterial strains. Indeed, in the case of Gram-negative *P. aeruginosa* PAO1 strain, no signs of cell division block were detected upon treatment with ApoB derived peptides, although significant alterations of cell morphology, with irregular and corrugated cell surfaces, signs of cytoplasm leakage and cell death, were detected. It has also to be emphasized that two out of four bacterial strains selected in the present study appear resistant to ApoB derived peptides antimicrobial activity, although they are characterized by negatively charged surfaces, as indicated by Zeta potential values determinations. In particular, in the case of Gram-positive *B. globigii* TNO BM013 and *S. aureus* MRSA WKZ-2 bacterial strains, Zeta potential values have been found to be -33 ± 3 and -28 ± 3 , respectively, but only *B. globigii* TNO BM013 cells were found to be susceptible to ApoB derived peptides antimicrobial activity. In the case of Gram-negative *P. aeruginosa* PAO1 and *P. aeruginosa* ATCC 27853 strains, instead, Zeta potential values were found to be very different, i.e. -23 ± 2 and -11 ± 2 mV, respectively. It is plausible that this dissimilarity reflects differences in bacterial membrane composition ultimately affecting peptide ability to interfere with bacterial cell viability. Since no significant effects on Zeta potential values were detected in the case of resistant bacterial cells treated with ApoB derived peptides, it has been hypothesized a failure of electrostatic interactions between negatively charged bacterial surfaces and positively charged peptides, with a consequent counteraction of ApoB derived peptides antimicrobial activity. Indeed, it has been extensively reported that electrostatic interactions play a pivotal role in the cell killing process mediated by antimicrobial peptides⁴². Based on obtained results, it has been hypothesized that some extracellular factors or bacterial membrane composition might interfere with electrostatic interactions between peptides and bacterial surfaces in the case of resistant bacterial cells. Since previous analyses by Far UV-CD suggested a direct binding of r(P)ApoB₁ peptide to bacterial LPS³⁰, experiments were here performed to verify whether ApoB derived peptides are able to directly interact with LPS molecules extracted from *P. aeruginosa* PAO1 and *P. aeruginosa* ATCC 27853 bacterial strains. Analyses, performed by isothermal titration calorimetry (ITC), indicated that both ApoB derived peptides are able to directly interact with LPS molecules extracted from the two bacterial strains, with no significant differences, at least when peptide binding to LPS molecules is tested in *in vitro* experiments. However, it has to be considered that, in physiological conditions, where up to 100,000 molecules of LPS are located at the surface of one single Gram-negative bacterium⁴³, several factors, such as membrane composition or extracellular microenvironment, might interfere with peptide binding to exposed LPS molecules. Based on this, we also performed a preliminary characterization of LPS molecules extracted from *P. aeruginosa* PAO1 and *P. aeruginosa* ATCC 27853 bacterial strains, in order to evaluate whether differences in LPS structures might be responsible for the efficacy or the inefficacy of ApoB derived peptides on Gram-negative bacterial strains. Performed analyses indicated the selective presence of 2-amino-2,6-dideoxy-D-galactopyranose (FucN) in the LPS of susceptible *P. aeruginosa* PAO1 bacterial strain, whereas LPS B-band was found to be absent in the case of resistant *P. aeruginosa* ATCC 27853 strain. Since the B-band is reported to display negative charges, such as those of the Man2N3NA residues³⁴, electrostatic interactions between positively charged ApoB derived peptides and LPS molecules exposed on *P. aeruginosa* PAO1 bacteria might involve these monosaccharides. Instead, the sole presence of the hydrophobic rhamnan chain (A-band) in the LPS of resistant *P. aeruginosa* ATCC 27853 strain could be responsible for the failure of the electrostatic interactions between peptides and bacterial

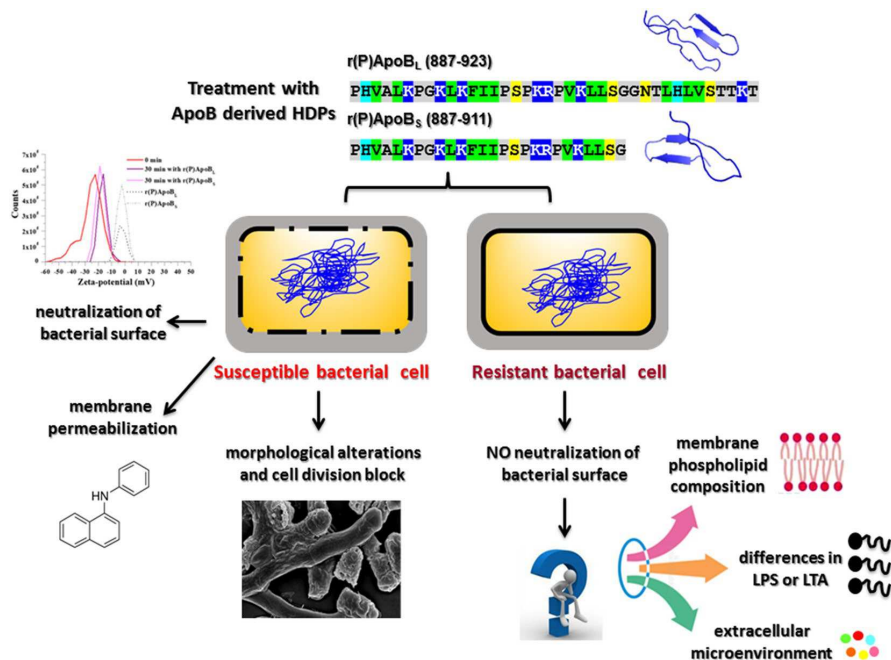


Figure 8. Schematic representation of the main experimental evidence herein collected.

surfaces. This might be one of the key factors responsible for the different response of the two Gram-negative bacterial strains to ApoB derived peptides toxicity.

Altogether, collected results indicate that ApoB derived peptides exert their antimicrobial activity by mainly targeting bacterial membrane and subsequently affecting intracellular molecules and/or processes, such as cell division (Fig. 8). Obtained findings also strongly indicate that an interference with electrostatic interactions between negatively charged bacterial surfaces and positively charged peptides, probably due to extracellular microenvironment or bacterial membrane composition, might counteract ApoB derived peptides antimicrobial activity (Fig. 8).

Materials and Methods

Materials. All the reagents were purchased from Sigma-Aldrich (Milan, Italy), unless differently specified. Chicken cathelicidin-2 (CATH-2) peptide was obtained from CPC Scientific Inc. (Sunnyvale, USA).

Recombinant production of ApoB derived peptides. Expression and isolation of recombinant peptides was carried out as previously described²⁰ with the only exception of a final gel-filtration step, that was added in order to remove salts used along the purification process and that tend to attach to the peptides, as previously reported^{44,45}.

Bacterial strains and growth conditions. Methicillin-resistant *Staphylococcus aureus* (MRSA WKZ-2), *Bacillus globigii* TNO BM013, *Pseudomonas aeruginosa* ATCC 27853, and *Pseudomonas aeruginosa* PAO1 bacterial strains were grown as previously described²⁰.

Anti-microbial activity assay. To test the anti-microbial activity of ApoB derived peptides, previously described experimental procedure was used²⁰. MIC₁₀₀ values correspond to the lowest concentration of peptide associated to no detectable bacterial growth.

Killing kinetic studies. To kinetically analyse bacterial killing by ApoB derived peptides, experiments were performed on *B. globigii* TNO BM013 and *P. aeruginosa* PAO1 strains as previously described²⁰.

Zeta potential measurements of bacterial cells in the presence of ApoB derived peptides. To perform analyses, bacteria were grown over-night in MHB medium, then diluted in fresh MHB, and incubated at 37 °C until logarithmic phase of growth was reached. Bacteria were then diluted to 4×10^6 CFU/mL in a final volume of 5 mL of NB 0.5X, and mixed with the peptide under test (1:1 v/v). In the case of bacterial strains susceptible to antimicrobial ApoB derived peptides, r(P)ApoB₁ and r(P)ApoB₃ were tested at concentrations corresponding to MIC₁₀₀ values. In the case of not responsive strains, instead, only the highest peptide concentration was tested (40 μM). At defined time intervals (0–180 min), Zeta potential values were determined. Zeta potential

measurements of control samples were carried out in NB 0.5X pH 7.4. To test different peptide concentrations, serial dilutions were performed, in order to mix bacteria and peptides at a ratio of 1:1 v/v. The Zeta potential of bacterial cells was determined at 25 °C from the mean of 3 independent measurements (30 runs each), in the absence and in the presence of different peptide concentrations. Zeta potential values were obtained by phase analysis light scattering (PALS) in a Zetasizer Nano ZS 90 device (Malvern, Worcestershire, UK), equipped with Helium–Neon laser (633 nm) as a source of light, with the detection at 173 degree scattering angle at room temperature (25 °C), using disposable Zeta cells with gold electrodes. Values of viscosity and refractive index were set to 0.8872 cP and 1.330, respectively.

NPN uptake assay. NPN uptake assays were carried out by following the previously described experimental procedure⁴⁶. To do this, 1-N-phenyl-naphthylamine (NPN) was diluted to 1 mM in 5 mM HEPES buffer pH 7.2. Control wells were prepared as follows: (i) buffer alone (1 mL); (ii) buffer (1 mL) and NPN (2 µL); (iii) bacteria in buffer (1 mL); (iv) bacteria in buffer (1 mL), NPN (2 µL). Antibiotics or peptides were mixed with bacterial suspension in Eppendorf tubes for 2 and 30 min, respectively, and then transferred into cuvettes. NPN was added immediately before the measurement of fluorescence; the values were recorded within 3 min. Fluorescence emission was detected at 420 nm upon excitation at 340 nm by using a PerkinElmer LS-55 luminescence spectrometer (Waltham, MA, USA). Each assay was performed at least three times. The results are expressed as NPN uptake factors, calculated by subtracting background, *i.e.* the value obtained in the absence of NPN.

Transmission electron microscopy. Bactericidal effects of ApoB derived peptides were also investigated by transmission electron microscopy (TEM) analyses, which required higher bacterial cell densities (2×10^8 CFU/mL). For this reason, additional colony count assays were performed to determine ApoB derived peptides MIC₁₀₀ values at this bacterial cell density. In the case of both peptides, a MIC₁₀₀ value of about 80 µM was determined. To perform analyses, *B. globigii* TNO BM013 and *P. aeruginosa* PAO1 strains were incubated with increasing concentrations of peptides (0–80 µM) for 3 hrs at 37 °C. Samples were then fixed with 2% glutaraldehyde (Polysciences, Eppelheim, Germany) in 5 mM CaCl₂, 10 mM MgCl₂ (both Merck, Darmstadt, Germany) in 0.1 M sodium cacodylate buffer pH 7.4 over-night at 4 °C. Bacteria treatment with peptides was stopped by adding the fixative and keeping the cells over-night at 4 °C. Cells were then washed 3 times by incubation in sodium cacodylate buffer for 10 min and embedded in 2% low-melting point agarose v/v. Cells were then post-fixed with 4% osmium tetroxide (Electron Microscopy Sciences, EMS, Hatfield, USA) and 1.5% K₄Fe(CN)₆·3H₂O (Merck, Darmstadt, Germany) in distilled water for 2 hrs at 4 °C. Upon cell washing with distilled water (5 times for 10 min), cells were incubated in 0.5% uranylacetate (EMS, Hatfield, USA) for 1 hr at 4 °C. After further washing with distilled water (3 times for 10 min), samples were embedded in Epon resin and ultrathin sections (50 nm) of each block were prepared by using a Leica UCT ultramicrotome (Leica, Vienna, Austria). Obtained sections were stained with uranyl acetate and lead citrate by using the Leica AC20 system (Leica, Vienna, Austria). TEM images have been acquired in bright field mode using a Philips EM 208 S transmission electron microscope with an accelerating voltage of 80 kV.

Scanning electron microscopy. Bacterial cells in exponential growth phase were grown for 3 hrs in NB 0.5X in microfuge tubes in the absence or in the presence of ApoB derived peptides. Also in this case, high bacterial cell densities were required (2×10^8 CFU/mL) for the analysis, and it should be underlined that, in these experimental conditions, peptides MIC₁₀₀ value was found to be about 80 µM. To perform scanning electron microscopy (SEM) analyses, *B. globigii* TNO BM013 and *P. aeruginosa* PAO1 strains were incubated with 40 µM peptides for 3 hrs at 37 °C. Following incubation, bacterial cells were centrifuged at 10,000 rpm at 4 °C and fixed in 2.5% glutaraldehyde. Following over-night incubation, bacterial cells were washed three times in distilled water (dH₂O) and then dehydrated with a graded ethanol series: 25% ethanol (1 × 10 min); 50% ethanol (1 × 10 min); 75% ethanol (1 × 10 min); 95% ethanol (1 × 10 min); 100% anhydrous ethanol (3 × 30 min). Bacterial cells deposited onto glass substrate were first sputter coated with a thin layer of Au-Pd (Sputter Coater Denton Vacuum Desk V) to allow subsequent morphological characterization using a FEI Nova NanoSEM 450 at an accelerating voltage of 5 kV with Everhart Thornley Detector (ETD) and Through Lens Detector (TLD) at high magnification.

Lipopolysaccharide (LPS) isolation, purification and characterization. Dried cells from *P. aeruginosa* PAO1 (1 g) and *P. aeruginosa* ATCC 27853 (0.9 g) were extracted by PCP method, *i.e.* by using phenol/chloroform/petroleum ether (2:5:8 v:v:v)⁴⁷. The yields of extracted LPS was found to be 9% and 5% for *P. aeruginosa* PAO 1 and *P. aeruginosa* ATCC 27853, respectively. Both extracts were analysed by 14% DOC-PAGE, that was performed by using Laemmli procedure^{48,49} and sodium deoxycholate (DOC) as detergent. LPS bands were visualized by silver staining as described previously⁵⁰. The glycosyl analysis was performed as previously reported⁵¹. Briefly, LPS samples (0.5 mg) were mixed with 1 mL of HCl/CH₃OH, subjected to methanolysis for 16 hrs at 80 °C, and then acetylated. Simultaneously, another sample of both native LPSs (0.5 mg) was firstly treated with HF (48%; 100 µL) and then subjected to methanolysis and acetylation. Finally, all the acetylated methyl glycosides (MGA) were analysed on an Agilent 7820 A GC System-5977B MSD spectrometer equipped with the automatic injector 7693A and a Zebtron ZB-5 capillary column (Phenomenex, Toornace, CA, USA; flow rate 1 mL/min; He as carrier gas). MGA were analysed using the following temperature program: 140 °C for 3 min, 140 °C → 240 °C at 3 °C/min.

Isothermal titration calorimetry. Interaction between ApoB derived peptides and LPS molecules extracted from *P. aeruginosa* PAO1 or *P. aeruginosa* ATCC 27853 bacterial strains was tested by isothermal titration calorimetry (ITC) experiments, which were carried out on a Low Volume NanoITC (TA instruments, Waters LLC, New Castle, USA) at 37 °C. To this purpose, LPS molecules were diluted to 0.5 mg/mL in 50% phosphate buffer (PBS), and vortexed for 5 min. Afterwards 190 µL of LPS suspension were added to the cell chamber. The

syringe was then filled with 50 μL of 266 μM peptide solutions in 50% PBS. Titrations were incremental with 2 μL injections at 300 seconds intervals. Control spectra, obtained by injection of the same amount of each peptide in buffer solution, were subtracted to correct for heat production upon peptide dilution. Collected data were analyzed by using Nano Analyze software (TA instruments, Waters LLC, New Castle, USA).

Statistical analysis. Statistical analysis was performed using a Student's t-Test. Significant differences were indicated as *($P < 0.05$), **($P < 0.01$) or ***($P < 0.001$).

Data Availability

All the data supporting the conclusions have been included within the article.

References

- Agerberth, B. *et al.* FALL-39, a putative human peptide antibiotic, is cysteine-free and expressed in bone marrow and testis. *Proc. Natl. Acad. Sci. USA* **92**, 195–199 (1995).
- Hancock, R. E. W. & Sahl, H. G. Antimicrobial and host-defense peptides as new anti-infective therapeutic strategies. *Nat. Biotechnol.* **24**, 1551–1557 (2006).
- Hancock, R. E. W. Mechanisms of action of newer antibiotics for Gram-positive pathogens. *Lancet Infect. Dis.* **95**, 209–218 (2005).
- Ostorhazi, E., Nemes-Nikodem, É., Knappe, D. & Hoffmann, R. *In vivo* activity of optimized apidaecin and onconin peptides against a multiresistant, KPC-producing *Klebsiella pneumoniae* strain. *Protein Pept. Lett.* **21**, 368–373 (2014).
- Steinstraesser, L., Kraneburg, U., Jacobsen, F. & Al-Benna, S. Host defense peptides and their antimicrobial-immunomodulatory duality. *Immunobiology* **216**, 322–333 (2011).
- Holz, M. A., Hofer, J., Steinberger, P., Pfistershammer, K. & Zlabinger, G. J. Host antimicrobial proteins as endogenous immunomodulators. *Immunol. Lett.* **119**, 4–11 (2008).
- Hancock, R. E. W. & Chapple, D. S. Peptide antibiotics. *Antimicrob. Agents Chemother.* **43**, 1317–1323 (1999).
- Papo, N. & Shai, Y. Host defense peptides as new weapons in cancer treatment. *Cell. Mol. Life Sci.* **62**, 784–790 (2005).
- Barns, K. J. & Weisshaar, J. C. Real-time attack of LL-37 on single *Bacillus subtilis* cells. *Biochim Biophys Acta* **1828**, 1511–1520 (2013).
- Zhang, L., Rozek, A. & Hancock, R. E. W. Interaction of cationic antimicrobial peptides with model membranes. *J. Biol. Chem.* **276**, 35714–35722 (2001).
- Yeaman, M. R. & Yount, N. Y. Mechanisms of antimicrobial peptide action and resistance. *Pharmacol. Rev.* **55**, 27–54 (2003).
- Joyce, G. H., Hammond, R. K. & White, D. C. Changes in membrane lipid composition in exponentially growing *Staphylococcus aureus* during the shift from 37 to 25 °C. *J. Bacteriol.* **104**, 323–330 (1970).
- Bozdogan, B., Esel, D., Whitener, C., Browne, F. A. & Appelbaum, P. C. Antibacterial susceptibility of a vancomycin-resistant *Staphylococcus aureus* strain isolated at the Hershey Medical Center. *J. Antimicrob. Chemother.* **52**, 864–868 (2003).
- Lee, M. T., Hung, W. C., Chen, F. Y. & Huang, H. W. Mechanism and kinetics of pore formation in membranes by water soluble amphipathic peptides. *Proc. Natl. Acad. Sci. USA* **105**, 5087–5092 (2008).
- Biaggi, M. H., Riske, K. A. & Lamy-Freund, M. T. Melanotropic peptides-lipid bilayer interaction. Comparison of the hormone alpha-MSH to a biologically more potent analog. *Biophys. Chem.* **67**, 139–149 (1997).
- Biaggi, M. H., Pinheiro, T. J., Watts, A. & Lamy-Freund, M. T. Spin label and 2H-NMR studies on the interaction of melanotropic peptides with lipid bilayers. *Eur. Biophys. J.* **24**, 251–259 (1996).
- Ramamoorthy, A., Thennarasu, S., Lee, D. K., Tan, A. & Maloy, L. Solid-state NMR investigation of the membrane-disrupting mechanism of antimicrobial peptides MSI-78 and MSI-594 derived from magainin 2 and melittin. *Biophys. J.* **91**, 206–216 (2006).
- Henzler Wildman, K. A., Lee, D. K. & Ramamoorthy, A. Mechanism of lipid bilayer disruption by the human antimicrobial peptide, LL-37. *Biochemistry* **42**, 6545–6558 (2003).
- Hong, M. & Su, Y. Structure and dynamics of cationic membrane peptides and proteins: Insights from solid-state NMR. *Protein Sci.* **20**, 641–655 (2011).
- Gaglione, R. *et al.* Novel human bioactive peptides identified in Apolipoprotein B: Evaluation of their therapeutic potential. *Biochem. Pharmacol.* **130**, 34–50 (2017).
- Pane, K. *et al.* Antimicrobial potency of cationic antimicrobial peptides can be predicted from their amino acid composition: Application to the detection of “cryptic” antimicrobial peptides. *J. Theor. Biol.* **419**, 254–265 (2017).
- Gaglione, R. *et al.* Insights into the anticancer properties of the first antimicrobial peptide from Archaea. *Biochim Biophys Acta Gen Subj* **1861**, 2155–2164 (2017).
- Bosso, A. *et al.* A new cryptic host defense peptide identified in human 11-hydroxysteroid dehydrogenase-1 β -like: from in silico identification to experimental evidence. *Biochim Biophys Acta Gen Subj* **1861**, 2342–2353 (2017).
- Zanfardino, A. *et al.* Human apolipoprotein E as a reservoir of cryptic bioactive peptides: The case of ApoE 133-167. *J. Pept. Sci.* **24**, e3095 (2018).
- Pizzo, E. *et al.* Novel bioactive peptides from PD-1/L1-2, a type 1 ribosome inactivating protein from *Phytolacca dioica* L. Evaluation of their antimicrobial properties and anti-biofilm activities. *Biochim Biophys Acta Biomembr* **1860**, 1425–1435.
- Kasety, G. *et al.* The C-terminal sequence of several human serine proteases encodes host defense functions. *J. Innate Immun.* **3**, 471–482 (2011).
- Lee, D. Y. *et al.* Histone H4 is a major component of the antimicrobial action of human sebocytes. *J. Invest. Dermatol.* **129**, 2489–2496 (2009).
- Beck, W. H. *et al.* Apolipoprotein A-I binding to anionic vesicles and lipopolysaccharides: role for lysine residues in antimicrobial properties. *Biochim Biophys Acta* **1828**, 1503–1510 (2013).
- van Dijk, A. *et al.* Chicken heterophils are recruited to the site of *Salmonella* infection and release antibacterial mature Cathelicidin-2 upon stimulation with LPS. *Mol. Immunol.* **46**, 1517–1526 (2009).
- MacGowan, A. P. *et al.* A new time-kill method of assessing the relative efficacy of antimicrobial agents alone and in combination developed using a representative beta-lactam, aminoglycoside and fluoroquinolone. *J. Antimicrob. Chemother.* **38**, 193–203 (1996).
- Dhariwal, A. K. & Tullu, M. S. Colistin: re-emergence of the ‘forgotten’ antimicrobial agent. *J. Postgrad. Med.* **59**, 208–215 (2013).
- González, C., Rubio, M., Romero-Vivas, J., González, M. & Picazo, J. J. Bacteremic pneumonia due to *Staphylococcus aureus*: A comparison of disease caused by methicillin-resistant and methicillin-susceptible organisms. *Clin. Infect. Dis.* **29**, 1171–1177 (1999).
- Arsenault, T. L. *et al.* Structural studies on the polysaccharide portion of A-band lipopolysaccharide from a mutant (AK1401) of *Pseudomonas aeruginosa* strain PAO1. *Can J Chem* **69**, 1273–1280 (1991).
- Sadovskaya, I. *et al.* Structural characterization of the outer core and the O-chain linkage region of lipopolysaccharide from *Pseudomonas aeruginosa* serotype O5. *Eur. J. Biochem.* **267**, 1640–1650 (2000).
- Fernandes, P. & Martens, E. Antibiotics in late clinical development. *Biochem. Pharmacol.* **133**, 152–163 (2017).
- Halder, S. *et al.* Alteration of Zeta potential and membrane permeability in bacteria: a study with cationic agents. *Springerplus* **4**, 672 (2015).

37. Yadavalli, S. S. *et al.* Antimicrobial peptides trigger a division block in *Escherichia coli* through stimulation of a signalling system. *Nat Commun* **7**, 12340 (2016).
38. Lutkenhaus, J. Regulation of cell division in *E. coli*. *Trends Genet.* **6**, 22–25 (1990).
39. Salomón, R. A. & Fariás, R. N. Microcin 25, a novel antimicrobial peptide produced by *Escherichia coli*. *J. Bacteriol.* **174**, 7428–7435 (1992).
40. Ishikawa, M., Kubo, T. & Natori, S. Purification and characterization of a dipteracin homologue from *Sarcophaga peregrina* (flesh fly). *Biochem. J.* **287**, 573–578 (1992).
41. Chileveru, H. R. *et al.* Visualizing attack of *Escherichia coli* by the antimicrobial peptide human defensin 5. *Biochemistry* **54**, 1767–1777 (2015).
42. Gaspar, D., Veiga, A. S., Sinthuvanich, C., Schneider, J. P. & Castanho, M. A. Anticancer peptide SVS-1: efficacy precedes membrane neutralization. *Biochemistry* **51**, 6263–6265 (2012).
43. Vincent, J. L., Opal, S. M., Marshall, J. C. & Tracey, K. J. Sepsis definitions: time for change. *Lancet* **381**, 774–775 (2013).
44. Bommarius, B. *et al.* Cost-effective expression and purification of antimicrobial and host defense peptides in *Escherichia coli*. *Peptides* **31**, 1957–1965 (2010).
45. Gaglione, R. *et al.* Cost-effective production of recombinant peptides in *Escherichia coli*. *N. Biotechnol.* **51**, 39–48 (2019).
46. Helander, I. M. & Mattila-Sandholm, T. Fluorometric assessment of gram-negative bacterial permeabilization. *J. Appl. Microbiol.* **88**, 213–219 (2000).
47. Galanos, C., Lüderitz, O. & Westphal, O. A new method for the extraction of R lipopolysaccharides. *Eur. J. Biochem.* **9**, 245–249 (1969).
48. Laemmli, U. K. Most commonly used discontinuous buffer system for SDS electrophoresis. *Nature* **227**, 680–685 (1970).
49. Carillo, S. *et al.* Structural investigation of the antagonist LPS from the cyanobacterium *Oscillatoria planktothrix* FP1. *Carbohydr. Res.* **388**, 73–80 (2014).
50. Tsai, C. M. & Frasch, C. E. A sensitive silver stain for detecting lipopolysaccharides in polyacrylamide gels. *Anal. Biochem.* **119**, 115–119 (1982).
51. Pieretti, G. *et al.* The complete structure of the core of the LPS from *Plesiomonas shigelloides* 302-73 and the identification of its O-antigen biological repeating unit. *Carbohydr. Res.* **345**, 2523–2528 (2010).

Acknowledgements

This research received no specific grant from any funding agency in the public, commercial, or not-for-profit sectors.

Author Contributions

R.G. conceived and performed most of the experiments; A.C., E.D.O., B.D.V., A.C. and R.D.G. performed the experiments and analysed the data; E.J.A.V. performed isothermal titration calorimetry studies and analysed the data; R.V., E.N., M.M.C. and C.D.R. conceived the experiments and discussed the results; A.A. conceived the experiments, analysed the data, discussed the results, and wrote the manuscript with the contribution of all the authors.

Additional Information

Supplementary information accompanies this paper at <https://doi.org/10.1038/s41598-019-43063-3>.

Competing Interests: The authors declare no competing interests.

Publisher's note: Springer Nature remains neutral with regard to jurisdictional claims in published maps and institutional affiliations.



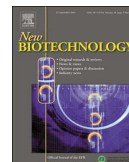
Open Access This article is licensed under a Creative Commons Attribution 4.0 International License, which permits use, sharing, adaptation, distribution and reproduction in any medium or format, as long as you give appropriate credit to the original author(s) and the source, provide a link to the Creative Commons license, and indicate if changes were made. The images or other third party material in this article are included in the article's Creative Commons license, unless indicated otherwise in a credit line to the material. If material is not included in the article's Creative Commons license and your intended use is not permitted by statutory regulation or exceeds the permitted use, you will need to obtain permission directly from the copyright holder. To view a copy of this license, visit <http://creativecommons.org/licenses/by/4.0/>.

© The Author(s) 2019



Contents lists available at ScienceDirect

New BIOTECHNOLOGY

journal homepage: www.elsevier.com/locate/nbt

Cost-effective production of recombinant peptides in *Escherichia coli*

Rosa Gaglione^a, Katia Pane^b, Eliana Dell'Olmo^a, Valeria Cafaro^c, Elio Pizzo^c,
Giuseppe Olivieri^{d,*,**}, Eugenio Notomista^c, Angela Arciello^{a,c,e,*}

^a Department of Chemical Sciences, University of Naples Federico II, 80126, Naples, Italy

^b IRCCS SDN, 80143, Naples, Italy

^c Department of Biology, University of Naples Federico II, 80126, Naples, Italy

^d Bioprocess Engineering, AlgaePARC, Wageningen University and Research, PO Box 16, 6700 AA, Wageningen, the Netherlands

^e Istituto Nazionale di Biostrutture e Biosistemi (INBB), Italy

ARTICLE INFO

Keywords:

Host defence peptides
Apolipoprotein B
Apolipoprotein A-I
Auto-inducing expression procedure
Cost-effective recombinant production
Techno-economic analysis

ABSTRACT

Among bioactive peptides, cationic antimicrobial peptides (AMPs), also referred to as host defence peptides (HDPs), are valuable tools to treat infections, being able to kill a wide variety of microbes directly and/or modulate host immunity. HDPs have great therapeutic potential against antibiotic-resistant bacteria, viruses and even parasites. However, high manufacturing costs have greatly limited their development as drugs, thus highlighting the need to develop novel and competitive production strategies. Here, a cost-effective procedure was established to produce the high amounts of peptides required for basic and clinical research. Firstly, a novel culture medium was designed, which was found to support significantly higher cell densities and recombinant expression levels of peptides under test compared to conventional media. The procedure has been also efficiently scaled up by using a 5 L fermenter, while the costs have been lowered significantly by developing a successful auto-induction strategy, which has been found to support higher yields of target constructs and cell biomass compared to conventional strategies based on expression induction by IPTG. Interestingly, it was estimated that by increasing production scale from 100 to 1000 mg/batch, unit costs decreased strongly from 253 to 42 €/mg. These costs appear highly competitive when compared to chemical synthesis strategies. Altogether, the data indicate that the strategy represents an important starting point for the future development of large-scale manufacture of HDPs.

Introduction

Both basic research and clinical applications require high quality peptides to be readily available in a cost-effective manner. This is the case for antimicrobial peptides (AMPs), also referred to as host defence peptides (HDPs), in view of their immunomodulatory properties. To date, more than 2500 HDPs have been identified [1]. Since they exhibit a wide spectrum of biological activities, their potential applications range from biomedical therapies to the food industry and agricultural area. In general, isolation of HDPs from natural sources is a labor intensive and time-consuming process, not suitable to obtain peptides in large amounts. Chemical synthesis, although very efficient, is complex and expensive [2], suited to obtain small amounts of peptides, but prohibitive when peptides longer than 30 amino acids or large

quantities of peptide are required. Costs are even higher in the case of lanthipeptides, ribosomally synthesized and post-translationally modified peptides having thioether cross-linked amino acids, lanthionines, as a structural element [3]. Indeed, industrial scale synthesis of lanthipeptides appears unprofitable, due to expensive raw materials and overall low yields, which culminate in exorbitant production costs in large scale process [4]. Based on this, chemical synthesis appears as an unsuitable platform for large-scale peptide production.

In this scenario, recombinant DNA technology provides economical means for peptide manufacture. However, although many HDPs have been successfully obtained through recombinant production in *Escherichia coli* [5,6], several difficulties have been encountered [6–8]. First, the antibacterial nature of the peptides makes them potentially lethal to the producing host. Secondly, their small size and cationic property make

Abbreviations: HDPs, host defence peptides; AMPs, antimicrobial peptides; TB, Terrific Broth; SB, Super Broth; RNase, ribonuclease; ONC, onconase; LB, Luria-Bertani broth; NAB, Notomista-Arciello broth; iNAB, auto-inducing Notomista-Arciello broth; IPTG, isopropyl-β-D-thiogalactopyranoside; ApoB, apolipoprotein B; ApoA-I, apolipoprotein A-I; TF-acetate, trifluoroacetate

* Corresponding author at: Department of Chemical Sciences, University of Naples Federico II, 80126, Naples, Italy.

** Corresponding author.

E-mail addresses: giuseppe.olivieri@wur.nl (G. Olivieri), anarciel@unina.it (A. Arciello).

<https://doi.org/10.1016/j.nbt.2019.02.004>

Received 15 December 2017; Received in revised form 12 February 2019; Accepted 16 February 2019

Available online 18 February 2019

1871-6784/© 2019 Elsevier B.V. All rights reserved.

them highly susceptible to proteolytic degradation [7,9]. A strategy that effectively overcomes both obstacles is peptide fusion to a carrier protein [7,10], from which the peptide of interest can be released by enzymatic or chemical cleavage at a specific site around the carrier-peptide junction [8]. The fusion design mimics the peptide precursor structure, with the carrier protein playing a similar role to the natural peptide pro-segment, thus protecting the host from the toxic peptide and the peptide from bacterial proteases [11]. Recently, the rational development of a new carrier protein for high yield production of recombinant peptides in *E. coli* has been described [12]. The denatured form of Onconase (ONC), a ribonuclease (RNase) from *Rana pipiens* [13], was found to be a highly suitable partner, since it can be expressed at very high levels in inclusion bodies (about 200–250 mg/L in Terrific Broth), is a small protein (104 aa), and its solubility is pH dependent (the denatured protein is soluble only at pH < 4.0), thus allowing the purification of peptides soluble at pH 7.0 by selective precipitation of the carrier. Moreover, the chimeric construct has been designed to contain a His tag sequence, located between the ONC and the peptide moieties, suitable for easy purification, a flexible linker (Gly-Thr-Gly) and a dipeptide (Asp-Pro), which is cleaved in acidic conditions, thus allowing the release of the peptide from the carrier [12]. The optimized procedure allows the purification of about 10–15 mg of pure peptide from 1 L of bacterial culture [12,14,15]. However, a cost analysis to evaluate the competitiveness of the production process has not yet been performed. Here, we describe the development of a novel growth medium and the setting up of an auto-induction expression procedure with the ultimate goal of scaling up an efficient and commercially competitive production strategy, as confirmed by techno-economic analyses. The experimental strategy has been successfully applied to GKY20 peptide, a short cationic AMP derived from the C-terminus of human thrombin [12,16] and to two novel HDPs identified in an isoform of human Apolipoprotein B (ApoB) [15,17].

Materials and methods

Bacterial strains, plasmids and bacterial culture media

E. coli BL21(DE3) and *E. coli* BL21(DE3)pLysS strains were from AMS Biotechnology (Abingdon, UK). To produce recombinant constructs ONC-r(P)GKY20 [12], ONC-r(P)ApoB_L [15] and ONC-r(P)ApoB_S [15] in bacterial cells, the cDNAs encoding the antimicrobial peptides were cloned in the pET-22b(+) expression vector (Novagen, Merck Group, Darmstadt, Germany). In the case of His6-ApoA-I, the pET-20b(+) expression vector (Novagen) was used. Bacterial cultures were carried out accordingly to [18]. NZY medium was prepared accordingly to [18]. All the reagents were from Sigma-Aldrich (Milan, Italy), unless otherwise specified.

Shake flask expression

Expression of recombinant constructs was carried out as previously described [12,14,15] by using IPTG (isopropyl-β-D-thiogalactopyranoside) at a final concentration of 0.7 mM. Expression of recombinant constructs was carried out by shaking bacterial samples at 180 rpm at 37 °C. In the case of apolipoprotein A-I (ApoA-I) protein, an ApoA-I expressing pET20 plasmid in *E. coli* strain BL21(DE3)pLysS (ThermoFisher Scientific, Waltham, MA) was used, as previously described [19–21].

Bioreactor cultivation

Bioreactor cultivation was performed in a BioFlo 3000 system from New Brunswick Scientific Co. (Connecticut, USA). The instrument is endowed with a 5 L vessel, temperature control by a heating sleeve and an integrated cooling system, monitoring of airflow rate, and monitoring of pH values and dissolved O₂ levels through specific probes (Mettler Toledo S.p.A., Novate Milanese, Milan, Italy). The medium in bioreactor (3 L) was inoculated with *E. coli* BL21(DE3) or with *E. coli* BL21(DE3)

Table 1
NA bacterial growth medium composition.

Organic Components	
Industrial Tryptone	34 g/L
Betaine	0.12 g/L
NH ₃	0.075%
Citric Acid	3 g/L
Glycerol	1.2%
Glucose	4 g/L
Buffer Components Concentration	
KH ₂ PO ₄	23 g/L
K ₂ HPO ₄	125 g/L
C-Goodies	0.5%
Salts	
MgSO ₄	30.1 g/L
FeSO ₄ * 7 H ₂ O	4.75 g/L
MgO	5.4 g/L
CaCO ₃	1.0 g/L
ZnSO ₄ * 7 H ₂ O	0.72 g/L
MnSO ₄ * 1 H ₂ O	0.56 g/L
CuSO ₄	0.125 g/L
CoSO ₄ * H ₂ O	0.14 g/L
H ₃ BO ₃	0.03 g/L
NiCl ₂	0.004 g/L
Na ₂ MoO ₄	0.006 g/L
HCl 37%	24.5 mL/L

pLysS cells, previously transformed with recombinant vectors, and incubated overnight at 37 °C in 150 mL of antibiotic-supplemented medium (OD_{600 nm} = 2–4). Sterile antifoam A emulsion (Sigma-Aldrich, Milan, Italy) was added manually (0.01% v/v final concentration) under aseptic conditions prior to overnight incubation. To avoid undesirable growth of non-transformed bacterial cells upon ampicillin degradation, antibiotic was regularly added to bacterial cells at a rate of 100 mg/h by using a fermenter peristaltic pump. During the whole fermentation process, the stirring speed was kept constant at 300 rpm, with an air flow rate of 10 cm³/sec, and temperature was kept constant at 37 °C. When bacterial culture in the bioreactor reached an OD_{600 nm} of 3–5, protein expression was induced by adding 0.7 mM IPTG by using a fermenter peristaltic pump. A time of 30 min after IPTG addition was defined as the start time (t = 0 h). In the case of the auto-induction expression procedure, 30 min after bacteria inoculation into the bioreactor was defined as the start time (t = 0 h). Bioreactor cultivation was carried out for a total of 24 h. For each experimental condition, bioreactor cultivations were performed at least twice for each expressed protein construct.

Biomass determination

For both shake flask and bioreactor cultivations, OD_{600 nm} measurements were performed on triplicate samples by using a Photometer UV-2600 (Shimadzu Europa GmbH, Duisburg, F.R. Germany), with samples diluted in complete medium. For cell dry weight determination, samples (25 mL) were harvested, centrifuged for 20 min at 6000 rpm, and washed 3 times with 0.9% NaCl, then dried overnight at 80 °C, and lyophilized before weighing.

Analyses of expression levels

For both shake flask and bioreactor cultivations, at established time intervals, bacterial aliquots (corresponding to 0.125 OD_{600 nm}) were withdrawn and solubilized in lysis buffer (0.125 M Tris-HCl pH 6.8 containing 2% SDS and 10% glycerol), in order to determine recombinant construct expression levels by 15% SDS-PAGE. Protein band intensities were detected by densitometric analyses using a ChemiDoc Imaging System (Bio-Rad, California, USA). In order to estimate

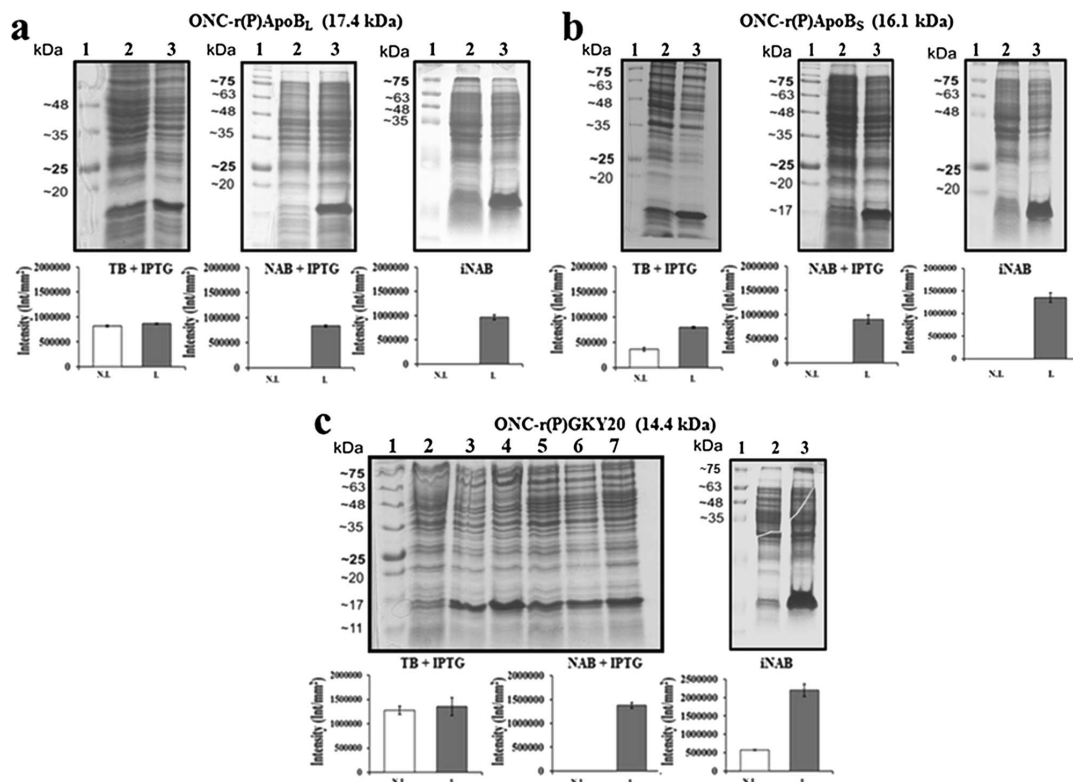


Fig. 1. Analysis by SDS-PAGE of total proteins extracted from non-induced (N.I., lane 2) and induced bacterial cells (L., lane 3) transformed with pET recombinant plasmids encoding ONC-r(P)ApoB₁ (a), ONC-r(P)ApoB₅ (b), or ONC-r(P)GKY20 (c) constructs in shake flasks. Densitometric analyses of protein bands with a molecular weight corresponding to that of ONC-r(P)ApoB₁ (17.4 kDa), ONC-r(P)ApoB₅ (16.1 kDa), or ONC-r(P)GKY20 (14.4 kDa) are reported as histograms in a, b, and c, respectively. In each panel, from left to the right, analysis of protein expression was performed in TB medium with IPTG induction, in NAB with IPTG induction and in iNAB, respectively. For the left gel of panel c, protein standards (lane 1), non-induced cells in NAB (lane 2), induced cells in NAB with IPTG (lanes 3 and 4), non-induced cells in TB (lane 5), induced cells in TB with IPTG (lanes 6 and 7). Molecular weights of expressed protein bands were determined on the basis of calibration curves, prepared for each gel by plotting electrophoretic mobility (mm) of visible standard proteins as a function of known molecular weights.

recombinant constructs expression levels, the intensity of protein bands with the expected electrophoretic mobility was referred to a calibration curve obtained by analyzing increasing defined amounts of bovine serum albumin (BSA, Sigma-Aldrich, Milan, Italy).

Techno-economic analysis

The analysis of the costs of peptide production was performed by implementing the process sections in SuperPro Designer 9.0 (Intelligen Inc., Thessaloniki, Greece). In the case of each unit operation, mass and energy balances were performed to evaluate chemical demand, electricity consumption and utilities duties. In Supplementary Fig. S1 and S2, the flow-sheet of the entire process is reported. As shown, the process consisted of 3 sections: (i) fermentation, (ii) protein extraction and (iii) purification (Supplementary Fig. S1 and S2). Step 1 (fermentation) comprised 3 stages: (i) pre-culture carried out in shake flasks, (ii) fermentation and (iii) sample harvesting by centrifugation. Extraction consisted of four washing-centrifugation steps according to [12]. Purification was performed by expanded bed chromatography followed by diafiltration. Thereafter, peptide was released by acidic hydrolysis of the chimeric construct, *i.e.* onconase-peptide. Onconase was then selectively precipitated and removed by centrifugation, whereas the soluble peptide was dried by lyophilization and stored prior to solubilization in an appropriate buffer. The chosen scenario describes first the production costs on a small production scale of 100 mg of peptide *per*

batch, which is related to a 5 L fermenter volume. The production process has then been scaled up to 10 times by simulating the case of a small-medium enterprise. Italy was chosen as the location to determine the costs of labor, electricity and other utilities, as reported in Table S1.

Capital (CAPEX) and Operating Expenditures (OPEX) were calculated according to the procedure reported in Table S2. The overall Lang factor of the process was about 8, which is in line with indications for high value product from microbial processes [22]. Costs of chemicals were taken from bulk quotations kindly provided by Sigma-Aldrich (Milan, Italy), PanReac AppliChem (Maryland Heights, MO, USA) and GE Healthcare Europe GmbH (Milan, Italy), as reported in Table S3. A detailed batch schedule was implemented by reporting operations associated with each unit, according to the procedure reported in Supplementary Figs. S1 and S2. Major equipment depreciation was evaluated by assuming a 10-year lifetime and an interest rate of 2–3%. To take into account maintenance, 330 days of production *per* year were considered. The process was initially fixed at a laboratory scale by considering a working fermenter volume of 5 L, and then scaled up to 50 L for future scenarios. Fermenter cost was scaled according to power law exponents suggested by Kalk and Langlykke [22]. Costs of other equipment were scaled up according to the model provided by SuperPro Designer. Wastewater treatment was fixed to 0.4 € m⁻³ [23]. Since the entire process was carried out under batchwise conditions, the labour demand was fixed to one direct labour hour *per* hour for all the procedures described in each step.

Table 2

Expression levels of recombinant constructs and OD_{600 nm} values of bacterial cultures before and after expression induction in TB and NAB by using IPTG as inducer, or at the end of the expression protocol by using iNAB. Results of representative experiments are reported.

Flask Expression			
TB medium (induction by IPTG 0.7 mM)			
Recombinant construct	Expression level (g/L)	OD _{600 nm} before induction	Final OD _{600 nm}
ONC-r(P)ApoB _L	0.51 ± 0.42	3.2 ± 0.11	5.7 ± 0.09
ONC-r(P)ApoB _S	0.66 ± 0.21	2.8 ± 0.02	7 ± 0.2
ONC-r(P)GKY20	0.44 ± 0.11	3.4 ± 0.2	6.6 ± 0.4
NAB medium (induction by IPTG 0.7 mM)			
Recombinant construct	Expression level (g/L)	OD _{600 nm} before induction	Final OD _{600 nm}
ONC-r(P)ApoB _L	0.80 ± 0.51	4.6 ± 0.36	9.5 ± 0.92
ONC-r(P)ApoB _S	1.07 ± 0.13	4.3 ± 0.29	9.1 ± 1.21
ONC-r(P)GKY20	0.50 ± 0.33	5 ± 0.55	8.3 ± 1.16
auto-inducing NAB medium			
Recombinant construct	Expression level (g/L)	Final OD _{600 nm}	
ONC-r(P)ApoB _L	1.25 ± 0.34	5.2 ± 1.81	
ONC-r(P)ApoB _S	2.05 ± 0.66	4 ± 1.93	
ONC-r(P)GKY20	1.03 ± 0.24	2.7 ± 1.48	
Fermenter Expression			
NAB medium (induction by IPTG 0.7 mM)			
Recombinant construct	Expression level (g/L)	OD _{600 nm} before induction	Final OD _{600 nm}
ONC-r(P)ApoB _L	2.36 ± 0.33	3 ± 1.12	8 ± 0.96
ONC-r(P)ApoB _S	1.44 ± 0.27	5 ± 0.85	7.9 ± 0.64
ONC-r(P)GKY20	1.17 ± 0.19	4 ± 1.06	6.3 ± 1.03
auto-inducing NAB medium			
Recombinant construct	Expression level (g/L)	Final OD _{600 nm}	
ONC-r(P)ApoB _L	3.1 ± 0.19	10.5 ± 1.61	
ONC-r(P)ApoB _S	2.5 ± 0.31	12 ± 1.96	
ONC-r(P)GKY20	2 ± 0.14	5 ± 1.77	

Results

Bacterial growth medium design

A novel semi-defined rich medium was developed, designated Notomista-Arciello broth (NAB), with the aim of obtaining high cell densities and significantly higher expression levels of recombinant peptides and proteins. The composition of NAB is reported in Table 1. As will be noted, the medium is composed of inexpensive, readily available components, and contains defined amounts of each of them. In particular, yeast extract has been replaced by known growth factors, in order to obtain a chemically defined medium rather than a complex crude extract whose composition varies not only depending on the manufacturer but also from batch to batch of the same manufacturer [24]. In NAB, yeast extract has been primarily replaced by tryptone, which has a defined amino acidic composition. As different batches of tryptone can contain different amounts of lactose, 4 g/L glucose has been added to NAB (Table 1), to avoid undesirable basal induction of recombinant protein expression. NAB also contains a mixture of salts providing optimal amounts of required metals (e.g. Mg, Ca, Zn, Fe, Mn, Cu, etc.), usually acting as cofactors for essential enzymatic reactions. Glycerol (1.2%) was added as the main carbon source. Ammonium citrate was added both as a source of inorganic nitrogen and as an additional buffer system. Furthermore, since citrate acts as a chelating agent, its presence is fundamental to avoid precipitation of transition metal cations and also promotes iron uptake [24]. Finally, betaine was added as one of the best osmolytes for *E. coli* [25], that is able to synthesize it from choline, a component likely present in yeast extract but not in tryptone.

To verify the efficiency of NAB for *E. coli* culture and recombinant protein production, a comparison was first performed between TB (Terrific Broth) and NAB in shake flask cultures. For this, *E. coli* BL21(DE3) strain was used as a host to produce recombinant bioactive peptides. Since the peptides GKY20, ApoB887-923, and ApoB887-911, upon cleavage of the chimeric construct in acidic conditions, are released with an additional proline residue at the N-terminus, they are termed r(P)ApoB_L, r(P)ApoB_S, and r(P)GKY20. Similarly, fusion proteins with onconase (ONC) are termed ONC-r(P)ApoB_L, ONC-r(P)ApoB_S, and ONC-r(P)GKY20, respectively. To compare TB and NAB, bacterial cells, transformed with pET recombinant plasmids, were grown in 50 mL of medium containing 100 µg/mL ampicillin, and then used to inoculate 1 L of ampicillin containing medium. The culture was incubated at 37 °C up to an OD_{600 nm} of 1–3.5. Expression of recombinant constructs was induced by addition of 0.7 mM IPTG. Cells were harvested after overnight induction by centrifugation and lysed in order to analyze recombinant constructs expression by 15% SDS-PAGE (Fig. 1a–c). With NAB, higher expression levels were reached for ONC-r(P)ApoB_L and ONC-r(P)ApoB_S recombinant constructs (Fig. 1a, b, and Table 2). In particular, expression levels were found to be 1.5 and 1.6 times higher in NAB than in TB for ONC-r(P)ApoB_L and ONC-r(P)ApoB_S recombinant constructs, respectively (Table 2). For the ONC-r(P)GKY20 construct, in contrast, the effects of NAB on expression levels were found to be slight. Moreover, in all the cases, we observed a strong decrease of basal expression in NAB compared to TB (Fig. 1a–c). Expression levels were determined on the basis of densitometric analyses of protein bands on SDS-PAGE gels (Materials and Methods). It can also be noted that faster growth kinetics were observed in NAB compared to TB. In fact, by monitoring biomass increase on the basis of OD_{600 nm} values, it was observed that in the early stationary phase, the point selected for IPTG addition, higher cell densities were achieved in NAB compared to TB. In Table 2, results of representative experiments are reported. Time-course experiments were also performed by monitoring bacterial growth on the basis of absorbance values at 600 nm and protein construct expression yield by SDS-PAGE analyses, followed by evaluation of intensity values of protein bands of interest. Both bacterial growth and protein expression yield were monitored at regular time intervals for 24 h. Results for ONC-r(P)ApoB_L and ONC-r(P)ApoB_S constructs in TB and NAB are reported in Supplementary Figs. 3 and 4. It can be seen that, over 24 h cultivation, biomass and protein construct expression yields progressively increased in both media. Moreover, final expression yields of protein constructs appeared significantly higher in NAB than in TB. These findings suggest that NAB is able to support higher biomass and protein product expression yields than conventional TB, at least in the case of the linear peptides under test.

Set up of an auto-induction protocol

To further improve and to significantly lower the costs of the production procedure, an auto-induction protocol was set up. An auto-induction medium was first developed, characterized by a well-balanced combination of different carbon sources and other essential nutrients, thus allowing cultures to grow to high cell densities and to support the expression of the target chimeric proteins at high levels. Indeed, NAB was conceived to possess the mineral salt formulation required for a successful auto-induction procedure [27]. Hence, to establish an efficient auto-induction protocol, NAB was supplemented with 0.4% glycerol (54 mM) and 1.92 g/L lactose (5.6 mM) [28]. Glucose was added at a concentration of 0.5 g/L (2.8 mM) [28] to promote rapid cell growth in the early stages of the culture, while also preventing uptake and metabolism of inducing sugar (lactose). In this way, lactose was consumed only after glucose exhaustion, with a consequent automatic induction of recombinant protein expression under the control of the T7 promoter. Indeed, *E. coli* has specific preferences with respect to alternative carbon sources and can switch between them in a specific order (diauxic shift) [29]. Unlike experimental procedures based on the

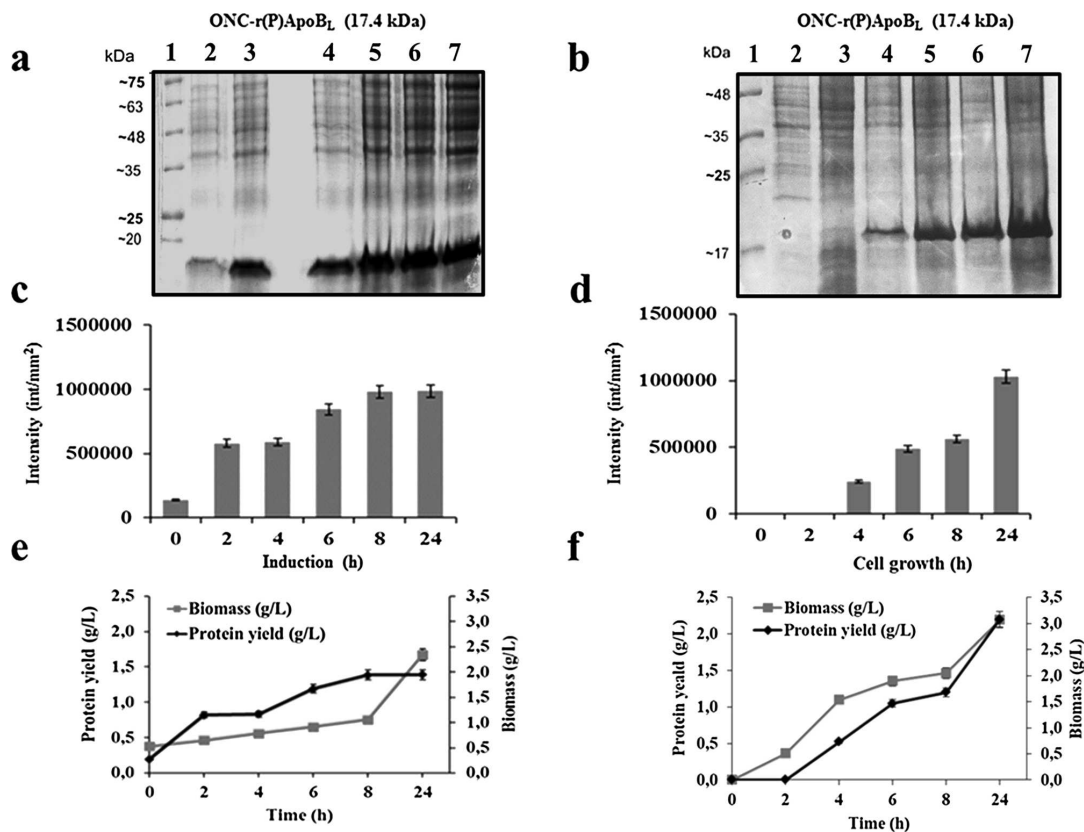


Fig. 2. Analysis by SDS-PAGE of total proteins extracted from bacterial cells transformed with pET recombinant plasmid encoding ONC-r(P)ApoB_L construct (a, b). Analyses are representative of fermentation processes carried out either in classical NAB (panels a, c, and e) or in iNAB (panels b, d, and f). Samples were collected at different time intervals along the fermentation process in batch reactor. In (a), protein standards (lane 1), non-induced cells (lane 2), and cells after 2 h induction (lane 3), 4 h induction (lane 4), 6 h induction (lane 5), 8 h induction (lane 6), and 24 h induction (lane 7). In (b), protein standards (lane 1), cells at time 0 (lane 2), and after 2 h growth (lane 3), 4 h growth (lane 4), 6 h growth (lane 5), 8 h growth (lane 6), and 24 h growth (lane 7). Molecular weight of expressed protein band was determined on the basis of calibration curves, prepared for each gel by plotting electrophoretic mobility (mm) of visible standard proteins as a function of known molecular weights. Densitometric analyses of protein bands with a molecular weight corresponding to that of ONC-r(P)ApoB_L construct (17.4 kDa) are reported as histograms (c, d). Chimeric construct expression levels (g/L) and biomass (cell dry weight, g/L) are reported as a function of time (h) in e and f.

use of IPTG, induction of protein expression is automatic and thus bacterial cell growth does not need to be monitored. Furthermore, to achieve sustained bacterial growth during the induction phase, glycerol is provided in auto-inducing media together with lactose [28,30]. NAB containing the above reported doses of glucose, glycerol and lactose has been termed auto-inducing NAB (iNAB).

To set up the auto-induction procedure, bacteria were transformed with pET recombinant plasmids, and grown in 50 mL of standard NAB containing 100 µg/mL ampicillin, at 37 °C overnight. Bacterial cultures were then used to inoculate 1 L of ampicillin containing iNAB. The culture was then incubated at 37 °C for 24 h, in order to allow automatic induction of chimeric protein expression. Following incubation, cells were harvested by centrifugation and lysed in order to analyze recombinant construct expression by 15% SDS-PAGE (Fig. 1a–c). Significantly higher expression levels were observed for all the constructs under test (Fig. 1a–c, and Table 2), which were found to be 1.5–2 times higher than those observed in NAB under IPTG induction (Table 2). However, it should be noted that saturation densities (OD_{600 nm} values at the end of the experiment) were significantly lower than those observed in the “classical” protocol (NAB with the addition of IPTG). This is in agreement with previous findings indicating that, in shake flask cultivations, lactose auto-induction generally occurs in the active

growth phase, with a possible consequent inactivation of bacterial cell growth [28,31].

Scale up of the production procedure

In order to scale up the production procedure, a fermentation process was set up using a 5 L fermenter. As before, the production procedure was optimized by using classical NAB and IPTG induction, and then the recombinant construct expression yields were compared with those obtained in iNAB, in order to set up a competitive and cost-effective process. Transformed bacterial cells were inoculated into 150 mL of standard NAB containing 100 µg/mL of ampicillin and 4 g/L glucose, and incubated at 37 °C overnight. Bacterial cultures were then diluted into 3 L (dilution 1:20 v/v) of NAB into a 5 L batch reactor. Since in stirred bioreactors a higher gas–liquid oxygen transfer is generally achieved than in shake flasks [31], oxygen was not expected to be a limiting factor. Oxygen saturation was maintained above 60% throughout the cultivation. Throughout the fermentation process, the stirring speed was kept constant at 300 rpm, with an air flow rate of 10 cm³/sec. To overcome drawbacks associated with ampicillin degradation, the antibiotic was added to bacterial cells at a rate of 100 mg/h using a fermenter peristaltic pump. In fact, a fundamental problem associated with the use

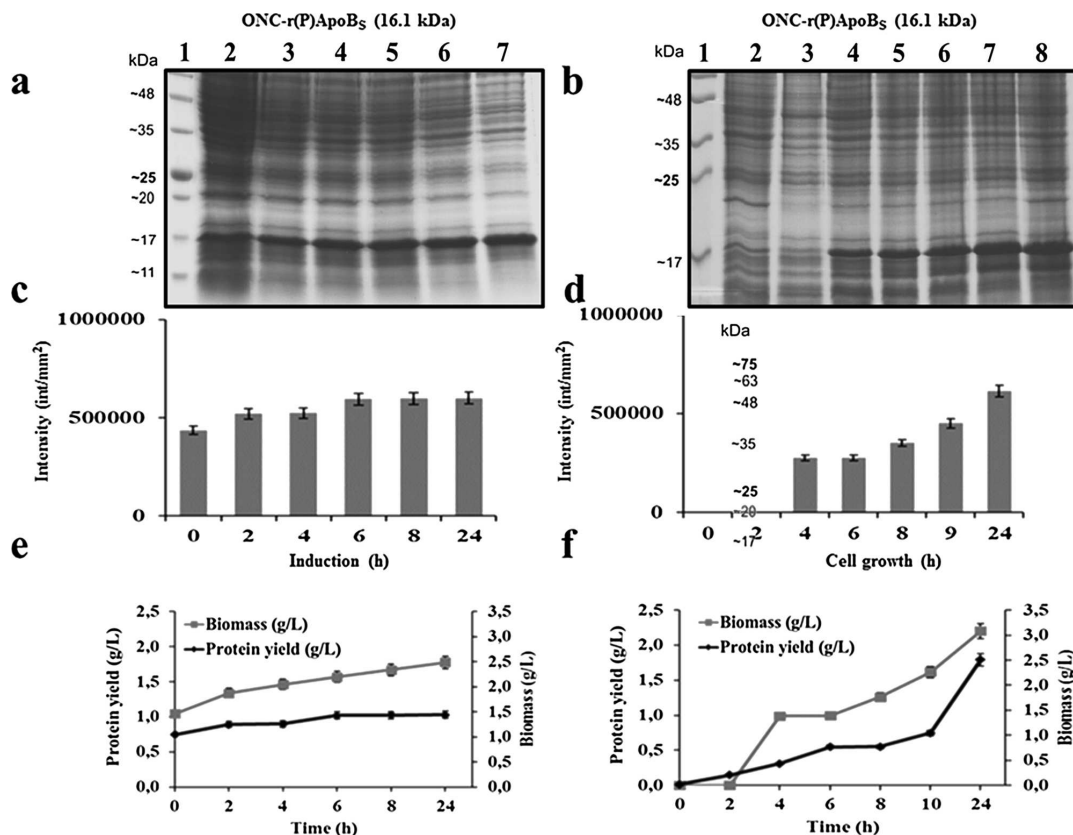


Fig. 3. Analysis by SDS-PAGE of total proteins extracted from bacterial cells transformed with pET recombinant plasmid encoding ONC-r(P)ApoB₅ construct (a, b). Analyses are representative of fermentation processes carried out either in classical NAB (panels a, c, and e) or in iNAB (panels b, d, and f). Samples were collected at different time intervals along the fermentation process in batch reactor. In a, protein standards (lane 1), non-induced cells (lane 2), after 2 h induction (lane 3), 4 h induction (lane 4), 6 h induction (lane 5), 8 h induction (lane 6) and 24 h induction (lane 7). In b, protein standards (lane 1), cells at time 0 (lane 2), after 2 h growth (lane 3), 4 h growth (lane 4), 6 h growth (lane 5), 8 h growth (lane 6), 9 h growth (lane 7) and 24 h growth (lane 8). Molecular weight of expressed protein band has been determined on the basis of calibration curves, prepared for each gel by plotting electrophoretic mobility (mm) of visible standard proteins as a function of known molecular weights. Densitometric analyses of protein bands with a molecular weight corresponding to that of ONC-r(P)ApoB₅ construct (16.1 kDa) are reported as histograms (c, d). Chimeric construct expression levels (g/L) and biomass (cell dry weight, g/L) are reported as a function of time (h) in e and f.

of ampicillin resistance as a selection mechanism is the rapid degradation of the antibiotic by the extracellular enzyme β -lactamase [32,33]. For the BL21(DE3) host strain containing the pET-type vectors, the half-life of 100 μ g/mL ampicillin is reported to be 30 min for mid-log phase cells grown in a fermenter [34]. By regularly adding ampicillin, it was possible to prevent plasmid loss, with consequent improvement of expression yields. The fermentation process was carried out at 37 °C up to OD_{600 nm} of about 4. At this stage, expression of recombinant constructs was induced by addition of 0.7 mM IPTG. Fermentation was carried out for 24 h. At the end of the fermentation process, cells were collected by using a peristaltic pump, harvested by centrifugation, and lysed in order to analyze recombinant constructs expression by 15% SDS-PAGE (Figs. 2–4). In all cases, expression of recombinant chimeric constructs began at about 2–4 h after IPTG addition, reaching a maximum at 8 h (Figs. 2–4a,c,e), and expression levels were found to be significantly higher than those observed in shake flask cultures carried out in NAB upon IPTG induction (Fig. 1 and Table 2). Instead, saturation densities (OD_{600 nm} values at the end of fermentation process) were similar to those obtained in shake flask cultures (Table 2). Biomass was monitored on the basis of cell dry weight and represented as a curve (Figs. 2–4e), which was similar to that representing the yield (g/L) of recombinant chimeric constructs (Figs. 2–4e).

Once the validity of the experimental strategy on a larger scale was verified, it was applied to the auto-induction procedure, in order to develop a cost-effective production process suitable for industrial purposes. The same experimental procedure described above was performed with the exception that *E. coli* BL21(DE3) cells, once transformed with recombinant pET-22b(+) expression vectors, were incubated overnight at 37 °C in 150 mL of NAB supplemented with ampicillin (0.1 mg/mL), but lacking glucose, glycerol and lactose. Following incubation, cell cultures were diluted 1:20 (v/v) in 3 L of iNAB into a 5 L batch reactor. Experimental conditions identical to those described above were applied, with the exception of IPTG addition, since recombinant expression of chimeric constructs was automatically induced by lactose present in the medium. At defined time intervals, bacterial aliquots (corresponding to 0.125 OD_{600 nm}) were withdrawn and lysed to determine recombinant constructs expression levels by 15% SDS-PAGE (Figs. 2–4b,d,f). Recombinant expression of chimeric constructs was found to begin at 2–4 h, indicating that, at this time, glucose probably decreased and lactose began to be metabolized, with a consequent inducing effect. In these experimental conditions, expression levels were found to reach a maximum at 24 h. In all cases, recombinant construct expression levels were significantly higher than those obtained either under the same experimental conditions using

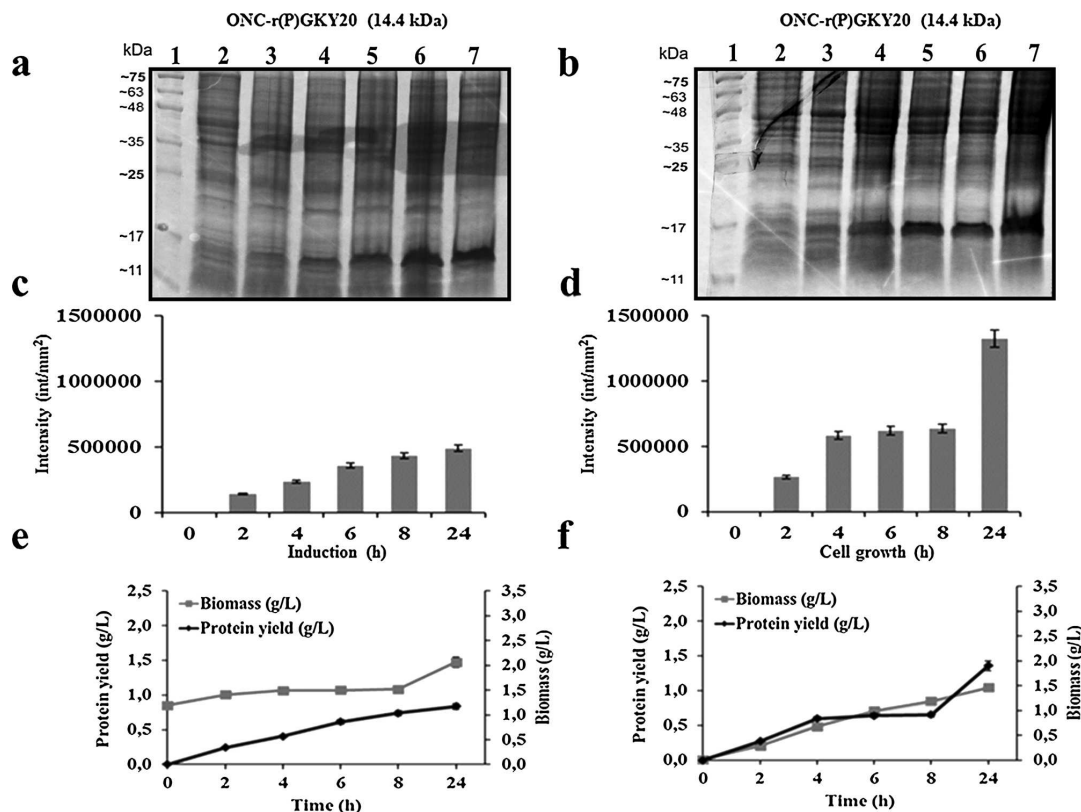


Fig. 4. Analysis by SDS-PAGE of total proteins extracted from bacterial cells transformed with pET recombinant plasmid encoding ONC-r(P)GKY20 construct (a, b). Analyses are representative of fermentation processes carried out either in classical NA medium (panels a, c, and e) or in iNAB (panels b, d, and f). Samples were collected at different time intervals along the fermentation process in batch reactor. In a, protein standards (lane 1), non-induced cells (lane 2), after 2 h induction (lane 3), 4 h induction (lane 4), 6 h induction (lane 5), 8 h induction (lane 6), and 24 h induction (lane 7). In b, protein standards (lane 1), cells at time 0 (lane 2), after 2 h growth (lane 3), 4 h growth (lane 4), 6 h growth (lane 5), 8 h growth (lane 6) and 24 h growth (lane 7). Molecular weight of expressed protein band has been determined on the basis of calibration curves, prepared for each gel by plotting electrophoretic mobility (mm) of visible standard proteins as a function of known molecular weights. Densitometric analyses of protein bands with a molecular weight corresponding to that of ONC-r(P)GKY20 construct (14.4 kDa) are reported as histograms (c, d). Chimeric construct expression levels (g/L) and biomass (cell dry weight, g/L) are reported as a function of time (h) in e and f.

classical NAB (Figs. 2–4 and Table 2) or in shake flask cultures by using iNAB (Table 2). Similar results were also obtained by analyzing saturation densities ($\text{OD}_{600 \text{ nm}}$ values at the end of fermentation process), which were higher than those obtained under the same experimental conditions using classical NAB under IPTG induction for all the constructs, with the exception of ONC-r(P)GKY20. In the last case, biomass growth in batch reactor was found to be similar in both experimental conditions (Table 2).

It can be highlighted that the set up procedure is of general validity and may be applied to any recombinant soluble protein expressed in *E. coli*. To demonstrate this, the auto-induction protocol was applied to the production of recombinant Apolipoprotein A-I (ApoA-I). Soluble ApoA-I expression levels were significantly higher in iNAB than in classical NZY medium upon IPTG induction in shake flasks (Supplementary Fig. S6), in agreement with data showing ApoA-I instability in bacterial expression systems [35].

Estimation of HDP production costs from laboratory to larger scale

The procedure to isolate pure recombinant HDPs has been described previously [12,14,15]. Briefly, upon recovery from inclusion bodies, the chimeric protein was purified by nickel affinity chromatography

(Fig. 5). The peptide was then released from the carrier onconase by hydrolysis in acidic conditions. Since the carrier is insoluble at neutral or alkaline pH, the peptide is isolated from insoluble components by repeated cycles of centrifugation, and finally lyophilized. By applying this procedure to fermentation process carried out in iNAB, peptide purity was 99% with a yield of about 40–50 mg/L. A final gel-filtration step was added, in order to remove salts used along the purification process and that tend to attach to the peptides [36]. This step is responsible for the loss of a significant amount of peptide (~50%), with a consequent final yield of about 20–25 mg of pure peptide per L of bacterial culture.

Fig. 6 reports the breakdown of peptide unit cost (€/mg) as a function of the production scale expressed as mg/batch, in the case of the fermentation process performed in iNAB. It can be seen that, at a small production scale (5 L fermenter), the cost is about 250 €/mg and is mainly determined by the labour cost and by the capital investment due to main equipment costs and additional fixed costs required to maintain equipment. When the production scale is increased up to 200, 500 and 1000 mg/batch, the unit cost decreases sharply to 136, 65 and 42 €/mg, respectively. In the last case (1000 mg/batch), labour and chemical costs become the only relevant factors, which is typical of a production scale [24]. In order to identify possible process bottlenecks,

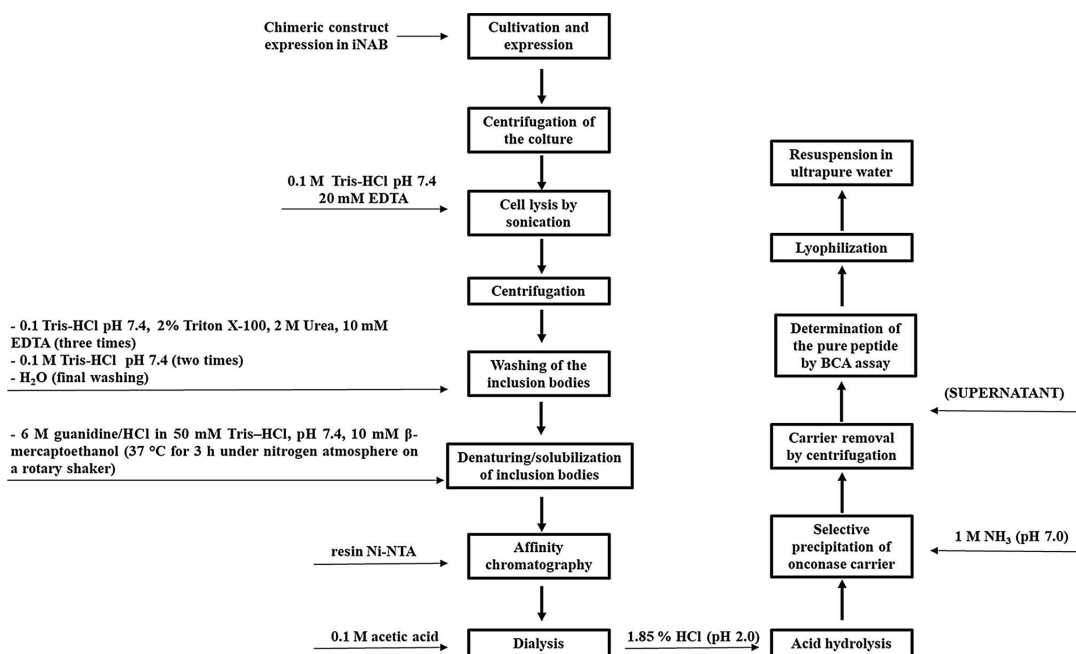


Fig. 5. Block flow diagram representing the production and purification process of recombinant HDPs.

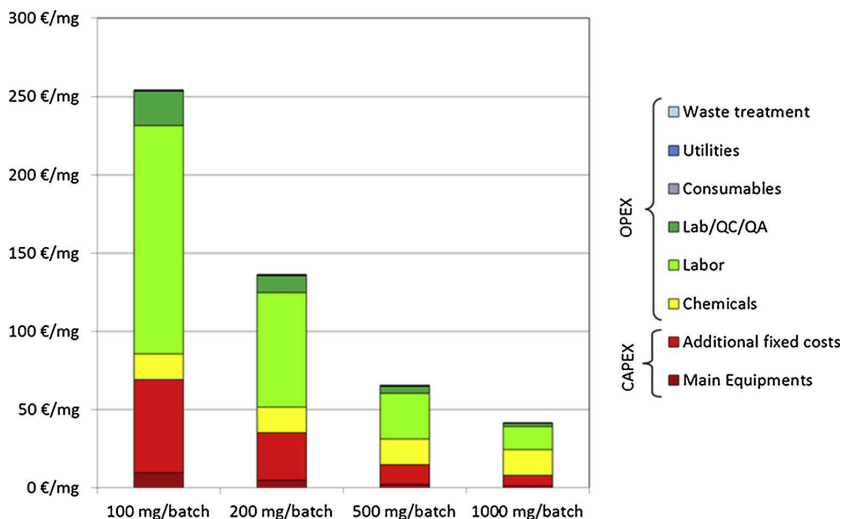


Fig. 6. Breakdown of peptide unit production cost as a function of production scale.

costs have also been analyzed by considering the contribution of each step in the process (fermentation, extraction and purification) (Fig. 7). More than the half of the costs derive from the final purification step and this contribution increases with increasing production scale. The labour costs, in contrast, decrease by increasing production scale. However, at 1 g/batch scale, labour still accounts for 1/3 rd of the whole unit production cost, and the purification process still accounts for more than the half. To further reduce the unit cost, it would be advisable to shorten the schedule and the total time of the procedures associated with the purification step or to automate them. Indeed, a reduction of 50% of the whole labour task in the purification step could

lead to a further decrease of the unit cost to 35 €/mg. The demand for chemicals, required to solubilise inclusion bodies and to perform expanded bed chromatography, strongly affects the overall large scale process costs. Indeed, chemicals demand is responsible for up to 1/3 rd of the unit cost at a production scale of 1 g/batch. In particular, the requirement for guanidine accounts for more than 80% of the chemical costs and, consequently, is responsible for more than 25% of the whole peptide unit cost. Hence, alternative methods to solubilize inclusion bodies should be tested in the future. It can also be highlighted that determined unit costs appear really competitive when considering the cost of chemical synthesis (Table 3). Indeed, those reported in Table 3

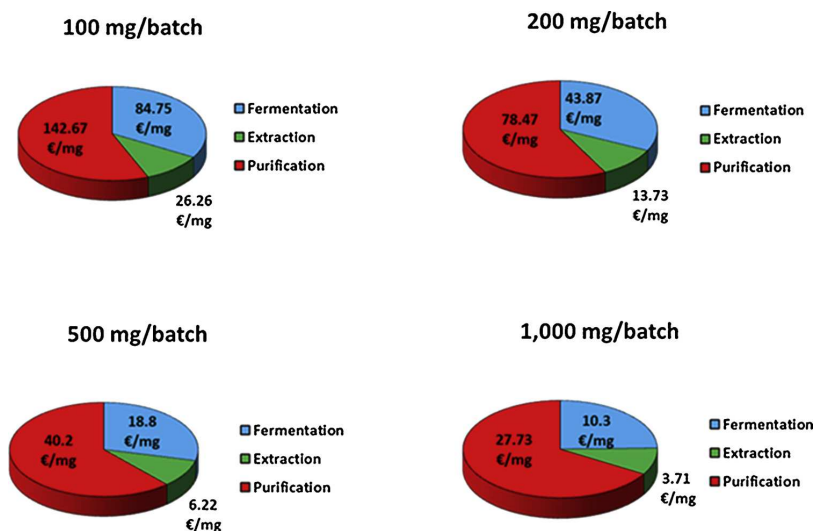


Fig. 7. Impact of production process steps (fermentation, extraction and purification) on peptide unit production costs.

Table 3

Quotations for peptide synthesis obtained from three companies. Company identities not disclosed.

Peptide	Purity	Sequence	Price company 1	Price company 2	Price company 3
r(P)ApoB ₁	> 95%	PHVALKPGKGLKFIIPSPKRPVKLLSGGNTLHLVSTTKT	€ 304 1 mg	€ 171 1 mg	€ 520 1 mg
r(P)ApoB ₂	> 95%	PHVALKPGKGLKFIIPSPKRPVKLLSG	€ 188 1 mg	€ 117 1 mg	€ 410 1 mg
r(P)GKY20	> 95%	PGKYGFYTHVRLKKWQIKVI	€ 152 1 mg	€ 84 1 mg	€ 260 1 mg

do not take into account trifluoroacetate (TF-acetate) exchange by another counter-ion, a step often required for synthetic cationic peptides, which are mainly obtained as TF-acetate salts [35]. Since TF-acetate strongly affects *in vitro* and *in vivo* studies [37–39], its removal is often necessary, with a consequent increase of chemical synthesis costs of about € 200. This provides a further key element attesting the competitiveness of the production procedure developed here.

Discussion

The past three decades have seen a rise in regulatory approval and sales of protein- and peptide-based therapeutics. To explore the pharmaceutical and therapeutic potential of HDPs, a cost-effective and scalable method to produce active and effective peptides is still required. Here, we set up a cost-effective procedure to produce high amounts of HDPs by developing a novel growth medium, NAB, comprising cheap, readily available components and defined amounts of each one. Among culture media, Luria-Bertani (LB) broth is the most commonly used for culturing *E. coli*, being rich in nutrients and with an optimal osmolarity for *E. coli* growth at early log phase. However, it is generally responsible for a cessation of bacterial cell growth at relatively low densities, mainly due to the presence of scarce amounts of carbohydrates and divalent cations [41]. Not surprisingly, when the amount of peptone or yeast extract is increased, higher cell densities are reached [28]. Similarly, divalent cation supplementation results in higher cell growth [28]. Glucose supplementation is of limited help because acid generation by glucose metabolism overwhelms the limited buffer capacity of LB [42,43]. If culture acidification poses a problem, the media can be buffered with phosphate salts. Indeed, this is the case of 2xYT, TB (Terrific Broth) and SB (Super Broth) media, which have been shown to be superior to LB to reach higher cell densities [28,44].

NAB, when applied to the production of the recombinant host

defence peptides under test, was found to support significantly higher cell densities and recombinant expression levels than conventional culture media. The production procedure was also efficiently scaled up and procedure costs significantly lowered by developing a successful auto-induction strategy. By this means, recombinant constructs expression was found to be mediated by a common and cheap sugar, such as lactose, instead of IPTG. Indeed, even if IPTG is generally required at submillimolar concentrations, its use might result in high cost accumulation for industrial purposes. IPTG substitution was also found to have further advantages, since this compound is not innocuous for bacterial cells [45,46]. Moreover, the auto-induction procedure was found to support significantly higher yields of target constructs than conventional strategies based on expression induction mediated by IPTG. When the procedure was scaled up by using a 5 L fermenter, expression levels of recombinant constructs (about 2–3 g/L) were found to be significantly higher than those obtained in shake flask cultures (about 1–2 g/L). A further main advantage of this procedure is the possibility of isolating the peptide of interest from its carrier protein by acidic conditions because of the presence of a dipeptide Asp-Pro between the peptide and the onconase moieties. This allows avoidance of the use of specific proteases [47], which would have made the production process too expensive and not suitable for industrial purposes. Moreover, the set up procedure is of general validity for application to recombinant soluble proteins expressed in *E. coli*, as demonstrated by applying the auto-induction protocol to the production of recombinant soluble Apo A-I.

Since the protocol to purify HDPs was previously optimized and found to provide high yields of pure peptides through a simple purification procedure (Fig. 5) [12,14,15], it is tempting to speculate that this optimized procedure might be successfully scaled up at an industrial scale. Thus, we estimated that by increasing the production scale to 200, 500 and 1000 mg/batch, unit costs fall to 136, 65 and 42

€/mg, respectively. These values appear highly competitive when considering chemical synthesis costs of the same peptides (Table 3). Indeed, they also appear competitive against the costs of a different linear helical peptide containing 37 amino acid residues, i.e. LL-37 human multifunctional cathelicidin-type host defence peptide endowed with antibacterial, antiviral, and immunomodulatory activities. Indeed, the cost of synthetic human LL-37 peptide is about 400 €/mg, whereas that of the recombinant protein precursor is about 1400 \$/mg. Altogether, these findings indicate that the herein set up production strategy appears competitive.

Conflict of interest

The authors declare that they have no conflict of interest.

Acknowledgements

This study was partially supported by the Italian Cystic Fibrosis Foundation (grant number 20/2014). We are deeply indebted to volunteers who devote many efforts in fundraising, in particular delegations from Palermo and Ragusa Vittoria Catania 2.

Appendix A. Supplementary data


Supplementary material related to this article can be found, in the online version, at doi:<https://doi.org/10.1016/j.nbt.2019.02.004>.

References

- Hancock REW, Haney EF, Gill EE. The immunology of host defence peptides: beyond antimicrobial activity. *Nat Rev Immunol* 2016;16:321–34.
- Andersson L, Blomberg L, Flegel M, Lepsa L, Nilsson B, Verlander M. Large-scale synthesis of peptides. *Biopolymers* 2000;55:227–50.
- Alvarez-Sieiro P, Montalbán-López M, Mu D, Kuipers OP. Bacteriocins of lactic acid bacteria: extending the family. *Appl Microbiol Biotechnol* 2016;100:2939–51.
- Ongey EL, Neubauer P. Lanthipeptides: chemical synthesis versus in vivo biosynthesis as tools for pharmaceutical production. *Microb Cell Fact* 2016;15:97.
- Ingham AB, Moore RJ. Recombinant production of antimicrobial peptides in heterologous microbial systems. *Biotechnol Appl Biochem* 2007;47:1–9.
- Li Y, Chen Z. RAPD: a database of recombinantly-produced antimicrobial Peptides. *FEMS Microbiol Lett* 2008;289:126–9.
- Li Y. Carrier proteins for fusion expression of antimicrobial peptides in *Escherichia coli*. *Biotechnol Appl Biochem* 2009;54:1–9.
- Li Y. Recombinant production of antimicrobial peptides in *Escherichia coli*: a review. *Protein Expr Purif* 2011;80:260–7.
- Di Gaetano S, Guglielmi F, Arciello A, Mangione P, Monti M, Pagnozzi D, et al. Recombinant amyloidogenic domain of ApoA-I: analysis of its fibrillogenic potential. *Biochim Biophys Res Commun* 2006;351:223–8.
- Guglielmi F, Monti DM, Arciello A, Torrassa S, Cozzolino F, Pucci P, et al. Enzymatically active fibrils generated by the self-assembly of the ApoA-I fibrillogenic domain functionalized with a catalytic moiety. *Biomaterials* 2009;30:829–35.
- Vassilevski AA, Kozlov SA, Grishin EV. Antimicrobial peptide precursor structures suggest effective production strategies. *Recent Pat Inflamm Allergy Drug Discov* 2008;2:58–63.
- Pane K, Durante L, Pizzo E, Varcamonti M, Zanfardino A, Sgambati V, et al. Rational design of a carrier protein for the production of recombinant toxic peptides in *Escherichia coli*. *PLoS One* 2016;11:e0146552.
- Notomista E, Cafaro V, Fusiello R, Bracale A, D'Alessio G, Di Donato A. Effective expression and purification of recombinant onconase, an antitumor protein. *FEBS Lett* 1999;463:211–5.
- Pane K, Sgambati V, Zanfardino A, Smaldone G, Cafaro V, Angrisano T, et al. A new cryptic cationic antimicrobial peptide from human apolipoprotein E with antibacterial activity and immunomodulatory effects on human cells. *FEBS J* 2016;283:2115–31.
- Gaglione R, Dell'Olimo E, Bosso A, Chino M, Pane K, Ascione F, et al. Novel human bioactive peptides identified in apolipoprotein B: evaluation of their therapeutic potential. *Biochem Pharmacol* 2017;130:34–50.
- Papareddy P, Rydengård V, Pasupuleti M, Walse B, Mörgelin M, Chalupka A, et al. Proteolysis of human thrombin generates novel host defense peptides. *PLoS Pathog* 2010;6:e1000857.
- Pane K, Durante L, Crescenzi O, Cafaro V, Pizzo E, Varcamonti M, et al. Antimicrobial potency of cationic antimicrobial peptides can be predicted from their amino acid composition: application to the detection of "cryptic" antimicrobial peptides. *J Theor Biol* 2017;419:254–65.
- Green MR, Hughes H, Sambrook J, MacCallum P. *Molecular cloning: a laboratory manual*. 4th edn. New York: Cold Spring Harbor Laboratory Press; 2012. p. 1890.
- Petrova J, Duong T, Cochran MC, Axelsson A, Mörgelin M, Roberts LM, et al. The fibrillogenic L178H variant of apolipoprotein A-I forms helical fibrils. *J Lipid Res* 2012;53:390–8.
- Del Giudice R, Arciello A, Itri F, Merlino A, Monti M, Buonanno M, et al. Protein conformational perturbations in hereditary amyloidosis: differential impact of single point mutations in ApoA1 amyloidogenic variants. *Biochim Biophys Acta* 2016;1860:434–44.
- Gaglione R, Smaldone G, Di Girolamo R, Piccoli R, Pedone E, Arciello A. Cell milieu significantly affects the fate of ApoA1 amyloidogenic variants: predestination or serendipity? *Biochim Biophys Acta* 2017;1862:377–84.
- Kalk JP, Langlykke AF. Cost estimation for biotechnology projects. In: Demain AL, Solomon NA, editors. *Manual of industrial microbiology and biotechnology*. Washington, DC: American Society for Microbiology; 1986. p. 363–85.
- Heinzel E, Biver A, Cooney C. *Development of sustainable bioprocesses*. West Sussex, England: John Wiley & Sons; 2006. p. 316.
- Huang CJ, Lin H, Yang X. Industrial production of recombinant therapeutics in *Escherichia coli* and its recent advancements. *J Ind Microbiol Biotechnol* 2012;39:383–99.
- Banerjee S, Paul S, Nguyen LT, Chu BC, Vogel HJ, FecB, a periplasmic ferric-citrate transporter from *E. coli*, can bind different forms of ferric-citrate as well as a wide variety of metal-free and metal-loaded tricarboxylic acids. *Metallomics* 2016;8:125–33.
- Krause M, Ukkonen K, Haataja T, Ruottinen M, Glumoff T, Neubauer A, et al. A novel fed-batch based cultivation method provides high cell-density and improves yield of soluble recombinant proteins in shaken cultures. *Microb Cell Fact* 2010;9:11.
- Studier FW. Protein production by auto-induction in high density shaking cultures. *Protein Expr Purif* 2005;41:207–34.
- Mostovenko E, Deelder AM, Palmblad M. Protein expression dynamics during *Escherichia coli* glucose-lactose diauxia. *BMC Microbiol* 2011;11:126.
- Blommel PG, Becker KJ, Duvnjak P, Fox BG. Enhanced bacterial protein expression during auto-induction obtained by alteration of lac repressor dosage and medium composition. *Biotechnol Prog* 2007;23:585–98.
- Mayer S, Junne S, Ukkonen K, Glazyrina J, Glauche F, Neubauer P, et al. Lactose autoinduction with enzymatic glucose release: characterization of the cultivation system in bioreactor. *Protein Expr Purif* 2014;94:67–72.
- Neubauer P, Hofmann K, Holst O, Mattiasson B, Kruschke P. Maximizing the expression of a recombinant gene in *Escherichia coli* by manipulation of induction time using lactose as inducer. *Appl Microbiol Biotechnol* 1992;36:739–44.
- Jung G, Denéfle P, Bequart J, Mayaux JF. High-cell density fermentation studies of recombinant *Escherichia coli* strains expressing human interleukin-1 beta. *Ann Inst Pasteur Microbiol* 1988;139:129–46.
- Hoffman BJ, Broadwater JA, Johnson P, Harper J, Fox BG, Kenealy WR. Lactose fed-batch overexpression of recombinant metalloproteins in *Escherichia coli* BL21 (DE3): process control yielding high levels of metal-incorporated, soluble protein. *Protein Expr Purif* 1995;6:646–54.
- Ryan RO, Forte TM, Oda MN. Optimized bacterial expression of human apolipoprotein A-I. *Protein Expr Purif* 2003;27:98–103.
- Bommarius B, Jessen H, Elliott M, Kindrachuk J, Pasupuleti M, Gieren H, et al. Cost-effective expression and purification of antimicrobial and host defense peptides in *Escherichia coli*. *Peptides* 2010;31:1957–65.
- Roux S, Zekri E, Rousseau B, Paternostre M, Cintrat JC, Nicolas F. Elimination and exchange of trifluoroacetate counter-ion from cationic peptides: a critical evaluation of different approaches. *J Pept Sci* 2008;14:354–9.
- Pini A, Luzzi L, Bernini A, Brunetti J, Falciani C, Scali S, et al. Efficacy and toxicity of the antimicrobial peptide M33 produced with different counter-ions. *Amino Acids* 2012;43:467–73.
- Andrushchenko VV, Vogel HJ, Prenner EJ. Optimization of the hydrochloric acid concentration used for trifluoroacetate removal from synthetic peptides. *J Pept Sci* 2007;13:37–43.
- Sezonov G, Joseleau-Petit D, D'Ari R. *Escherichia coli* physiology in Luria-Bertani broth. *J Bacteriol* 2007;189:8746–9.
- Weuster-Botz D, Altenbach-Rehm J, Arnold M. Parallel substrate feeding and pH-control in shaking-flasks. *Biochem Eng J* 2001;7:163–70.
- Scheidle M, Dittrich B, Klinger J, Ikeda H, Klee D, Büchs J. Controlling pH in shake flasks using polymer-based controlled-release discs with pre-determined release kinetics. *BMC Biotechnol* 2011;11:25.
- Madurawe RD, Chase TE, Tsao EI, Bentley WE. A recombinant lipoprotein antigen against Lyme disease expressed in *E. coli*: fermentor operating strategies for improved yield. *Biotechnol Prog* 2000;16:571–6.
- Andrews KJ, Hegeman GD. Selective disadvantage of non-functional protein synthesis in *Escherichia coli*. *J Mol Evol* 1976;8:317–28.
- Malakar P, Venkatesh KV. Effect of substrate and IPTG concentrations on the burden to growth of *Escherichia coli* on glycerol due to the expression of Lac proteins. *Appl Microbiol Biotechnol* 2012;93:2543–9.
- Zhou QF, Luo XG, Ye L, Xi T. High-level production of a novel antimicrobial peptide peritrem in *Escherichia coli* by fusion expression. *Curr Microbiol* 2007;54:366–70.

SPECIAL ISSUE ARTICLE

Human apolipoprotein E as a reservoir of cryptic bioactive peptides: The case of ApoE 133-167

Anna Zanfardino¹ | Andrea Bosso¹ | Giovanni Gallo¹ | Valeria Pistorio² |
Michela Di Napoli¹ | Rosa Gaglione³ | Eliana Dell'Olmo³ | Mario Varcamonti¹ |
Eugenio Notomista¹ | Angela Arciello^{3,4} | Elio Pizzo¹ 

¹ Department of Biology, University of Naples Federico II, 80126 Naples, Italy

² Department of Molecular Medicine and Medical Biotechnologies, University of Naples Federico II, Naples, Italy

³ Department of Chemical Sciences, University of Naples Federico II, 80126 Naples, Italy

⁴ INBB—Istituto Nazionale Biostrutture e Biosistemi, Rome, Italy

Correspondence

Elio Pizzo, Department of Biology, University of Naples Federico II, 80126 Naples, Italy.
Email: elipizzo@unina.it

Funding information

Italian Cystic Fibrosis Foundation, Grant/Award Number: 16/2017

Bioactive peptides derived from the receptor-binding region of human apolipoprotein E have previously been reported. All these peptides, encompassing fragments of this region or designed on the basis of short repeated cationic sequences identified in the same region, show toxic activities against a broad spectrum of bacteria and interesting immunomodulatory effects. However, the ability of these molecules to exert antibiofilm properties has not been described so far. In the present work, we report the characterization of a novel peptide, corresponding to residues 133 to 167 of human apolipoprotein E, here named ApoE (133-167). This peptide, besides presenting interesting properties comparable with those reported for other ApoE-derived peptides, such as a direct killing activity against a broad spectrum of bacteria or the ability to downregulate lipopolysaccharide-induced cytokine release, is also endowed with significant antibiofilm properties. Indeed, the peptide is able to strongly affect the formation of the extracellular matrix and also the viability of encapsulated bacteria. Noteworthy, ApoE (133-167) is not toxic toward human and murine cell lines and is able to assume ordered conformations in the presence of membrane mimicking agents. Taken together, collected evidences about biological and structural properties of ApoE (133-167) open new perspectives in the design of therapeutic agents based on human-derived bioactive peptides.

KEYWORDS

antimicrobial peptides, apolipoprotein E, bacterial biofilm, inflammation, lipopolysaccharide

1 | INTRODUCTION

Human apolipoprotein E (ApoE) is a circulating glycoprotein with a molecular mass of ~34 kDa; it is mainly involved in the clearance of cholesterol and other lipids from the blood circulation via binding to cell surface ApoE receptors.¹ In humans, there are 3 common isoforms, with different affinities for LDL receptor,^{2,3} produced by hepatocytes, macrophages, and adipocytes in the peripheral tissues and in astrocytes, microglia, and vascular mural cells in central nervous system.⁴ Plasma ApoE is preferentially associated to very low density lipoprotein particles, whereas it is found in high-density lipoprotein-like particles in the CNS.^{5,6} Brain ApoE is primarily derived from de

novo synthesis because the blood-brain barrier limits ApoE transport into and out of the brain.⁷ Apolipoprotein E consists of 2 main structural domains connected by a hinge region.⁸ The N-terminal domain (residues 1-167) consists of a 4 alpha helix bundle containing the receptor binding region (residues 130-162), whereas the C-terminal domain (residues 206-299) consists of 3 alpha helices and represents the major lipid/lipoprotein binding region. Upon binding to lipids, ApoE undergoes a major conformational change and forms a molecular envelope around the surface of the phospholipid outer shell of a nascent lipoprotein particle.⁹ Apolipoprotein E receptor-binding region retains the biological activities of the whole protein, as for instance COG-133 that shows pharmacological properties, such as

antiinflammatory and neuroprotective activities.^{10,11} Other reports, focused on monomeric and dimeric synthetic peptides encompassing ApoE amino acids 130 to 169, revealed the importance of α -helical conformations and of positively charged amino acids.¹² Several recent reports are focused on the study of ApoE-derived peptide antimicrobial and immunomodulatory properties.^{13–15} They have been identified in the receptor binding region, or they have been obtained by combining clusters of residues identified in the same region. For most of these peptides, the antimicrobial and immunomodulatory properties have been analyzed. Interestingly, the most active antimicrobial peptides were found to partially or almost completely cover the receptor binding region (residues 130–162), thus revealing that amino acidic composition could be determinant for their effective interaction with bacterial membrane.^{16,17} Recently, our research group has developed a bioinformatics method that identifies antimicrobial peptides within the sequences of larger protein precursors and quantitatively predicts their antibacterial activity.¹⁸ The method assigns an antimicrobial score to peptides based on their net charge, hydrophobicity and length, and 2 bacterial strain-dependent weight factors.¹⁸ By means of this method, we have already reported the characterization of novel human peptides^{19,20} including an exhaustive structural and functional study of a cryptic peptide identified in human ApoE (residues 133–150).¹⁵ We deeply characterized the ability of ApoE (133–150) to assume stable conformations in the presence of membrane mimicking agents and LPS as well as its antibacterial and immunomodulatory properties.¹⁵ Very interestingly, the antimicrobial score plot derived by the *in silico* analysis of ApoE (Figure S1) showed that, in addition to the local maximum corresponding to region 133 to 150, a further maximum was present (indicated by the black arrow on the right in Figure S1). This maximum, corresponding to region 133 to 167, has a score of 12.3, ie, only slightly higher than the score of region 133 to 150 (11.8). Based on these considerations, we hypothesized that ApoE (133–167) could possess antimicrobial properties comparable with those reported for other ApoE-derived peptides and that, at the same time, it could exert additional activities related to its length (35 residues) and amino acidic composition, the latter virtually able to drive the peptide to acquire a larger helical conformation. Accordingly, the aim of this study was to analyze ApoE (133–167) antimicrobial activity on planktonic and sessile bacteria, its effects on eukaryotic cells, its conformation in the presence of membrane mimicking agents, and its antiinflammatory properties.

2 | MATERIALS AND METHODS

2.1 | Bacterial strains and growth conditions

Bacterial strains used in this study were *Escherichia coli* ATCC 25922, *E. coli* DH5 α , *Bacillus subtilis* PY79, *Bacillus globigii* TNO BMO13, *Pseudomonas aeruginosa* PAO1 wild type, *P. aeruginosa* KK27 (cystic fibrosis clinical isolate kindly provided by Dr Alessandra Bragonzi), *P. aeruginosa* ATCC 27853, methicillin-resistant *Staphylococcus aureus* WK22 (MRSA WK22), *S. aureus* ATCC 6538P, *S. aureus* ATCC 29213, and *Salmonella enteritidis* 706 RIVM. All bacterial strains were grown in Mueller Hinton Broth (MHB, Becton Dickinson Difco,

Franklin Lakes, NJ) and on tryptic soy agar (Oxoid Ltd., Hampshire, UK). In all the experiments, bacteria were inoculated and grown overnight in MHB at 37°C and then transferred to a fresh MHB tube and grown to midlogarithmic phase.

2.2 | Eukaryotic cell lines

THP-1 cells, a pro-monocytic cell line, were cultured in RPMI 1640 (Sigma Aldrich, Milan, Italy), supplemented with 10% fetal bovine serum (HyClone, GE Healthcare Lifescience, Chicago, IL), 10-mM Hepes, 0.1-mM MEM nonessential amino acids, 1-mM sodium pyruvate, and 1% penicillin/streptomycin (Sigma Aldrich, Milan, Italy), in a 5% CO₂ humidified atmosphere at 37°C. THP-1 cells were differentiated with phorbol 12-myristate 13-acetate (Sigma-Aldrich, Milan, Italy) at a concentration of 10 ng/mL in RPMI 1640 supplemented with 1% fetal bovine serum (HyClone, GE Healthcare Lifescience, Chicago, IL). HaCat, HeLa, HEK-293, CaCo-2, and RAW 264.7 cells were from ATCC, Manassas, VA. Cells were cultured in Dulbecco's modified Eagle's medium (Sigma Aldrich, Milan, Italy), supplemented with 10% fetal bovine serum (HyClone, GE Healthcare Lifescience, Chicago, IL) and antibiotics, in a 5% CO₂ humidified atmosphere at 37°C.

2.3 | Antimicrobial activity assays

The antimicrobial activity of ApoE-derived peptides against planktonic bacteria was evaluated by broth microdilution method, performed as previously described for antimicrobial peptides²¹ with minor modifications. Briefly, a single colony of each strain was resuspended in 5 mL of TY medium (Difco, Detroit, MI) and incubated overnight at 37°C. When the culture reached OD_{600nm} of 1 unit, it was diluted 1:100 (vol/vol) in 2-mM phosphate buffered saline (PBS) pH 7.0. Then, to test the effects of peptides on bacterial viability, samples (500 μ L final volume) were prepared by diluting bacterial cells (20 μ L) in growth medium containing the molecules under test at the desired concentration. The samples were then incubated at 37°C under stirring at 150 rpm for 4 hours. Subsequently, serial dilutions of all the samples were plated on TY-agar and incubated overnight at 37°C. The percentage of viable cells was finally evaluated by colony counting.²² All the experiments were carried out in triplicate. To determine the minimal inhibitory concentration values, assays were performed as previously described elsewhere.^{19,20} Briefly, bacteria were grown to midlogarithmic phase at 37°C and then diluted to 1×10^6 CFU/mL in Difco 0.5 \times Nutrient Broth (Becton-Dickenson, Franklin Lakes, NJ) containing increasing amounts of ApoE (133–167) or ApoE (133–150; 0–40 μ M). Starting from a peptide stock solution, 2-fold serial dilutions were sequentially carried out, accordingly to broth microdilution method.²³ Following overnight incubation, MIC₁₀₀ values were determined as the lowest peptide concentration responsible for no visible bacterial growth.

2.4 | ATP leakage measurements

MRSA WKZ-2 and *E. coli* ATCC 25922 were grown to midlogarithmic phase in MHB at 37°C. Bacteria were then centrifuged and diluted to 2×10^7 CFU/mL in MHB medium diluted 1:100 (vol/vol) in PBS at pH 7.0. In the case of each diluted sample, 60 μ L of bacterial

suspension was incubated with 60 μ L of peptide solution (0.5 or 2 μ M for ApoE-derived peptides, 0.5 μ M for positive control PMAP-36 peptide²¹) for 20 minutes at 37°C. The samples were then centrifuged, and the supernatant was stored at 4°C until further use. The bacterial pellet was suspended in lysis buffer (Roche Diagnostics Nederland B.V., Almere, the Netherlands) and further incubated at 100°C following the manufacturer instructions. Cell lysates were then centrifuged, and supernatants were kept on ice. Subsequently, both intracellular and extracellular ATP levels were determined by using the Roche ATP bioluminescence kit HS II, according to the manufacturer's instructions (Roche Diagnostics Nederland B.V., Almere, the Netherlands).

2.5 | Cytotoxicity on mammalian cells

Toxicity toward undifferentiated and differentiated THP-1, HaCat, HeLa, HEK-293, CaCo-2, and RAW 264.7 cells was assessed by performing the 3-(4,5-dimethylthiazol-2-yl)-2,5 diphenyltetrazolium bromide (MTT) reduction inhibition assay.²⁴ Cytotoxicity experiments were performed at least 4 times independently. In all the cases, cells were grown for 24 hours in the absence or in the presence of increasing concentrations of the peptide under test. Cell survival values are expressed as percentage of viable cells with respect to control untreated samples.

2.6 | Hemolytic assay

The hemolytic assay was performed as previously described.^{19,20} Briefly, ethylenediaminetetraacetic acid anticoagulated mouse blood was centrifuged for 10 minutes at 800 g at 20°C to obtain red blood cells, which were washed 3 times, and 200-fold diluted in PBS. Subsequently, 75- μ L aliquots of red blood cells were added to 75- μ L peptide solutions (final concentration ranging from 0 to 80 μ M) in 96-well microtiter plates, and the mixture was incubated for 1 hour at 37°C. A solution of 0.2% (vol/vol) Triton X-100 served as a control for complete lysis. Supernatants, collected after centrifugation, were transferred into polystyrene 96-wells plates, and absorbance was measured at 405 nm by using an automatic plate reader (FLUOstar Omega, BMG LABTECH, Germany). Hemolysis (%) was calculated as follows: $[(Abs_{405\text{ nm}} \text{ peptide} - Abs_{405\text{ nm}} \text{ blank}) / (Abs_{405\text{ nm}} \text{ 0.2\% Triton} - Abs_{405\text{ nm}} \text{ blank})] \times 100$.

2.7 | Circular dichroism analyses

Circular dichroism (CD) experiments were performed on a Jasco J-810 CD spectropolarimeter. The cell path length was 0.1 cm. Circular dichroism spectra were collected at 20°C in the 200 to 260-nm (far-UV) interval, with a 10-nm/min scan rate, 2-nm bandwidth, and a 4-second response. Spectra are reported in mean residue ellipticity, calculated by dividing the total molar ellipticity by the number of amino acids in the molecule. Lyophilized peptides were dissolved in 50-mM sodium PBS at pH 7.4 at a concentration of 50 μ M. The spectra were signal-averaged over at least 3 scans, and the baseline was corrected by subtracting the background and reported without further signal processing. Circular dichroism spectra of the peptide were collected in the absence or in the presence of increasing concentrations of sodium dodecyl sulfate (SDS; 0-20mM,

Sigma Aldrich, Milan, Italy), trifluoroethanol (TFE, 0-30%, Sigma Aldrich, Milan, Italy), and lipopolysaccharide (LPS) from *P. aeruginosa* strain P10 or from a cystic fibrosis isolate strain KK27 tested at a concentration ranging from 0 to 0.8 mg/mL. Circular dichroism spectra were corrected by subtracting every time the contribution of the compound under test at any given concentration. Circular dichroism spectrum deconvolution was performed according to the Selcon method by using Dichroweb,²⁵ to estimate secondary structure contents.

2.8 | Real-time quantitative polymerase chain reaction

THP-1 undifferentiated cells were plated in 6-well plates at a density of 1×10^6 cells/well for 12 hours. The cells were then incubated with ApoE (133-150) or ApoE (133-167) at a concentration of 1 μ M (2.5 and 4.4 μ g/mL, respectively). Peptides were tested alone or in combination with LPS from *E. coli* O111:B4 (0.1 μ g/mL). After an incubation of 1 hour, the cells were collected and washed with cold PBS. Total RNA was extracted from cell pellet by using QIAGEN Rneasy Mini Kit (Qiagen, Hilden, Germany) according to the manufacturer's instructions. One microgram of total RNA was retrotranscribed by using Maxima Reverse Transcriptase (Thermo-Fisher Scientific, Waltham, MA) according to the manufacturer's instructions. Quantitative real-time polymerase chain reaction (qRT-PCR) amplifications were performed by using the Power SYBR Green PCR Master Mix (Thermo-Fisher Scientific, Waltham, MA) in Applied Biosystems 7500 real-time PCR Systems. The qRT-PCR conditions were 95°C for 15 minutes followed by 40 cycles of 95°C for 15 seconds, 59°C for 30 seconds, and 72°C for 30 seconds. The following primers were used for cDNA amplification: COX-2 5'-TCACGCATCAGTTTTCAA GA-3' (forward) and 5'-TCACCGTAAATATGATTTAAGTCCAC-3' (reverse); IL-8 5'-GGCACAAACTTTCAGAGACAG-3' (forward) and 5'-ACACAGAGCTGCAGAAATCAGG-3' (reverse); and as the house-keeping genes for the qRT-PCR reaction actin: 5'-ATTGCCGACAG GATCGAGAA-3' (forward) and 5'-GCTGATCCACATCTGCTGGAA-3' (reverse). Results were expressed as relative fold induction of the target genes relative to the reference gene. Calculations of relative expression levels were performed by using the $2^{-\Delta\Delta Ct}$ method and averaging the values of at least 3 independent experiments.¹⁵

2.9 | Antibiofilm activity

To test ApoE-derived peptide antibiofilm activity, bacteria were grown overnight in MHB (Becton Dickinson Difco, Franklin Lakes, NJ) and then diluted to 1×10^8 CFU/mL in BM2 medium²⁶ containing the peptide under test. Incubations were carried out for 24 hours to test peptide effects on biofilm formation.²⁰ At the end of the incubation, the crystal violet assay was performed. To do this, the planktonic culture was removed from the wells, which were washed 3 times with sterile PBS prior to staining with 0.04% crystal violet (Sigma Aldrich, Milan, Italy) for 20 minutes. The colorant excess was eliminated by 3 successive washes with sterile PBS. Finally, the crystal violet was solubilized with 33% acetic acid and samples optical absorbance

values were determined at 600 nm by using an automatic plate reader (MicrobetaWallac 1420, Perkin Elmer, Waltham, MA, USA).

2.10 | Analysis of static biofilm growth by confocal microscopy

Bacterial biofilm was grown on glass cover slips in 24-well plates in BM2 medium in static conditions at 37°C for 24 hours. To do this, *P. aeruginosa* PAO1 and MRSA WKZ-2 bacterial cells from an overnight culture were diluted to about 2×10^8 CFU/mL and then seeded into wells together with ApoE (133-167) or ApoE (133-150) at a concentration of 10 μ M. Following incubation (24 h at 37°C), nonadherent bacteria were removed by gently washing with sterile PBS. Glass cover slips were then mounted in PBS. Viability of cells embedded into biofilm structure was determined by sample staining with LIVE/DEAD® BacLight™ Bacterial Viability kit (Molecular Probes ThermoFisher Scientific, Waltham, MA, USA). Staining was performed accordingly to manufacturer instructions. Biofilm images were captured by using a confocal laser scanning microscopy (Zeiss LSM 710, Zeiss, Germany) and a 63 \times objective oil immersion system. Biofilm architecture was analyzed by using the Zen Lite 2.3 software package. Each experiment was performed in triplicate. All images were taken under identical conditions.

2.11 | Statistical analysis

Statistical analysis was performed by using a Student's *t* test. Significant differences were indicated as **P* < .05, ***P* < .01, or ****P* < .001.

3 | RESULTS AND DISCUSSION

3.1 | Recombinant production of ApoE (133-167)

Recombinant ApoE (133-167) has been produced by using a previously set up experimental procedure.²⁷ Briefly, ApoE (133-167) coding sequence was cloned into the expression vector pET22b⁽⁺⁾ downstream to ONC-DClass-H6 coding sequence.²⁷ The resulting fusion protein, composed by ApoE (133-167) fused to a mutated version of amphibian ribonuclease onconase, contains a His tag sequence, suitable for an easy purification of the fusion protein, between the onconase moiety and the ApoE moiety, a flexible linker (Gly-Thr-Gly), and a dipeptide (Asp-Pro), that allows to separate the carrier from

the peptide by mild acidic cleavage. After protein construct expression induction in *E. coli* cells strain BL21 (DE3), inclusion bodies were collected and washed. Protein construct was then purified by affinity chromatography. Pooled fractions were extensively dialyzed against 0.1 M acetic acid pH 3.0 at 4°C and finally clarified. Following the removal of any insoluble material by centrifugation and filtration, the sample containing the fusion construct was acidified to pH 2.0 with HCl to cleave the Asp-Pro linker peptide. Sample was then purged with N₂, and incubated at 60°C for 24 hours in a water bath. Following cleavage, the pH of the sample was increased to 7.0–7.2 by adding NH₃, and the sample was then incubated overnight at 28°C to selectively precipitate the carrier onconase. The released peptide was then isolated from the insoluble components through repeated cycles of centrifugation and finally lyophilized. The purity of the peptide was checked by SDS polyacrylamide gel electrophoresis and by mass spectrometry analyses. Only peptides purified to the >95% level were subjected to further analyses. The same experimental procedure was used to express and purify ApoE (133-150) peptide.¹⁵

3.2 | Antimicrobial activity of recombinant ApoE (133-167)

To evaluate the antibacterial activity of ApoE (133-167), antimicrobial assays were carried out on a panel of Gram-negative and Gram-positive bacterial strains (Table 1).

Apolipoprotein E (133-167) antimicrobial activity was analyzed accordingly to broth microdilution method.²³ By performing this assay, minimal inhibitory concentration values were found to be comprised between 1.2 and 40 μ M against all the tested strains. As expected from their very similar AS values (12.3 and 11.8), the toxicity of ApoE (133-167) was found to be comparable with that exerted by the previously described ApoE (133-150) peptide,¹⁵ used as control peptide. This was also confirmed when the killing rate of the 2 ApoE-derived peptides was analyzed on 2 Gram-positive and 2 Gram-negative bacteria. Indeed, the toxicity curves obtained for the 2 peptides were found to be identical (see figure S2A-D).

To further investigate about the antimicrobial activity of ApoE (133-167), it has been also performed an alternative assay to define whether the peptide was lytic. Antimicrobial peptides generally kill bacterial cells by forming pores into membranes, thus determining the leakage of small molecules, such as ATP, which is synthesized on the inner side of the membrane. To verify if ApoE (133-167) was able

TABLE 1 Minimum inhibitory concentration (MIC₁₀₀, μ M) values of apolipoprotein E (ApoE)-derived peptides against a panel of Gram-positive and Gram-negative bacteria

Gram-Positive Strains	ApoE (133-150) MIC ₁₀₀ Values (μ M)	ApoE (133-167)	Gram-Negative Strains	ApoE (133-150) MIC ₁₀₀ Values (μ M)	ApoE (133-167)
MRSA WKZ-2	10	5	<i>Escherichia coli</i> ATCC 25922	10	10
<i>S. aureus</i> ATCC 29213	5	5	<i>Pseudomonas aeruginosa</i> ATCC 27853	10	5
<i>B. globigii</i> TNO BMO13	1.2	1.2	<i>S. enteritidis</i> 706 RIVM	20	10
			<i>Pseudomonas aeruginosa</i> PAO1	20	40

Values were obtained from a minimum of 3 independent trials.

to induce ATP release, we performed an assay to detect the leakage of this nucleotide. To this purpose, *MRSA* WKZ-2 and *E. coli* ATCC 25922 bacterial strains were treated with 2 different doses of both ApoE-derived peptides (see section 2). As shown in Figure 1, the presence

of ATP in the culture media was clearly evident; hence, we can confidently suppose that ApoE (133-167) as well as ApoE (133-150) exert a lytic effect on both bacterial strains, with *MRSA* WKZ-2 cells being particularly sensitive to the peptide.

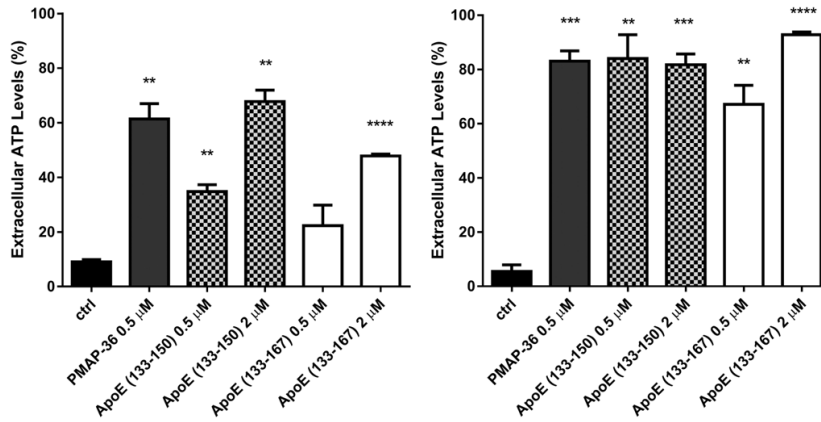


FIGURE 1 Apolipoprotein E-derived induced ATP leakage in (left) *Escherichia coli* ATCC 25922 and (right) *MRSA* WKZ-2 upon treatment with 0.5 or 2- μ M peptide. PMAP-36, a canonical pore forming peptide, was used as positive control.²¹ The assays were performed in 3 independent experiments

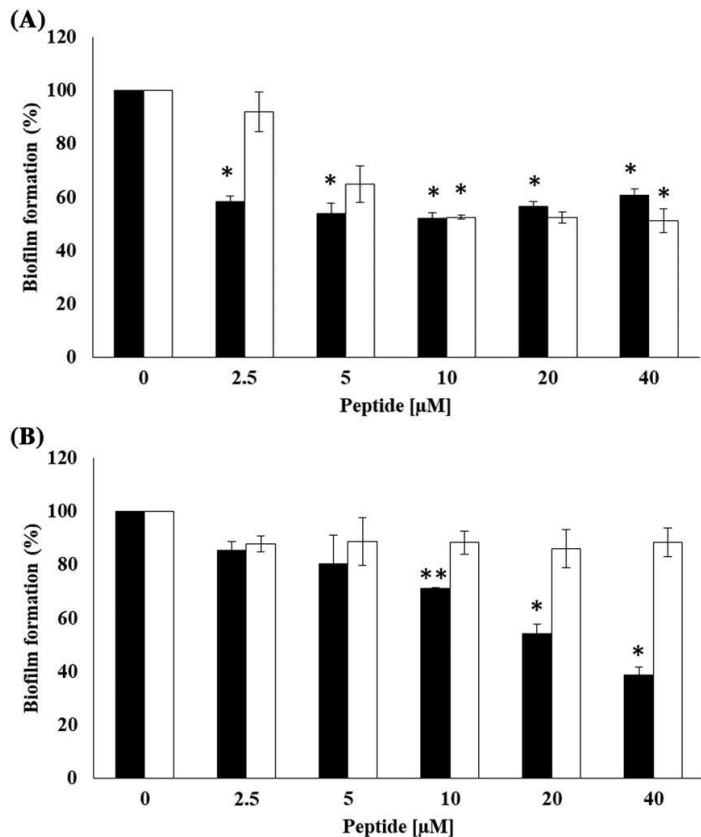


FIGURE 2 Antibiofilm activity of ApoE (133-167), black bars, and ApoE (133-150), white bars, on (A) *MRSA* WKZ-2 and (B) *Pseudomonas aeruginosa* PAO1 strains in BM2 medium. The effects of increasing concentrations of peptides were evaluated on biofilm formation. Biofilm was stained with crystal violet and measured at 600 nm. Data represent the mean (\pm standard deviation, SD) of at least three independent experiments, each one carried out with triplicate determinations. * $P < .05$ or ** $P < .01$ was obtained for control versus treated samples

3.3 | Antibiofilm properties of ApoE (133-167)

Antibiofilm peptides represent a very promising approach to treat biofilm-related infections generally recalcitrant to conventional antibiotics.²⁸ To verify whether ApoE (133-167) peptide exerts antibiofilm activity, we tested its effects on biofilm formation. To do this, we incubated MRSA WKZ-2 and *P. aeruginosa* PAO1 cells with ApoE (133-167) for 24 hours at 37°C. The same experimental procedure was also applied to ApoE (133-150) because its antibiofilm activity has not been characterized yet. By crystal violet assay, both peptides were found to strongly inhibit (about 40% inhibition) MRSA WKZ-2 biofilm formation (Figure 2A). However, it has to be noticed that ApoE (133-150) is effective at a concentration (10 µM) corresponding to its MIC₁₀₀ value on planktonic cells. Based on this, we may not exclude that peptide effects on bacterial biofilm are indeed related to its ability to directly kill planktonic cells. In the case of *P. aeruginosa* PAO1, instead, only ApoE (133-167) was found to exert a significant effect on biofilm formation (about 60% inhibition at 20 µM), whereas the shorter peptide was found to be almost inactive (Figure 2B). We also analyzed the effects of the 2 peptides on biofilm formation by confocal microscopy. To this purpose, bacterial cells were incubated with peptides (10 µM) for 24 hours at 37°C in static conditions. Ciprofloxacin antibiotic was used as a positive control (Figures 3 and 4). Following incubation, samples were double stained (Syto9/PI mixture) to discriminate between live and dead bacterial cells embedded

into biofilm structure. As shown in Figure 3, a dramatic decrease of cell cohesion with respect to control sample was observed upon treatment with both peptides in the case of MRSA WKZ-2. This indicates a drastic inhibition of biofilm formation, in agreement with crystal violet observations. Moreover, in both cases, a significant increase in cell death was observed (Figure 3). As previously reported, for ApoE (133-150) peptide, we may not exclude that its effects on bacterial biofilm are indeed related to its toxicity toward planktonic cells because peptide concentrations lower than 10 µM were found to be ineffective on biofilm formation. When peptide effects on *P. aeruginosa* PAO1 biofilm formation were analyzed, we observed that both peptides induce a dramatic decrease of cell cohesion, although only ApoE (133-167) peptide induces a significant increase in cell death (Figure 4). This might justify the results obtained by crystal violet assay, indicating that the shorter peptide has almost no effect on *P. aeruginosa* PAO1 biofilm formation (Figure 4). Altogether, these findings support the hypothesis that ApoE (133-167) peptide is endowed with additional properties absent or limited in the case of ApoE (133-150).

3.4 | Cytotoxicity assays of ApoE (133-167) on eukaryotic cells

The promising interest in the use of antimicrobial peptides as alternative antibiotics stems from their selective toxicity toward bacterial

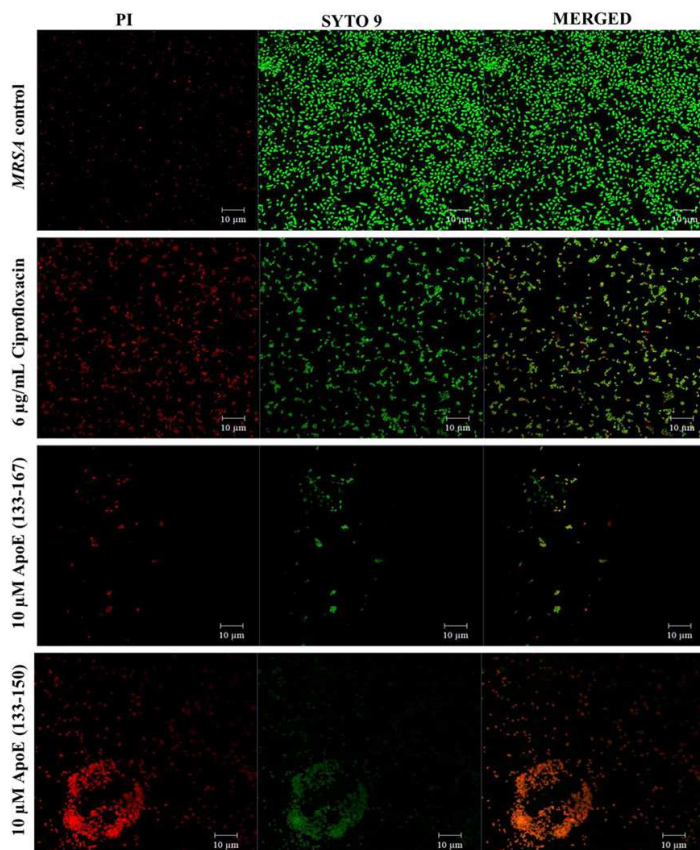


FIGURE 3 Effect of ApoE (133-167) and ApoE (133-150) on MRSA WKZ-2 biofilm grown in BM2 medium and visualized by controlled low strength material. Bacterial biofilm was cultivated in BM2 medium for 24 hours at 37°C together with each peptide (10 µM) or ciprofloxacin used as positive control (6 µg/mL). Biofilm images were captured by using a confocal laser scanning microscopy (Zeiss LSM 710, Zeiss, Germany) and a 63× objective oil immersion system. Biofilm architecture was analyzed by using the Zen Lite 2.3 software package. Each experiment was performed in triplicate. Scale bars correspond to 10 µm in all the cases

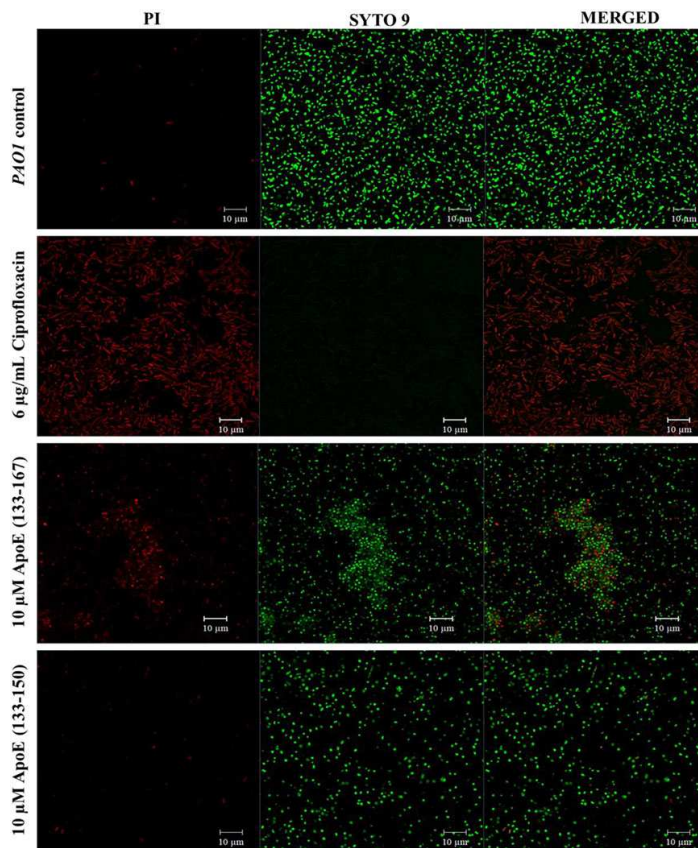


FIGURE 4 Effect of ApoE (133-167) and ApoE (133-150) on *Pseudomonas aeruginosa* PAO1 biofilm grown in BM2 medium and visualized by controlled low strength material. Bacterial biofilm was cultivated in BM2 medium for 24 hours at 37°C together with each peptide (10 µM) or ciprofloxacin used as positive control (6 µg/mL). Biofilm images were captured by using a confocal laser scanning microscopy (Zeiss LSM 710, Zeiss, Germany) and a 63× objective oil immersion system. Biofilm architecture was analyzed by using the Zen Lite 2.3 software package. Each experiment was performed in triplicate. Scale bars correspond to 10 µm in all the cases

cells.²⁹ We thus analyzed the cytotoxic effects and possible hemolytic effects of ApoE (133-167). As shown in figure S3A and B, the addition of peptide increasing concentrations (from 0.6 to 40 µM) to either differentiated or undifferentiated human THP-1 cells for 24 hours at 37°C did not result in any significant reduction in cell viability. Moreover, ApoE (133-167) was found to be not hemolytic for murine erythrocytes, as reported in figure S3C. This suggests that the presence of this peptide in the systemic circulation would not cause toxic effects on the blood cells, thus confirming the ability of this promising peptide to selectively recognize distinctive structural targets on bacterial cell membranes. Apolipoprotein E (133-167) peptide eventual toxicity was also tested on human keratinocytes (HaCat cells); human tumor cell line, such as HeLa, HEK-293, and CaCo-2 cells; and on murine macrophage RAW 264.7 cells. In all the cases, no significant cytotoxicity was detected (data not shown), clearly demonstrating that this peptide exerts selective toxic effects on prokaryotic cells.

3.5 | Conformational analyses of ApoE (133-167)

Apolipoprotein E (133-167) peptide conformation was analyzed by Far-UV CD. We found that the peptide is largely unstructured in PBS and that it assumes an increasingly ordered conformation in the presence of membrane mimicking agents, such as TFE and SDS micelles (Figure 5A and B). This clearly indicates that, similarly to other

cationic antimicrobial peptides,^{19,20} ApoE (133-167) is prone to assume a stable conformation when interacting with membrane mimicking agents. At the highest concentrations of TFE and SDS, the CD spectra showed 2 broad minima, at 208 and 222 nm, respectively, and 1 maximum at <200 nm, indicative of a putative alpha-helical conformation. It is worth noting that the maximal structured conformation was observed at a TFE concentration of about 30%, thus indicating a high propensity of ApoE (133-167) to acquire an ordered structure.

To further characterize the structural properties of ApoE (133-167), we analyzed by CD spectroscopy its binding to LPS, the main constituent of the outer membrane of Gram-negative bacteria (Figure 5C and D). When ApoE (133-167) was analyzed in the presence of increasing concentrations (0.05 to 0.8 mg/mL) of LPS purified from 2 different strains of *P. aeruginosa* (strain P10 and a cystic fibrosis isolate strain KK27), 2 minima around 208 and 222 nm appeared, clearly suggesting that the peptide is able to adopt a helical conformation upon interaction with this bacterial wall determinant (Figure 5C and D).

3.6 | ApoE (133-167) interaction with LPS

Because data obtained by CD analyses suggested an interaction between ApoE (133-167) and LPS, it seemed intriguing to provide a functional evidence for this hypothesis. To this purpose, we

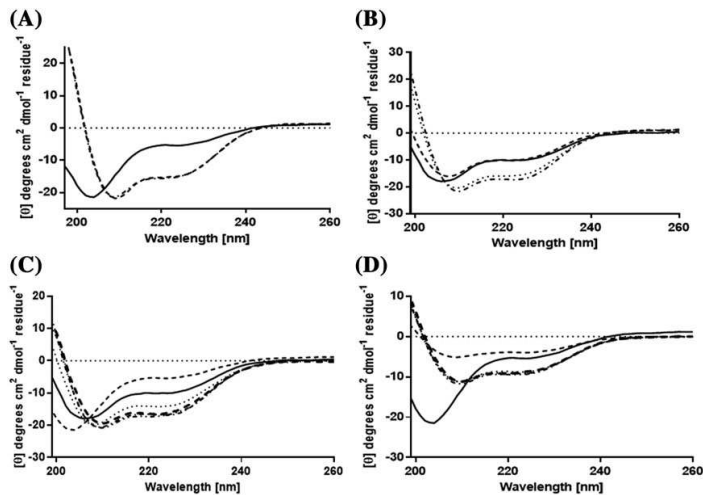


FIGURE 5 Far-UV circular dichroism spectra of ApoE (133-167); continuous line) in the presence of increasing concentrations of (A) sodium dodecyl sulfate, (B) tetrafluoroethylene, and (C and D) lipopolysaccharide

performed vitality assays by incubating LPS isolated from *E. coli* O11: B4 with 4.4 $\mu\text{g}/\text{mL}$ of ApoE (133-167) for 30 minutes at 37°C. Mixtures were then added to *E. coli* ATCC 25922 cells for 4 hours. The same experimental procedure was also applied to ApoE (133-150). As reported in figure S4, bacterial vitality upon treatment with ApoE (133-167)/LPS mixture was found to be significantly lower than that observed upon administration of the peptide alone. In the case of ApoE (133-150) peptide, instead, no differences were detected when the peptide was administered alone or in combination with LPS. This might indicate that, in our experimental conditions, ApoE (133-167) peptide is indeed sequestered by LPS, thus exerting a lower antimicrobial activity. This opens a new scenario in which ApoE (133-167) peptide biological activities go beyond its antimicrobial properties.

3.7 | Effects of ApoE (133-167) on the expression of LPS-induced inflammatory cytokines

The data described above would indicate that ApoE (133-167) is able to assume ordered conformations in the presence of LPS as well as to presumably interact with this endotoxin, thus determining a subsequent mitigation of intracellular signaling cascade induced by the recognition of the LPS by the core receptor complex composed of LPS-binding protein, CD14, Toll-like receptor 4, and MD-2.³⁰ As the ability of host defense peptides to bind to LPS could be associated to a mitigation of inflammatory cytokine production,³¹ to confirm the hypothesis that also ApoE (133-167) might elicit antiinflammatory effects on human cells, it seemed appropriate to analyze its effects on the LPS induced IL-8 and Cox2 expression in human monocytic THP-1 cells in comparison with the effects exerted by ApoE (133-150), for which antiinflammatory properties have already been demonstrated.¹⁵

As shown in Figure 6, in THP-1 undifferentiated cells stimulated with LPS in the presence of ApoE (133-167), a significant decrease in mRNA expression of both IL-8 and Cox-2, with respect to cells treated with LPS alone, was observed. According to Pane et al 2016,¹⁵ ApoE (133-150) was also able to influence mRNA expression

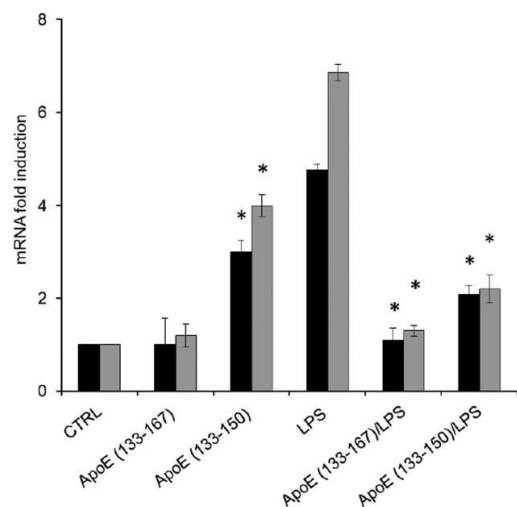


FIGURE 6 Influence of ApoE (133-167) and ApoE (133-150) on gene expression of COX-2 (black bars) and IL-8 (gray bars) in THP-1 cells treated with a mixture of 1- μM ApoE derived peptide, 2.5 $\mu\text{g}/\text{mL}$ for ApoE (133-150) and 4.4 $\mu\text{g}/\text{mL}$ for ApoE (133-167) and LPS (0.1 $\mu\text{g}/\text{mL}$) from *Escherichia coli* O111:B4. The results were expressed as relative fold induction respect to actin. Data were the average of 3 independent experiments \pm SE

of these 2 cytokines, although to a lesser extent with respect to ApoE (133-167). This corroborates the hypothesis that ApoE (133-167) could possess in its composition and in its structure key responsive LPS scavenger determinants that are absent or limited, instead, in other ApoE-derived peptides.

4 | CONCLUSIONS

Recently, by a bioinformatics approach, we identified a cryptic peptide including the receptor binding region of ApoE, characterized by the

highest antimicrobial score among all putative or already reported ApoE-derived peptides.

Based on its length and composition, we hypothesized that this peptide, here named ApoE (133-167), could be antimicrobial but present also additional properties associated to its ability to acquire a large amphipathic conformation.

Interestingly, ApoE (133-167) was found to be able to assume a regular helical conformation in the presence of detergents and exopolysaccharides (as LPS) and to present a broad antimicrobial activity, being effective also on clinical isolates. In spite of this, our truly striking evidence is that Apo E (133-67) also showed a potent ability to inhibit biofilm formation of both Gram-positive and Gram-negative bacteria, as well as to induce a significant decrease of bacteria encapsulated in their self-produced extracellular polymeric matrix. This finding is even more significant if we consider that ApoE (133-167) revealed other intriguing properties, such as (i) the ability to interact with LPS, thus showing a potential scavenger propensity of this endotoxin; (ii) the absence of toxicity when administered to human cells; and (iii) the ability to downregulate LPS-induced proinflammatory cytokine expression.

Generally, antimicrobial peptides do not necessarily interact with a specific intracellular target that bacteria can mask or modify by genetically acquiring resistance. It should also be emphasized that this positive aspect, associated to additional biological properties of cryptic peptides, as shown for ApoE (133-167), could open an appealing future scenario in which peptides might effectively and selectively operate in conditions in which antibiotics fail. Moreover, the ability of some peptides to synergistically act in combination with conventional antibiotics²⁰ might allow the future design of combinatorial therapeutic approaches, which might succeed especially in those cases in which the infection is particularly difficult to eradicate due to biofilm formation.

ACKNOWLEDGEMENTS

This research was supported by the Italian Cystic Fibrosis Foundation (grant number 16/2017). We are deeply indebted to volunteers who devote many efforts in fundraising, in particular delegations "Gruppo di Sostegno FFC di San Giovanni Rotondo," "Delegazione FFC di Reggio Calabria," and Guadagnin srl.

ORCID

Elio Pizzo  <http://orcid.org/0000-0002-3652-8865>

REFERENCES

- Getz GS, Reardon CA. Apoprotein E as a lipid transport and signaling protein in the blood, liver, and artery wall. *J Lipid Res.* 2009;50 Suppl: S156-S161.
- Phillips MC. Apolipoprotein E isoforms and lipoprotein metabolism. *IUBMB Life.* 2014;66(9):616-623.
- Johnson LA, Olsen RH, Merkens LS, et al. Apolipoprotein E-low density lipoprotein receptor interaction affects spatial memory retention and brain ApoE levels in an isoform-dependent manner. *Neurobiol Dis.* 2014;64:150-162.
- Mahley RW. Apolipoprotein E: cholesterol transport protein with expanding role in cell biology. *Science.* 1988;240(4852):622-630.
- Mahley RW. Central nervous system lipoproteins: ApoE and regulation of cholesterol metabolism. *Arterioscler Thromb Vasc Biol.* 2016;36(7):1305-1315.
- Wang H, Eckel RH. What are lipoproteins doing in the brain? *Trends Endocrinol Metab.* 2014;25(1):8-14.
- Zlokovic BV. Cerebrovascular effects of apolipoprotein E: implications for Alzheimer disease. *JAMA Neurol.* 2013 Apr;70(4):440-444.
- Giau VV, Bagyinszky E, An SS, Kim SY. Role of apolipoprotein E in neurodegenerative diseases. *Neuropsychiatr Dis Treat.* 2015;11:1723-1737.
- Saito H, Dhanasekaran P, Baldwin F, Weisgraber KH, Lund-Katz S, Phillips MC. Lipid binding-induced conformational change in human apolipoprotein E. Evidence for two lipid-bound states on spherical particles. *J Biol Chem.* 2001;276(44):40949-40954.
- Laskowitz DT, Thekdi AD, Thekdi SD, et al. Downregulation of microglial activation by apolipoprotein E and apoE-mimetic peptides. *Exp Neurol.* 2001;167(1):74-85.
- Sarantseva S, Timoshenko S, Bolshakova O, et al. Apolipoprotein E-mimetics inhibit neurodegeneration and restore cognitive functions in a transgenic Drosophila model of Alzheimer's disease. *PLoS one.* 2009;4(12):e8191.
- Clay MA, Anantharamaiah GM, Mistry MJ, Balasubramaniam A, Harmony JA. Localization of a domain in apolipoprotein E with both cytostatic and cytotoxic activity. *Biochemistry.* 1995;34(35): 11142-11151.
- Forbes S, McBain AJ, Felton-Smith S, Jowitt TA, Birchenough HL, Dobson CB. Comparative surface antimicrobial properties of synthetic biocides and novel human apolipoprotein E derived antimicrobial peptides. *Biomaterials.* 2013;34(22):5453-5464.
- Wang CQ, Yang CS, Yang Y, Pan F, He LY, Wang AM. An apolipoprotein E mimetic peptide with activities against multidrug-resistant bacteria and immunomodulatory effects. *J Pept Sci.* 2013;19(12):745-750.
- Pane K, Sgambati V, Zanfardino A, et al. A new cryptic cationic antimicrobial peptide from human apolipoprotein E with antibacterial activity and immunomodulatory effects on human cells. *FEBS J.* 2016;283(11):2115-2131.
- Wilson C, Wardell MR, Weisgraber KH, Mahley RW, Agard DA. Three-dimensional structure of the LDL receptor-binding domain of human apolipoprotein E. *Science.* 1991;252(5014):1817-1822.
- Raussens V, Slupsky CM, Ryan RO, Sykes BD. NMR structure and dynamics of a receptoractive apolipoprotein E peptide. *J Biol Chem.* 2002;277(32):29172-29180.
- Pane K, Durante L, Crescenzi O, et al. Antimicrobial potency of cationic antimicrobial peptides can be predicted from their amino acid composition: application to the detection of "cryptic" antimicrobial peptides. *J Theor Biol.* 2017;419:254-265.
- Bosso A, Pirone L, Gaglione R, et al. A new cryptic host defense peptide identified in human 11-hydroxysteroid dehydrogenase-1 β -like: from in silico identification to experimental evidence. *Biochim Biophys Acta.* 2017;1861(9):2342-2353.
- Gaglione R, Dell'Olmo E, Bosso A, et al. Novel human bioactive peptides identified in apolipoprotein B: evaluation of their therapeutic potential. *Biochem Pharmacol.* 2017;130:34-50.
- Scocchi M, Zelezetsky I, Benincasa M, Gennaro R, Mazzoli A, Tossi A. Structural aspects and biological properties of the cathelicidin PMAP-36. *FEBS J.* 2005;272(17):4398-4406.
- Pizzo E, Varcamonti M, Di Maro A, Zanfardino A, Giancola C, D'Alessio G. Ribonucleases with angiogenic and bactericidal activities from the Atlantic salmon. *FEBS J.* 2008;275(6):1283-1295.
- Wiegand I, Hilpert K, Hancock RE. Agar and broth dilution methods to determine the minimal inhibitory concentration (MIC) of antimicrobial substances. *Nat Protoc.* 2008;3(2):163-175.
- Boukamp P, Popp S, Altmeyer S, et al. Sustained non tumorigenic phenotype correlates with a largely stable chromosome content during long-term culture of the human keratinocyte line HaCaT. *Genes Chromosom Cancer.* 1997;19(4):201-214.

25. Whitmore L, Wallace BA. Protein secondary structure analyses from circular dichroism spectroscopy: methods and reference databases. *Biopolymers*. 2008;89(5):392-400.
26. Li J, Kleintschek T, Rieder A, et al. Hydrophobic liquid-infused porous polymer surfaces for antibacterial applications. *ACS Appl Mater Interfaces*. 2013;5(14):6704-6711.
27. Pane K, Durante L, Pizzo E, et al. Rational design of a carrier protein for the production of recombinant toxic peptides in *Escherichia coli*. *PLoS one*. 2016;11(1):e0146552.
28. Pletzer D, Coleman SR, Hancock RE. Anti-biofilm peptides as a new weapon in antimicrobial warfare. *Curr Opin Microbiol*. 2016;33:35-40.
29. Takahashi D, Shukla SK, Prakash O, Zhang G. Structural determinants of host defense peptides for antimicrobial activity and target cell selectivity. *Biochimie*. 2010;92(9):1236-1241.
30. Park BS, Lee JO. Recognition of lipopolysaccharide pattern by TLR4 complexes. *Exp Mol Med*. 2013;45(12):e66.
31. Wang C, Shen M, Zhang N, et al. Reduction impairs the antibacterial activity but benefits the LPS neutralization ability of human enteric defensin 5. *Sci Rep*. 2016;6(1):22875. <https://doi.org/10.1038/srep22875>

SUPPORTING INFORMATION

Additional supporting information may be found online in the Supporting Information section at the end of the article.

How to cite this article: Zanfardino A, Bosso A, Gallo G, et al. Human apolipoprotein E as a reservoir of cryptic bioactive peptides: The case of ApoE 133-167. *J Pep Sci*. 2018;e3095. <https://doi.org/10.1002/psc.3095>



Novel human bioactive peptides identified in Apolipoprotein B: Evaluation of their therapeutic potential



Rosa Gaglione^{a,b}, Eliana Dell'Olmo^a, Andrea Bosso^{b,c}, Marco Chino^a, Katia Pane^c, Flora Ascione^d, Francesco Itri^a, Sergio Caserta^{d,e,f}, Angela Amoresano^a, Angelina Lombardi^a, Henk P. Haagsman^b, Renata Piccoli^{a,g}, Elio Pizzo^c, Edwin J.A. Veldhuizen^b, Eugenio Notomista^c, Angela Arciello^{a,g,*}

^a Department of Chemical Sciences, University of Naples Federico II, 80126 Naples, Italy

^b Department of Infectious Diseases and Immunology, Division Molecular Host Defence, Faculty of Veterinary Medicine, Utrecht University, Utrecht, The Netherlands

^c Department of Biology, University of Naples Federico II, 80126 Naples, Italy

^d Department of Chemical, Materials and Production Engineering, University of Naples Federico II, 80125 Naples, Italy

^e CEINGE Biotecnologie Avanzate, Via Sergio Pansini, 5, 80131 Naples, Italy

^f Consorzio Interuniversitario Nazionale per la Scienza e Tecnologia dei Materiali (INSTM), Udr INSTM Napoli Federico II, P.le Tecchio, 80, 80125 Naples, Italy

^g Istituto Nazionale di Biostrutture e Biosistemi (INBB), Italy

ARTICLE INFO

Article history:

Received 2 December 2016

Accepted 23 January 2017

Available online 25 January 2017

Keywords:

Host defence peptides
Apolipoprotein B
Immunomodulation
Lipopolysaccharide
Bacterial biofilm
Combination therapy
Wound healing
Biocompatibility

ABSTRACT

Host defence peptides (HDPs) are short, cationic amphipathic peptides that play a key role in the response to infection and inflammation in all complex life forms. It is increasingly emerging that HDPs generally have a modest direct activity against a broad range of microorganisms, and that their anti-infective properties are mainly due to their ability to modulate the immune response. Here, we report the recombinant production and characterization of two novel HDPs identified in human Apolipoprotein B (residues 887–922) by using a bioinformatics method recently developed by our group. We focused our attention on two variants of the identified HDP, here named r(P)ApoB_L and r(P)ApoB_S, 38- and 26-residue long, respectively. Both HDPs were found to be endowed with a broad-spectrum antimicrobial activity while they show neither toxic nor haemolytic effects towards eukaryotic cells. Interestingly, both HDPs were found to display a significant anti-biofilm activity, and to act in synergy with either commonly used antibiotics or EDTA. The latter was selected for its ability to affect bacterial outer membrane permeability, and to sensitize bacteria to several antibiotics. Circular dichroism analyses showed that SDS, TFE, and LPS significantly alter r(P)ApoB_L conformation, whereas slighter or no significant effects were detected in the case of r(P)ApoB_S peptide. Interestingly, both ApoB derived peptides were found to elicit anti-inflammatory effects, being able to mitigate the production of pro-inflammatory interleukin-6 and nitric oxide in LPS induced murine macrophages. It should also be emphasized that r(P)ApoB_L peptide was found to play a role in human keratinocytes wound closure *in vitro*. Altogether, these findings open interesting perspectives on the therapeutic use of the herein identified HDPs.

© 2017 Elsevier Inc. All rights reserved.

Abbreviations: MRSA, methicillin-resistant *Staphylococcus aureus*; VRE, vancomycin-resistant enterococci; HDPs, host defence peptides; AMPs, antimicrobial peptides; LPS, lipopolysaccharide; ApoE, Apolipoprotein E; ApoB, Apolipoprotein B; LDL, low-density lipoprotein; IL-10, interleukin-10; MIC, minimal inhibitory concentration; TSA, Tryptic Soy Agar; AS, absolute score; MHB, Muller Hinton Broth; NB, Nutrient Broth; IPTG, isopropyl-β-D-thiogalactopyranoside; TFE, trifluoroethanol; SDS, sodium dodecyl sulfate; FIC, fractional inhibitory concentration; EDTA, ethylenediaminetetraacetic acid; IL-6, interleukin-6; NO, nitric oxide; CATH-2, cathelicidin-2; ONC, onconase; PBS, phosphate-buffered saline; CD, circular dichroism; MTT, 3-(4,5-dimethylthiazol-2-yl)-2,5-diphenyltetrazolium bromide; MALDI-MS, matrix assisted laser desorption ionisation mass spectrometry; RBCs, red blood cells; WH, wound healing.

* Corresponding author at: Department of Chemical Sciences, University of Naples Federico II, 80126 Naples, Italy

E-mail address: anarciel@unina.it (A. Arciello).

1. Introduction

The excessive and sometimes improper use of antibiotics has been responsible for the development of resistant bacterial isolates, the so-called 'superbugs', such as methicillin-resistant *Staphylococcus aureus* (MRSA) [1], vancomycin-resistant enterococci (VRE), and multidrug-resistant *Pseudomonas*, *Klebsiella*, and *Acinetobacter* [2]. This made the search for novel antimicrobial therapies and approaches imperative. In this scenario, the broad immunomodulatory properties of naturally occurring host defence peptides (HDPs) have attracted considerable attention. HDPs, also known as antimicrobial peptides (AMPs), are evolutionarily conserved molecules of the innate immune system. They are a

key element of the ancient, nonspecific innate defence system in most multicellular organisms, representing the first line of defence against invading microbes [3,4]. Found in all complex living organisms, HDPs have first attracted considerable attention for their modest antimicrobial activity directed towards a broad spectrum of pathogens including bacteria, viruses, fungi, and protozoa [3,4]. Natural HDPs have a size ranging from 12 to 50 amino acids, are mostly cationic owing to the presence of high levels of lysine and arginine residues, and contain over 50% hydrophobic amino acids [3,5]. These properties are at the basis of HDPs' ability to interact with membranes, and, in some cases, to penetrate cell membranes. In model systems, HDPs associate preferentially with negatively charged membranes of bacteria-like composition, but many peptides are also able to translocate into host cells. To date, the molecular bases of their selectivity towards bacterial membranes are still poorly understood [6]. It has been suggested that HDPs tend to translocate into bacterial cells owing to the presence of a large electrical potential gradient [7]. However, although HDPs' direct antimicrobial mechanism of action against bacteria mainly involves interaction with the bacterial membrane, multiple targets have been identified, such as cell wall peptidoglycans, cytosolic RNA, proteins, or cytosolic enzymes/chaperones [6,8]. Hence, the selection of resistance mechanisms in bacteria is improbable, since the removal of a single target, e.g. by mutation, would still allow other targets to mediate HDPs direct killing activity [8]. However, it is becoming increasingly evident that these peptides are endowed with a wide range of biological activities, such as multispecies anti-biofilm properties, modulation of innate immune response, and anticancer, analgesic, antioxidant and anti-inflammatory activities [3,9–13]. Therefore, although these bioactive peptides were often named AMPs, more recently they have been termed as HDPs to describe more appropriately the breadth of their activities [14]. Due to HDPs' multifunctional properties, as well as to the increased bacterial resistance to conventional antibiotics, these peptides have great chance to be used as anti-infective and immunomodulatory therapeutics. Although very few HDPs are currently in use in the market, many of them are progressing through clinical trials for the treatment of diseases including microbial infections, organ failure, immune disorders, wound healing, diabetes and cancer [15,16]. Currently, most of the therapies based on HDPs that have entered clinical trials were designed for topical applications [17], presumably due to issues concerning their stability and toxicity [18].

Natural cationic HDPs are encoded by genes from many organisms. In mammals, HDPs are expressed in a variety of cell types including monocytes/macrophages, neutrophils, epithelial cells, keratinocytes, and mast cells [19–21]. They are usually synthesized as pro-peptides from which mature and biologically active HDPs are released by bacterial and/or host proteases [20]. Apolipoproteins are a source of bioactive peptides. Previous reports have shown that peptides derived from the cationic receptor binding region of Apolipoprotein E (ApoE141–149) are endowed with broad anti-infective activity [22]. Apolipoprotein B (ApoB) also contains two LDL (low-density lipoprotein) receptor binding domains, namely region A (ApoB3147–3157) and region B (ApoB3359–3367). Region B, more uniformly conserved across species and primarily involved in receptor binding, has been found to be endowed with a significant antiviral activity [22]. Moreover, peptides derived from ApoB have been already used in vaccine preparations to treat atherosclerosis [23]. When ApoE deficient mice have been immunized with ApoB661–680 and ApoB3136–3155 peptides, a significant increase of the levels of peptide-specific immunoglobulins was detected accompanied by a concomitant increase of secreted interleukin-10 (IL-10) levels, with no effect on IFN- γ expression levels, thus indicating that ApoB derived peptides are able to modulate the immune response [23].

Recently, our group developed an *in silico* method [K. Pane et al. submitted, 24] to identify HDPs in protein precursors and to predict quantitatively their antibacterial activity. This method assigns to any given peptide an antimicrobial score, called “absolute score” (AS), on the basis of net charge, hydrophobicity and length of the peptide and of two bacterial strain-dependent weight factors defining the contribution of charge and hydrophobicity to the antimicrobial activity. We demonstrated that AS is directly proportional to the antimicrobial activity of HDPs expressed as Log(1000/MIC), where MIC is the minimal inhibitory concentration of the peptide. Score values lower than 6.5 are considered not significant as they correspond to predicted MIC values higher than 200 μ M, while for score values higher than about 10 the linear relationship is no longer valid, and an increase in the score does not necessarily correspond to a concomitant increase in the antimicrobial activity. In order to analyse a protein potentially bearing hidden antimicrobial regions, the AS values of all the peptides of the desired length contained in a precursor protein can be plotted as a function of peptide sequence and length, thus obtaining an accurate map of the antimicrobial activity determinants. This method allows the identification of novel HDPs within the sequence of known proteins (“cryptic” HDPs), as demonstrated by the identification of a novel cationic HDP endowed with antibacterial and immunomodulatory activities in human ApoE [24], and in the transcription factor Stf76 from the archaeon *Sulfolobus islandicus*. In the last case, peptide VVL-28 represents the first antimicrobial peptide derived from an archaeal protein [25].

On the basis of the interesting results obtained in the case of human ApoE, we applied our *in silico* analysis method to a human Apolipoprotein B (ApoB) isoform [26,27]. In Fig. 1, the isometric plot of region 882–929 of this ApoB variant is shown. An absolute maximum, corresponding to region 887–922 (AS = 12.0), and a relative maximum, corresponding to residues 887–909 (AS = 10.6), are shown (Fig. 1). Even if several ApoB functional regions have already been analysed, and in some cases biologically active peptides were obtained [22,23], to the best of our knowledge, this is the first report identifying ApoB region 887–922 as a source of HDPs.

Here, we report the recombinant production and characterization of two variants of the putative HDP identified by our bioinformatics method in human ApoB, i.e. peptides ApoB887–923 and ApoB887–911. Both peptides include at the C-terminal side one (as in the case of ApoB887–923), or two (as in the case of ApoB887–911) small uncharged residues (serine, glycine or threonine), which are not present in the regions highlighted in the AS plot (Fig. 1). These residues have been arbitrarily included to avoid that the negatively charged C-terminus of the peptide is adjacent to the antimicrobial region.

To evaluate the therapeutic potential of these peptides, we analysed their structure, antimicrobial and anti-biofilm activities, the ability to act in synergy with conventional antibiotics, their anti-inflammatory and wound healing properties, and their possible toxic effects on eukaryotic cells.

2. Materials and methods

2.1. Bacterial strains and growth conditions

Eight bacterial strains were used in the present study, i.e. *E. coli* ATCC 25922, methicillin-resistant *Staphylococcus aureus* (MRSA WKZ-2), *Salmonella enteritidis* 706 RIVM, *Bacillus globigii* TNO BM013, *Bacillus licheniformis* ATCC 21424, *Staphylococcus aureus* ATCC 29213, *Pseudomonas aeruginosa* ATCC 27853, and *Pseudomonas aeruginosa* PAO1. All bacterial strains were grown in Muller Hinton Broth (MHB, Becton Dickinson Difco, Franklin Lakes, NJ)

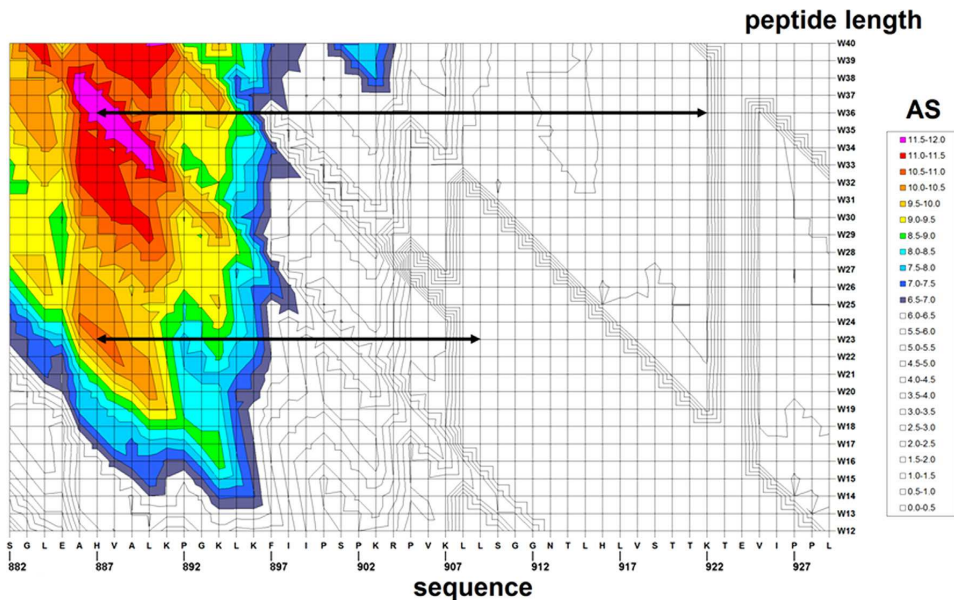


Fig. 1. Isometric plot showing the absolute score values (AS) of peptides with a length ranging from 12 to 40 residues (W12–W40) in the region 882–929 of ApoB. Colors were used to highlight AS values higher than 6.5, and corresponding to predicted MIC values on *S. aureus* lower than 200 μM .

and on Tryptic Soy Agar (TSA; Oxoid Ltd., Hampshire, UK). In all the experiments, bacteria were inoculated and grown overnight in MHB at 37 °C. The next day, bacteria were transferred to a fresh MHB tube and grown to mid-logarithmic phase.

2.2. Cell culture

Murine RAW 264.7 cells, malignant SVT2 murine fibroblasts (BALBc 3T3 cells transformed by SV40 virus), parental murine BALBc 3T3 cells, and human HeLa and HaCaT cells were from ATCC, Manassas, VA. Cells were cultured in Dulbecco's modified Eagle's medium (Sigma Aldrich, Milan, Italy), supplemented with 10% foetal bovine serum (HyClone, GE Healthcare Lifescience, Chicago, IL) and antibiotics, in a 5% CO₂ humidified atmosphere at 37 °C.

2.3. Synthetic peptides

CATH-2 peptide was obtained from CPC Scientific Inc. (Sunnyvale, USA), and LL-37 peptide was from Sigma Aldrich, Milan, Italy.

2.4. Expression and isolation of recombinant ApoB derived peptides

Expression and isolation of recombinant peptides was carried out as previously described [24,28]. Briefly, *E. coli* BL21(DE3) cells were transformed with pET recombinant plasmids, and grown in 10 mL of Terrific Broth medium (TB) containing 100 $\mu\text{g}/\text{mL}$ of ampicillin, at 37 °C up to OD_{600nm} of 2. These cultures were used to inoculate 1 L of TB/ampicillin medium. Glucose at final concentration of 4 g/L was added to cultures to limit protein expression before induction with IPTG. Cultures were incubated at 37 °C up to OD_{600nm} of 3.5–4. Expression of recombinant proteins was induced by addition of IPTG (isopropyl- β -D-thiogalactopyranoside) at final concentration of 0.7 mM. Cells were harvested after overnight induction by centrifugation at 8,000g for 15 min at 4 °C and washed with 50 mM Tris–HCl buffer pH 7.4. The bacterial pellet was suspended in 50 mM Tris–HCl buffer pH 7.4 containing 10 mM

ethylenediaminetetraacetic acid (EDTA), and sonicated in a cell disruptor (10 x 1 min cycle, on ice). The suspension was then centrifuged at 18,000g for 60 min at 4 °C. The insoluble fractions were washed three times in 0.1 M Tris–HCl buffer pH 7.4 containing 10 mM EDTA, 2% Triton X-100, and 2 M urea, followed by repeated washes in 0.1 M Tris–HCl buffer pH 7.4. Following washing steps, 100 mg of fusion proteins were dissolved in 10 mL of denaturing buffer (6 M guanidine/HCl in 50 mM Tris–HCl, pH 7.4) containing 10 mM β -mercaptoethanol. Mixtures were incubated at 37 °C for 3 h under nitrogen atmosphere on a rotary shaker, and then centrifuged at 18,000g for 60 min at 4 °C. Soluble fractions were then collected and purified by affinity chromatography on Ni Sepharose™ 6 Fast Flow resin (GE Healthcare Lifescience, Chicago, IL). The chromatographic fractions were analysed by 15% SDS/PAGE, pooled, and extensively dialyzed against 0.1 M acetic acid pH 3 at 4 °C. Any insoluble material was removed by centrifugation and filtration. The sample containing the fusion construct was then acidified to pH 2.0 by the addition of 0.6 M HCl to allow the cleavage of Asp-Pro linker peptide, purged with N₂, and incubated at 60 °C for 24 h in a water bath. The pH was then increased to 7–7.2 by the addition of 1 M NH₃, and incubated overnight at 28 °C to selectively precipitate the carrier ONC-Dcless-H6, that is insoluble at neutral or alkaline pH values. The peptides were isolated from insoluble components by repeated cycles of centrifugation, and finally lyophilized. Their purity was checked by SDS/PAGE and mass spectrometry analyses. Lyophilized peptides were then dissolved in pure water, unless differently specified, and quantified by BCA assay (ThermoFisher Scientific, Waltham, MA).

2.5. Mass spectrometry analyses

Matrix-assisted laser desorption/ionisation mass spectrometry (MALDI-MS) was carried out on a 4800 Plus MALDI TOF/TOF mass spectrometer (Applied Biosystems, Framingham, MA) equipped with a nitrogen laser (337 nm). The peptide samples (1 mL) were mixed (1:1, v/v) with a 10 mg/mL solution of a-cyano-4-

hydroxycinnamic acid in acetonitrile/50 mM citrate buffer (70:30 v/v). Mass calibration was performed using external peptide standards purchased from Applied Biosystems, Framingham, MA. Spectra were acquired using 5,000 shots/spectrum in a mass (m/z) range of 1,000–5,000 amu and raw data were analysed using Data Explorer Software provided by the manufacturer.

2.6. Circular dichroism spectroscopy

CD experiments were performed on a Jasco J-815 circular dichroism spectropolarimeter, calibrated for intensity with ammonium [D10] camphorsulfonate ($[\theta_{290.5}] = 7,910 \text{ deg cm}^2 \text{ dmol}^{-1}$). The cell path length was 0.01 cm. CD spectra were collected at 25 °C in the 190–260 nm (far-UV) at 0.2 nm intervals, with a 20 nm/min scan rate, 2.5 nm bandwidth and a 16 s response. Spectra are reported in terms of mean residue ellipticity, calculated by dividing the total molar ellipticity by the number of amino acids in the molecule. Each spectrum was corrected by subtracting the background, and reported without further signal processing. Lyophilized peptides were dissolved in ultra-pure water (Romil, Waterbeach, Cambridge, GB) at a concentration of 100 μM , determined on the basis of peptide dry weight and BCA assay (Thermo-Fisher Scientific, Waltham, MA). CD spectra of the peptides were collected in the absence or in the presence of increasing concentrations of trifluoroethanol (TFE, Sigma Aldrich, Milan, Italy), SDS (Sigma Aldrich, Milan, Italy) or lipopolysaccharide (LPS) from *E. coli* 0111:B4 strain (Sigma Aldrich, Milan, Italy). CD spectra were corrected by subtracting every time the contribution of the compound under test at any given concentration. CD spectra deconvolution was performed by using the program PEPFIT, that is based on peptide-derived reference spectra [29], in order to estimate secondary structure contents. A Microsoft Excel-ported version of PEPFIT was used for convenience [30].

2.7. Measurement of IL-6 release

IL-6 levels were determined by ELISA assay (DuoSet ELISA kits, R&D Systems, Minneapolis, MN) following the manufacturer's instructions. Briefly, RAW 264.7 cells (5×10^4) were seeded into 96-well microtiter plates, and grown to semi-confluency. After 24 h, the culture medium was replaced with fresh medium containing the peptide under test (5 or 20 μM) in the presence or in the absence of LPS from *Salmonella Minnesota* (50 ng/mL, Sigma Aldrich, Milan, Italy) for 24 h at 37 °C. When the protective effect of peptides was evaluated, cells were pre-incubated with the peptide under test (5 or 20 μM) for 2 h at 37 °C. Following treatment, cells were washed three times with PBS prior to incubation with LPS (50 ng/mL) for further 24 h at 37 °C. In each case, at the end of incubation, the culture supernatants were collected, and centrifuged at 5,000 rpm for 3 min at room temperature, in order to remove cell debris. Samples were then analysed by reading absorbance values at 450 nm using 550 nm as a reference wavelength at an automatic plate reader (FLUOstar Omega, BMG LABTECH, Ortenberg, Germany).

2.8. Determination of NO production

To determine the levels of NO released by RAW 264.7 cells, a colorimetric assay based on the use of Griess reagent (Sigma Aldrich, Milan, Italy) was performed. The levels of nitrite (NO_2^-) in cell supernatants were determined on the basis of a reference curve obtained by testing increasing concentrations (from 1 to 50 μM) of sodium nitrite dissolved in water. Briefly, cell culture supernatants were mixed with equal volumes of 1% sulphanyl-amide dissolved in 2.5% phosphoric acid, and incubated for 5 min at room temperature. Samples were then diluted 1:1 (v/v) with

0.1% N-(1-naphthyl) ethylenediamine dihydrochloride, and incubated for further 5 min at room temperature. Absorbance values were then determined at 520 nm using an automatic plate reader (FLUOstar Omega, BMG LABTECH, Ortenberg, Germany).

2.9. Antimicrobial activity assay

The antimicrobial activity of ApoB derived peptides was tested towards eight bacterial strains, i.e. *E. coli* ATCC 25922, methicillin-resistant *Staphylococcus aureus* (MRSA WKZ-2), *Salmonella enteritidis* 706 RIVM, *Bacillus globigii* TNO BM013, *Bacillus licheniformis* ATCC 21424, *Staphylococcus aureus* ATCC 29213, *Pseudomonas aeruginosa* ATCC 27853, and *Pseudomonas aeruginosa* PAO1. In each case, bacteria were grown to mid-logarithmic phase in MHB at 37 °C. Cells were then diluted to 2×10^6 CFU/mL in Nutrient Broth (Difco, Becton Dickinson, Franklin Lakes, NJ) containing increasing amounts of either r(P)ApoB_L or r(P)ApoB_S peptide (0,625–40 μM). In each case, starting from a peptide stock solution, twofold serial dilutions were sequentially carried out, accordingly to broth microdilution method [31]. Following overnight incubation, MIC₁₀₀ values were determined as the lowest peptide concentration responsible for no visible bacterial growth.

2.10. Killing kinetics studies

To kinetically analyse bacterial killing by ApoB derived peptides, experiments were performed on *E. coli* ATCC 25922 and *Bacillus licheniformis* ATCC 21424 strains. To this purpose, bacteria were grown overnight in MHB medium, then diluted in fresh MHB, and incubated at 37 °C until logarithmic phase of growth was reached. Bacteria were then diluted to 4×10^6 CFU/mL in a final volume of 150 μL of Nutrient Broth 0.5X (Difco, Becton Dickinson, Franklin Lakes, NJ), and mixed with the peptide under test (1:1 v/v). For each strain, increasing concentrations of peptide were analysed (ranging from 0 to 20 μM or from 0 to 10 μM in the case of *E. coli* ATCC 25922 and *Bacillus licheniformis* ATCC 21424 strains, respectively). At defined time intervals, samples (20 μL) were serially diluted (from 10- to 10,000-fold), and 100 μL of each dilution was plated on TSA. Following an incubation of 16 h at 37 °C, bacterial colonies were counted.

2.11. Synergy evaluation

Synergism between ApoB derived peptides and antimicrobial agents was assessed by the so called “checkerboard” assay against *S. aureus* MRSA WKZ-2, *E. coli* ATCC 25922, *P. aeruginosa* ATCC 27853, *P. aeruginosa* PAO1, and *S. aureus* ATCC 29213 strains. To this purpose, ApoB derived peptides were tested in combination with EDTA or antibiotics, such as ciprofloxacin, colistin, erythromycin, kanamycin sulfate, and vancomycin. All these antimicrobial agents were from Sigma Aldrich, Milan, Italy. Twofold serial dilutions of each ApoB derived peptide and each antimicrobial agent were tested in combination on each strain tested. To do this, we tested peptide concentrations ranging from 0 to 20 μM . Compound concentrations tested on each strain are reported in Table 1. The fractional inhibitory concentration (FIC) index was calculated as follows: $\text{FIC}_A + \text{FIC}_B$, where $\text{FIC}_A = \text{MIC}$ of drug A in combination/MIC of drug A alone, and $\text{FIC}_B = \text{MIC}$ of drug B in combination/MIC of drug B alone. FIC indexes ≤ 0.5 were classified as synergism, whereas FIC indexes between 0.5 and 4 were associated to additive or “no interaction” effects [32]. Antagonism is usually associated to a FIC index > 4 .

Table 1
Range of antimicrobial agent concentrations tested on each strain for combination therapy analyses.

	<i>S. aureus</i> ATCC 29213	<i>S. aureus</i> MRSA WKZ-2	<i>P. aeruginosa</i> ATCC 27853	<i>P. aeruginosa</i> PAO1	<i>E. coli</i> ATCC 25922
Ciprofloxacin	0–0.5 µg/mL	0–1 µg/mL	0–2 µg/mL	0–1 µg/mL	0–0.03 µg/mL
Colistin	0–8 µg/mL	0–8 µg/mL	0–4 µg/mL	0–4 µg/mL	0–8 µg/mL
Erythromycin	0–4 µg/mL	0–4 µg/mL	0–16 µg/mL	0–128 µg/mL	0–128 µg/mL
Vancomycin	0–0.25 µg/mL	0–0.5 µg/mL	0–32 µg/mL	0–4 µg/mL	0–0.25 µg/mL
Kanamycin	0–0.5 µg/mL	0–0.125 µg/mL	0–64 µg/mL	0–8 µg/mL	0–0.125 µg/mL
EDTA	0–24.53 µg/mL	0–49.07 µg/mL	0–392.5 µg/mL	0–196.2 µg/mL	0–98.14 µg/mL

Each antimicrobial agent was tested for synergistic effects with ApoB derived peptides (0–20 µM) within the concentration range listed in the table, depending from the sensitivity of the specific bacterial strain.

2.12. Anti-biofilm activity

Anti-biofilm activity of ApoB derived peptides was tested on *S. aureus* MRSA WKZ-2, *E. coli* ATCC 25922, *P. aeruginosa* ATCC 27853, and *P. aeruginosa* PAO1 strains. Bacteria were grown overnight in MHB (Becton Dickinson Difco, Franklin Lakes, NJ), and then diluted to 1×10^8 CFU/mL in BM2 medium [33] containing increasing peptide concentrations (0–1 µM). Incubations with the peptides were carried out either for 4 h, in order to test peptide effects on biofilm attachment, or for 24 h, in order to test peptide effects on biofilm formation. When peptide effects on preformed biofilm were evaluated, bacterial biofilms were formed for 24 h at 37 °C, and then treated with increasing concentrations (0–1 µM) of the peptide under test. In all the cases, at the end of the incubation, the crystal violet assay was performed. To do this, the planktonic culture was removed from the wells, which were washed three times with sterile PBS prior to staining with 0.04% crystal violet (Sigma Aldrich, Milan, Italy) for 20 min. The colorant excess was eliminated by three successive washes with sterile PBS. Finally, the crystal violet was solubilised with 33% acetic acid and samples optical absorbance values were determined at 630 nm by using a microtiter plate reader (FLUOstar Omega, BMG LABTECH, Germany). To determine the percentage of viable bacterial cells inside the biofilm structure, upon biofilm disruption with 0.1% Triton X-100 (Sigma Aldrich, Milan, Italy), bacterial cells were ten-fold diluted on solid TSA and incubated for 16 h at 37 °C. Once evaluated the number of colony forming units, bacterial cell survival was calculated as follows: $(CFU_{in\ treated\ sample}/CFU_{in\ untreated\ sample}) \times 100$.

2.13. Cytotoxicity assays

Cytotoxic effects of ApoB derived peptides on RAW 264.7 cells were determined by using the cell proliferator reagent WST-1 (Roche Applied Science, Mannheim, Germany). To this purpose, RAW 264.7 cells were plated into 96-well plates at a density of 5×10^4 cells in 100 µL medium per well, and incubated overnight at 37 °C. Afterwards, cells were treated with increasing concentrations (0–20 µM) of the peptide under test for 24 h at 37 °C. Following incubation, peptide-containing medium was removed, and 100 µL of fresh medium containing 10% WST-1 reagent was added to each well. Following an incubation of 30 min at 37 °C in the dark, sample absorbance values were measured at 450 nm using 650 nm as a reference wavelength at a microtiter plate reader (FLUOstar Omega, BMG LABTECH, Germany).

Cytotoxic effects of peptides on the viability of malignant SVT2 murine fibroblasts, parental murine BALBc 3T3 fibroblasts, human HeLa cells, and human HaCaT keratinocytes were determined by using the 3-(4,5-dimethylthiazol-2-yl)-2,5-diphenyltetrazolium bromide (MTT) assay (Sigma Aldrich, Milan, Italy), as previously described [34]. Briefly, cells were seeded into 96-well plates at a density of 5×10^3 /well in 100 µL medium per well, and incubated overnight at 37 °C. Afterwards, cells were treated with increasing

concentrations (0–20 µM) of the peptide under test for 24 h at 37 °C. Following incubation, the peptide-containing medium was removed, and 100 µL of MTT reagent, dissolved in DMEM without phenol red (Sigma Aldrich, Milan, Italy), were added to the cells (100 µL/well) at a final concentration of 0.5 mg/mL. After 4 h at 37 °C, the culture medium was removed and the resulting formazan salts were dissolved by the addition of isopropanol containing 0.1 N HCl (100 µL/well). Absorbance values of blue formazan were determined at 570 nm using an automatic plate reader (Microbeta Wallac 1420, Perkin Elmer).

In all the cases, cell survival was expressed as the percentage of viable cells in the presence of the peptide under test, with respect to control cells grown in the absence of the peptide.

2.14. Haemolytic activity

The release of haemoglobin from mouse erythrocytes was used as a measure for the haemolytic activity of ApoB derived peptides. To do this, EDTA anti-coagulated mouse blood was centrifuged for 10 min at 800g at 20 °C, in order to obtain red blood cells (RBCs), which were washed three times, and 200-fold diluted in PBS. Subsequently, 75 µL aliquots of RBCs were added to 75 µL peptide solutions (final concentration ranging from 0 to 20 µM) in 96-well microtiter plates, and the mixture was incubated for 1 h at 37 °C. Following the incubation, the plate was centrifuged for 10 min at 1,300g at 20 °C, and 100 µL supernatant of each well were transferred to a new 96-well plate. Absorbance values were determined at 405 nm by using an automatic plate reader (FLUOstar Omega, BMG LABTECH, Germany), and the percentage of haemolysis was calculated by comparison with the control samples containing no peptide (negative control) or 0.2% (v/v) Triton X-100 (positive control, complete lysis). Haemolysis (%) = $[(Abs_{405\ nm\ peptide} - Abs_{405\ nm\ negative\ control}) / (Abs_{405\ nm\ 0.2\% \text{ Triton}} - Abs_{405\ nm\ negative\ control})] \times 100$.

2.15. Wound healing assay

Wound healing activity of r(P)ApoB₁ peptide was evaluated *in vitro* as previously described [35]. Human HaCaT keratinocytes were seeded into 12-well plates at a density of 6.3×10^5 cells/well in 1 mL medium per well. Following an incubation of 24 h at 37 °C, cells were pre-treated with 3 µM mitomycin C for 30 min, in order to inhibit cell proliferation [36]. Cell monolayers were then wounded with a pipette tip to remove cells from a specific region of the monolayer. The culture medium was then removed and the cells were washed twice with PBS. Cells were then incubated with fresh culture medium containing increasing concentrations of r(P)ApoB₁ peptide (0–0.5–10–20 µM). Wound closure was then followed by multiple field time-lapse microscopy (TLM) experiments, using an inverted microscope (Zeiss Axiovert 200, Carl Zeiss, Germany) equipped with an incubator to control temperature, humidity and CO₂ percentage [37,38]. Images were iteratively acquired in phase contrast with a CCD video camera (Hamamatsu

Orca AG, Japan) by using a $5\times$ objective. The microscope was also equipped with a motorized stage and focus control (Marzhauser, Germany) enabling automated positioning of the acquired samples. The workstation was controlled through a homemade software in Labview. Each cell sample was analysed in duplicate, and in any case at least two fields of view were selected. Since three independent experiments were carried out, from 8 to 12 independent fields of view were analysed for each sample. The delay between consecutive imaging of the same field of view was set to 15 min. The wound closure dynamics were quantified by using a homemade automated image analysis software, that allowed to measure the size of the wound area for each time point (A). For each field of view, determined values were normalized with respect to the value of the wound area at time 0 (A_0), and plotted as function of time. After an initial lag phase, the wound area was found to decrease with a constant velocity [39,40]. By reporting A/A_0 values as a function of time, a linear decrease was observed for A/A_0 values lower than 0.8 (Fig. 9b). For each sample, the lag time t_l was calculated as the time required to obtain an initial wound closure corresponding to $A/A_0 = 0.8$. Being R^2 typically higher than 0.98, the linear range of the curve was fitted, and the slope ($-\alpha$) was considered a measure of the wound closure velocity. The values of wound closure velocity obtained for each field of view from

three independent experiments were averaged (α), and normalized with respect to the value of the corresponding control sample ($\alpha/\alpha_{\text{contr}}$). For each peptide concentration tested, $\alpha/\alpha_{\text{contr}}$ values obtained from three independent experiments were averaged and the standard error of the mean was calculated to account for reproducibility [41].

2.16. Statistical analysis

Statistical analysis was performed using a Student's *t*-Test. Significant differences were indicated as * ($P < 0.05$), ** ($P < 0.01$) or *** ($P < 0.001$).

3. Results

3.1. Recombinant production of ApoB derived peptides

Expression of HDPs in bacterial cells can be deleterious to the host due to their toxicity. For this reason, we used a procedure to produce HDPs as fusion proteins with onconase (ONC), a frog ribonuclease that mediates the delivery to inclusion bodies very efficiently, as previously described [24,27], thus avoiding toxicity problems. DNA sequences encoding peptide ApoB887-923 or

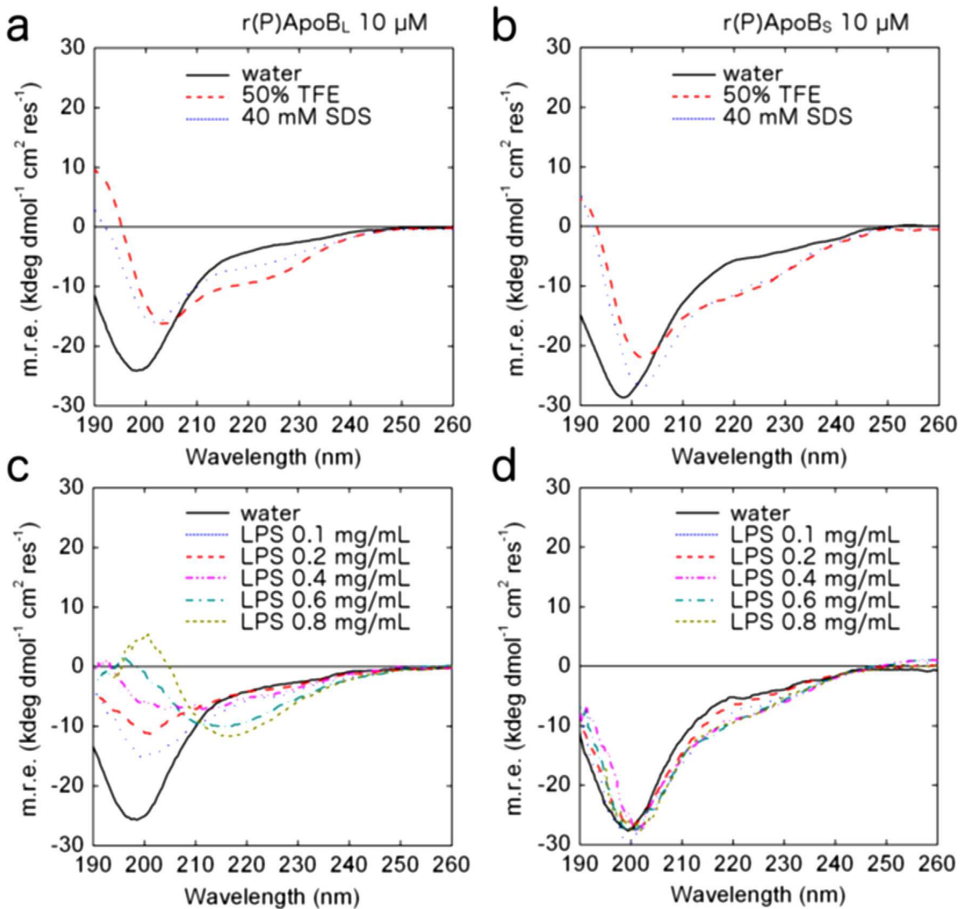


Fig. 2. Far-UV CD spectra of recombinant peptides r(P)ApoB_L (a, c) and r(P)ApoB_S (b, d) at a concentration of 10 μM in the presence of increasing concentrations of membrane-mimicking agents TFE or SDS at micellar concentrations (a, b) or of LPS (c, d).

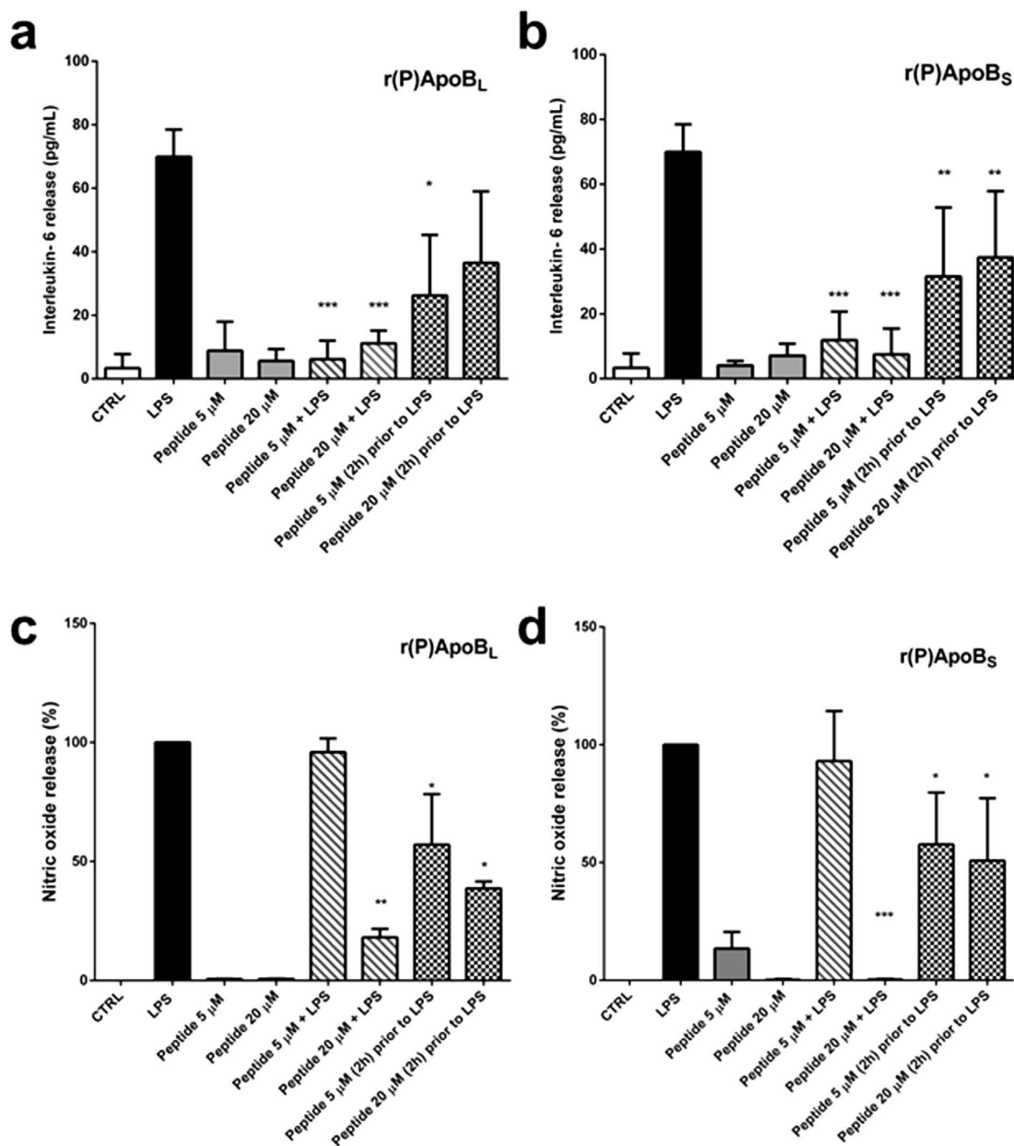


Fig. 3. Effects of ApoB derived peptides on the release of IL-6 (a, b) and NO (c, d) in mouse macrophages RAW 264.7 stimulated with LPS (50 ng/mL) from *Salmonella Minnesota*. The effects of r(P)ApoB_L (a, c) and r(P)ApoB_S (b, d) peptides were evaluated either co-incubating cells with the peptide under test (5 or 20 μM) and LPS (oblique grey lanes) or by treating cells with the peptide under test (5 or 20 μM) for 2 h at 37 °C prior to incubation with LPS (chessboard bars). Results were compared to those obtained in the case of control untreated cells (white bars), cells stimulated with the LPS alone (black bars), or cells incubated with two different concentrations (5 or 20 μM) of peptide (grey bars). Data represent the mean (±standard deviation, SD) of at least three independent experiments, each one carried out with triplicate determinations. *P < 0.05, **P < 0.01, or ***P < 0.001 were obtained for control versus treated samples.

peptide ApoB887-911, synthesized by MWG Biotech in conformity with the *E. coli* codon usage, were cloned into the expression vector pET22b(+), downstream to a sequence encoding a mutated form of ONC. The resulting fusion proteins contain a His tag sequence, positioned between the ONC and the peptide moieties, suitable for an easy purification of the fusion protein, a flexible linker (Gly-Thr-Gly), and a dipeptide (Asp-Pro), which is cleaved in mild acidic conditions thus allowing the release of the peptide from the carrier. Since the carrier is insoluble at neutral or alkaline pH, ApoB

derived peptides were isolated from insoluble components by repeated cycles of centrifugation, and finally lyophilized. Peptides' purity was checked by SDS/PAGE and matrix assisted laser desorption ionisation (MALDI) mass spectrometry analyses. Recombinant peptides were found to be 99% pure. Molecular mass values of ApoB887-923 and ApoB887-911 were found to be 4,072.3 Da (Theoretical MH⁺ 4072.7) and 2,820.9 Da (Theoretical MH⁺ 2820.2), respectively, values which are in agreement with the expected molecular weights of the peptides with the addition of a Pro

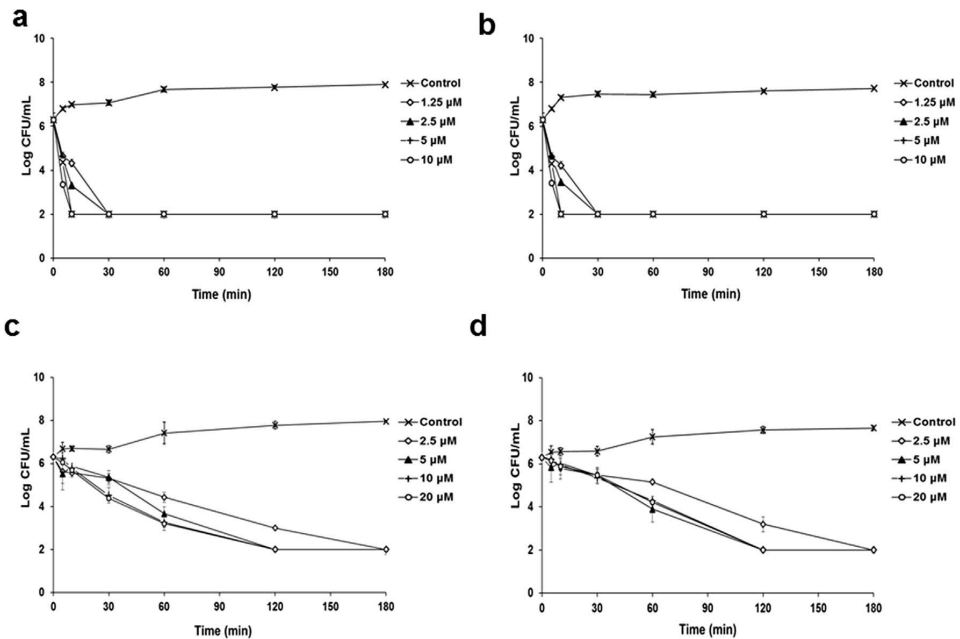


Fig. 4. Time killing curves obtained by incubating *Bacillus licheniformis* ATCC 21424 (a, b) and *E. coli* ATCC 25922 (c, d) strains with increasing concentrations of r(P)ApoB₁ (a, c) or r(P)ApoB₅ (b, d) peptides for different lengths of time. Data represent the mean (\pm standard deviation, SD) of at least three independent experiments, each one carried out with triplicate determinations.

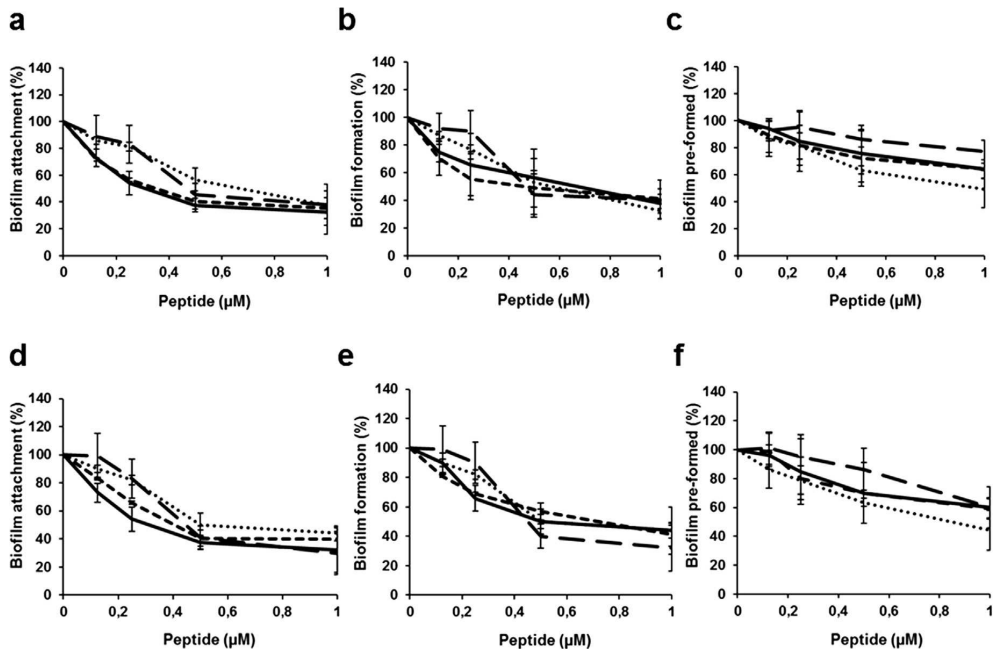


Fig. 5. Anti-biofilm activity of r(P)ApoB₁ (—), r(P)ApoB₅ (---), CATH-2 (---), and LL-37 (●●●) peptides on *E. coli* ATCC 25922 (a, b, c) and *S. aureus* MRSA WKZ-2 (d, e, f) strains in BM2 medium. The effects of increasing concentrations of peptides were evaluated either on biofilm attachment (a, d), biofilm formation (b, e), or on pre-formed (c, f) biofilm. Biofilm was stained with crystal violet and measured at 630 nm. Data represent the mean (\pm standard deviation, SD) of at least three independent experiments, each one carried out with triplicate determinations. For all the experimental points, *P < 0.05, **P < 0.01, or ***P < 0.001 were obtained for control versus treated samples.

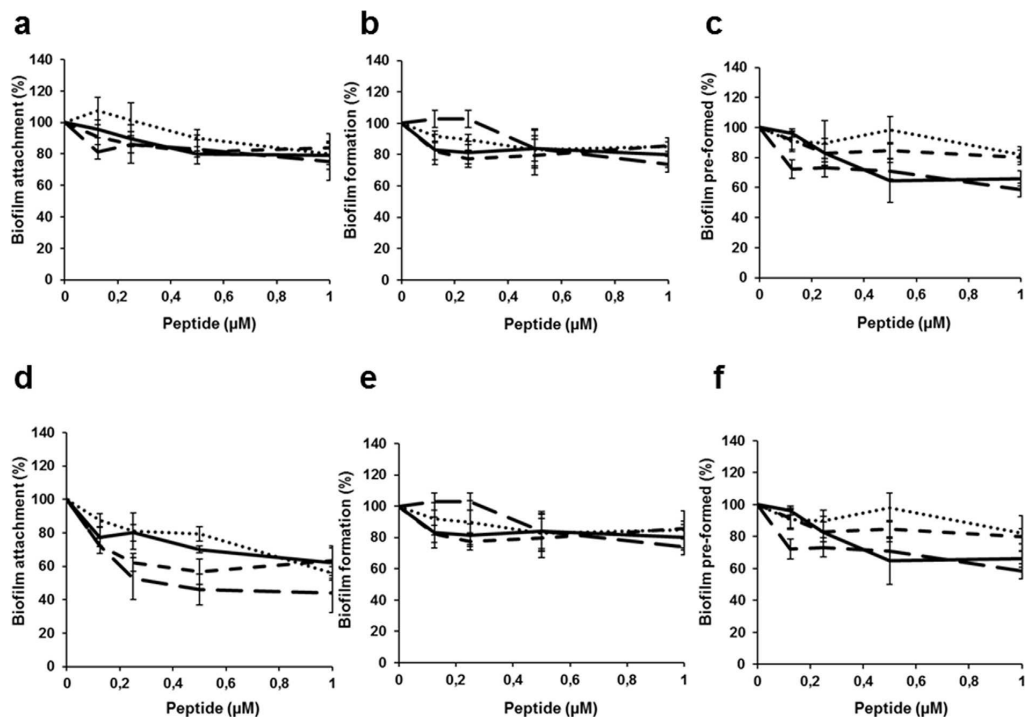


Fig. 6. Anti-biofilm activity of r(P)ApoB_L (—), r(P)ApoB_S (---), CATH-2 (····), and LL-37 (—•••) peptides on *P. aeruginosa* ATCC 27853 (a, b, c) and *P. aeruginosa* PAO1 (d, e, f) strains in BM2 medium. The effects of increasing concentrations of peptides were evaluated either on biofilm attachment (a, d), biofilm formation (b, e), or on pre-formed (c, f) biofilm. Biofilm was stained with crystal violet and measured at 630 nm. Data represent the mean (±standard deviation, SD) of at least three independent experiments, each one carried out with triplicate determinations. For all the experimental points, *P < 0.05, or **P < 0.01 were obtained for control versus treated samples.

residue deriving from the cleavage of the Asp-Pro bond. The final yield of peptides ApoB887-923 and ApoB887-911, here named r(P)ApoB_L and r(P)ApoB_S, was about 7 and 4 mg/L of bacterial culture, respectively.

3.2. Conformational analyses of r(P)ApoB_L and r(P)ApoB_S peptides by Far-UV circular dichroism

To analyse the secondary structure of recombinant ApoB derived peptides, we performed Far-UV CD spectra, and found that both peptides are largely unstructured in pure water (Fig. 2a and b). We also evaluated the effects of membrane-mimicking agents, such as TFE and SDS at micellar concentrations, on peptide conformation. We found that r(P)ApoB_L secondary structure shifts mainly towards an α -helical conformation in presence of both membrane-mimicking agents, and only a partial (<10%) increase in β -strand content is observed (Table 2). This is clearly evidenced by the presence of two broad minima at around 208 and 222 nm, and a maximum at <200 nm (Fig. 2a). A similar behavior has been described for different HDPs [24,42,43], and suggests that r(P)ApoB_L peptide is prone to assume a specific ordered conformation when interacting with membrane-mimicking agents. Similar effects, even if significantly less pronounced, were observed in the case of r(P)ApoB_S peptide (Fig. 2b and Table 2). No appreciable β -strand formation was observed for this peptide, probably indicating that, in the r(P)ApoB_L peptide, β -strand propensity is mainly localized in the C-terminus region.

We also analysed by CD spectroscopy the effects of the endotoxin LPS (lipopolysaccharide), the predominant glycolipid in the outer membrane of Gram-negative bacteria [44], on the peptide

conformations (Fig. 2c and d and Table 2). When r(P)ApoB_L secondary structure was analysed in the presence of increasing concentrations (from 0.1 to 0.8 mg/mL) of *E. coli* LPS, the progressive appearance of a maximum at approximately 200 nm and of a minimum at approximately 218 nm suggested that the peptide tends to assume a prevalently β -strand conformation, probably induced by its interaction with LPS (Fig. 2c and Table 2). As expected on the basis of previous analyses, in which r(P)ApoB_S does not show any β -strand content, no significant effects were observed in the case of r(P)ApoB_S (Fig. 2d and Table 2) under the experimental conditions tested.

3.3. Analysis of the immunomodulatory activity of r(P)ApoB_L and r(P)ApoB_S peptides

Based on CD analyses, we hypothesized that an interaction between r(P)ApoB_L peptide and LPS occurs. Since it is widely reported that HDPs are able to mitigate the pro-inflammatory effects induced by endotoxins [45], we tested the anti-inflammatory properties of ApoB derived peptides by monitoring their effects on LPS induced interleukin-6 (IL-6) release, as well as on nitric oxide (NO) release in murine macrophages (RAW 264.7 cell line). In fact, it is known that, upon activation by internal and external stimuli, macrophages produce and secrete various endogenous inflammatory mediators, such as nitric oxide (NO) and pro-inflammatory cytokines, including interleukin-6 [46,47].

To test the effects of ApoB derived peptides on the release of IL-6, ELISA assays were performed on LPS stimulated RAW 264.7 cells. As shown in Fig. 3a and b, a significant release of IL-6 was observed in control cells incubated with LPS from *Salmonella*

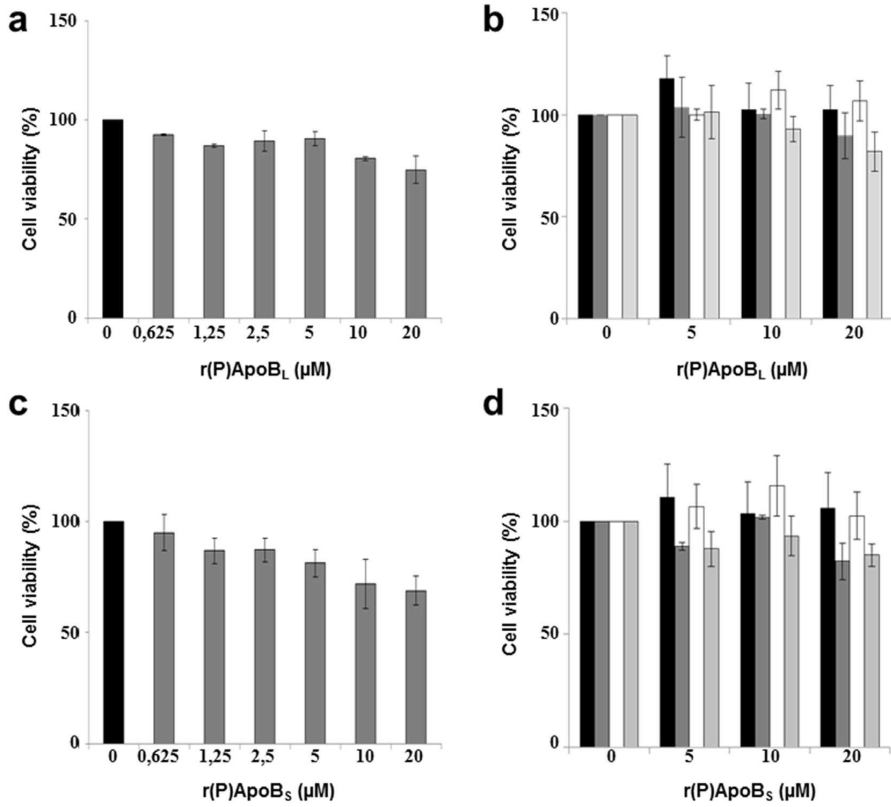


Fig. 7. Effects of r(P)ApoB_L (a, b) and r(P)ApoB_S (c, d) peptides on the viability of RAW 264.7 (a, c), BALBc3T3 (black bars in b, d), SVT2 (dark grey bars in b, d), Hela (white bars in b, d), and HaCaT (light grey bars in b, d) cells. Cell viability was assessed by WST-1 (a, c) or MTT (b, d) assay, and expressed as the percentage of viable cells with respect to controls (untreated cells). Error bars indicate standard deviations obtained from at least three independent experiments, each one carried out with triplicate determinations.

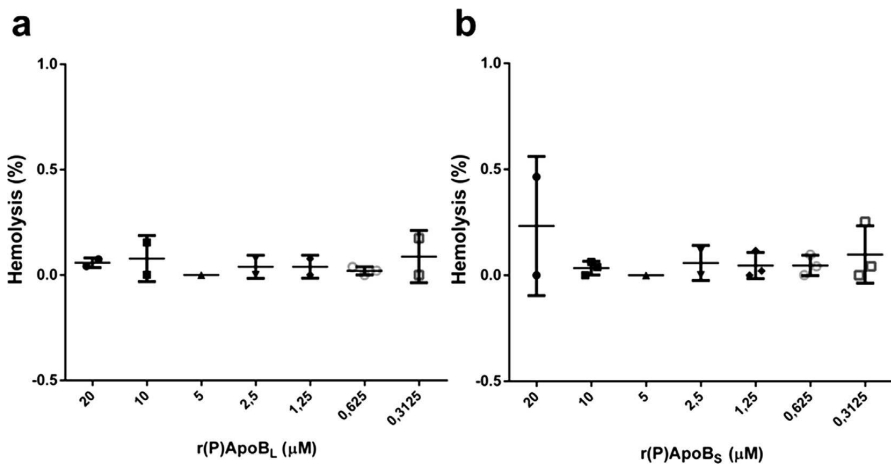


Fig. 8. Haemolytic activity of r(P)ApoB_L (a) and r(P)ApoB_S (b) peptides towards murine red blood cells (RBCs) after 1 h of incubation at 37 °C. Data represent the mean (±standard deviation, SD) of at least three independent experiments, each one carried out with triplicate determinations.

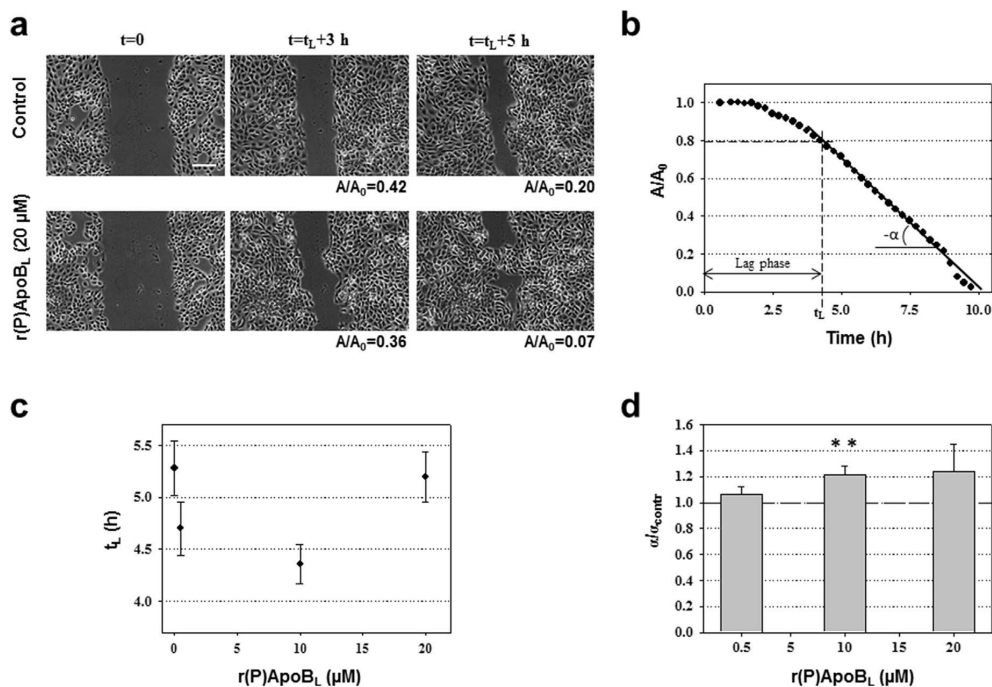


Fig. 9. Wound healing activity of r(P)ApoB_L peptide on HaCaT cells monolayer. Cells were pre-treated for 30 min with 3 μM mitomycin C, and then wounded prior to incubation with r(P)ApoB_L peptide (0.5–10–20 μM) for 12 h at 37 °C. Images were acquired for untreated HaCaT cells and for cells treated with 20 μM peptide (a). The lag phase time (t_L) corresponds to the time interval before the linear decrease of the wound area. Images were acquired at time t = 0 (a, on the left), 3 h after t_L (a, in the middle) and 5 h after t_L (a, on the right). For each sample, A/A₀ values are reported, where A is the wound area after a specific incubation time and A₀ is the wound area at time 0. Scale bar = 150 μm. In (b), evolution in time of the wound area (A), normalized with respect to A₀, is reported for a control sample. A homemade automated image analysis software was used to measure the size of the cell-free area (A) for each time point. For A/A₀ values < 0.8, a linear correlation with the incubation time was found. The slope -α of the linear fit, reported as a continuous line, represents a measure of the wound closure velocity. In (c), determined t_L values are reported as a function of peptide concentration (0–0.5–10–20 μM). In (d), wound closure velocity (α), normalized with respect to control sample (α_{contr}), is reported as a function of peptide concentration (0.5–10–20 μM). The dashed line corresponds to α/α_{contr} = 1. In (c) and (d), each data point represents the mean (±standard error) of three independent experiments. **P < 0.01 was obtained for control versus treated samples.

Table 2
Analysis of r(P)ApoB_L and r(P)ApoB_S peptides secondary structure.

	H ₂ O			TFE		
	α-Helix (%)	β-Strand (%)	Random coil (%)	α-Helix (%)	β-Strand (%)	Random coil (%)
r(P)ApoB _L	5	12	83	26	18	56
r(P)ApoB _S	7	3	90	26	0	74
	SDS			LPS		
	α-Helix (%)	β-Strand (%)	Random coil (%)	α-Helix (%)	β-Strand (%)	Random coil (%)
r(P)ApoB _L	17	21	62	11	64	25
r(P)ApoB _S	29	3	68	18	2	80

Secondary structure content of ApoB derived peptides in water and in the presence of trifluoroethanol (TFE), sodium dodecyl sulfate (SDS), and lipopolysaccharide (LPS), calculated by means of PEPFIT program.

Minnesota (50 ng/mL). When murine macrophages were incubated with LPS (50 ng/mL) in the presence of either r(P)ApoB_L (Fig. 3a) or r(P)ApoB_S (Fig. 3b) peptide (two different peptide concentrations), a strong decrease of IL-6 release was observed with respect to LPS induced control cells. Moreover, we found that both peptides have a significant protective effect on LPS stimulated RAW 264.7 cells. In fact, when macrophages were pre-treated for 2 h with either r(P)ApoB_L or r(P)ApoB_S peptide and then incubated for further 24 h with LPS, a significant decrease of IL-6 release was observed (Fig. 3a and b).

Similar results were observed when the effects of ApoB derived peptides were tested on NO release (Fig. 3c and d). Also in this case, following co-incubation of cells with LPS from *Salmonella Minnesota* and either r(P)ApoB_L or r(P)ApoB_S peptide, a significant attenuation of NO release with respect to control cells was detected (Fig. 3c and d). However, in this case, it has to be noticed that a significant effect of peptides on NO release was observed only at the highest peptide concentration tested (20 μM), while at 5 μM concentration both peptides were found to be almost ineffective (Fig. 3c and d). However, when RAW 264.7 cells were

pre-treated for 2 h with 5 or 20 μM of either r(P)ApoB_L or r(P)ApoB_S peptide and subsequently stimulated for 24 h with LPS (50 ng/mL), a significant reduction of NO release was observed even at 5 μM peptide concentration (Fig. 3c and d), thus confirming the protective effect of both peptides on LPS stimulated RAW 264.7 cells.

3.4. Antimicrobial activity of r(P)ApoB_L and r(P)ApoB_S peptides

The antibacterial activity of recombinant ApoB derived peptides was determined by measuring their MIC₁₀₀ values on a panel of Gram-negative and Gram-positive bacterial strains (Table 3). A significant antimicrobial activity of r(P)ApoB_L and r(P)ApoB_S peptides was detected towards four out of eight strains tested, i.e. *E. coli* ATCC 25922, *P. aeruginosa* PAO1, *B. globigii* TNO BM013, and *B. licheniformis* 21424, for which almost identical MIC₁₀₀ values were calculated for both ApoB derived peptides. Notably, MIC₁₀₀ values were found to be comparable or even significantly lower than those determined when control cathelicidin-2 (CATH-2), a known HDP from chicken [48], was tested (Table 3). These data indicate that r(P)ApoB_L and r(P)ApoB_S peptides are endowed with a broad-range antimicrobial activity, being effective on both Gram-negative and Gram-positive bacterial strains. On the other hand, ApoB derived peptides were found to be ineffective towards *P. aeruginosa* ATCC 27853, methicillin-resistant *S. aureus* (MRSA WKZ-2), and *S. aureus* 29213 (Table 3), while, in the case of *S. enteritidis* 706 RIVM, a significant antibacterial effect was elicited only by r(P)ApoB_L peptide.

To analyse the kinetic of peptides bactericidal activity, kinetic killing curves were obtained by treating *E. coli* ATCC 25922 and *B. licheniformis* ATCC 21424 strains, highly susceptible to both peptides (Table 3), with increasing concentrations of either r(P)ApoB_L or r(P)ApoB_S for different times (0–180 min). We found that, at the highest peptide concentrations tested (5–10 μM), *B. licheniformis* cells were killed within 10 min, while at the lowest peptide concentrations (1.25–2.5 μM) the same effect was obtained within 30 min (Fig. 4a and b). When peptides were tested on *E. coli* ATCC 25922 at high concentrations (5–10 μM), bacterial cells were killed within 120 min, while at the lowest peptide concentration (2.5 μM) the same effect was obtained within 180 min (Fig. 4c and d).

3.5. Combination therapy analyses

To potentiate the antimicrobial efficacy of recombinant ApoB derived peptides for therapeutic purposes, especially against *P. aeruginosa* and *S. aureus* strains, we carried out combination

therapy analyses by concomitantly administrating peptides and antibiotics in various combinations to bacteria. One of the best known tests to evaluate synergism between two compounds is the so called “chequerboard” experiment, in which a two-dimensional array of serial concentrations of test compounds is used as the basis for calculation of a fractional inhibitory concentration (FIC) index to demonstrate that paired combinations of agents can exert inhibitory effects that are more than the sum of their effects alone [32]. It is generally accepted that FIC indexes ≤ 0.5 are indicative of “synergy”; FIC indexes comprised between >0.5 and 4.0 are, instead, associated to “additive” or “no interaction” effects, whereas FIC indexes >4.0 are indicative of “antagonism” [32].

As reported in Table 4, all the combinations tested were found to be effective, either with additive or synergistic effects between peptides and antibiotics. Notably, no FIC indexes higher than 2 were measured.

The most potent combinations were obtained in the presence of EDTA, which was selected for its ability to affect bacterial outer membrane permeability, thus sensitizing bacteria to a number of antibiotics [49–51]. Very pronounced synergistic effects were observed for both ApoB derived peptides in combination with EDTA on *S. aureus* MRSA WKZ-2 and both *P. aeruginosa* strains.

Both peptides were found to act synergistically with (i) ciprofloxacin on all the strains tested (Table 4); (ii) colistin on all the strains tested, except for *S. aureus* ATCC 29213 (Table 4); (iii) vancomycin on *S. aureus* MRSA WKZ-2, *P. aeruginosa* strains and *E. coli* ATCC 25922 (Table 4); (iv) erythromycin on *P. aeruginosa* ATCC

Table 4
Combination therapy analyses.

Bacterial strains	Antibiotic	ΣFICI^a	
		r(P)ApoB _L	r(P)ApoB _S
Methicillin resistant <i>S. aureus</i> MRSA WKZ-2	Ciprofloxacin	0.328	0.365
	Colistin	0.340	0.350
	Erythromycin	1.094	1.375
	Vancomycin	0.425	0.316
	Kanamycin	2.000	0.387
	EDTA	0.278	0.360
<i>S. aureus</i> ATCC 29213	Ciprofloxacin	0.340	0.413
	Colistin	1.049	1.024
	Erythromycin	1.049	1.146
	Vancomycin	1.049	1.097
	Kanamycin	1.049	0.352
	EDTA	1.049	0.351
<i>P. aeruginosa</i> ATCC 27853	Ciprofloxacin	0.347	0.328
	Colistin	0.267	0.255
	Erythromycin	0.389	0.170
	Vancomycin	0.379	0.306
	Kanamycin	0.479	1.030
	EDTA	0.333	0.089
<i>P. aeruginosa</i> PAO1	Ciprofloxacin	0.396	0.444
	Colistin	0.144	0.266
	Erythromycin	0.569	0.556
	Vancomycin	0.500	0.486
	Kanamycin	0.507	0.389
	EDTA	0.396	0.438
<i>E. coli</i> ATCC 25922	Ciprofloxacin	0.363	0.442
	Colistin	0.438	0.292
	Erythromycin	1.243	1.292
	Vancomycin	0.428	0.426
	Kanamycin	0.603	0.572
	EDTA	0.729	0.750

Fractional inhibitory concentration (FIC) indexes determined for r(P)ApoB_L and r(P)ApoB_S peptides tested in combination with antibiotics or EDTA on Gram-positive and Gram-negative bacterial strains. Indexes were obtained from a minimum of three independent experiments, each one carried out with triplicate determinations.

Table 3
Antibacterial activity of ApoB derived peptides.

	MIC ₁₀₀ (μM)		
	r(P)ApoB _L	r(P)ApoB _S	CATH-2
Gram-negative strains			
<i>Escherichia coli</i> ATCC 25922	10	10	10
<i>Pseudomonas aeruginosa</i> ATCC 27853	>40	>40	10
<i>Pseudomonas aeruginosa</i> PAO1	20	20	20
<i>Salmonella enteritidis</i> 706 RIVM	10	>40	10
Gram-positive strains			
<i>Staphylococcus aureus</i> MRSA WKZ-2	>40	>40	10
<i>Bacillus globigii</i> TNO BMO13	5	2.5	5
<i>Bacillus licheniformis</i> ATCC 21424	1.25	1.25	20
<i>Staphylococcus aureus</i> ATCC 29213	>40	>40	10

Minimum Inhibitory Concentration (MIC, μM) values determined for r(P)ApoB_L and r(P)ApoB_S peptides tested on a panel of Gram-positive and Gram-negative bacterial strains. Chicken CATH-2 peptide was used as a positive control. Values were obtained from a minimum of three independent experiments.

27853 (Table 4). In the latter case, a FIC index of 0.38 and 0.17 for r(P)ApoB_L and r(P)ApoB_S peptides, respectively, was obtained. In the case of kanamycin, the response varied depending on the peptide and the specific bacterial strain. In fact, r(P)ApoB_L was found to act synergistically with this antibiotic prevalently on Gram-negative bacteria, particularly on the *P. aeruginosa* strains, whereas r(P)ApoB_S peptide was found to be very active in the presence of kanamycin against both *S. aureus* strains as well as against *P. aeruginosa* PAO1 strain (FIC indexes < 0.4).

It should be emphasized that combinations of ApoB derived peptides with antibiotics or EDTA were found to have a strong antimicrobial activity also towards strains on which the peptides alone were found to be ineffective, such as both *S. aureus* strains and *P. aeruginosa* ATCC 27853 (Table 3). Notably, we did not observe any antagonistic interactions between the peptides and the antimicrobials under test.

3.6. Anti-biofilm activity of r(P)ApoB_L and r(P)ApoB_S peptides

Anti-biofilm peptides represent a very promising approach to treat biofilm-related infections and have an extraordinary ability to interfere with various stages of the biofilm growth mode [52]. To test whether recombinant ApoB derived peptides are endowed with anti-biofilm activity, we performed experiments on different bacterial strains, such as *E. coli* ATCC 25922, *Pseudomonas aeruginosa* PAO1, *Pseudomonas aeruginosa* ATCC 27853, and methicillin-resistant *Staphylococcus aureus* MRSA WKZ-2 in BM2 medium. The same experiments were also performed using LL-37 control peptide, that is a human antimicrobial peptide known to have a significant anti-biofilm activity against multidrug-resistant bacterial strains [53]. We also tested for the first time CATH-2 anti-biofilm activity. Three different approaches were followed. At first, we tested the peptide effects on biofilm attachment. To do this, the bacterial culture, following overnight growth, was diluted in BM2 medium containing increasing concentrations of the peptide under test (0–1 μM), and incubated for 4 h at 37 °C. Following incubation, biofilm analysis by crystal violet staining revealed a significant dose-dependent inhibition of biofilm attachment in the case of *E. coli* ATCC 25922 (Fig. 5a) and *S. aureus* MRSA WKZ-2 (Fig. 5d) strains treated with r(P)ApoB_L (continuous line in Fig. 5a, d) or r(P)ApoB_S (smaller dashed line in Fig. 5a, d) peptides. Similar results were obtained on these two strains in the case of peptides CATH-2 (larger dashed line in Fig. 5a, d) and LL-37 (dotted line in Fig. 5a, d). Strong effects were also displayed by ApoB derived peptides on biofilm attachment in the case of *P. aeruginosa* PAO1 strain (Fig. 6d). A less pronounced effect of ApoB derived peptides (about

20% inhibition of biofilm formation) was observed, instead, on *P. aeruginosa* ATCC 27853 biofilm attachment (Fig. 6a).

Second, we tested the effect of ApoB derived peptides on biofilm formation. To investigate this phenomenon, we followed the experimental procedure described above with the only exception that bacterial cells were incubated with increasing concentrations of peptides for 24 h at 37 °C. Also in this case, we observed a significant dose-dependent inhibition of biofilm formation in the case of *E. coli* ATCC 25922 (Fig. 5b) and *S. aureus* MRSA WKZ-2 (Fig. 5e) strains treated with r(P)ApoB_L (Fig. 5b, e) or r(P)ApoB_S (Fig. 5b, e) peptides. Similar effects were elicited by peptides CATH-2 (Fig. 5b, e) and LL-37 (Fig. 5b, e). ApoB derived peptides strongly affected also *P. aeruginosa* PAO1 biofilm formation (Fig. 6e). In the case of *P. aeruginosa* ATCC 27853, instead, a less pronounced effect (about 20% biofilm formation inhibition) was observed for all the peptides under test (Fig. 6b).

Third, we tested the effect of ApoB derived peptides on preformed biofilms. By incubating preformed biofilms of *E. coli* ATCC 25922 (Fig. 5c) and *S. aureus* MRSA WKZ-2 (Fig. 5f) strains with increasing concentrations of r(P)ApoB_L (Fig. 5c, f) or r(P)ApoB_S (Fig. 5c, f), we found a significant reduction (about 50%), an effect even stronger than that observed in the case of CATH-2 peptide (Fig. 5c, f). Similar results were observed in the case of *P. aeruginosa* PAO1 strain (Fig. 6f). On the other hand, when the peptides were tested on *P. aeruginosa* ATCC 27853 preformed biofilm, a slight effect (about 20% reduction) was observed for all the peptides except for CATH-2, which was found to have a strong effect (about 50% reduction, Fig. 6c).

We also evaluated the percentage of viable bacterial cells inside the biofilm structure by colony counting assay. We found that, even at the highest ApoB derived peptides concentrations tested, a significant percentage of bacterial cells appeared to be still alive (Table 5). Similar results were also obtained in the case of LL-37 and CATH-2 control peptides on both *P. aeruginosa* strains (Table 5), even if it has to be noticed that, in the case of biofilm formation, both control peptides affected the viability of *P. aeruginosa* PAO1 cells more than ApoB derived peptides (Table 5). CATH-2 and LL-37 control peptides were also found to strongly impair the viability of *E. coli* ATCC 25922 and *S. aureus* MRSA WKZ-2 cells in the case of biofilm eradication (Table 5).

3.7. Biocompatibility of r(P)ApoB_L and r(P)ApoB_S peptides

The development of HDPs as therapeutic agents is strictly related to their selective toxicity towards bacterial cells [54]. The presence of zwitterionic phospholipids and cholesterol on the

Table 5
Effects of peptides on the viability of bacterial cells inside the biofilm structure.

	In biofilm attachment (%)				In biofilm formation (%)				In biofilm eradication (%)			
	r(P)ApoB _L	r(P)ApoB _S	CATH-2	LL-37	r(P)ApoB _L	r(P)ApoB _S	CATH-2	LL-37	r(P)ApoB _L	r(P)ApoB _S	CATH-2	LL-37
<i>E. coli</i>												
ATCC 25922	105±7	101±9	15±5	97±8	79±7	79±9	40±3	73±12	83±14	80±5	15±2	37±6
MRSA WKZ-2	90±7	102±9	35±5	70±4	66±7	60±8	23±3	69±12	66±11	70±3	10±2	17±6
<i>P. aeruginosa</i>												
ATCC 27853	76±11	68±10	91±5	60±13	66±13	64±14	96±16	77±15	70±15	59±9	59±12	69±5
<i>P. aeruginosa</i>												
PAO1	52±12	77±15	45±7	47±7	55±14	57±14	35±16	25±14	44±15	86±6	50±10	58±9

Effects of r(P)ApoB_L, r(P)ApoB_S, CATH-2, and LL-37 peptides (1 μM) on the viability of bacterial cells inside the biofilm structure. To determine the percentage of viable bacterial cells, biofilm was lysed with Triton X-100 (0.1%), bacterial cells were ten-fold diluted, and colonies were counted after an incubation of 16 h at 37 °C. Data are expressed as percentage with respect to control untreated samples, and represent the mean (±standard deviation, SD) of at least three independent experiments, each one carried out with triplicate determinations. For all the experimental points, *P < 0.05, or **P < 0.01 were obtained for control versus treated samples.

outer leaflet of eukaryotic cell membranes largely accounts for the preference of HDPs for bacterial membranes over eukaryotic membranes [55,56]. To deepen on the therapeutic potential of ApoB derived peptides, we analysed their cytotoxic effects towards a panel of mouse and human eukaryotic cells. The addition of increasing concentrations (from 0.625 to 20 μM) of ApoB derived peptides to mouse macrophages Raw 264.7 cells for 24 h did not result in any significant reduction in cell viability (Fig. 7a and c). A slight toxicity was detected only at the highest peptide concentrations tested (10 and 20 μM in Fig. 7a and c). We also tested ApoB derived peptides on murine embryo fibroblasts BALBc 3T3 and their tumor counterpart, *i.e.* SVT2 simian virus 40-transformed cell line (Fig. 7b and d). A slight toxicity (10–20%) was detected only in the case of SVT2 cells at the highest concentration tested (20 μM in Fig. 7b and d). Moreover, no significant toxic effects were detected when ApoB derived peptides were assayed on human cervical cancer HeLa cells (Fig. 7b and d), while a slight toxicity (~20%) was observed in the case of human keratinocytes (HaCaT cells) at the highest concentration (20 μM in Fig. 7b and d). ApoB derived peptides were also tested on murine red blood cells (RBCs) to exclude haemolytic effects. As shown in Fig. 8, both peptides did not exert any lytic effect on mouse RBCs, even at the highest concentration tested (20 μM).

3.8. Wound healing activity of r(P)ApoB_L peptide

Numerous studies support the hypothesis that human HDPs promote wound healing in skin, by modulating cytokine production, cell migration, proliferation and, in some cases, angiogenesis [57]. Based on this, we performed experiments to test whether r(P)ApoB_L peptide is able to stimulate wound re-epithelialization by human keratinocytes (HaCaT cell line). To this purpose, we performed a classical *in vitro* wound healing assay to evaluate peptide effects on cell migration. HaCaT cell monolayers were pre-treated with 3 μM mitomycin C for 30 min, and then wounded with a pipette tip to remove cells from a specific region of the monolayers. Cells were then washed with PBS and incubated with r(P)ApoB_L (0, 0.5, 10, and 20 μM). As it is well known that the spreading of cells in the wound area is due to two mechanisms, *i.e.* cell motility and cell proliferation [37,40,58], a pre-treatment with mitomycin C allowed us to exclude any influence of cell proliferation on the wound healing process.

In Fig. 9a, we reported the images acquired during a time-lapse wound healing experiment on control cells, and on cells treated with 20 μM r(P)ApoB_L peptide at three time points, *i.e.* at time 0 and at 3 and 5 h after the lag time (t_L), defined as a transient time period (t_L) before the linear decrease of the wound area (see below). By the comparison of the images of treated and untreated cells at each time point, it emerged that the cells treated with 20 μM peptide were able to close the wound faster than the control cells. In order to quantify the wound closure, we used an automated image analysis software, that allowed us to measure the size of the cell-free area (A) for each time point. The obtained values were normalized with respect to the value measured at time 0 (A_0) for each field of view, and plotted as a function of time (Fig. 9b). In Fig. 9a, at $t = 5$ h after t_L , A/A_0 values were found to be 0.20, and 0.07 for the control sample, and for the cells treated with 20 μM peptide, respectively. This evidence suggests that r(P)ApoB_L peptide might be able to stimulate wound re-epithelialization by human keratinocytes. As shown in Fig. 9b, where A/A_0 values of control cells are reported as a function of time, after an initial lag phase (t_L), the wound area decreases with a constant velocity. The initial lag phase, corresponding to a transient time period (t_L) before the linear decrease of the wound area, has been observed for all the analysed samples, and has been found

to range between 3 and 5 h independently from peptide concentrations under test (Fig. 9c).

As the slope (α) of the line represents the measure of the wound closure velocity, each α value calculated in the presence of the peptide was normalized with respect to the value calculated for untreated cells (α_{contr}), and plotted as a function of peptide concentration (Fig. 9d). It appeared that the cells treated with the peptide show an increased wound closure velocity with respect to the control cells ($\alpha/\alpha_{\text{contr}} > 1$). In particular, in the case of the cells treated with 10 μM peptide, an increment of about 20% in the normalized wound closure velocity ($\alpha/\alpha_{\text{contr}} = 1.21$, data statistically significant) was observed. When cells were treated with 20 μM peptide, a slightly higher value of the normalized wound closure velocity was measured ($\alpha/\alpha_{\text{contr}} = 1.23$). However, in the latter case, a higher data variability was observed (larger error bar), leading to a limited statistical significance of the result.

Overall, our results indicate that r(P)ApoB_L peptide is able to promote the migration and the consequent wound healing in HaCaT keratinocyte monolayers when tested at concentration values ranging between 0.5 and 20 μM .

4. Discussion

Recently, an abundance of multidrug-resistant bacteria has emerged, whereas very few classes of new antibiotics have been discovered. The knowledge that HDPs may prevent infections in many organisms opened interesting perspectives to the applications of these peptides as a new class of antimicrobials. In fact, they initially attracted attention solely for their direct antimicrobial activity, and were studied as promising alternative antibiotic candidates due to their prospective potency, rapid action, and broad spectrum of activity against Gram-negative and Gram-positive bacteria, viruses, fungi and parasites [59,60]. To date, more than 1,000 natural cationic HDPs with antimicrobial properties have been identified [61]. These peptides constitute a major component of the ancient, nonspecific innate defence system in most multicellular organisms [3,19,59,60]. However, it has to be emphasized that most natural HDPs have, indeed, modest direct antimicrobial activities, and exhibit multiple mechanisms of action, with a consequent low potential to induce *de novo* resistance [59]. This class of peptides includes both the bioactive peptides displaying direct antimicrobial activity and those that stimulate the immune system to clear or prevent an infection [59,61]. In mammals, the expression of mature and biologically active HDPs requires a proteolytic cleavage event determining the release of the “cryptic” bioactive peptide from its precursor protein [62]. In fact, it should be emphasized that a wide variety of human proteins, whose primary functions are not necessarily related to host defence, contain HDPs hidden inside their sequences [63,64]. Fascinatingly, human proteome could be seen as a yet unexplored source of bioactive peptides with potential pharmacological applications. In this context, apolipoproteins have been identified as a source of bioactive peptides displaying broad anti-infective and antiviral activities [22]. Indeed, the presence of antiviral peptides hidden within apolipoprotein sequences may be related to the fact that lipoproteins and viruses share a similar cell biological niche, having a comparable size and displaying similar interactions with mammalian cells and receptors [22]. ApoB is one of the several apolipoproteins that play key roles in lipoprotein metabolism [65], and represents the ligand for receptor-mediated removal of low density lipoprotein particles from circulation [65]. ApoB contains two LDL (low-density lipoprotein) receptor binding domains, namely region A (ApoB3147–3157) and region B (ApoB3359–3367), which is more uniformly conserved across species and that has been found to be endowed with a significant antiviral activity

[22]. Moreover, ApoB derived peptides have been already used in vaccine preparations to treat atherosclerosis [23]. Here, we applied our *in silico* analysis method to a human ApoB isoform [26,27] and identified a novel “cryptic” HDP (region 887–922). To the best of our knowledge, this ApoB region has never been analysed before, since all the previously identified biologically active ApoB peptides are far from the high scoring region identified in the present work [22,23]. By applying our *in silico* analysis, we identified an absolute maximum score, corresponding to region 887–922 (Fig. 1), and a relative maximum score, corresponding to residues 887–909 (Fig. 1). Here, we focused our attention on these two ApoB sequences by producing in bacterial cells two recombinant HDPs, here named r(P)ApoB_L and (P)ApoB_S, 38- and 26-residue long, respectively. Both recombinant peptides were found to exhibit antibacterial activities against both Gram-positive and Gram-negative strains, including the pathogenic strains *P. aeruginosa* PAO1 and *B. globigii* TNO BM013, while having negligible cytotoxic effects on a panel of human and murine cell lines. Time killing curves also indicated that peptides exert a strong bactericidal activity against susceptible strains. However, it has to be underlined that ApoB derived peptides were found to be ineffective towards *P. aeruginosa* ATCC 27853, methicillin-resistant *S. aureus* (MRSA WKZ-2), and *S. aureus* ATCC 29213 strains, while, in the case of *S. enteritidis* 706 RIVM strain, a significant antibacterial effect was displayed only by r(P)ApoB_L peptide. This observation is in agreement with previous findings indicating that most natural cationic antimicrobial peptides do not appear to be highly optimized for direct antimicrobial activity, since it is likely that multiple modestly active peptides with concomitant immunomodulatory activities work effectively in combination and/or when induced or delivered to sites of infection [66]. Indeed, considering this, we performed combination therapy analyses and found that both ApoB derived peptides are able to synergistically act with either commonly used antibiotics or EDTA, the latter selected for its ability to affect bacterial outer membrane permeability, thus sensitizing bacteria to a number of antibiotics [49–51]. Interestingly, synergistic effects were observed towards most of the strains under test, including methicillin-resistant *S. aureus* MRSA WKZ-2, on which peptides alone were found to be ineffective even at high concentrations (40 μM). Although the use of a single agent to treat pathogens is the most common practice in clinics, combination therapy approaches have several advantages, such as low potential to induce resistant phenotype, efficacy at lower drug doses, with a consequent mitigation of toxic effects, and possibility to target a broad spectrum of pathogens [67]. Interestingly, both r(P)ApoB_L and r(P)ApoB_S peptides showed synergism with systemic antibiotic ciprofloxacin against all the strains under test (FIC indexes ranging from 0.3 to 0.44). This would allow to significantly lower the doses of the antibiotic in the combination therapy approaches, with a consequent decrease of the appearance of resistant clinical isolates, an undesired phenomenon strongly affecting ciprofloxacin efficacy [68]. ApoB derived peptides also showed synergistic effects with colistin and vancomycin against most of the strains under test (FIC indexes ranging from 0.14 to 0.5). Since both colistin and vancomycin are responsible for toxic effects at high concentrations [67,69], a combination therapeutic approach based on a reduced frequency of antibiotic administration and/or exposure to antibiotic may offer several advantages over conventional dosing schemes. However, the most potent synergism was observed for both ApoB derived peptides in combination with EDTA, with FIC indexes ranging from 0.089 to 0.4. In the case of *P. aeruginosa* strains, synergism might be associated to EDTA ability to combine with magnesium ions playing a key role in the self-interaction of LPS molecules, with a consequent LPS release determining an increased permeability of bacterial membrane [50]. This might ultimately facilitate peptide internalization into bacterial

cells, thus potentiating the peptide antimicrobial activity. EDTA is also known to determine the release of endogenous phospholipases, with a consequent alteration of Gram-negative bacteria outer membrane [70]. In the case of *S. aureus* strains, the increase of bacterial membrane permeability might be due to the ability of EDTA to solubilize extracellular polymeric substances [71], mainly composed by exopolysaccharides and playing a key role in biofilm establishment.

It should be highlighted that, although in some cases FIC indexes very close to 0.5 make it difficult to discriminate between synergistic and additive effects, no antagonistic interactions were observed between peptides and antimicrobials. Furthermore, combinations of ApoB derived peptides with antibiotics and EDTA were found to have a strong antimicrobial activity also towards strains on which the peptides alone were found to be ineffective, such as both *S. aureus* strains and *P. aeruginosa* ATCC 27853, indicating that in drug combinations a reciprocal facilitation and potentiation of different mechanisms of action is realized.

Interestingly, ApoB derived peptides are also endowed with anti-biofilm activity. Microorganisms growing in a biofilm state are very resilient to the treatment by many antimicrobial agents. Indeed, biofilm infections are a significant problem in chronic and long-term infections, including those colonizing medical devices and implants [52]. Specific cationic HDPs have recently been described to have multispecies anti-biofilm activity, which is independent of their activity against planktonic bacteria [9]. We found that ApoB derived peptides are effective on biofilm formation and biofilm attachment, and, even more interestingly, they strongly affect pre-formed biofilms. Furthermore, ApoB derived peptides display anti-biofilm activity even on bacterial strains not sensitive to the peptide antimicrobial activity, such as *S. aureus* MRSA WKZ-2, and, in the case of sensitive strains, even at peptide concentrations (0.625–1 μM) significantly lower than those required to directly kill planktonic cells. This is in agreement with previous reports indicating that LL-37 peptide potently inhibits the formation of bacterial biofilms *in vitro* at the very low and physiologically meaningful concentration of 0.5 μg/mL, significantly lower than that required to kill or inhibit bacterial growth (64 μg/mL) [72]. As a consequence of this, it should be emphasized that even at the highest ApoB derived peptides concentrations tested, a significant percentage of bacterial cells inside the biofilm structure appeared to be still alive. This was observed for both ApoB derived peptides and LL-37 control peptide, while it was less pronounced in the case of CATH-2 peptide. Based on this, it is tempting to speculate that successful therapeutic approaches could be designed by combining anti-biofilm peptides and conventional antibiotics ineffective on biofilm, but effective on bacterial cells entrapped into the biofilm structure.

From a structural point of view, by Far UV-CD analyses, we found that ApoB derived peptides are unstructured in aqueous buffer, and tend to assume a conformation in the presence of membrane mimicking agents. In the presence of increasing concentrations of LPS, r(P)ApoB_L peptide was found to gradually assume a defined structure, what suggests a direct binding of this peptide to LPS. This was not observed, instead, in the case of r(P)ApoB_S peptide. It has also to be highlighted that both r(P)ApoB_L and r(P)ApoB_S peptides are endowed with immunomodulatory activities by significantly decreasing the release of pro-inflammatory IL-6 and NO in LPS induced murine RAW 264.7 macrophages. Both ApoB derived peptides were found to efficiently act either when the cells were co-incubated with the peptide under test in the presence of LPS or when the cells were pre-treated with the peptide for 2 h and then incubated with LPS for further 24 h, thus indicating that both peptides are able to display a significant protective action. However, it has to be noticed that, differently from r(P)ApoB_L peptide, r(P)ApoB_S was found to play anti-

inflammatory activities, when co-incubated with LPS, only at the highest peptide concentration tested (20 μM), whereas both r(P) ApoB₅ concentrations (5 and 20 μM) were found to efficiently exert a protective effect. This might be due to the fact that ApoB derived peptides probably act through different mechanisms, with r(P) ApoB_L peptide mainly acting by binding to LPS and consequently interfering with its activity on target cells, and r(P)ApoB₅ peptide mainly acting on cell membrane and competing with LPS for the binding to specific cell sites. Therefore, a complex picture emerges, in agreement with the observation that HDPs immunomodulatory activities are extremely diverse [14]. Further experiments will allow us to elucidate the molecular mechanisms at the basis of ApoB derived peptides anti-inflammatory effects, which might include multiple aspects, such as stimulation of chemotaxis, suppression of bacterial induced pro-inflammatory cytokine production, regulation of neutrophil and epithelial cell apoptosis, modulation of cellular differentiation pathways, and promotion of angiogenesis and wound healing. As for the last aspect, in agreement with previous findings on LL-37 human peptide [73,74], we found that r(P)ApoB_L peptide is able to stimulate human keratinocytes wound re-epithelialization *in vitro*, an evidence that opens new and interesting perspectives on future topical applications of this human HDP.

It has to be underlined that, although there are very few HDPs currently in use in the market, many are progressing through clinical trials that have focused on topic rather than systemic treatment because of peptides potential toxicity. However, it is conceivable that judicious formulations of HDPs for a clinical use, e.g. peptide inclusion in liposomal nanoparticles, will avoid undesired toxicity and degradation, thus allowing a sustainable HDPs delivery [18]. Here, we show that both ApoB derived peptides are not toxic for eukaryotic cells and do not determine any haemolytic effect when tested on murine red blood cells. These observations associated to their multifunctional properties and to their ability to synergistically act in combination with conventional antibiotic drugs open interesting perspectives to their therapeutic applications.

Conflict of interest statement

None declared.

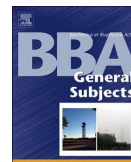
Acknowledgements

We acknowledge "Programma di scambi internazionali con Università ed Istituti di ricerca stranieri per la mobilità di breve durata di docenti, ricercatori e studiosi" of the University of Naples Federico II, that financially supported scientific exchanges between Universities of Naples and Utrecht. The technical expert assistance by Dr. Johanna L. M. Tjeerdsma-van Bokhoven is acknowledged.

References

- [1] M.T. Parker, J.H. Hewitt, Methicillin resistance in *Staphylococcus aureus*, *Lancet* 1 (1970) 800–804.
- [2] J.N. Pendleton, S.P. Gorman, B.F. Gilmore, Clinical relevance of the ESKAPE pathogens, *Exp. Rev. Anti Infect. Ther.* 11 (2013) 297–308.
- [3] M. Zasloff, Antimicrobial peptides of multicellular organisms, *Nature* 415 (2002) 389–395.
- [4] D.A. Phoenix, S.R. Dennison, F. Harris, Antimicrobial Peptides: Their History, Evolution, and Functional Promiscuity, Wiley, 2013.
- [5] R.E. Hancock, R. Lehrer, Cationic peptides: a new source of antibiotics, *Trends Biotechnol.* 16 (1998) 82–88.
- [6] J.D. Hale, R.E. Hancock, Alternative mechanisms of action of cationic antimicrobial peptides on bacteria, *Exp. Rev. Anti Infect. Ther.* 5 (2007) 951–959.
- [7] E.C. Spindler, J.D. Hale, T.H. Jr Giddings, R.E. Hancock, R.T. Gill, Deciphering the mode of action of the synthetic antimicrobial peptide Bac8c, *Antimicrob. Agents Chemother.* 55 (2012) 1706–1716.
- [8] C.D. Fjell, J.A. Hiss, R.E. Hancock, G. Schneider, Designing antimicrobial peptides: form follows function, *Nat. Rev. Drug Discov.* 11 (2012) 37–51.
- [9] C. de la Fuente-Nunez, F. Refouveille, E.F. Haney, S.K. Straus, R.E. Hancock, Broad-spectrum anti-biofilm peptide that targets a cellular stress response, *PLoS Pathog.* 10 (2014) e1004152.
- [10] A.F.G. Cicero, F. Fogacci, A. Colletti, Potential role of bioactive peptides in prevention and treatment of chronic diseases: a narrative review, *Br. J. Pharmacol.* (2016), <http://dx.doi.org/10.1111/bph.13608>.
- [11] R.E.W. Hancock, M.G. Scott, The role of antimicrobial peptides in animal defences, *Proc. Natl. Acad. Sci. U.S.A.* 97 (2000) 8856–8861.
- [12] D. Yang, A. Biragyn, D.M. Hoover, J. Lubkowski, J.J. Oppenheim, Multiple roles of antimicrobial defensins, cathelicidins, and eosinophil-derived neurotoxin in host defense, *Annu. Rev. Immunol.* 22 (2004) 181–215.
- [13] D. Yang, A. Biragyn, L.W. Kwak, J.J. Oppenheim, Mammalian defensins in immunity: more than just microbicidal, *Trends Immunol.* 23 (2002) 291–296.
- [14] A.T.Y. Yeung, S.L. Gellatly, R.E.W. Hancock, Multifunctional cationic host defence peptides and their clinical applications, *Cell. Mol. Life Sci.* 68 (2011) 2161–2176.
- [15] D.M. Easton, A. Nijnik, M.L. Mayer, R.E.W. Hancock, Potential of immunomodulatory host defence peptides as novel anti-infectives, *Trends Biotechnol.* 27 (2009) 582–590.
- [16] T.A. Waldmann, Immunotherapy: past, present and future, *Nat. Med.* 9 (2003) 269–277.
- [17] J. Kindrachuk, E. Scruten, S. Attah-Poku, K. Bell, A. Potter, L.A. Babiuk, P.J. Griebel, S. Napper, Stability, toxicity, and biological activity of host defence peptide BMAP28 and its inverted and retro-inverted isomers, *Biopolymers* 96 (2013) 14–24.
- [18] M. Sobczak, C. Dębek, E. Ołędzka, R. Kozłowski, Polymeric systems of antimicrobial peptides – strategies and potential applications, *Molecules* 18 (2013) 14122–14137.
- [19] K.L. Brown, R.E.W. Hancock, Cationic host defence (anti-microbial) peptides, *Curr. Opin. Immunol.* 18 (2006) 24–30.
- [20] E. Guaní-Guerra, T. Santos-Mendoza, S.O. Lugo-Reyes, L.M. Terán, Antimicrobial peptides: general overview and clinical implications in human health and disease, *Clin. Immunol.* 135 (2010) 1–11.
- [21] N. Mookherjee, R.E.W. Hancock, Cationic host defence peptides: innate immune regulatory peptides as a novel approach for treating infections, *Cell. Mol. Life Sci.* 64 (2007) 922–933.
- [22] B.A. Kelly, I. Harrison, A. McKnight, C.B.B. Dobson, Anti-infective activity of apolipoprotein domain derived peptides *in vitro*: identification of novel antimicrobial peptides related to apolipoprotein B with anti-HIV activity, *BMC Immunol.* 11 (2010) 13.
- [23] C. Pierides, A. Bermudez-Fajardo, G.N. Fredrikson, J. Nilsson, E. Oviedo-Orta, Immune responses elicited by apoB-100-derived peptides in mice, *Immunol. Res.* 56 (2013) 96–108.
- [24] K. Pane, V. Sgambati, A. Zanfardino, G. Smaldone, V. Cafaro, T. Angrisano, E. Pedone, S. Di Gaetano, D. Capasso, E.F. Haney, V. Izzo, M. Varcamonti, E. Notomista, R.E. Hancock, A. Di Donato, E. Pizzo, A new cryptic cationic antimicrobial peptide from human apolipoprotein E with antibacterial activity and immunomodulatory effects on human cells, *FEBS J.* 283 (2016) 2115–2131.
- [25] E. Notomista, A. Falanga, S. Fusco, L. Pirone, A. Zanfardino, S. Galdiero, M. Varcamonti, E. Pedone, P. Contursi, The identification of a novel *Sulfolobus islandicus* CAMP-like peptide points to archaeal microorganisms as cell factories for the production of antimicrobial molecules, *Microb. Cell Fact.* 14 (2015) 126.
- [26] S.H. Chen, C.Y. Yang, P.F. Chen, D. Setzer, M. Tanimura, W.H. Li, A.M. Gotto, L. Chan, The complete cDNA and amino acid sequence of human apolipoprotein B-100, *J. Biol. Chem.* 261 (1986) 12918–12921.
- [27] C.Y. Yang, Z.W. Gu, S.A. Weng, T.W. Kim, S.H. Chen, H.J. Pownall, P.M. Sharp, S. W. Liu, W.H. Li, A.M. Jr, Gotto, Structure of apolipoprotein B-100 of human low density lipoproteins, *Arteriosclerosis* 9 (1989) 96–108.
- [28] K. Pane, L. Durante, E. Pizzo, M. Varcamonti, A. Zanfardino, V. Sgambati, A. Di Maro, A. Carpentieri, V. Izzo, A. Di Donato, V. Cafaro, E. Notomista, Rational design of a carrier protein for the production of recombinant toxic peptides in *Escherichia coli*, *PLoS ONE* 11 (2016) e0146552.
- [29] J. Reed, T.A. Reed, A set of constructed type spectra for the practical estimation of peptide secondary structure from circular dichroism, *Anal. Biochem.* 254 (1997) 36–40.
- [30] M.A. Amon, M. Ali, V. Bender, K. Hall, M.-I. Aguilar, J. Aldrich-Wright, N. Manolios, Kinetic and conformational properties of a novel T-cell antigen receptor transmembrane peptide in model membranes, *Peptide Sci.* 14 (2008) 714–724.
- [31] I. Wiegand, K. Hilpert, R.E. Hancock, Agar and broth dilution methods to determine the minimal inhibitory concentration (MIC) of antimicrobial substances, *Nat. Protoc.* 3 (2008) 163–175.
- [32] F.C. Odds, Synergy, antagonism, and what the checkerboard puts between them, *J. Antimicrob. Chemother.* 52 (2003) 1.
- [33] J. Li, T. Kleintschek, A. Rieder, Y. Cheng, T. Baumbach, U. Obst, T. Schwartz, P.A. Levkin, Hydrophobic liquid-infused porous polymer surfaces for antibacterial applications, *ACS Appl. Mater. Interfaces* 5 (2013) 6704–6711.
- [34] A. Arciello, N. De Marco, R. Del Giudice, F. Guglielmi, P. Pucci, A. Relini, D.M. Monti, R. Piccoli, Insights into the fate of the N-terminal amyloidogenic polypeptide of ApoA-I in cultured target cells, *J. Cell Mol. Med.* 15 (2011) 2652–2663.

- [35] C.C. Liang, A.Y. Park, J.L. Guan, In vitro scratch assay: a convenient and inexpensive method for analysis of cell migration in vitro, *Nat. Protoc.* 2 (2007) 329–333.
- [36] A. Di Grazia, F. Cappiello, A. Imanishi, A. Mastrofrancesco, M. Picardo, R. Paus, M.L. Mangoni, The frog skin-derived antimicrobial peptide esculentin-1a(1–21)NH₂ promotes the migration of human HaCaT keratinocytes in an EGF receptor-dependent manner: a novel promoter of human skin wound healing? *PLoS ONE* 10 (2015) e0128663.
- [37] F. Ascione, S. Caserta, S. Guido, Wound healing revisited: a transport phenomena approach, *Chem. Eng. Sci.* 160 (2017) 200–209.
- [38] F. Ascione, A. Vasaturo, S. Caserta, V. D'Esposito, P. Formisano, S. Guido, Comparison between fibroblast wound healing and cell random migration assays in vitro, *Exp. Cell Res.* 347 (2016) 123–132.
- [39] A.Q. Cai, K.A. Landman, B.D. Hughes, Multi-scale modeling of a wound-healing cell migration assay, *J. Theor. Biol.* 245 (2007) 576–594.
- [40] P.K. Maini, D.L.S. McElwain, D.I. Leavesley, Traveling wave model to interpret a wound-healing cell migration assay for human peritoneal mesothelial cells, *Tissue Eng.* 10 (2004) 475–482.
- [41] G. Cumming, F. Fidler, D.L. Vaux, Error bars in experimental biology, *J. Cell Biol.* 177 (2007) 7–11.
- [42] A.P. Subasinghage, D. O'Flynn, J.M. Conlon, C.M. Hewage, Conformational and membrane interaction studies of the antimicrobial peptide alyteserin-1c and its analogue [E4K]alyteserin-1c, *Biochim. Biophys. Acta* 2011 (1808) 1975–1984.
- [43] R. Gopal, J.S. Park, C.H. Seo, Y. Park, Applications of circular dichroism for structural analysis of gelatin and antimicrobial peptides, *Int. J. Mol. Sci.* 13 (2012) 3229–3244.
- [44] Y.J. Na, S.B. Han, J.S. Kang, Y.D. Yoon, S.K. Park, H.M. Kim, K.H. Yang, C.O. Joe, Lactoferrin works as a new LPS-binding protein in inflammatory activation of macrophages, *Int. Immunopharmacol.* 4 (2004) 1187–1199.
- [45] Y.J. Seo, K.T. Lee, J.R. Rho, J.H. Choi, Phorbaketol A, isolated from the marine sponge phorbasp sp., exerts its anti-inflammatory effects via NF-kappaB inhibition and heme oxygenase-1 activation in lipopolysaccharide-stimulated macrophages, *Mar. Drugs* 13 (2015) 7005–7019.
- [46] A. Gossiau, S. Li, C.T. Ho, K.Y. Chen, N.E. Rawson, The importance of natural product characterization in studies of their anti-inflammatory activity, *Mol. Nutr. Food Res.* 55 (2011) 74–82.
- [47] C. Nathan, Points of control in inflammation, *Nature* 420 (2002) 846–852.
- [48] A. van Dijk, M.H. Tersteeg-Zijdeveld, J.L. Tjeerdsma-van Bokhoven, A.J. Jansman, E.J. Veldhuizen, H.P. Haagsman, Chicken heterophils are recruited to the site of *Salmonella* infection and release antibacterial mature cathelicidin-2 upon stimulation with LPS, *Mol. Immunol.* 46 (2009) 1517–1526.
- [49] M. Vaara, Agents that increase the permeability of the outer membrane, *Microbiol. Rev.* 56 (1992) 395–411.
- [50] R.E. Hancock, Alterations in outer membrane permeability, *Annu. Rev. Microbiol.* 38 (1984) 237–264.
- [51] A.H. Delcour, Outer membrane permeability and antibiotic resistance, *Biochim. Biophys. Acta* 1794 (2009) 808–816.
- [52] D. Pletzer, S.R. Coleman, R.E.W. Hancock, Anti-biofilm peptides as a new weapon in antimicrobial warfare, *Curr. Opin. Microbiol.* 33 (2016) 35–40.
- [53] X. Feng, K. Sambanthamoorthy, T. Palys, C. Paranavithana, The human antimicrobial peptide LL-37 and its fragments possess both antimicrobial and antibiofilm activities against multidrug-resistant *Acinetobacter baumannii*, *Peptides* 49 (2013) 131–137.
- [54] D. Takahashi, S.K. Shukla, O. Prakash, G. Zhang, Structural determinants of host defense peptides for antimicrobial activity and target cell selectivity, *Biochimie* 92 (2010) 1236–1241.
- [55] K.A. Brogden, Antimicrobial peptides: pore formers or metabolic inhibitors in bacteria? *Nat. Rev. Microbiol.* 3 (2005) 238–250.
- [56] D.I. Chan, E.J. Prenner, H.J. Vogel, Tryptophan- and arginine-rich antimicrobial peptides: structures and mechanisms of action, *Biochim. Biophys. Acta* 1758 (2006) 1184–1202.
- [57] M.L. Mangoni, A.M. McDermott, M. Zasloff, Antimicrobial peptides and wound healing: biological and therapeutic considerations, *Exp. Dermatol.* 25 (2016) 167–173.
- [58] A. Tremel, A. Cai, N. Tirtaatmadja, B.D. Hughes, G.W. Stevens, K.A. Landman, A. J. O'Connor, Cell migration and proliferation during monolayer formation and wound healing, *Chem. Eng. Sci.* 64 (2009) 247.
- [59] R.E.W. Hancock, K.L. Brown, N. Mookherjee, Host defence peptides from invertebrates—emerging antimicrobial strategies, *Immunobiology* 211 (2006) 315–322.
- [60] R.E.W. Hancock, G. Diamond, The role of cationic anti-microbial peptides in innate host defences, *Trends Microbiol.* 8 (2000) 402–410.
- [61] A.K. Marr, W.J. Gooderham, R.E.W. Hancock, Antibacterial peptides for therapeutic use: obstacles and realistic outlook, *Curr. Opin. Pharmacol.* 6 (2006) 468–472.
- [62] E. Guani-Guerra, T. Santos-Mendoza, S.O. Lugo-Reyes, L.M. Terán, Antimicrobial peptides: general overview and clinical implications in human health and disease, *Clin. Immunol.* 135 (2010) 1–11.
- [63] P. Papareddy, M. Kalle, G. Kasetty, M. Mörgelin, V. Rydengård, B. Albiger, K. Lundqvist, M. Malmsten, A. Schmidtchen, C-terminal peptides of tissue factor pathway inhibitor are novel host defense molecules, *J. Biol. Chem.* 285 (2010) 28387–28398.
- [64] E. Andersson, V. Rydengard, A. Sonesson, M. Mørgelin, L. Björck, A. Schmidtchen, Antimicrobial activities of heparin-binding peptides, *Eur. J. Biochem.* 271 (2004) 1219–1226.
- [65] S.G. Young, Recent progress in understanding apolipoprotein B, *Circulation* 82 (1990) 1574–1594.
- [66] O.L. Franco, Peptide promiscuity: an evolutionary concept for plant defense, *FEBS Lett.* 585 (2011) 995–1000.
- [67] H.M. Nguyen, C.J. Graber, Limitations of antibiotic options for invasive infections caused by methicillin-resistant *Staphylococcus aureus*: is combination therapy the answer? *J. Antimicrob. Chemother.* 65 (2010) 24–36.
- [68] G.S. Tillotson, I. Dorrian, J. Blondeau, Fluoroquinolone resistance: mechanisms and epidemiology, *J. Med. Microbiol.* 46 (1997) 457–461.
- [69] M.E. Evans, D.J. Feola, R.P. Rapp, Polymyxin B sulfate and colistin: old antibiotics for emerging multidrug-resistant gram-negative bacteria, *Ann. Pharmacother.* 33 (1999) 960–967.
- [70] H. Nakaido, M. Vaara, Molecular basis of bacterial outer membrane permeability, *Microbiol. Rev.* 49 (1985) 1–32.
- [71] S.L. Percival, P. Kite, K. Eastwood, R. Murga, J. Carr, M.J. Arduino, Tetrasodium EDTA as a novel central venous catheter lock solution against biofilm, *Infect. Control Hosp. Epidemiol.* 2 (2005) 515–519.
- [72] J. Overhage, A. Campisano, M. Bains, E.C. Torfs, B.H. Rehm, R.E.W. Hancock, Human host defense peptide LL-37 prevents bacterial biofilm formation, *Infect. Immun.* 76 (2008) 4176–4182.
- [73] J.D. Heilborn, M.F. Nilsson, G. Kratz, G. Weber, O. Sørensen, N. Borregaard, M. Stähle-Bäckdahl, The cathelicidin anti-microbial peptide LL 37 is involved in re epithelialization of human skin wounds and is lacking in chronic ulcer epithelium, *J. Invest. Dermatol.* 120 (2003) 379–389.
- [74] R. Shaykhiiev, C. Beisswenger, K. Kändler, J. Senske, A. Püchner, T. Damm, J. Behr, R. Bals, Human endogenous antibiotic LL-37 stimulates airway epithelial cell proliferation and wound closure, *Am. J. Physiol. Lung Cell. Mol. Physiol.* 289 (2005) L842–L848.



Insights into the anticancer properties of the first antimicrobial peptide from Archaea



Rosa Gaglione^{a,1}, Luciano Pirone^{b,1}, Biancamaria Farina^{b,c,1}, Salvatore Fusco^{d,i,1}, Giovanni Smaldone^e, Martina Aulitto^d, Eliana Dell'Olmo^a, Emanuela Roscetto^f, Annarita Del Gatto^{b,g}, Roberto Fattorusso^{g,h}, Eugenio Notomista^d, Laura Zaccaro^{b,g}, Angela Arciello^{a,i,*}, Emilia Pedone^{b,g,***,2}, Patrizia Contursi^{d,***,2}

^a Department of Chemical Sciences, University of Naples Federico II, 80126 Naples, Italy

^b Institute of Biostructures and Bioimaging, Italian Research National Council, Naples, Italy

^c Advanced Accelerator Applications, 81100 Caserta, Italy

^d Department of Biology, University of Naples Federico II, Complesso Universitario Monte S. Angelo, Via Cinthia, 80126 Naples, Italy.

^e IRCCS SDN, Via E. Gianturco 113, 80143 Naples, Italy

^f Department of Molecular Medicine and Medical Biotechnology, Federico II University Medical School, Italy

^g Research Centre on Bioactive Peptides (CIRPeB), University of Naples "Federico II", Via Mezzocannone 16, 80134 Naples, Italy

^h Department of Environmental, Biological and Pharmaceutical Sciences and Technologies, University of Campania-Luigi Vanvitelli, 81100 Caserta, Italy

ⁱ National Institute of Biostructures and Biosystems (INBB), Italy

^j Division of Industrial Biotechnology, Department of Biology and Biological Engineering, Chalmers University of Technology, Göteborg, Sweden

ARTICLE INFO

Keywords:

Antimicrobial peptide

Anticancer peptide

Sulfolobus

Archaea

Peptide-membrane interactions

ABSTRACT

Background: The peptide VLL-28, identified in the sequence of an archaeal protein, the transcription factor Stf76 from *Sulfolobus islandicus*, was previously identified and characterized as an antimicrobial peptide, possessing a broad-spectrum antibacterial activity.

Methods: Through a combined approach of NMR and Circular Dichroism spectroscopy, Dynamic Light Scattering, confocal microscopy and cell viability assays, the interaction of VLL-28 with the membranes of both parental and malignant cell lines has been characterized and peptide mechanism of action has been studied.

Results: It is here demonstrated that VLL-28 selectively exerts cytotoxic activity against murine and human tumor cells. By means of structural methodologies, VLL-28 interaction with the membranes has been proven and the binding residues have been identified. Confocal microscopy data show that VLL-28 is internalized only into tumor cells. Finally, it is shown that cell death is mainly caused by a time-dependent activation of apoptotic pathways.

Conclusions: VLL-28, deriving from the archaeal kingdom, is here found to be endowed with selective cytotoxic activity towards both murine and human cancer cells and consequently can be classified as an ACP.

General significance: VLL-28 represents the first ACP identified in an archaeal microorganism, exerting a trans-kingdom activity.

1. Introduction

Antimicrobial peptides (AMPs) are short peptides endowed with direct and broad-spectrum antimicrobial activity and represent essential components of the innate immune system of higher eukaryotes, being the first line of defense against microbial invasions [1,2]. In

addition to a direct antimicrobial action, AMPs show a wide panel of biological activities including anti-inflammatory, anti-viral, chemoattractive and pro-angiogenic activity [1,3–6]. AMPs are very heterogeneous in length, amino-acid composition, secondary structure and mechanism of action; however, the majority of them shows a peculiar abundance of cationic and hydrophobic residues. These AMPs, also

* Correspondence to: A. Arciello, Department of Chemical Sciences, University of Naples Federico II, 80126 Naples, Italy.

** Correspondence to: E. Pedone, Institute of Biostructures and Bioimaging, Italian Research National Council, Naples, Italy.

*** Corresponding author.

E-mail addresses: anarciel@unina.it (A. Arciello), empedone@unina.it (E. Pedone), contursi@unina.it (P. Contursi).

¹ These authors equally contributed.

² These authors equally contributed to the study and are therefore both last names on this manuscript.

called Host Defence Peptides (HDPs) [7], kill bacterial cells through a specific mechanism i.e. targeting bacterial membranes [2,6,8]: the net positive charge drives the adsorption of the peptide onto the surface of bacterial membranes which are richer in anionic lipids than eukaryotic membranes, hence the hydrophobic residues mediate the insertion of the peptide into the membrane. The accumulation of peptide molecules in the membrane causes the alteration of its structure/permeability, accompanied by a severe impairment of the membrane functions that eventually lead to the death of bacterial cells, often by cell lysis [2,6,8]. Since eukaryotic plasma membranes show an asymmetric distribution of negatively charged phospholipids, generally present only in the inner leaflet of the membrane, HDPs are not able to effectively adsorb to eukaryotic cells. The presence of cholesterol further prevents the insertion into and the perturbation of the eukaryotic membranes. Nonetheless, it is worth mentioning that at high concentration several HDPs become toxic also for eukaryotic cells.

Intriguingly, several AMPs endowed with anti-cancer activity [9] are defined as “anti-cancer peptides” (ACPs), because they show a much stronger toxicity for cancer cells than that towards normal cells. This differential toxicity has been attributed to the fact that transformation of eukaryotic cells is often associated to alterations of the membrane composition [10], such as: i) loss of the asymmetric distribution of phospholipids with exposure of phosphatidylserine on the outer leaflet, ii) increased production of anionic lipids (e.g. sulfated lipids), sialic acid containing glycolipids and glycoproteins, and sometimes iii) decreased production of cholesterol. Altogether these events lead to an augmented negative charge at the external surface of tumor cells that, in turn, would favor the binding of ACPs. However, differently from bacterial killing mechanisms, the death of tumor cells is not necessarily due to accumulation of the peptide into the membrane followed by their lysis. Indeed, in several cases it has been demonstrated that ACPs are internalized and the cell death occurs upon the interaction with one or more intracellular targets, such as mitochondria, DNA, cytoplasmic and nuclear proteins (e.g. HSP70 [11] and DNA polymerase β [12], respectively). Moreover, it is worth noting that these ACPs usually induce apoptosis rather than necrosis [9].

Due to the severe side effects of conventional chemotherapeutic agents and the ability of some tumor cells to develop the multidrug resistant phenotype, ACPs have attracted considerable attention. Indeed, these peptides could help to develop a new generation of anti-cancer drugs with a mechanism of action well distinguished from those of conventional chemotherapeutic agents.

As not all the HDPs are ACPs and the killing mechanism seems to differ for each ACP and tumor cell line, the rationale development of new antitumor agents based on CAMPs/ACPs requires further investigations. In particular, the identification and characterization of new ACPs could help to better define the requirements for a strong and selective antitumor activity.

Recently, we have developed an *in silico* tool allowing to identify HDP-like peptides hidden into the sequences of proteins not necessarily involved in host defense [13]. Using this tool we have already identified three new human HDPs [14–16]. Furthermore, we have demonstrated that DNA binding proteins can be a convenient source of new HDP-like peptides by identifying the first HDP from an archaeal protein, the transcription factor Stf76 encoded by the hybrid plasmid-virus pSSVx from *Sulfolobus islandicus* [17]. This archaeal HDP, named VLL-28 from its sequence [16], has a broad-spectrum antibacterial activity and exhibits selective leakage and fusogenic capability on vesicles with a lipid composition similar to that of bacterial membranes. Moreover, we have shown that VLL-28 retains the ability of the parental protein to bind nucleic acids (both single and double strand DNA). Using a fluorescent derivative, we have demonstrated that VLL-28 localizes not only on the cell membrane but also in the cytoplasm of *Escherichia coli*, thus suggesting that it could target both membranes and intracellular components of bacterial cells.

Here we report for the first time the characterization of the

antitumor activity of VLL-28. By means of a multidisciplinary approach including biochemical, cellular biology and spectroscopic techniques, the action mechanism of VLL-28 has been elucidated. Intriguingly, it has been proved to be an effective ACP able to selectively kill tumor cells by inducing apoptosis.

2. Materials and methods

2.1. Peptide synthesis reagents

Polypropylene reaction vessels and sintered polyethylene frits were supplied by Alltech Italia (Milan, Italy). NovaSyn TGR resin, 2-(1H-benzotriazole-1-yl)-1,1,3,3-tetramethyluronium hexafluorophosphate (HBTU), cyano-hydroxyimino-acetic acid ethyl ester (Oxyma) and all amino acids were purchased from Novabiochem-Merck (Nottingham, U.K.). *N,N'*-diisopropylethylamine (DIPEA), piperidine, Kaiser test, trifluoroacetic acid (TFA), scavengers, fluorescein isothiocyanate (FITC) and *N*-methylmorpholine (NMM) were purchased from Sigma-Aldrich (Milan, Italy). *N,N*-Dimethylformamide (DMF) was purchased from CARLO ERBA Reagents (Milan, Italy). Acetonitrile (ACN), dichloromethane (DCM) and diethyl ether were purchased from VWR International (Milan, Italy). All aqueous solutions were prepared by using water obtained from a Milli-Q gradient A-10 system (Millipore, 18.2 M Ω -cm, organic carbon content \geq 4 μ g/L).

2.2. Peptide synthesis

VLL-28 and FITC-VLL-28 (VLL-28 derivative with an additional glycine residue at the C-terminus as spacer and a lysin residue for FITC labeling) peptides were manually synthesized using the fluorenylmethyloxycarbonyl (Fmoc) solid-phase strategy (0.2 mmol). The syntheses were performed on NovaSyn TGR resin (loading 0.24 mmol/g), using all standard amino acids. The Fmoc protecting group was removed by treatment with 30% piperidine in DMF (3 \times 10 min). The amino acids in 10-fold excess were pre-activated with HBTU (9.8 equiv)/Oxyma (9.8 equiv)/DIPEA (10 equiv) in DMF for 5 min and then added to the resin suspended in DMF. The reaction was performed for 1 h and the coupling efficiency was assessed by the Kaiser test. In the case of FITC-VLL-28 peptide, once synthesis was completed, the ivDde protecting group of Lys(ivDde) residue was selectively removed by treatment of the peptidyl resin with a solution of 2% hydrazine in DMF (20 \times 3 min). FITC labeling was then performed with 2 equiv of fluorescein isothiocyanate and 4 equiv of NMM in DMF for 5 h.

The peptides were finally cleaved off the resins by treatment with a mixture of trifluoroacetic acid (TFA)/water/triisopropylsilane (95:2.5:2.5 v/v/v) for 3 h at room temperature. The resins were filtered, the crude peptides were precipitated with diethyl ether, dissolved in H₂O/ACN solution, and lyophilized. The products were purified by preparative RP-HPLC on a Shimadzu system equipped with a UV-visible detector SPD10A using a Phenomenex Jupiter Proteo column (21.2 \times 250 mm; 4 μ m; 90 \AA) and a linear gradient of H₂O (0.1% TFA)/ACN (0.1% TFA) from 10%–55% of ACN (0.1% TFA) in 15 min at a flow rate of 20 mL/min. The collected fractions containing the peptides were lyophilized giving a final yield of about 35% of each pure product. The identity and purity of the compounds were assessed by the AGILENT Q-TOF LC/MS instrument equipped with a diode array detector combined with a dual ESI source on a Agilent C18 column (2.1 \times 50 mm; 1.8 μ m; 300 \AA) at a flow rate of 200 μ L/min and a linear gradient of H₂O (0.01% TFA)/ACN (0.01% TFA) from 5%–70% of ACN (0.01% TFA) in 15 min.

2.3. Cell culture

Malignant SVT2 murine fibroblasts (BALBc 3T3 cells transformed by SV40 virus), parental BALBc 3T3 murine cells, and HEK-293 human embryonic kidney cells were cultured in Dulbecco's Modified Eagle's

Medium (Sigma-Aldrich), supplemented with 10% fetal bovine serum (HyClone), 2 mM L-glutamine and antibiotics, in a 5% CO₂ humidified atmosphere at 37 °C. HRCE (Human Renal Cortical Epithelial) cells (InnoproT) were cultured in basal medium, supplemented with 2% fetal bovine serum, epithelial cell growth supplement and antibiotics, all from InnoproT, in a 5% CO₂ humidified atmosphere at 37 °C [18].

2.4. Cytotoxicity assays

Cells were seeded in 96-well plates (100 µL per well) at a density of 5×10^3 per well (SVT2, HEK-293, and HRCE cells) or 2.5×10^3 per well (BALBc 3T3 cells). VLL-28 peptide was added to the cells 24 h after seeding for time- and dose-dependent cytotoxic assays. At the end of incubation, cell viability was assessed by the MTT assay, as previously described [19]. In brief, MTT reagent, dissolved in DMEM in the absence of phenol red (Sigma-Aldrich), was added to the cells (100 µL per well) to a final concentration of 0.5 mg/mL. After a 4-h incubation at 37 °C, the culture medium was removed and the resulting formazan salts were dissolved by adding isopropanol containing 0.1 N HCl (100 µL per well). Absorbance values of blue formazan were determined at 570 nm using an automatic plate reader (MicrobetaWallac 1420, Perkin Elmer). Cell survival was expressed as percentage of viable cells in the presence of the peptide, with respect to control cells grown in the absence of the peptide. In all of the experiments described in this paper, controls were performed by supplementing the cell cultures with identical volumes of peptide buffer for the same time span. Obtained data represent the mean (\pm standard deviation) of at least 4 independent experiments, each one carried out with triplicate determinations. Statistical analysis was performed using a Student's *t*-Test, and significant differences were indicated as *($P < 0.05$), **($P < 0.01$) or ***($P < 0.001$).

2.5. Analysis of cell death

Cells were plated in 6-well plates (1 mL per well) at a density of 1×10^6 cells per well in complete medium for 24 h and then exposed to 20 µM VLL-28 for 6, 12 or 24 h to prepare cell lysates. Both untreated and treated cells were scraped off in PBS, centrifuged at $1000 \times g$ for 10 min and resuspended in lysis buffer (1% NP-40 in PBS, pH 7.4) containing protease inhibitors. After 30 min of incubation on ice, lysates were centrifuged at $14,000 \times g$ for 30 min at 4 °C. Upon determination of total protein concentration in the supernatant by the Bradford assay, samples were analyzed by SDS-PAGE followed by Western blotting using specific antibodies directed towards procaspase-3 (Cell Signaling Technology) or p62 (Novus Biologicals) proteins. For normalization to internal standard signals, antibodies against β -actin (Sigma-Aldrich) were used. In parallel experiments, cells were treated with puromycin (10 µg/mL) for 12 h or with rapamycin (20 µM) for 24 h, which were used as positive controls for apoptosis and autophagy induction, respectively.

For morphological analyses, cells were seeded on glass coverslips in 24-well plates and grown to semi-confluency. Cells were then incubated for 72 h with 20 µM VLL-28 peptide in complete medium, after which cells were washed with PBS, fixed for 10 min at room temperature (RT) with 4% paraformaldehyde in PBS and mounted in 50% glycerol in PBS. Samples were then examined using a confocal laser-scanner microscope Zeiss LSM 700. All images were taken under identical conditions.

2.6. Fluorescence studies

Fluorescence analyses were performed as previously described [20]. Briefly, cells were seeded on glass coverslips in 24-well plates, grown to semi-confluency, and then incubated for 12 h with 20 µM FITC-labeled VLL-28. Following incubation, cells were washed with PBS and then fixed for 10 min at RT with 4% paraformaldehyde in PBS. Cell membranes were labeled by incubating the cells with Wheat Germ

Agglutinin (WGA, 5 µg/mL) Alexa Fluor®594 Conjugate (ThermoFisher Scientific) for 10 min at RT. Cells were then washed twice in PBS following the manufacturer's instructions. Confocal microscopy analyses were performed with a confocal laser-scanner microscope Zeiss LSM 700.

2.7. Circular dichroism analyses

Far-UV CD spectra were recorded on a Jasco J-810 spectropolarimeter (JASCO Corp) equipped with a PTC-423S/15 Peltier temperature controller in the wavelength interval of 198–260 nm. Experiments were performed using a 20 µM VLL-28 solution (in PBS pH 7.4) in a 0.1 cm path-length quartz cuvette as already reported in Notomista et al. [16].

CD spectra in the presence of intact cells were registered using 8×10^5 BALBc 3T3 cells or SVT2 cells at different incubation times (0, 10, 30, 60 min and 24 h) in PBS buffer at 20 °C. The baseline was corrected by subtracting the spectrum of the cells alone at the same time of incubation [21–23].

2.8. Membrane preparation

Membranes used in NMR experiments were isolated from BALBc 3T3 or SVT2 cells and obtained as reported in Farina et al. [24]. In details, cells were detached from the flask with trypsin and washed twice with PBS. Then the cells were transferred into homogenization buffer containing PBS and homogenized by means of a pellet pestle (Sigma). Particulate matter was removed by centrifuging at 3500 rpm for 15 min. The supernatant was then centrifuged at 28000 rpm for 1 h at 4 °C. The pellet was washed and centrifuged at 28000 rpm for 30 min at 4 °C. 180 µL of PBS plus 20 µL D₂O were added to the pellet, and the membrane was re-suspended by 20 passages through a 25 gauge needle.

2.9. NMR spectroscopy

All NMR experiments were carried out at 298 K using an Inova 600 MHz spectrometer (Varian Inc., Palo Alto, CA, USA), equipped with a cryogenic probe optimized for ¹H detection.

NMR samples were prepared as follows. For chemical shift assignment and conformational analysis, 1 mg of VLL-28 was dissolved either in 500 µL sodium phosphate 20 mM pH 7.0 with 10% v/v D₂O or in 500 µL of the same buffer containing 25% (v/v) TFE (2,2,2-trifluoroethanol-D3 99.5% isotopic purity, Sigma-Aldrich). One-dimensional (1D) ¹H spectra were acquired with a spectral width of 7191.66 Hz, relaxation delay 1.03 s, 7k data points for acquisition and 16k for transformation. Bi-dimensional (2D) [¹H, ¹H] total correlation spectroscopy (TOCSY) [25], double quantum filtered correlated spectroscopy (COSY) [26] and nuclear Overhauser effect spectroscopy (NOESY) [27] were acquired with 32 or 64 scans per t1 increment with a spectral width of 7191.66 Hz along both t1 and t2, 2048 \times 256 data points in t2 and t1, respectively, and recycle delay 1.0 s. Water suppression was achieved by means of Double Pulsed Field Gradient Spin Echo (DPFGSE) sequence [28,29]. TOCSY experiments were recorded using a DIPSI-2 mixing scheme of 70 ms with 7.7 kHz spin-lock field strength. NOESY spectra were carried out with a mixing time of 250 ms. Data were typically apodized with a square cosine window function and zero filled to a matrix of size 4096 \times 1024 before Fourier transformation and baseline correction.

According to the procedure recently reported [24] for interaction studies of VLL-28 with intact cells and isolated membranes of BALBc 3T3 and SVT2 cell lines, pellet of 18×10^6 cells and membranes from 18×10^6 cells, obtained as reported above, were re-suspended in 150 µL of PBS buffer (pH 7.4) and 10% ²H₂O, to obtain reference spectra, or of VLL-8 (430 µM) in PBS buffer. STD spectra were acquired with 10,000 scans with on-resonance irradiation at 0.2 ppm or 5.2 ppm for saturation of membrane proteins or lipids resonances, respectively,

and off-resonance irradiation at 30 ppm. A train of 40 Gaussian shaped pulses of 50 ms with 1 ms delay between pulses were used, for a total saturation time of 2 s. STD spectra were obtained by internal subtraction of saturated spectrum from off-resonance spectrum by phase cycling. STD spectrum of the only peptide was also acquired and did not show any signal. 2D [¹H, ¹H] TOCSY and NOESY spectra of VLL-28 in presence of isolated membranes were also acquired, similarly to those of the peptide alone.

All NMR data were processed with the software VNMRJ 1.1.D (Varian Inc.). 1D spectra were analyzed using ACD/NMR Processor 12.0 [www.acdlabs.com]. 2D TOCSY, COSY and NOESY spectra for proton chemical shift assignment were analyzed using Homoscope, a tool available in CARA (Computer Aided Resonance Assignment) software. Chemical shift assignments of VLL-28 in the absence of TFE are referred to residual water proton signals, (4.75 ppm), whereas in 25% TFE to residual TFE proton signals (3.88 ppm). Chemical shift deviations from random coil values for H α were calculated using the ChemShiftDeviationsFile script available in CARA.

2.10. Zeta-potential measurements of bacterial and eukaryotic cells in the presence of VLL-28

BL21 (DE3) *E. coli* cells were plated on Luria-Bertani agar overnight at 37 °C. An isolated bacterial colony was used to inoculate Mueller Hinton Broth (MHB; OXOID, Hampshire, UK), and the bacterial culture was allowed to grow overnight at 37 °C. 100 μ L of culture was used to freshly inoculate 5 mL of MHB. The suspension was incubated at 37 °C for ~2 h, until a final bacterial concentration of $\sim 3 \times 10^8$ colony forming units per mL (CFU/mL) was reached ($OD_{600nm} \sim 0.1$). Bacterial suspensions were diluted using fresh MHB to 3×10^7 CFU/mL for zeta-potential studies. Afterwards, cells were centrifuged at $12,000 \times g$ for 5 min, and washed three times using 20 mM sodium phosphates buffer, pH 7.4. The zeta-potential of bacterial cells was determined at 25 °C from the mean of 3 measurements (50 runs each), in the absence and presence of different VLL-28 concentrations (0–10 μ M). Zeta-potential values were obtained by phase analysis light scattering (PALS) in a Zetasizer Nano ZS (Malvern Instruments, Malvern, UK), using disposable zeta cells with gold electrodes. Values of viscosity and refractive index were set to 0.8872 cP and 1.330, respectively.

Confluent BALBc 3T3 and SVT2 cells were washed with PBS buffer followed by trypsinization. Zeta potential measurements of eukaryotic cells were performed using the Diffusion Barrier Technique (Malvern, Application Note). 4×10^5 cells were dispensed into the disposable zeta cells with gold electrodes in PBS with and without the peptide (from 0 to 50 μ M) and allowed to equilibrate for 30 min at 37 °C. One measurement (~70 runs each) was performed with a constant voltage of 40 V. The complete experiment was carried out at least two times using independent cellular suspensions.

3. Results and discussion

3.1. Selective antitumor action of VLL-28 peptide

To assess whether VLL-28 was endowed with anti-cancer activity, cytotoxicity assays were performed on malignant SVT2 mouse fibroblasts and parental non-malignant BALBc 3T3 mouse fibroblasts. Interestingly, these studies have shown that the peptide VLL-28 exerts a dose- and time-dependent inhibition of viability on malignant SVT2 murine fibroblasts (see Fig. 1a). Conversely, the peptide was found to be inactive towards the non-malignant line of BALBc 3T3 fibroblasts (Fig. 1b). This evidence was also confirmed by morphological analyses through light microscopy, where a severe alteration of cell morphology with the presence of cell debris was observed only in the case of SVT2 cancer cells, with an IC₅₀ value of 10 μ M at 72 h (Fig. S1). Remarkably, this peptide was also found to be effective and selective against human tumor cell lines, as demonstrated by MTT assays performed on

transformed HEK-293 cells (with an IC₅₀ value of 10 μ M at 72 h) and human primary renal cortical epithelial (HRCE) cells (Fig. S2). In agreement with these results, it has been previously reported that other AMPs, which are toxic for bacteria but not for normal mammalian cells, are instead cytotoxic for cancer cells [30].

3.2. Internalization of VLL-28 peptide

Most AMPs and ACPs share a common membranolytic mechanism of action that results first either in the selective disruption or permeation of the cancer cell membrane and then in the swelling of mitochondria. Nonetheless, a non-membranolytic mechanism of action is increasingly recognized as an alternative ACPs mechanism [31]. To test whether the selective antitumor activity of VLL-28 was associated to a membranolytic mechanism and/or to its internalization, we performed experiments by using the peptide labeled with fluorescein isothiocyanate (FITC). To this purpose, SVT2 and BALBc 3T3 cells were incubated for 12 h with 20 μ M FITC-labeled VLL-28, since this concentration of peptide turned out to be the most effective in terms of cytotoxicity. As shown in Fig. 2a, in the case of SVT2 cells, VLL-28 fluorescent signal appears to be mostly intracellular already after 12 h of incubation, thus indicating that the peptide is internalized into the target cancer cells. On the other hand, the peptide (green) mainly colocalizes with WGA (red) at the plasma membrane in BALBc 3T3 cells (as indicated by arrows in Fig. 2b). The lack of VLL-28 internalization into these latter cells is consistent with the absence of cytotoxicity emerged from viability tests (Fig. 1b). Fluorescent staining was found to be specific, as no fluorescent signals were observed in the absence of FITC-labeled peptide (data not shown). Since the internalization has been observed at a time point preceding the cell death (48–72 h), the molecular target of VLL-28 might be a not yet identified intracellular component.

3.3. VLL-28 CD analyses in the presence of intact eukaryotic cells

Since differences in the plasma membrane composition between normal and cancer cells are supposed to contribute to the selective permeability and toxicity of ACPs towards the latter, we resolved to examine if the presence of the two different cell lines affects differently the secondary structure of VLL-28. Interestingly, VLL-28 CD spectra registered in the presence of either BALBc 3T3 or SVT2 whole cells revealed a different behavior (Fig. 3). In particular, in the presence of BALBc 3T3 cells, VLL-28 seems to gradually get structured over time until a prevalence of helical structure is observed upon 1 h incubation (Fig. 3a). Indeed, the spectrum shows two minima, at 208 and 222 nm, typical of helical structure, in agreement with CD data obtained in the presence of *n*-dodecyl-phosphatidylcholine (DPC), a well-known eukaryotic membrane mimetic agents [16]. Differently, in the presence of SVT2 intact cells, a drop in the CD signal is observed suggesting a fast internalization process of VLL-28, occurring already after 10 min (Fig. 3b), as confirmed by confocal microscopy data (Fig. 2).

3.4. NMR conformational analysis of VLL-28

In order to gain insight into the mechanism of action of VLL-28 and provide information on the basis of the different behaviors of VLL-28 with regard to the two studied cell lines, a NMR conformational analysis of the peptide in the absence and in the presence of TFE, a well-known structuring solvent, has been initially carried out (Figs. S3 and S4). According with what previously observed by CD analysis [16], VLL-28 does not adopt a well-defined conformation in phosphate neutral solution, as indicated by sharp and low-dispersed resonances in both the amide/aromatic and the aliphatic regions (Fig. S3a). Upon addition of TFE (25% v/v), amide, aromatic and aliphatic proton resonances resulted significantly more dispersed (Fig. S3b). In particular, the tryptophan side chain H_N, clearly distinguishable at 10.14 ppm in

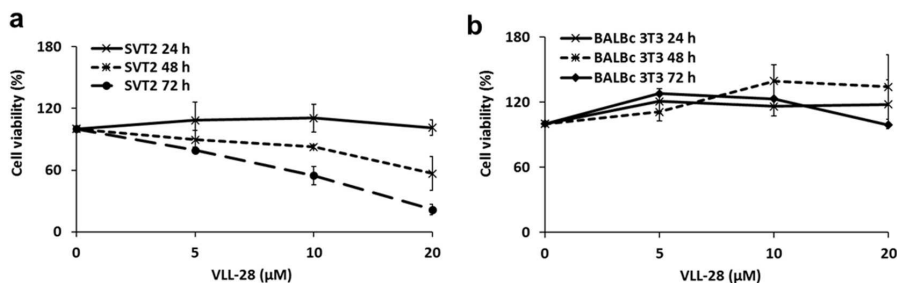


Fig. 1. Effects of the peptide VLL-28 on the SVT2 (a) and BALBc 3T3 (b) cell viability. MTT assays were performed on cells treated with increasing amounts of the peptide (5, 10 and 20 μM) for different time spans (24, 48 and 72 h). The viability of cell samples was expressed as the percentage of MTT reduction with respect to control cells, tested under the same conditions but in the absence of the peptide. Data represent the mean (\pm standard deviation, SD) of at least 4 independent experiments, each one carried out with triplicate determinations. * $P < 0.05$, ** $P < 0.01$, or *** $P < 0.001$ were obtained for control versus treated samples in the case of SVT2 cells treated with VLL-28 peptide for 48 and 72 h.

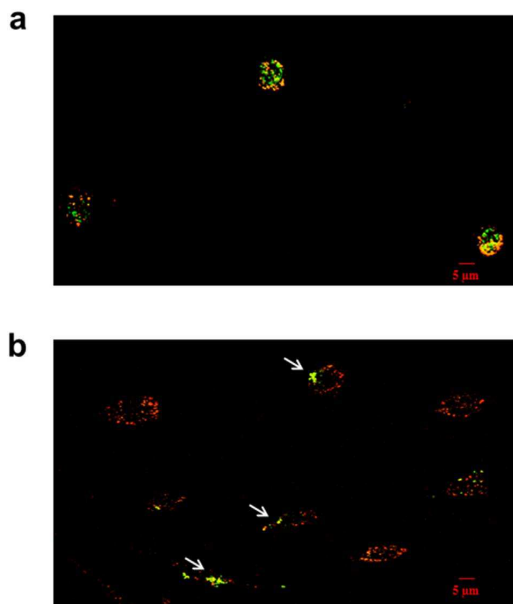


Fig. 2. Internalization of VLL-28 peptide in SVT2 (a) and BALBc 3T3 (b) cells. Cells were cultured on coverslips, incubated for 12 h with 20 μM VLL-28 peptide (green) and stained with WGA (5 μg/mL, Alexa Fluor[®]594 Conjugate). Cells were analyzed by confocal microscopy.

the absence of TFE (Fig. S3a, left), exhibits up-field shift at 9.94 ppm upon addition of TFE (Fig. S3b, left), possibly induced by an aromatic-aromatic long-range interaction. Moreover, 2D [¹H, ¹H] NOESY spectrum of VLL-28 peptide contains a consistent higher number of cross-peaks with respect to that recorded in the absence of TFE, indicating a more structured conformation (Fig. S4). Almost complete assignment of proton resonances of VLL-28 has been achieved in 25% TFE by using a combination of TOCSY and NOESY spectra, according to the standard procedures (Table S1).

To assess the secondary structure of VLL-28 in 25% TFE, analyses of the H_α chemical shift deviations from random coil values ($\Delta\delta H_{\alpha}$) and of the NOE patterns were performed. Interestingly, two regions encompassing residues V³⁷-R⁴⁸ and V⁵⁰-S⁵⁹ showed large negative deviations ($\Delta\delta H_{\alpha} < -0.1$ ppm), suggesting that the peptide mostly assumes a helical conformation, which is lost in the last C-terminal amino acids (Fig. 4a). Accordingly, H_N-H_N NOEs, together with H_{αi}-H_{Ni+3} and H_{αi}-H_{βi+3} NOEs, were observed starting from residues V³⁷ to S⁵⁹ only in the presence of TFE (Fig. 4b and c), further confirming the helical

structure of that region in TFE.

3.5. STD NMR interaction studies of VLL-28 with tumor and normal cell membranes and definition of its binding epitopes

To identify binding residues of VLL-28 saturation transfer difference (STD) NMR binding experiments of the peptide in the presence of intact SVT2 and BALBc 3T3 cells [32], as well as of their isolated membranes, were performed. Unfortunately, ¹H NMR VLL-28 proton resonances vanish in the presence of each of the two cell lines, thus hampering a detailed molecular analysis of the VLL-28 interaction with the cellular membranes (data not shown).

Very recently, we described the use of native cell membranes to overcome peptide cell internalization issues in “on-cell” NMR binding experiments [24]. This approach provides a significant improvement of NMR peptide spectra with respect to those acquired by using intact cells. Particularly, in the presence of isolated membranes, the ¹H NMR signals of the peptide are sharper and better resolved, the STD signals appear significantly stronger, and background signals of the cellular components result much weaker in both the ¹H and the STD spectra [24]. On the basis of the biochemical evidences of peptide internalization (see above), we carried out STD NMR experiments of the VLL-28 peptide in the presence of isolated membranes.

Interestingly, ¹H NMR peptide signals resulted well visible in the presence of both SVT2 and BALBc 3T3 cell membranes as in the sole buffer (Fig. S5), thus allowing to perform STD NMR binding studies. In particular, we evaluated the binding capability of VLL-28 to the two different components of the cell membrane, proteins and lipids, acquiring STD spectra at two different saturation frequencies, i.e. one to selectively saturate proteins (0.2 ppm) and another one to saturate lipids (5.2 ppm) [33]. Remarkably, the ¹H STD spectra showed that VLL-28 receives a detectable saturation transfer in the presence of cell membranes only when lipids are saturated (Fig. 5). This effect, which is negligible in the absence of cell membranes (Fig. 5b), provides a direct observation of the binding of VLL-28 to the lipid component of the cell membranes. This finding is in agreement with previous results showing that the peptide is able to interact with lipids mimicking bacterial membranes [16]. It is worth of note that differences in the STD spectra were observed for BALBc 3T3 and SVT2 cell membranes (Fig. 5). In particular, a higher number of STD signals, with stronger intensities, was observed in the presence of BALBc 3T3 cell membranes compared with those of SVT2 (Fig. 6a). In particular, all the binding residues of VLL-28 to the SVT2 cell membranes are in common with that of the BALBc 3T3 cell membranes. Specifically, VLL28 residues involved in both BALBc 3T3 and SVT2 interaction are G⁴⁹, Y⁵² and W⁵⁵ (Fig. 6b, highlighted in magenta). Moreover, one or both of the two threonine residues, T⁴¹ and T⁴³, appear involved in the VLL-28 interaction with both cell lines. On the other hand, Q⁴⁷, V⁵⁰, I⁵¹ and F⁵⁸, together with the acetyl N-terminal, show protons that are saturated only in the

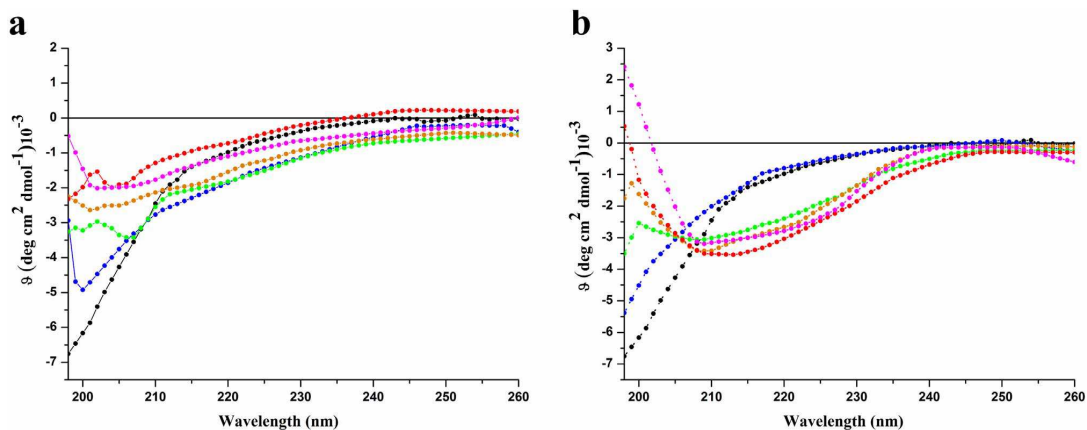


Fig. 3. Far UV VLL-28 CD spectra (black) recorded in the presence of a) BALBc 3T3 cells and b) SVT2 cells at 0 (blue), 10 (green), 30 (orange), 60 (red) min and 24 h (magenta) of incubation.

presence of BALBc 3T3 membranes (Fig. 6b, highlighted in red). Furthermore, strong STD effects were observed for side-chains of arginine and lysine residues. However, due to the spectral overlap and to the presence of a high number of basic residues in the peptide sequence they could not be identified unambiguously. Moreover, methyl of leucine (L) and valine (V) localized in the N-terminal region, seem to be involved as well.

Overall, these data indicate that the interaction of VLL-28 with cell membranes is mediated by the N-terminal and the central regions (V³⁷-F⁵⁸) (Fig. 6), which interestingly correspond to the portions of the

peptide that assume helical conformation in presence of TFE. Specifically, the binding to both the cell membranes seems to be mainly mediated by aromatic and basic residues, as could be expected for peptide-lipid interactions.

Different STD intensities of the peptide induced by the interaction with BALBc 3T3 and SVT2 cell membranes are likely ascribed to a different interaction mechanism between the peptide and the two membranes. In particular, stronger STD effects observed in the presence of non-tumor BALBc 3T3 membranes indicates that a fast-exchange equilibrium between the free form and a well-recognized bound

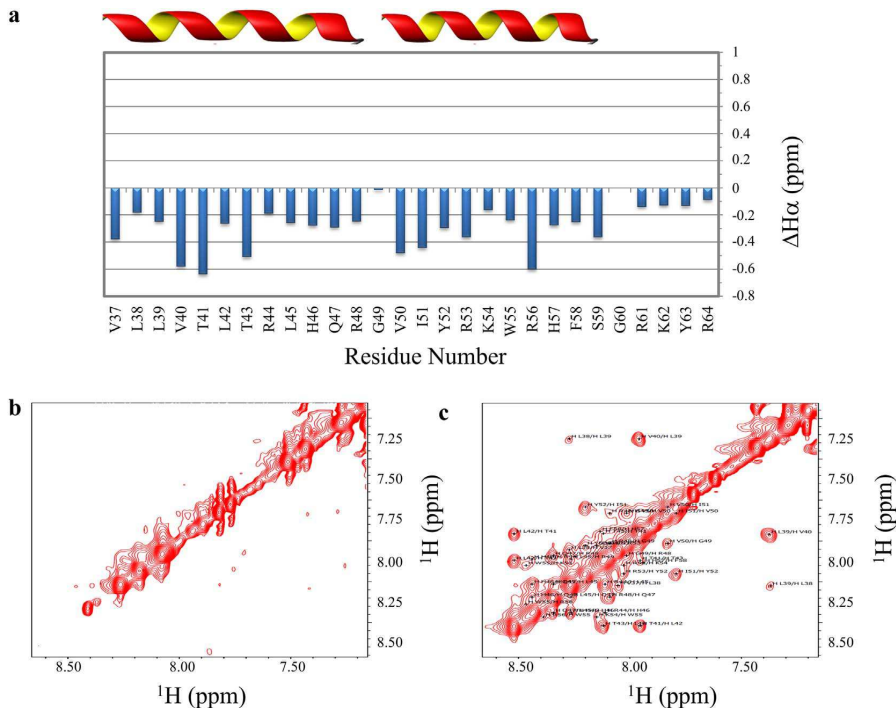


Fig. 4. (a) Chemical shift deviation from random coil values of H α backbone atoms ($\Delta H\alpha$) plotted as a function of residue number. Two segments with helical conformation encompassing residues V37-R58, V50-S59, as suggested from the $\Delta H\alpha$ s, are indicated above the plot. (b) and (c) Expansions of the H $_N$ -H $_N$ correlation region of the 2D [1H , 1H] NOESY spectra of VLL-28 in phosphate buffer pH 7.0 at 298 K in the absence and presence of TFE 25%, respectively. H $_N$ -H $_N$ + 1 cross-peaks, observed only in (C), are labeled.

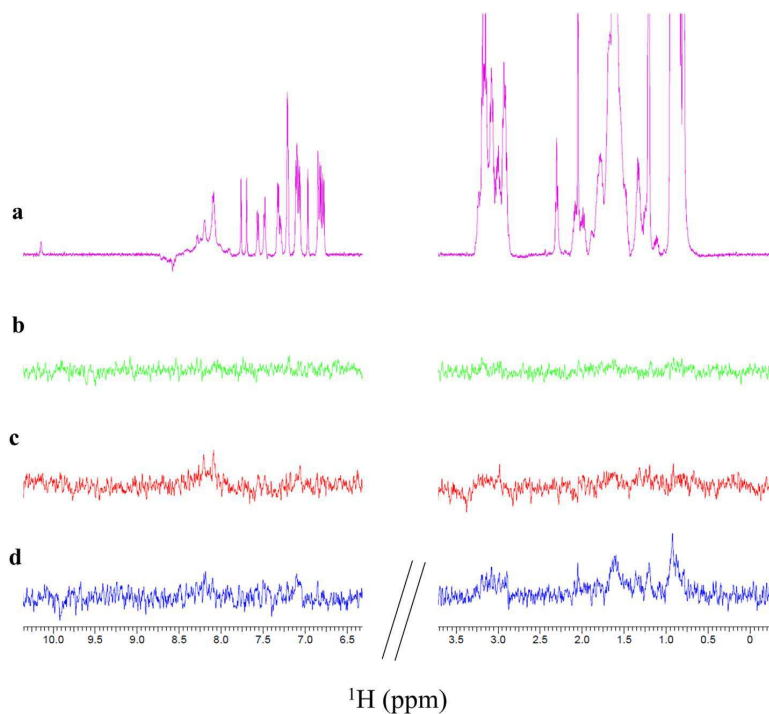


Fig. 5. Reference ^1H (a) and (STD)-NMR spectra of VLL-28 in the absence (b) and in the presence of SVT2 (C) and BALBc 3T3 (D) cell membranes.

conformation occurs. Since fast-exchange regime is observed with lower affinity interaction, this could explain the inability of VLL-28 to penetrate these cell membranes. Differently, the reduced STD effects, observed in the presence of SVT2 membranes, can be ascribed to a stronger interaction with the cell membranes possibly being the first step of an internalization process.

3.6. Effect of VLL-28 on zeta-potential of cell membranes

Zeta potential of cell membranes has been used as a possible marker for the assessment of membrane damage and could be suitable to study the permeabilizing property of the VLL-28 peptide [34]. Zeta potential analyses were performed on *E. coli*, BALBc 3T3 and SVT2 cells. The

measured zeta potential in our experimental conditions for the cells in the absence of any peptide is -43.93 mV for *E. coli* (Fig. S6), -6.91 mV for BALBc 3T3 and -11.2 mV for SVT2 cells, respectively, indicating that their surfaces are all negatively charged and, as already known, that the surface of the bacterial membranes is more negatively charged than mammalian cells [35,36]. This is due to both lipid composition and negatively charged cell surface macromolecules, as described also for other systems [9]. Furthermore, Z-potential measurements clearly demonstrated that the surface of SVT2 has a more negative charge than BALBc 3T3 cells. The addition of VLL-28 caused an increase of Z-potential values towards neutralization indicating that the peptide is interacting with the surface of all the cells tested (Fig. 7a and b and S6). Given the role of electrostatic interactions in driving the

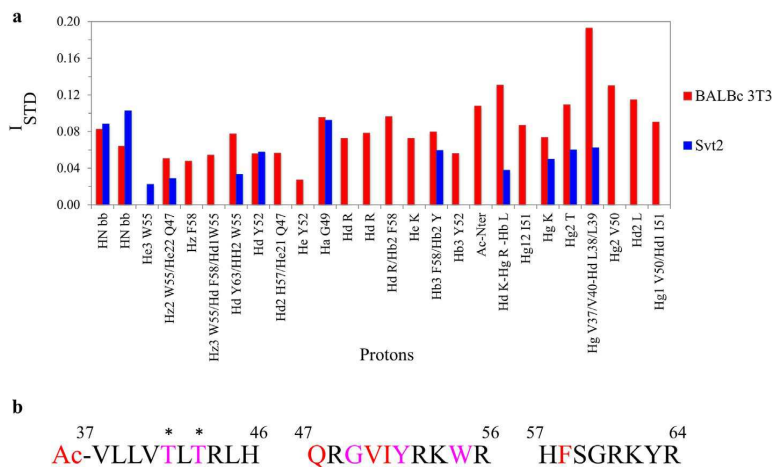


Fig. 6. (a) Bar graphs of STD signal intensities (I_{STD}) for the VLL-28 H^{N} /aromatic and aliphatic protons receiving saturation transfer in the presence of BALBc 3T3 (red bars) and SVT2 (blue bars) cell membranes. In the x-axis label, HNbb = not assigned backbone amide protons, R = $\text{R}^{\text{H4}}/\text{R}^{\text{H8}}/\text{R}^{\text{H3}}/\text{R}^{\text{H6}}/\text{R}^{\text{H4}}$, K = $\text{K}^{\text{H4}}/\text{K}^{\text{H4}}$, Y = $\text{Y}^{\text{H2}}/\text{Y}^{\text{H3}}$; L = $\text{L}^{\text{H8}}/\text{L}^{\text{H9}}$; T = $\text{T}^{\text{H1}}/\text{T}^{\text{H3}}$. (b) The VLL-28 sequence is reported. VLL-28 residues showing STD effect in the presence of the both cell membranes are highlighted in magenta, whereas those affected only in the presence of BALBc 3T3 in red. Asterisks indicate that, due to overlapped proton resonances, one or both the threonine are possibly involved in the interaction with BALBc 3T3 and SVT2 cell membranes. Residues that are not involved in the binding or that could not be identified unambiguously are indicated in black.

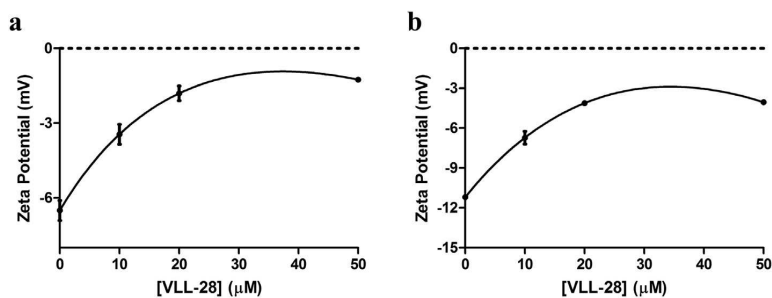


Fig. 7. a) VLL-28 effect on the Z-potential of BALBc 3T3 cells. b) VLL-28 effect on the Z-potential of SVT2 cells. At 4×10^5 cells/mL cells were incubated and stabilized for 30 min with different peptide concentrations and the potential was measured at 37 °C. Data represent the mean (\pm standard deviation, SD) of 2 independent experiments.

AMPs initial adsorption onto the extracellular surface, it is reasonable to question if VLL-28, as ACP, exerts the same kind of action. In accordance with the general mechanism of action of AMPs, VLL-28 fully neutralizes *E. coli* cell's surface potential to exert its antimicrobial action (Fig. S6). Differently, on eukaryotic cells, VLL-28 is able to increase the Z-potential but never reaching full neutralization even at concentrations ≥ 20 μM thus indicating that total surface neutralization is not necessary to elicit its anticancer action [37].

3.7. Cell death pathway activated by cell treatment with VLL-28

To elucidate cell death pathways selectively activated by cell treatment with VLL-28, we performed western blot analyses by using antibodies specifically recognizing pro-caspase-3 and p62 proteins. The activation of procaspase-3 to caspase-3 is a key event in the apoptotic execution phase, since caspase-3 is considered the most important among executioner caspases and is activated by any of the initiator caspases (caspase-8, caspase-9, or caspase-10) [38]. p62, instead, is generally used as a marker to study the autophagic flux, since it accumulates when autophagy is inhibited, whereas p62 decreased levels can be observed when autophagy is induced [39].

To get insight into cell death pathway induced by VLL-28, western blot analyses were performed on SVT2 cells in comparison with BALBc 3T3 (Fig. 8a–d). In SVT2 cells it was found a significant increase of p62 levels upon 6 h treatment with 20 μM VLL-28 (Fig. 8a, d), indicative of

a stress leading to cell death with a consequent block of autophagy flux [40]. Accordingly, procaspase-3 levels appear lower than in control cells upon 6 and 12 h treatment (Fig. 8a, b), indicating a significant (about 30%) activation of procaspase-3 to caspase-3 associated to apoptosis induction. This activation appears even stronger (about 50%) after 24 h of treatment (Fig. 8a, b), and is associated to a significant decrease of p62 levels (Fig. 8a, d), in agreement with a time-dependent activation of apoptotic cell pathway.

In the case of non-malignant BALBc 3T3 cells, instead, no significant effects on procaspase-3 levels were observed upon cell treatment with 20 μM VLL-28 peptide at different time intervals (6, 12 and 24 h) (Fig. 8b, c), in agreement with the results reported above. This indicates that these cells are not susceptible to VLL-28 peptide toxic effects. Moreover, no significant effects were observed also when p62 levels were analyzed, except for 72 h treatment, where a slight increase of p62 levels was observed (Fig. 8b, d). Since no effects on cell viability were detected by MTT assays, this might be indicative of a slight cell perturbation counteracted by autophagy activation.

Hence, experimental data revealed that VLL-28 exerts its action through a time-dependent activation of apoptotic cell pathways as demonstrated by the maturation of procaspase-3 to the caspase-3 [41]. This is in agreement with data reported in the literature indicating that several potential ACPs are able to induce apoptosis in human cancer cell lines of different origin, such as breast, uterine cervix, liver and prostate [9]. Apoptosis induction, with some degree of selectivity

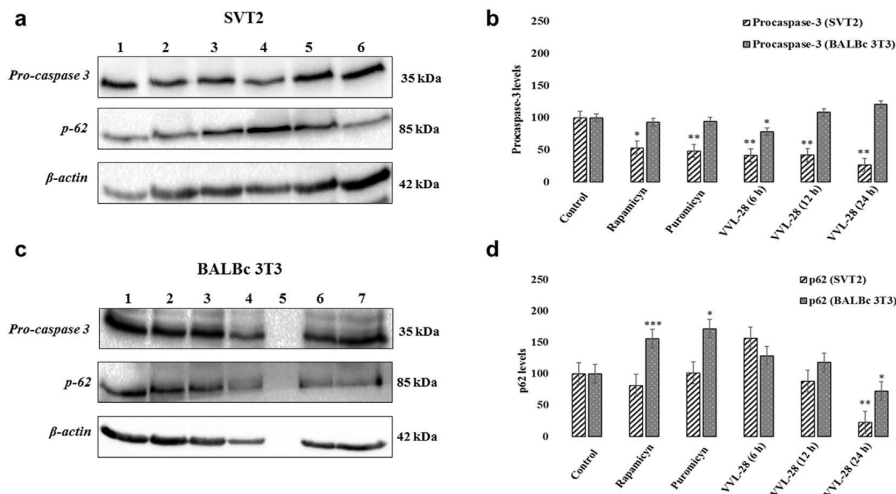


Fig. 8. Analysis of cell death pathway activated by the treatment with 20 μM VLL-28 peptide of SVT2 (a) and BALBc 3T3 (c) cells. Lane 1, cell lysate of untreated cells; lane 2, lysate of cells treated with rapamycin; lane 3, lysate of cells treated with puromycin; lane 4, lysate of cells treated with the peptide for 6 h; lane 5, lysate of cells treated with the peptide for 12 h; lane 6, lysate of cells treated with the peptide for 24 h. Western blots were performed by using antibodies directed towards procaspase-3, p62, and endogenous β-actin used as an internal standard (a, c). Densitometric analyses of protein bands specifically recognized by anti-procaspase-3 and anti-p62 antibodies are reported in b and d, respectively, where data represent the mean (\pm standard deviation, SD) of 3 independent experiments. * $P < 0.05$, ** $P < 0.01$, *** $P < 0.001$ were obtained for control versus treated samples.

towards cancer cells, has been described also in the case of ACPs effective on metastatic tumor cells or on cancer endothelial cells [9]. Since metastases are the main cause of conventional therapy failure, peptides able to specifically interfere with the process of metastases formation by stimulating apoptosis induction in neoplastic cells represent valuable resources in cancer treatment [9]. These observations associated to the strong and selective toxic effects exerted by VLL-28 peptide towards cancer cells open interesting perspective to future applications of this peptide.

4. Concluding remarks

The cytotoxic activities of several AMPs turn this group of molecules into an amazing pool of new templates for anticancer drug development [42]. Accordingly, VLL-28, previously identified as an AMP [16], is here found to be endowed also with selective cytotoxic activity towards both murine and human cancer cells, thus pointing to VLL-28 as a potential chemotherapeutic agent. Microorganisms belonging to the archaeal kingdom have been so far considered as source of biotechnologically relevant enzymes and proteins [43–51], but there are no reports regarding potential ACPs isolated from this kingdom. This paper represents the first evidence that archaeal microorganisms could bear also an unexplored repertoire of such kind of molecules exerting a trans-kingdom action. Given the intrinsic stability to physical and chemical agents of Stf76, the parental source of VLL-28, it is foreseen that VLL-28 might be a promising “lead compound” for future development of novel drugs, upon chemical modifications, i.e. D-amino acids, an all-hydrocarbon bridge, and/or modified amide bonds to further increase its stability to proteases [22].

Transparency document

The <http://dx.doi.org/10.1016/j.bbagen.2017.06.009> associated with this article can be found, in online version.

Appendix A. Supplementary data

Supplementary data to this article can be found online at <http://dx.doi.org/10.1016/j.bbagen.2017.06.009>.

References

- [1] S.C. Mansour, O.M. Pena, R.E. Hancock, Host defense peptides: front-line immunomodulators, *Trends Immunol.* 35 (2014) 443–450.
- [2] J. Wiesner, A. Vilcinskas, Antimicrobial peptides: the ancient arm of the human immune system, *Virulence* 1 (2010) 440–464.
- [3] A.L. Hilchie, K. Wuerrh, R.E.W. Hancock, Immune modulation by multifaceted cationic host defense (antimicrobial) peptides, *Nat. Chem. Biol.* 9 (2013) 761–768.
- [4] K.C.L. Mulder, L.A. Lima, V.J. Miranda, S.C. Dias, O.L. Franco, Current scenario of peptide-based drugs: the key roles of cationic antitumor and antiviral peptides, *Front. Microbiol.* 4 (2013).
- [5] M. Pushpanathan, P. Gunasekaran, J. Rajendran, Antimicrobial peptides: versatile biological properties, *Int. J. Pept. Biol.* 2013 (2013) 675391.
- [6] S. Riedl, D. Zwytyck, K. Lohner, Membrane-active host defense peptides — challenges and perspectives for the development of novel anticancer drugs, *Chem. Phys. Lipids* 164 (2011) 766–781.
- [7] R.E.W. Hancock, E.F. Haney, E.E. Gill, The immunology of host defence peptides: beyond antimicrobial activity, *Nat. Rev. Immunol.* 16 (2016) 321–334.
- [8] V. Teixeira, M.J. Feio, M. Bastos, Role of lipids in the interaction of antimicrobial peptides with membranes, *Prog. Lipid Res.* 51 (2012) 149–177.
- [9] D. Gaspar, A.S. Veiga, M.R.B. Castanho, From antimicrobial to anticancer peptides. A review, *Front. Microbiol.* 4 (2013).
- [10] G. Gabernet, A.T. Muller, J.A. Hiss, G. Schneider, Membranolytic anticancer peptides, *Med. Chem. Commun.* 7 (2016) 2232–2245.
- [11] A.L. Rerole, J. Gobbo, A. De Thonel, E. Schmitt, J.P. Pais de Barros, A. Hammann, D. Lanneau, E. Fourmaux, O.N. Demidov, O. Mischeau, L. Lagrost, P. Colas, G. Kroemer, C. Garrido, Peptides and aptamers targeting HSP70: a novel approach for anticancer chemotherapy, *Cancer Res.* 71 (2011) 484–495.
- [12] I. Kuriyama, A. Miyazaki, Y. Tsuda, H. Yoshida, Y. Mizushima, Inhibitory effect of novel somatostatin peptide analogues on human cancer cell growth based on the selective inhibition of DNA polymerase beta, *Bioorg. Med. Chem.* 21 (2013) 403–411.
- [13] K. Pane, L. Durante, O. Crescenzi, V. Cafaro, E. Pizzo, M. Varcamonti, A. Zanfardino, V. Izzo, A. Di Donato, E. Notomista, Antimicrobial potency of cationic antimicrobial peptides can be predicted from their amino acid composition: application to the detection of “cryptic” antimicrobial peptides, *J. Theor. Biol.* 419 (2017) 254–265.
- [14] R. Gaglione, E. Dell’Omo, A. Bosso, M. Chino, K. Pane, F. Ascione, F. Itri, S. Caserta, A. Amoresano, A. Lombardi, H.P. Haagsman, R. Piccoli, E. Pizzo, E.J. Veldhuizen, E. Notomista, A. Arciello, Novel human bioactive peptides identified in apolipoprotein B: evaluation of their therapeutic potential, *Biochem. Pharmacol.* (2017).
- [15] K. Pane, V. Sgambati, A. Zanfardino, G. Smaldone, V. Cafaro, T. Angrisano, E. Pedone, S. Di Gaetano, D. Capasso, E.F. Haney, V. Izzo, M. Varcamonti, E. Notomista, R.E.W. Hancock, A. Di Donato, E. Pizzo, A new cryptic cationic antimicrobial peptide from human apolipoprotein E with antibacterial activity and immunomodulatory effects on human cells, *FEBS J.* 283 (2016) 2115–2131.
- [16] E. Notomista, A. Falanga, S. Fusco, L. Pirone, A. Zanfardino, S. Galdiero, M. Varcamonti, E. Pedone, P. Contursi, The identification of a novel *Sulfolobus islandicus* CAMP-like peptide points to archaeal microorganisms as cell factories for the production of antimicrobial molecules, *Microb. Cell Factories* 14 (2015).
- [17] P. Contursi, B. Farina, L. Pirone, S. Fusco, L. Russo, S. Bartolucci, R. Fattorusso, E. Pedone, Structural and functional studies of Stf76 from the *Sulfolobus islandicus* plasmid-virus pSVX: a novel peculiar member of the winged helix-turn-helix transcription factor family, *Nucleic Acids Res.* 42 (2014) 5993–6011.
- [18] E. Galano, A. Arciello, R. Piccoli, D.M. Monti, A. Amoresano, A proteomic approach to investigate the effects of cadmium and lead on human primary renal cells, *Metallomics* 6 (2014) 587–597.
- [19] D.M. Monti, D. Guarnieri, G. Napolitano, R. Piccoli, P. Netti, S. Fusco, A. Arciello, Biocompatibility, uptake and endocytosis pathways of polystyrene nanoparticles in primary human renal epithelial cells, *J. Biotechnol.* 193 (2015) 3–10.
- [20] A. Arciello, N. De Marco, R. Del Giudice, F. Guglielmi, P. Pucci, A. Relini, D.M. Monti, R. Piccoli, Insights into the fate of the N-terminal amyloidogenic polypeptide of ApoA-I in cultured target cells, *J. Cell. Mol. Med.* 15 (2011) 2652–2663.
- [21] G. Smaldone, D. Diana, L. Pollegioni, S. Di Gaetano, R. Fattorusso, E. Pedone, Insight into conformational modification of alpha-synuclein in the presence of neuronal whole cells and of their isolated membranes, *FEBS Lett.* 589 (2015) 798–804.
- [22] I. de Paola, L. Pirone, M. Palmieri, N. Balasco, L. Esposito, L. Russo, D. Mazza, L. Di Marcotullio, S. Di Gaetano, G. Malgieri, L. Vitagliano, E. Pedone, L. Zaccaro, Cullin3-BTB interface: a novel target for stapled peptides, *PLoS One* 10 (2015).
- [23] S. Correale, C. Esposito, L. Pirone, L. Vitagliano, S.D. Gaetano, E. Pedone, A biophysical characterization of the folded domains of KCTD12: insights into interaction with the GABAB2 receptor, *J. Mol. Recognit.* 26 (2013) 488–495.
- [24] B. Farina, I. de Paola, L. Russo, D. Capasso, A. Liguoro, A. Del Gatto, M. Saviano, P.V. Pedone, S. Di Gaetano, G. Malgieri, L. Zaccaro, R. Fattorusso, A combined NMR and computational approach to determine the RGDchi-hiC-alpha(v)beta(3) integrin recognition mode in isolated cell membranes, *Chem. Eur. J.* 22 (2016) 681–693.
- [25] A. Bax, D.G. Davis, Mlev-17-based two-dimensional homonuclear magnetization transfer spectroscopy, *J. Magn. Reson.* 65 (1985) 355–360.
- [26] M. Rance, O.W. Sorensen, G. Bodenhausen, G. Wagner, R.R. Ernst, K. Wuthrich, Improved spectral resolution in cosy 1H NMR spectra of proteins via double quantum filtering, *Biochem. Biophys. Res. Commun.* 117 (1983) 479–485.
- [27] A. Kumar, R.R. Ernst, K. Wuthrich, A two-dimensional nuclear Overhauser enhancement (2D NOE) experiment for the elucidation of complete proton-proton cross-relaxation networks in biological macromolecules, *Biochem. Biophys. Res. Commun.* 95 (1980) 1–6.
- [28] T.L. Hwang, A.J. Shaka, Water suppression that works — excitation sculpting using arbitrary wave-forms and pulsed-field gradients, *J. Magn. Reson. Ser. A* 112 (1995) 275–279.
- [29] C. Dalvit, Efficient multiple-solvent suppression for the study of the interactions of organic solvents with biomolecules, *J. Biomol. NMR* 11 (1998) 437–444.
- [30] D.W. Hoskin, A. Ramamoorthy, Studies on anticancer activities of antimicrobial peptides, *BBA-Biomembranes* 1778 (2008) 357–375.
- [31] F. Schweizer, Cationic amphiphilic peptides with cancer-selective toxicity, *Eur. J. Pharmacol.* 625 (2009) 190–194.
- [32] G. Malgieri, C. Avitabile, M. Palmieri, L.D. D’Andrea, C. Isernia, A. Romanelli, R. Fattorusso, Structural basis of a temporin 1b analogue antimicrobial activity against gram negative bacteria determined by CD and NMR techniques in cellular environment, *ACS Chem. Biol.* 10 (2015) 965–969.
- [33] X. Pan, M. Wilson, C. McConville, M.-A. Brundler, T.N. Arvanitis, J.P. Shockcor, J.L. Griffin, R.A. Kauppinen, A.C. Peet, The lipid composition of isolated cytosolic lipid droplets from a human cancer cell line, *BE(2)M17*, *Mol. BioSyst.* 8 (2012) 1694–1700.
- [34] S. Halder, K.K. Yadav, R. Sarkar, S. Mukherjee, P. Saha, S. Halder, S. Karmakar, T. Sen, Alteration of zeta potential and membrane permeability in bacteria: a study with cationic agents, *Spring* 4 (2015).
- [35] R.E.W. Hancock, H.G. Sahl, Antimicrobial and host-defense peptides as new anti-infective therapeutic strategies, *Nat. Biotechnol.* 24 (2006) 1551–1557.
- [36] D. Gaspar, J.M. Freire, T.R. Pacheco, J.T. Barata, M.A.R.B. Castanho, Apoptotic human neutrophil peptide-1 anti-tumor activity revealed by cellular biomechanics, *BBA-Mol. Cell. Res.* 1853 (2015) 308–316.
- [37] D. Gaspar, A.S. Veiga, C. Sinthuvanich, J.P. Schneider, M.A.R.B. Castanho, Anticancer peptide SVS-1: efficacy precedes membrane neutralization, *Biochemistry* 51 (2012) 6263–6265.
- [38] S. Elmore, Apoptosis: a review of programmed cell death, *Toxicol. Pathol.* 35 (2007) 495–516.
- [39] G. Bjorkoy, T. Lamark, S. Pankiv, A. Overvatn, A. Brech, T. Johansen, Monitoring

- autophagic degradation of P62/Sqstm1, *Methods Enzymol.* 452 (Pt B, 452) (2009) 181–197.
- [40] A. Gonzalez-Rodriguez, R. Mayoral, N. Agra, M.P. Valdecantos, V. Pardo, M.E. Miquilena-Colina, J. Vargas-Castrillon, O. Lo Iacono, M. Corazzari, G.M. Fimia, M. Piacentini, J. Muntane, L. Bosca, C. Garcia-Monzon, P. Martin-Sanz, A.M. Valverde, Impaired autophagic flux is associated with increased endoplasmic reticulum stress during the development of NAFLD, *Cell Death Dis.* 5 (2014).
- [41] Y. Huang, Q. Feng, Q. Yan, X. Hao, Y. Chen, Alpha-helical cationic anticancer peptides: a promising candidate for novel anticancer drugs, *Mini Rev. Med. Chem.* 15 (2015) 73–81.
- [42] C.M.A.R.B. D. Gaspar, Host Defense Peptides and Their Potential as Therapeutic Agents, (2016).
- [43] S. Prato, R.M. Vitale, P. Contursi, G. Lipps, M. Saviano, M. Rossi, S. Bartolucci, Molecular modeling and functional characterization of the monomeric primase-polymerase domain from the *Sulfolobus solfataricus* plasmid pIT3, *FEBS J.* 275 (2008) 4389–4402.
- [44] S. Fusco, Q. She, S. Bartolucci, P. Contursi, T(lys), a newly identified *Sulfolobus* spindle-shaped virus 1 transcript expressed in the lysogenic state, encodes a DNA-binding protein interacting at the promoters of the early genes, *J. Virol.* 87 (2013) 5926–5936.
- [45] S. Fusco, Q.X. She, G. Fiorentino, S. Bartolucci, P. Contursi, Unravelling the role of the F55 regulator in the transition from lysogeny to UV induction of *Sulfolobus* spindle-shaped virus 1, *J. Virol.* 89 (2015) 6453–6461.
- [46] S. Fusco, M. Aulitto, S. Bartolucci, P. Contursi, A standardized protocol for the UV induction of *Sulfolobus* spindle-shaped virus 1, *Extremophiles* 19 (2015) 539–546.
- [47] P. Contursi, S. Fusco, R. Cannio, Q.X. She, Molecular biology of fuselloviruses and their satellites, *Extremophiles* 18 (2014) 473–489.
- [48] P. Contursi, S. Fusco, D. Limauro, G. Fiorentino, Host and viral transcriptional regulators in *Sulfolobus*: an overview, *Extremophiles* 17 (2013) 881–895.
- [49] S. Bartolucci, P. Contursi, G. Fiorentino, D. Limauro, E. Pedone, Responding to toxic compounds: a genomic and functional overview of Archaea, *Front. Biosci. (Landmark Ed)* 18 (2013) 165–189.
- [50] P. Contursi, R. Cannio, Q.X. She, Transcription termination in the plasmid/virus hybrid pSSVx from *Sulfolobus islandicus*, *Extremophiles* 14 (2010) 453–463.
- [51] S. Prato, R. Cannio, H.P. Klenk, P. Contursi, M. Rossi, S. Bartolucci, pIT3, a cryptic plasmid isolated from the hyperthermophilic crenarchaeon *Sulfolobus solfataricus* IT3, *Plasmid* 56 (2006) 35–45.